
THE UNIVERSITY *of* EDINBURGH


# Functional analysis of DAZL-mediated translation activation during mammalian gametogenesis

**João Pedro Sousa Martins**
**BSc (Hons) Human Biology, Glamorgan University**
**MSc Reproductive and Developmental Biology, Imperial College, London**

**Thesis Submitted to the University of Edinburgh for the degree of**
Doctor of Philosophy

# Abstract

Gametogenesis is a highly complex process that requires stringent control of gene expression, in which translational regulation plays an essential role. Deleted in Azoospermia-like (DAZL) belongs to the DAZ family of RNA-binding proteins, which are restricted to germ cells, and regulate mRNA translation. Importantly, loss of function of these proteins results in infertility in both males and females in a wide variety of organisms.

A model for the mechanism by which DAZL stimulates translation has been proposed based on work in *Xenopus laevis* (*X. laevis*) oocytes. In this model, DAZL functions by recruiting the translation initiation factor poly(A)-binding protein (PABP) to the 3' untranslated region (UTR) of messenger RNAs. Simultaneous binding of PABP to Dazl and factors at the 5' end confers a "closed-loop" mRNA conformation, which promotes translation initiation.

To examine whether DAZL plays a similar role in mammals, co-expression of Dazl and PABP family members was investigated in fetal and adult mouse gonads. In contrast to *X. laevis*, mammals encode four cytoplasmic PABPs which share a similar domain organisation: PABP1, tPABP, ePABP and PABP4, of which PABP1 and PABP4 appear to be expressed in a wide range of tissues. Immunohistochemistry revealed that Dazl, Pabp1 and Pabp4 are all expressed in primordial germ cells (PGCs) but these show different expression patterns following germ cell sex differentiation. In adult testes Dazl is expressed in spermatogonia and spermatocytes, coinciding with the peak of Pabp4 expression. In contrast, the peak of Pabp1 expression occurs later than that of Dazl, with these proteins only being co-expressed in late pachytene and secondary spermatocyte phases. In adult ovaries, Pabp1, Pabp4 and Dazl are all expressed in the oocytes of primordial and primary follicles. Since both PABP family members are co-expressed with Dazl, the ability of DAZL to interact with PABP1 and PABP4 was investigated *in vitro* and *in vivo.* Surprisingly, these studies showed that DAZL discriminates between different PABP family members, only interacting with PABP1, providing the first report of a PABP-specific protein partner.

Several putative DAZL mutations have been identified in patients with impaired fertility. Two of these mutations, I37A and R115G, are located in the RNA recognition motif (RRM), a domain which is found in many RNA-binding proteins and mediates both RNA and protein interactions. Thus, the role of these mutations in the ability of DAZL to stimulate translation was investigated. To this end, a translational target of human DAZL (hDAZL) was sought. The 3'UTR of growth differentiation factor 9 (hGDF9) mRNA was found to confer regulation by hDAZL and thus the ability of mutant DAZLs to stimulate reporter mRNAs containing this 3'UTR was examined. This revealed that both mutations compromised the ability of hDAZL to stimulate hGDF9 translation, suggesting a causative effect. These results were further confirmed in assays in which hDAZL is artificially tethered to mRNAs. The ability of mutant hDAZLs to stimulate translation in this assay was compromised suggesting that loss of function is, at least in part, due to impaired protein-protein interactions rather than altered RNA-binding.

This work provides insights into the molecular mechanism by which DAZL stimulates the translation of specific mRNAs during mammalian gametogenesis and provides evidence that this function may play an important physiological role in human reproduction.

# Declaration

The studies undertaken for the completion of this thesis represent work performed by the author, except where acknowledged by reference. These have not been previously submitted for another degree or qualification.

João Pedro Sousa Martins
July 2012

# Acknowledgements

I thought I could dedicate each one of the following pages to all of the people that have helped me throughout the last 4 years, but there are simply not enough pages! Therefore, to all of you, I dedicate instead, each and single strand of hair that I have lost from my balding forehead during the course of this PhD.

This experience exposed me to challenges that I would have never been able to overcome without the help of a great group of friends.

First I would like to thank Niki. Despite being the most unlikely candidate for this tremendous endeavour she always believed in me. Thank you for your patience with my portugalinglish, for your guidance during this work, for teaching me how to see problems as solutions and solutions as new projects. This "thank you" needs to be extended way beyond the stereotypical acknowledgment towards the typical supervisor, because you were much more than that, thank you for your respect, discretion and foremost for your honesty. Without you things would for sure been horribly different. I will always be in-debt to you.

I would also like to thank the other members of the Gray lab, Bill, Ross, Richard, Barbara, Matt, Hannah and Lora for making each day in the lab feel much more than just work.

Thank you to Professor McNeilly, Dr McNeilly and Dr Childs for the helpful discussions, always over a nice coffee, regarding applied reproductive biology topics, and Dr Ian Adams and Dr O'Hara for teaching me the difference between testicles and ovaries, regarding fetal mice. Thanks to Mike Millar and Sheila MacPherson for their help with my infinite histology problems.

I also need to acknowledge and thank Moh for helping me to start my PhD and with my move to Edinburgh.

And now "proper" Kate Winslet style …

A special thank you goes to Ross, which even without being asked, helped me a lot when I started my PhD, by trying endlessly to teach me basic molecular techniques (now, that explains everything).

A big thank you also to the entire McNeilly lab, Alan, Linda, Dr McNeilly (there should always be space for manners and respect), Kasia and Sarah for making me feel so welcome, in spite of my *sui generis* ways. Thank you for adopting me as a self proclaimed "honorary" member. I promise I have learned my lessons; The Queen Rules, "keep yer Heid" and chocolate go "out of date" if it is not instantly devoured. Don't worry BBFs I will keep in touch through facebook on my iPhone/Pad.

A humongous thank you to my friends Ale, Cris, Sana, Rafa, Vanessa, James, John, Mike and Eva, for being there for me when I needed the most even despite my, sometimes, arrogate, stern, egotistical and prepotent attitude towards a friendly hug.

I need also to acknowledge Batman, Robin and Sweetcheeks, (not entirely sure why, maybe) for helping me to realise that there are people way more weird than me… and that ultimately there is always North Bridge, seriously, Thanks Dr S.

Thank you to everyone at the MRC-CRH, especially to Sharon, Laura, Erin, Julia, Hazel, Julie, Debs and Uma for being such great friends, coping with all my passive aggressive ways, my nakedness and "frapes".

Thank you to Barbara and Andrew for understanding me even without the need of words, for understanding that I am border line impossible, defensive and stubborn … but hopefully still on the good side!?

I know that the space is sparse and I shouldn't repeat people but I can never thank enough two of the greatest people that I have ever met, Sarah and Linda, thank you again for everything.

Thank you to Lawrence, Abdi and Richard for not forgetting the way to my office in the moment that I needed the most.

Thank you to Dougie and his immense patience, care and support and for telling me that the solution for a DAZL-PABP1 co-IP was 2 (sorry for sharing the secret). Thank you for turning my frown upside down.

The greatest "Obrigado" of all goes to my parents, Pai Martins and Mãe Lena, for making me feel like the luckiest son in the world, I will never be able to thank you enough for all that you did for me.

Thank you to Bruno, for "free-ing" me from the "tarantula killer" duties and taking care of the most important person in my world. And it is to her, my sister that I dedicate this work, after all, despite the fact that I was the boss I always had to do what you told me to. I wish I could one day show you how grateful I am for all of what you have done.

# Publications

-Gorgoni B, Richardson WA, Burgess HM, Anderson RC, Wilkie GS, Gautier P, Martins JP, Brook M, Sheets MD, Gray NK. (2011) **Poly(A)-binding proteins are functionally distinct and have essential roles during vertebrate development.** Proc Natl Acad Sci U S A. 10;108(19):7844-9.

# Poster presentations

-Sousa Martins JP, McCracken L and Gray NK **Characterization of Dazl-PABP interactions.** Translation UK, Warwick, 2009.

-Sousa Martins JP, McCracken L and Gray NK **Characterization of Dazl-PABP Interactions in Mammalian Gametogenesis.** Germ Cells, Cold Spring Harbor, New York, 2010.

-Sousa Martins JP and Gray NK **Characterization of Dazl-PABP Interactions in Mammalian Gametogenesis.** Society for Reproduction and Fertility, Brighton, 2011. (awarded the "SRF Poster Prize" and the "People's Choice Poster Prize")

-Sousa Martins JP and Gray NK **Putative mutations identified in patients with impaired fertility disrupt DAZL's ability to stimulate mRNA translation.** Translation UK, The University of Southampton, 2012.

# Abbreviations

**3'-UTR**..... 3' untranslated region
**4E-BP**..... eukaryotic initiation factor 4E binding protein
**5'-UTR**..... ..... 5' untranslated region

**β-Gal**..... β-galactosidase
**µg**..... microgram
**µl**..... microlitre
**µM**..... micromolar
**µm**..... micrometre

**A**..... adenosine
**AD**..... activation domain
**ARE**..... adenosine/uracil-rich element
**ARS**..... autoregulatory sequence
**A-site**..... aminoacyl site
**ATP**..... adenosine triphosphate

**BD**..... binding domain

**C**..... cytosine
**cDNA**..... complementary DNA
**Co-IP**..... protein complex immunoprecipitation
**CPE**..... cytoplasmic polyadenylation element
**CPEB**..... cytoplasmic polyadenylation element binding protein
**C-terminus**..... carboxyl terminus

**DAB**..... diaminobenzidinetrahydrochloride
**DAPI**..... 4', 6-diamidino-2-phenylindole
**DAZ**..... deleted in azoospermia
**DAZL**..... deleted in azoospermia-like
**dH2O**..... distilled water
**DMEM**..... Dulbecco's minimal essential medium
**DNA**..... deoxyribonucleic acid
**DNase**..... deoxyribonucleic acid nuclease
**dpc**..... days post coitum
**dpp**..... days postpartum
**DSB** ..... double strand breaks
**dsRNA**..... double stranded ribonucleic acid

***E. coli***..... *Escherichia coli*
**EDTA**..... ethylene diamine tetraacetic acid
**EGFP**..... enhanced green fluorescent protein
**eIF**..... eukaryotic initiation factor
**EJC**..... exon junction complex

**EMSA**..... electrophoresis mobility shift assay
**ePABP**..... embryonic polyadenylate binding protein
**eRF**..... eukaryotic release factor
**E-site**..... exit site

**FCS**..... fetal calf serum
**FSH**..... follicle-stimulating hormone

**G**..... guanosine
**g**..... gram
**GST**..... glutathione S-transferase
**GTP**..... guanosine triphosphate
**GTPase**..... guanosine triphosphatase
**GVBD**..... germinal vesicle breakdown e
**γH2AX**…….. phosphorylation of histone H2AX
**H2O**..... water
**Hela cell**..... Henrietta Lacks cell
**His**..... histidine
**HRP**..... horse radish peroxidase

**I37A**……. isoleucine to alanine substitution at aa 37 (hDAZL mutation)
**iPABP**..... inducible polyadenylate binding protein
**IPTG**..... isopropyl β-D-1-thiogalactopyranoside
**IRE**..... iron regulatory element
**IRES**..... internal ribosome entry site
**IRP**..... iron regulatory protein

**Kb**..... kilobase
**Kd**..... dissociation constant
**KDa**..... kilodalton

**L**..... litre
**LH**..... luteinising hormone
**LSU**..... large ribosomal subunit

**M**..... molar
**Met-tRNAi**..... initiator transfer ribonucleic acid
**mg**..... milligram
**miRISC**..... microribonucleic acid induced silencing complex
**miRNA**..... microribonucleic acid
**ml**..... millilitre
**mM**..... millimolar
**mm**..... millimetre
**mRNA**..... messenger ribonucleic acid
**mRNP**..... messenger ribonucleoprotein
**mTOR**..... mammalian target of rapamycin

**N10C** …… asparagine to cysteine substitution at aa 10 (hDAZL mutation)
**ng**..... nanogram
**nl**..... nanolitre
**nM**..... nanomolar
**nm**..... nanometre
**NMD**..... nonsense mediated decay
**NSP3**..... non-structural protein 3
**nt**..... nucleotide
**N-terminus**..... amino terminus

**O.D.**..... optical density
**Oligo**..... oligonucleotide
**ORF**..... open reading frame

**P6H**…….. proline to histidine substitution at aa 6 (hDAZL mutation)
**PABC**..... polyadenylate binding protein carboxy terminus
**PABP**..... polyadenylate binding protein
**PABP1**..... polyadenylate binding protein 1
**PABP4**..... polyadenylate binding protein 4
**PABP5**..... polyadenylate binding protein 5
**PABPN1**..... nuclear polyadenylate binding protein
**PAGE**..... polyacrylamide gel electrophoresis
**PAIP-1**..... polyadenylate binding protein interacting protein 1
**PAIP-2**..... polyadenylate binding protein interacting protein 2
**PAM**..... polyadenylate binding protein interacting motif
**PAN2**..... polyadenylate nuclease 2
**PAN3**..... polyadenylate nuclease 3
**PAP**..... polyadenylate polymerase
**PARN**..... polyadenylate ribonuclease
**PCR**..... polymerase chain reaction
**PFA**..... paraformaldehyde
**pg**..... picogram
**PIC**..... preinitiation complex
**PKR**..... protein kinase R
**pM**..... picomolar
**poly(A)**..... polyadenylate

**QPCR**..... quantitative polymerase chain reaction

**R115G**……. argenine to glycine substitution at aa 115 (hDAZL mutation)
**rcf**..... relative centrifugal force
**RNA**..... ribonucleic acid
**RNA-BP**..... ribonucleic acid binding protein
**RNAi**..... ribonucleic acid interference
**RNase**..... ribonucleic acid nuclease
**rpm**..... revolutions per minute
**RRL**..... rabbit reticulocyte lysate

**RRM**..... ribonucleic acid recognition motifs
**rRNA**..... ribosomal ribonucleic acid
**RT-PCR**..... reverse transcription polymerase chain reaction

**SAP**..... shrimp alkaline phosphatase
**SC**..... synaptonemal complex
**Sycp1**..... synaptonemal complex protein 1
**Sycp2**..... synaptonemal complex protein 2
**Sycp3**..... synaptonemal complex protein 3
**SG**..... stress granule
**siRNA**..... short interfering ribonucleic acid
**SXL**..... sex lethal

**T**..... thymidine
**TC**..... ternary complex
**TD-NEM**..... transcription dependent nuclear export motif
**TOP**..... terminal oligopyrimidine
**tPABP**..... testis polyadenylate binding protein
**tRNA**..... transfer ribonucleic acid

**U**.....uracil
**uAUG**.....upstream AUG
**uORF**.....upstream open reading frame

**WT**.....wild-type

**X-Gal**.....bromochloroindolylgalactopyranoside
**XRN1**.....exoribonuclease 1

**Y2H**.....yeast two-hybrid

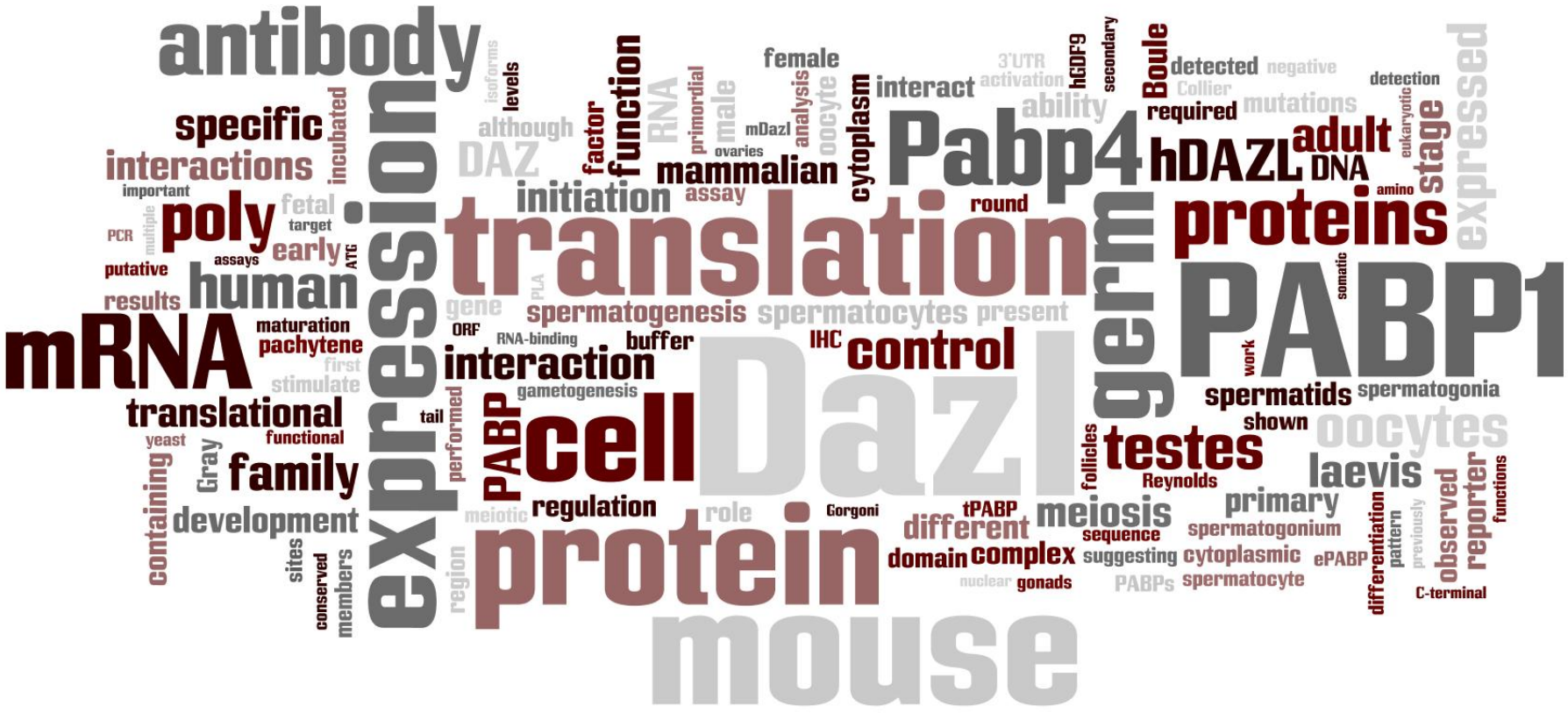
antibody
expression
translation
Dazl
PABP1
mouse
protein
cell
mRNA
Pabp4
germ
proteins
hDAZL
specific
interactions
poly
human
translational
family
development
control
interaction
testes
oocytes
laevis
meiosis
primary
spermatids
spermatogonia
spermatogenesis
spermatocytes
expressed
function
mammalian
initiation
DAZ
RNA
PABP
regulation
different
complex
domain
sequence
suggesting
cytoplasmic
spermatogonium
spermatocyte
gonads
PABPs
ePABP
observed
reporter
differentiation
C-terminal
adult
stage
DNA
Boule
Reynolds
Gray
Gorgoni
Collier
Xenopus
mDazl
hGDF9
IHC
ORF
RNA-binding
PLA
PCR
ATG
tPABP
pachytene
maturation
buffer
gametogenesis
functional
yeast
tail
performed
meiotic
role
region
sites
conserved
members
containing
follicles
shown
work
somatic
eukaryotic
detection
negative
detected
required
mutations
ability
interact
activation
3'UTR
secondary
female
male
primordial
ovaries
analysis
oocyte
cytoplasm
factor
isoforms
levels
incubated
important
multiple
fetal
target
early
assays
putative
results
gene
present
round
assay
although
amino
first
stimulate
pathway
nuclear
PABPs
previously
pattern
functions

# Table of contents

# List of figures

## Chapter 1



## Chapter 2

## Chapter 3

## Chapter 4

## Chapter 5

## Chapter 6

## Appendix 1



## Appendix 2



## Appendix 3



## Appendix 4

# List of tables

## Chapter 1



## Chapter 2



## Chapter 3



## Chapter 5

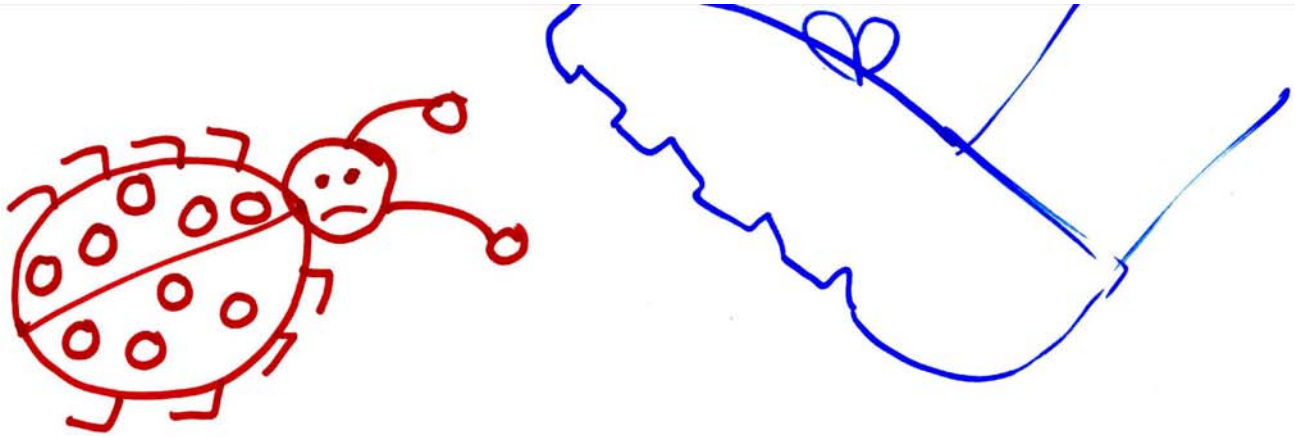

1 bug was hurt in
the printing of this thesis.

D.McN

# Chapter 1
# Literature Review

# 1.1 Mammalian Gametogenesis

Gametogenesis is a complex process that results in the production of haploid gametes (oocytes and sperm), which transmit genetic information to the next generation. Oogenesis and spermatogenesis involve multiple rounds of mitosis followed by meiosis and maturation. These are sexually dimorphic processes however, with important differences in timing, gamete number and error occurrence. Germ cells do not develop autonomously, but work closely together with somatic cells, in a bidirectional program of developmental control (Murray *et al.*, 2010). The regulation of this multi-step process requires stringent control of gene expression by a plethora of mechanisms that are only starting to be understood.

## 1.1.1 Primordial Germ cells

In mouse the earliest identifiable cells of the germ cell lineage occur at 6.25 days post coitum (dpc) (Ohinata *et al.*, 2005). At this stage a small group of six cells expressing the transcriptional repressor Blimp1 (McLaren and Lawson, 2005) can be detected in the proximal epiblast adjacent to the extraembryonic ectoderm (Lawson and Hage, 1994). Blimp1 has been proposed to regulate this lineage by repressing the expression of the somatic cell specific *Hox* genes (Ohinata *et al.*, 2005, Saitou *et al.*, 2005, Vincent *et al.*, 2005). By 7.5 dpc 40 migrating cells expressing Blimp1 can be detected. It is thought that this increase in numbers is due to a rise in cells expressing Blimp1 and division of some of the original Blimp1-expressing cells (McLaren and Lawson, 2005). At this stage these germ cell lineage restricted cells start expressing Stella (also known as PCG7 and Dppa3) (Saitou *et al.*, 2002), a factor that prevents DNA demethylation (Nakamura *et al.*, 2007) and are known as primordial germ cells (PGCs).

During migration and following their arrival at the genital ridges, between 10.5 and 11.5 dpc, the PGCs continue to proliferate with an estimated 4000 sexually indistinguishable PGCs being present by 12 dpc. By 13.5 dpc the developing gonads contain around 24,000 germ cells known as gonocytes since they are now committed to sex specific pathways (Monk and McLaren, 1981, Tam and Snow, 1981).

### 1.1.2 Sex Differentiation

Although genetic sex is determined at fertilization, differences between the germ cells only become evident after they reach the genital ridges (reviewed in (Kocer *et al.*, 2009)). After undergoing one last common round of mitosis at 12.5 dpc they commit to sex-specific pathways that ultimately lead to oocyte and spermatozoa production. The sexual identity of germ cells is determined by a combination of sex chromosomes and the somatic environment surrounding the germ cells (reviewed in (Murray *et al.*, 2010)). In male mice, sex differentiation of germ cells is preceded by the transient expression of the HMG-box transcription factor sex-determining region of the Y (Sry) at 10.5 dpc (Figure 1.1). Sry up-regulates the transcription factor Sox9 inducing Sertoli cell differentiation (Sekido *et al.*, 2004, Sekido and Lovell-Badge, 2008) which in turn conditions germ cells to a male specific pathway. By inducing expression of the fibroblast growth factor 9 (Fgf9) Sox9 reinforces male development through a positive feedback and represses female development (Colvin *et al.*, 2001). In females, absence of Sry leads to up-regulation of the signalling molecules Rspo1 and Wnt4, which down-regulate Sox9, leading to the germ cells entering meiosis at 13.5 dpc (Figure 1.1). Retinoic acid (RA) is another modulator of germ cell sex differentiation. Despite being present in both male and female urogenital region, levels of RA are considerably higher in the developing ovaries (Bowles *et al.*, 2006, Koubova *et al.*, 2006). RA promotes the expression of *Stra8* in the mouse ovary from 12.5 dpc (Chuma and Nakatsuji, 2001), a protein essential for the initiation of meiosis (Anderson *et al.*, 2008). In males high levels of the P450 enzyme Cyp26b1, metabolises RA and inhibits male germ cells from entering meiosis (Bowles *et al.*, 2006, Koubova *et al.*, 2006, Bowles and Koopman, 2007). Nanos2, an RNA binding protein, is also involved in a male sexual development. This is specifically expressed in males, following Fgf9 expression (Tsuda *et al.*, 2003), and represses Stra8 expression therefore repressing entry into meiosis (Suzuki and Saga, 2008). There are also studies that report the existence of other meiosis preventing substances secreted by Sertoli cells within the testicular cords. For instance leukaemia inhibitory factor (LIF) expression is stronger in the embryonic testes than in ovaries and it was shown to prevent meiosis (Farini *et al.*, 2005).

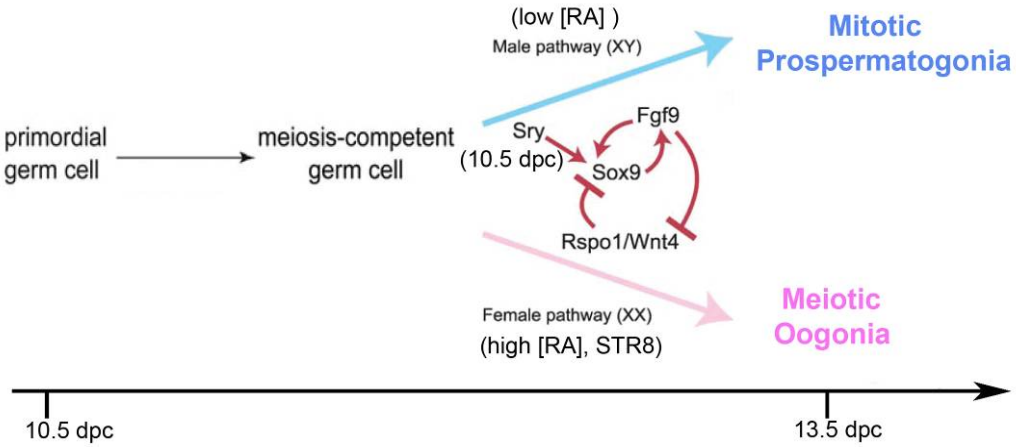


**Figure 1.1 - Germ cell sex determination in mice.** Schematic diagram showing differentiation of germ cells towards a sex specific pathway in the developing gonads. In red, changes in gene expression that drive differentiation of supporting somatic cells. Blue – male specific pathway; pink – female specific pathway. [RA] – retinoic acid concentration; dpc – days post coitum. Adapted from (Lin *et al.*, 2008) and (Kocer *et al.*, 2009).

## 1.1.3 Oogenesis

### 1.1.3.1 Fetal development

In the genital ridges of 13.5 dpc female mice, oogonia cluster together in small groups surrounded by a basement membrane referred to as "germ cell nests". These proliferating oogonia are linked by extended intracellular bridges which allow for an exchange of molecules and may account for the developmental synchronization within each cluster (Pepling and Spradling, 1998). At this stage, oogonia initiate prophase of meiosis I (Figure 1.2) which can be subdivided into leptotene, zygotene and pachytene until they reach the diplotene stage where they arrest in a state known as the dictyate arrest (Baillet and Mandon-Pepin, 2011) until puberty.

In the developing ovaries the quiescent oocytes become associated with somatic cells, presumptive granulosa cells (Byskov, 1975), and depend on these for survival. The granulosa cells surround the oocyte and enclose themselves within a basement membrane, forming a primordial follicle (Hirshfield and DeSanti, 1995). At birth, oocytes that have not been incorporated into primordial follicles undergo atresia. At this point the ovary contains a finite, non-renewable and ever-diminishing reserve of oocytes, which becomes depleted through life (Kerr *et al.*, 2006).

However, this idea has been contested (Johnson *et al.*, 2004, Johnson *et al.*, 2005), but only very recently has it become more accepted that oogonial stem cells may be present in postnatal ovaries both in rodents and humans (White *et al.*, 2012). In particular, this report showed that the adult ovary of reproductive-age women possess oogonial stem cells that can be propagated and differentiated *in vitro* to generate oocytes both *in vitro* and *in vivo*. However, the predominant view is still that that newborn ovaries contain a finite and non-renewable pool of primordial follicles.

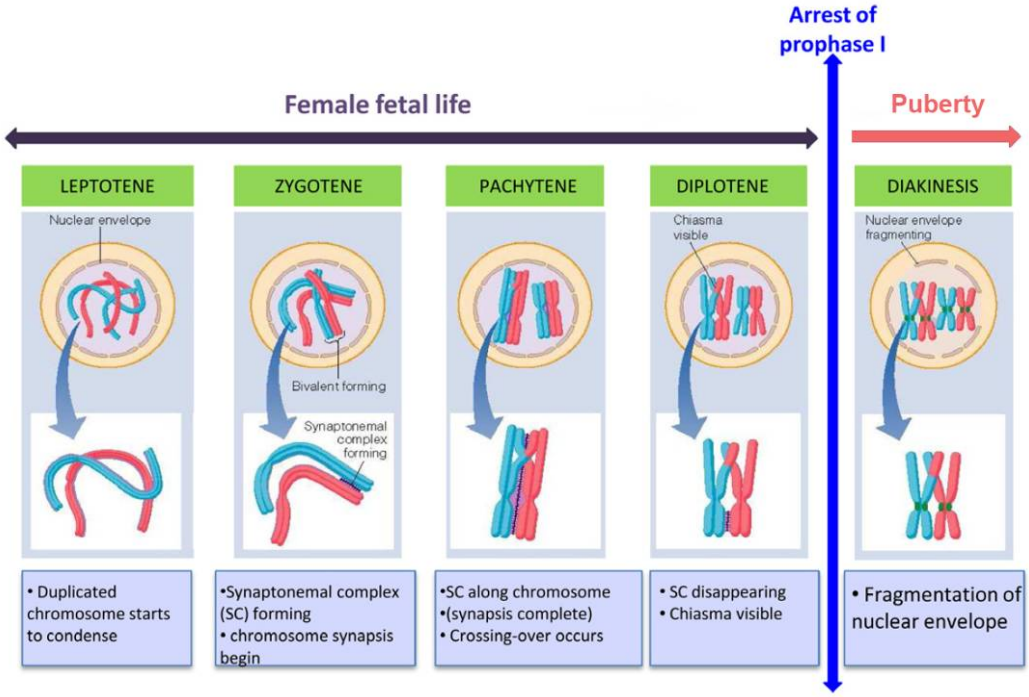


**Figure 1.2 - Prophase I stages.** Chromosomal changes with the progression of meiosis. In females meiosis starts during fetal life and reaches dictyate arrest (arrest of prophase I). Meiosis is only resumed again after puberty. From (Baillet and Mandon-Pepin, 2011).

The number of germ cell in females results from a number of factors, as they can succumb to apoptosis and die during fetal development, undergo atresia at any stage of the female reproductive life or, for a very small number (of the original millions) be recruited from the pool of primordial follicles to develop, and if acquire dominance be ovulated (Kerr *et al.*, 2006). Once the ovaries become completely depleted of germ cells, females enter menopause which corresponds to the termination of ovarian function. Therefore it is important that the recruitment of

germ cells to either undergo atresia or ovulation is tightly controlled, to ensure that a supply of oocytes is not exhausted prematurely leading to premature ovarian failure (POF) also known as premature ovarian insufficiency (POI).

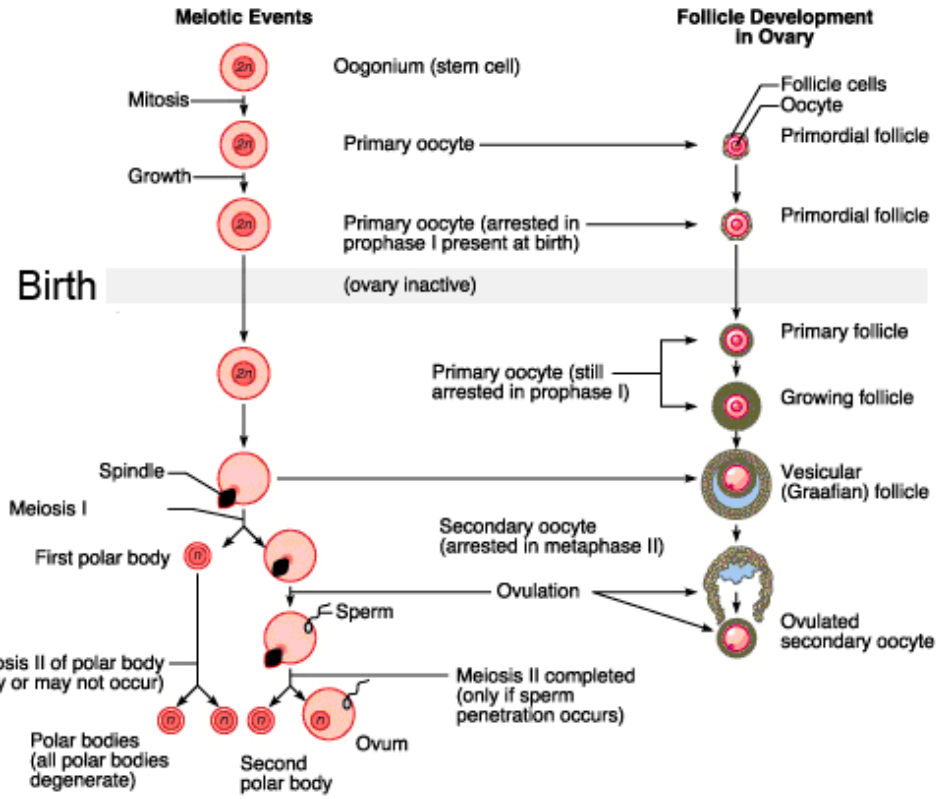


**Figure 1.3 - Mammalian female gametogenesis.** Mammalian female gametogenesis comprises two interlinked but distinct events, with meiotic events related to oogenesis and folliculogenesis related to development of the somatic cells that support the developing oocyte. From http://seem2success.com/wp-content/uploads/2012/02/oogenesis.jpg .

### 1.1.3.2 Folliculogenesis

Folliculogenesis describes the coordinated development between oocytes (oogenesis) and the surrounding somatic cells, which are important sites of steroidogenesis (Figure 1.3). These intrinsically linked events are dependent on bidirectional communication between the oocytes and the granulosa cells within the follicle (Eppig, 2001), e.g. removal of oocytes from follicles results in a failure of granulosa cells to differentiate and proliferate (Sugiura *et al.*, 2005). Follicles also contain theca cells, which are recruited to the follicle later in development. Oocyte-thecal cell communication is also important, e.g. oocyte derived growth and

differentiation factor 9 (GDF9) appears to be required for androgen biosynthesis by the thecal cells (Solovyeva *et al.*, 2000) which is in turn important for folliculogenesis.

After birth a selected number of primordial follicles become committed to growth. Their recruitment is thought to be negatively regulated by AMH (anti-Müllerian hormone) (Durlinger *et al.*, 2002), since the number of follicles undergoing growth increases in AMH null mice. The single layer of flattened granulosa cells differentiates and proliferates to form primary and then secondary follicles surrounded by a single and then double layer of cuboidal granulosa cells. After this initial hormone independent growth, follicles become responsive to follicle-stimulating hormone (FSH) which leads to the formation of early antral follicles, characterised by fluid filled spaces between the proliferating granulosa cells (reviewed in (Adashi, 1994, Canipari, 2000). These spaces eventually get amalgamated into one large fluid filled antral cavity. The FSH responsive antral follicle becomes FSH-dependent and grows substantially due to increased proliferation of the follicular cells and an increased volume of follicular fluid, composed of water, serum proteins, steroid hormones and electrolytes. Only a very small number of follicles achieve dominance capacity, the ability to respond to luteinising hormone (LH) and ovulate, with the remaining developing follicles succumbing to atresia. From primordial until late antral follicles, the oocyte remains in dictyate arrest but grows substantially ((Hsieh *et al.*, 2009) reviewed in (Richards *et al.*, 2002)).

#### 1.1.3.3 Oocyte maturation and the completion of meiosis II

In the pre-ovulatory follicle, the oocyte undergoes meiotic maturation and granulosa cells undergo important phenotypic changes that results in ovulation with the ruptured follicle releasing a mature oocyte which is ready to be fertilised. This process is triggered by an LH surge from the pituitary. It is the somatic cells which respond to this LH surge underlining the importance of somatic-germ cell communication ((Chen *et al.*, 1990, Tirone *et al.*, 1997) reviewed in (Conti *et al.*, 2011)). The resumption of meiosis occurs in response to the flow of cyclic AMP from the granulosa cells (Wert and Larsen, 1990) being suppressed which initiates a

number of intracellular signalling cascades culminating in germinal vesicle breakdown (GVBD) and the extrusion of the first polar body followed by a subsequent meiosis II arrest at metaphase. Meiosis II is only completed following fertilisation (reviewed in (Baker and Spears, 1999, Eppig, 2001, Richards, 2005)). Following ovulation the follicular cells undergo further differentiation to form the *corpus luteum* (Richards, 2005).

### 1.1.4 Spermatogenesis

In mouse fetal testes, germ cells confined within the mesenchymal tissue stop mitotic proliferation and are prevented from entering meiosis. Prior to puberty a surge of steroids drives Sertoli cell maturation which restarts mitosis (Weinbaeur and Niechlag, 1993, Sharpe, 1994). In mammals, a pool of spermatogonia acts as precursor cells proliferating through mitotic division in a process called spermatocytogenesis. These spermatogonia either continue to divide to maintain this pool, or become spermatocytes entering meiosis I before undergoing spermatidogenesis in which the now haploid germ cells differentiate into round spermatids and then elongate to form spermatozoa (Clermont, 1972, Russel, 1993) (Figure 1.4). In mice, this process takes 35 days and can be divided in twelve stages (Russell *et al.*, 1990), which are described in detail in the relevant result sections. In mice, the spermatogenic wave progresses in topographically well-coordinated manner. In humans this pattern is not as clear as the tubules progress with a "helical" organization (Johnson, 2007).

During spermatocytogenesis, progressive rounds of cell division produce three distinct spermatogonial cell populations: undifferentiated, dividing and differentiated spermatogonia (Hermo *et al.*, 2009). Undifferentiated spermatogonia are known as type A-single ($A_s$), and dividing spermatogonia as paired and aligned spermatogonia ($A_{pr}$ and $A_{al}$). These differentiate into $A_1$-$A_2$-$A_3$-$A_4$ spermatogonia, followed by intermediate and B-spermatogonia. B-spermatogonia undergo a last round of mitosis before differentiating into primary spermatocytes (Hermo *et al.*, 2009). Despite this being the commonly accepted pathway for the initial steps of spermatogenesis, there is still some debate regarding A spermatogonia differentiation. Specifically, whether differentiation results from a symmetrical

division with $A_s$ cell committed to renewal or differentiation, or asymmetrical with one daughter cell committed to renewal and the other to differentiation (Oatley and Brinster, 2008).

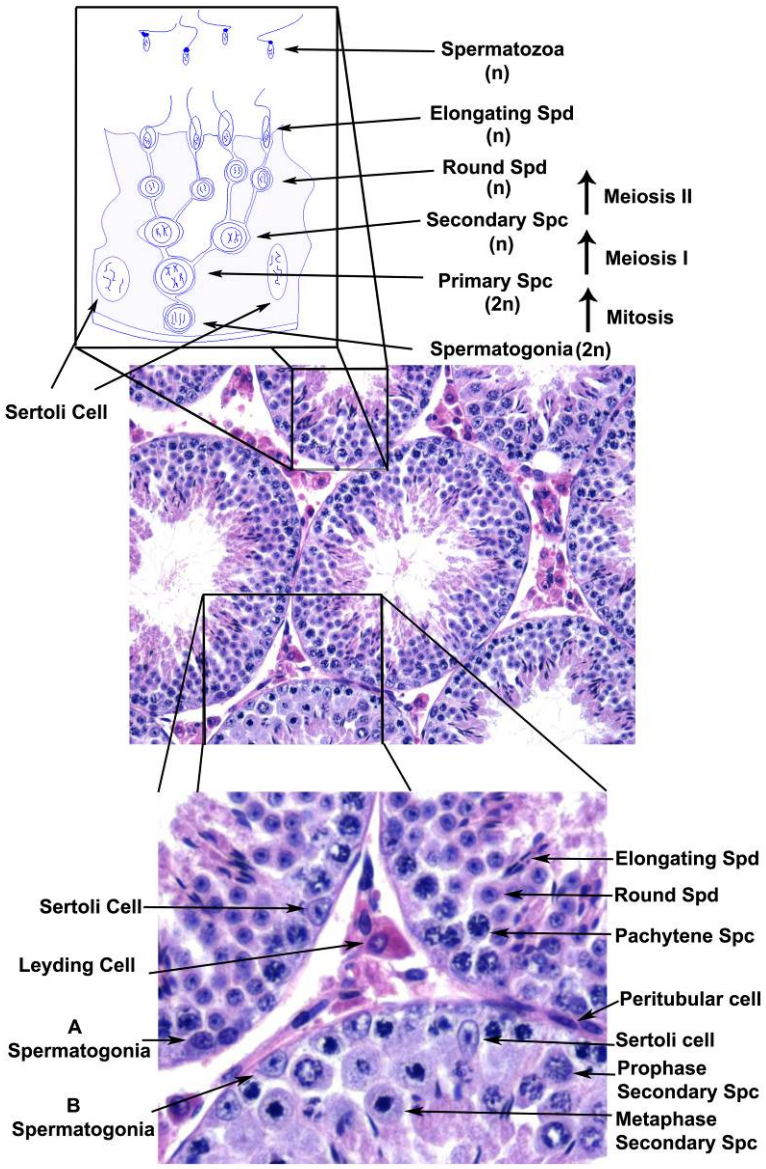


**Figure 1.4 - Mouse spermatogenesis**. Schematic diagram of mouse spermatogenesis progression. H&E staining of mouse adult testis depicting different cell phases. n - chromosome number.

In the final mitosis, B-spermatogonia produce two primary spermatocytes which enter meiosis, starting with prophase I. Prophase I accounts for 90% of the time spent in meiosis during spermatogenesis, and the DNA processes follows those outlined in figure 1.2. However in males this is only started at puberty. Briefly:

primary spermatocytes engage in meiosis starting a prophase I, and proceed through leptotene, zygotene and pachytene spermatocytes, followed by diplotene (Zickler and Kleckner, 1999) and a meiosis I to meiosis II transition. Following meiosis I each primary spermatocyte has given rise to two secondary spermatocytes, containing two sister chromatids. These secondary spermatocytes engage in a new round of cell division without DNA replication, meiosis II, which is a very rapid process and therefore rarely observed in fixed sections. The resulting round spermatids each contain one set of sister chromatids. A more detailed description of meiosis is provided in section 1.1.5.

In the last stage of spermatogenesis, the spermatids undergo profound morphological changes known as spermiogenesis. One of the most striking changes is the reduction in nuclear volume, facilitated by the almost complete replacement of histones by protamines which allow denser DNA packaging, maintaining it in a highly condensed transcriptionally-inactive state (Brewer *et al.*, 1999, Braun, 2001). Head elongation starts at spermatid phase 9. During this process the spermatid head starts to form a "cap". This structure contains important digestive enzymes that allow the spermatozoa to break through the zona pellucida of the ovum (Abou-Haila and Tulsiani, 2000). During the spermatid elongation phase, the cytoplasm is displaced towards the caudal end of the spermatid and eventually sloughs off as a residual body and is phagocytosed by the Sertoli cells and drawn down towards the basement membrane. During elongation a tail is also generated to allow forward propulsion of the sperm. Despite, being morphologically mature, these spermatozoa lack motility which is only acquired with passage through the efferent ducts and epididymis.

Many of the features of spermatogenesis have been discerned by studying the first wave of spermatogenesis, as during this timeframe cells progress synchronously through the different developmental phases (Table 1.1 and Figure 1.5). However, the initial stages and subsequent waves differ in that differentiated spermatogonia are thought to arise directly from prospermatogonia rather than from undifferentiated spermatogonia previously derived from prospermatogonia (Yoshida *et al.*, 2006). Throughout adult life a stem-cell population of mitotically dividing male germ cells is retained which the testis, providing continuous waves of spermatogenesis (Handel and Eppig, 1998, Morelli and Cohen, 2005).

| Cell types | Days post-partum | | | | | | | |
|---|---|---|---|---|---|---|---|---|
| | **6** | **8** | **10** | **12** | **14** | **16** | **18** | **20** |
| Prespermatogonia | 16 | - | - | - | - | - | - | - |
| A Spermatogonia | - | 17 | 7 | 7 | 6 | 9 | 3 | 4 |
| B spermatognia | - | 10 | 11 | 8 | 6 | 8 | 7 | 6 |
| Preletotene Spermatocytes | - | - | 15 | 11 | 9 | 5 | 10 | 7 |
| Leptotene spermatocytes | - | - | 15 | 12 | 13 | 5 | 5 | 9 |
| Zygotene spermatocytes | - | - | - | 23 | 14 | 7 | 8 | 8 |
| Pachytene spermatocytes | - | - | - | - | 15 | 27 | 36 | 33 |
| Secondary spermatocytes | - | - | - | - | - | - | 1 | 1 |
| Round spermatids | - | - | - | - | - | - | 1 | 4 |
| Sertoli cells | 84 | 73 | 52 | 39 | 37 | 39 | 29 | 28 |

**Table 1.1 - Temporal appearance of spermatogenic cells.** Adapted from (Bellve *et al.*, 1977).

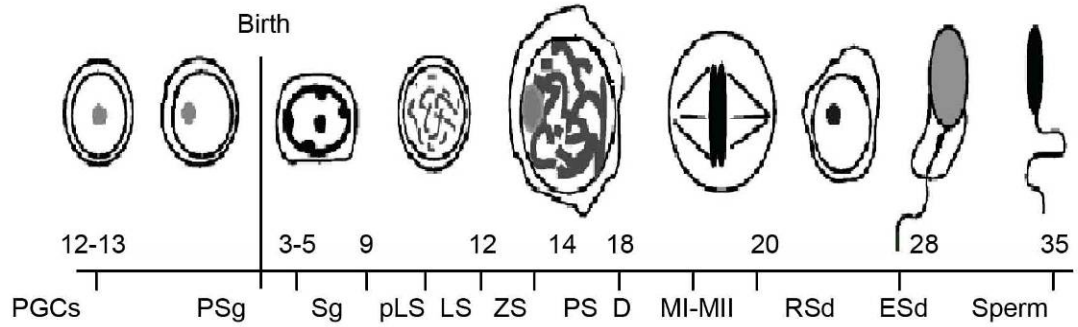


**Figure 1.5 - First wave of mouse spermatogenesis.** Schematic representation of male germ cell development in mouse. PGCs –primordial germ cells; PSg – prospermatogonia; Sg – spermatogonia; pLs –preleptotene spermatocyte; LS – Leptotene spermatocyte; ZS – zygotene spermatocyte; PS – pachytene spermatocyte; D- diplotene spermatocyte; MI-MII – meiosis 1 to meiosis 2 transition; RSd – round spermatid; ESd – elongating spermatid. Adapted from (Meikar *et al.*, 2011).

## 1.1.5 Meiotic division

Meiosis is a specialised mode of cell division in which a diploid precursor cell generates four haploid cells. Meiosis is distinct from mitosis in that cells undergo one round of DNA replication followed by two cell divisions known as meiosis I and meiosis II. In a pre-meiotic event, maternal and paternal homologous chromosomes replicate to produce sister chromatids (Figure 1.6). Initiation of meiosis is characterised by the formation of double strand breaks (DSB), marked by the phosphorylation of histone H2AX (γH2AX) (Mahadevaiah *et al.*, 2001). Homologous recombination allows for the exchange of DNA at DSBs between sister

chromatids (reviewed in (Marston and Amon, 2004)) which are held together by cohesions (Pelttari *et al.*, 2001, Prieto *et al.*, 2001) and the synaptonemal complex (SC). The axial element of the SC starts to form at leptotene (Keeney *et al.*, 1997), concomitantly with homologous chromosome pairing (Schalk *et al.*, 1998, Yang *et al.*, 2008a, Yang *et al.*, 2008b), and is mainly composed of synaptonemal complex protein 2 (Sycp2) and Sycp3. Whereas the transversal element of the SC, mainly composed by Sycp1, only starts to form at zygotene (Meuwissen *et al.*, 1992) (Figure 1.7).

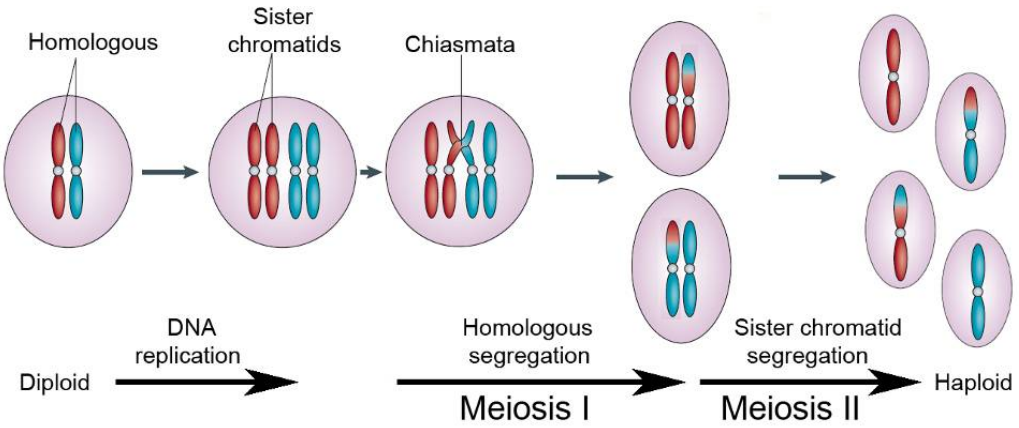


**Figure 1.6 - Meiotic progression.** Following replication of the homologous chromosomes, recombination is initiated by the formation of double strand breaks. Through the action of recombinases, opposite strands of homologous chromosomes form cross-strand exchanges known as crossing overs. The contact point between both chromatid strands is known as chiasmata. Following recombination, cells undergoes two rounds of chromosome segregation, resulting after meiosis I in two cells each containing 2 sister chromatids, and after meiosis II four daughter cells each with 1 sister chromatid (haploid). Adapted from (Marston and Amon, 2004)

The complete attachment of the SC along the full length of the chromosome arms marks the start of the pachytene phase. At pachytene, γH2AX is no longer associated with the chromosomes suggesting that DBS have been repaired. Following pachytene of prophase I, through diplotene and diakinesis SC disassembly occurs but the crossover points, known as chiasmata, keep homologous chromosomes together. During prometaphase, microtubules from opposing poles of the cell attach the centromeres and create a tension force resisted by the chiasmata. This tension aligns the homologous chromosomes along the metaphase plate (Toth *et al.*, 2000, Petronczki *et al.*, 2003). Chiasmata resolution occurs by a loss of

peripheral cohesion at the arms of sister chromatids, resulting in homologous chromosome segregation (Buonomo *et al.*, 2000, Kudo *et al.*, 2006). Following meiosis I, centromeric cohesion is retained (Kitajima *et al.*, 2006), and regulates the alignment of sister chromatids at metaphase II. Proteolysis of the remaining cohesion allows progression to anaphase II (Kudo *et al.*, 2006) and the formation of haploid gametes each with one sister chromatid.

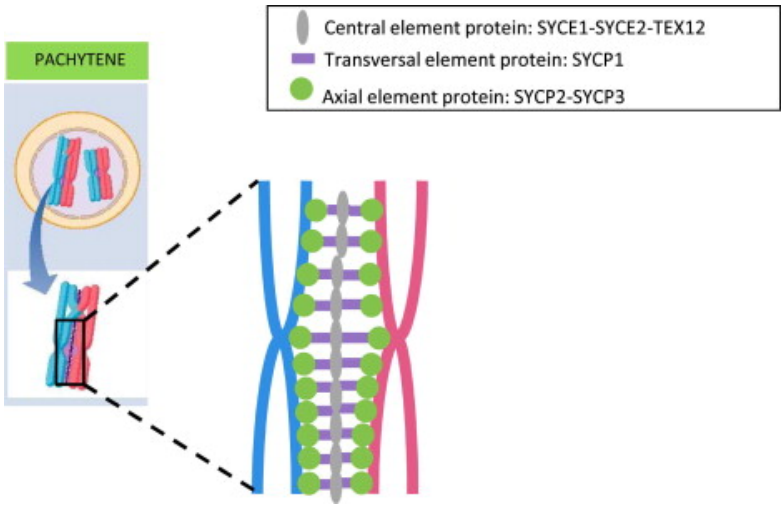


**Figure 1.7 - Synaptonemal complex.** Schematic representation of the synaptonemal complex (SC) at the pachytene phase of prophase I. SC is formed by three different elements, the central, transversal and axial elements. The SC is essential for homologous chromosome pairing and is present from leptotene to pachytene-diplotene phase. From (Baillet and Mandon-Pepin, 2011)

## 1.2 Gene expression

Gene expression refers to the multi-step process by which DNA is transcribed into RNA and then translated into protein. Control can be exerted at multiple stages including transcription, mRNA processing, export, translation or turnover (Figure 1.8) (reviewed in (Orphanides and Reinberg, 2002, Villard, 2004). However, recent work has uncovered the importance of post-transcriptional regulatory mechanisms and in particular translational control in biological processes such as gametogenesis ((Schwanhausser *et al.*, 2011) reviewed in (Lackner and Bahler, 2008)). This may, in part, stem from the periods of transcriptional quiescence during spermatogenesis and oogenesis which mean that changes in the patterns of protein synthesis are dependent

on the activation, repression or destruction of mRNAs transcribed at earlier stages (Prasad *et al.*, 2008, Standart and Minshall, 2008).

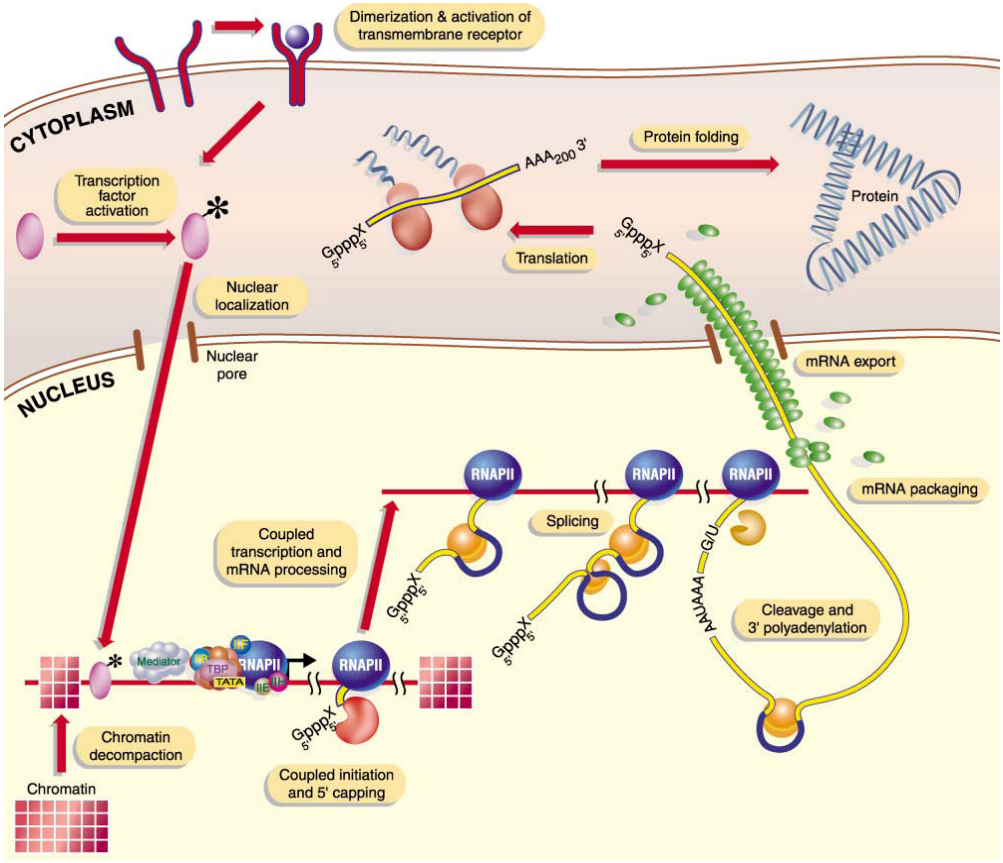


**Figure 1.8 - Eukaryotic gene expression.** Schematic representation of the different steps of gene expression in eukaryotic cells. Regulation can be transcriptional or post-transcriptional, with the latter occurring both within the nucleus and the cytoplasm. From (Orphanides and Reinberg, 2002).

## 1.2.1 mRNA translation control

During transcription and processing of pre-mRNAs in the nucleus, the mRNA is bound by proteins that escort it through the nuclear pores to the cytoplasm (Figure 1.8) (Le Hir *et al.*, 2000a, Le Hir *et al.*, 2000b, Le Hir *et al.*, 2001, Stewart, 2007). Whilst many of these factors, including the nuclear cap complex and nuclear poly(A)-binding protein (PABPN1), are replaced by cytoplasmic counterparts, e.g. eukaryotic translation initiation factor (eIF) 4F and PABP (reviewed in (Carmody and Wente, 2009) other nuclear proteins remain bound to mRNAs and can affect their utilisation (e.g. direct their localisation or efficient translation).

Translational regulation classically refers to a change in the rate of protein synthesis without a corresponding change in mRNA levels (Newbury, 2006). However in many cases, changes in translation are accompanied by downstream changes in mRNA stability as these processes are intimately linked. Translational regulation allows for rapid, temporal and or spatial control of gene expression (Mignone *et al.*, 2002), and in a few exceptional cases can also contribute to protein diversity (Atkins *et al.*, 1990).

There are two main types of quantitative translational regulation, namely global, which affects most cellular mRNAs, or specific, which regulates the activity of a single or a subset of mRNAs (Gebauer and Hentze, 2004). These processes are not exclusive and can occur simultaneously to promote a rapid reprogramming of cellular protein synthesis (Gray and Wickens, 1998, Spriggs *et al.*, 2010). Although translation elongation and termination are subject to regulation, by far the majority of mechanisms act at the level of initiation (Gray and Wickens, 1998).

### 1.2.2 Translation initiation

In eukaryotes, mRNAs leave the nucleus with a 5' $m^7G$ cap structure and a tail of approximately 250 adenosines (poly(A)-tail) at the 3'end, features which are fundamental determinants of translation initiation. As such, the functions of the proteins/protein complexes which bind to them are often the targets of regulation.

Initiation is a complex multi-step process that requires at least 12 eukaryotic initiation factors (eIFs), and which is not yet fully delineated. The following brief description reflects the current prevailing model (detailed reviews on initiation can be found (Sonenberg and Hinnebusch, 2009a, Jackson *et al.*, 2010)).

Initiation starts with the joining of the ternary complex (eIF2, GTP and Met-tRNAi) to the 40S ribosomal subunit to form a 43S pre-initiation complex (PIC). This processes is mediated by a complex series of interactions between eIF1, eIF1A, eIF5, eIF3, eIF2 and the 40S subunit (Majumdar *et al.*, 2003).

The first mRNA-dependent step is binding of the cap by eIF4F also known as the cap-binding complex. eIF4F consists of the cytoplasmic cap-binding protein eIF4E, the scaffold protein eIF4G and the DEAD-box RNA helicase eIF4A. The interaction between eIF4G and eIF4E enhances eIF4E binding to the cap structure

(Yanagiya *et al.*, 2012). Most mRNAs contain some degree of secondary structure that needs to be removed to facilitate binding of the 43S PIC (Pestova *et al.*, 2007a), a function that is mediated by the RNA helicase eIF4A, whose function is stimulated by eIF4F and eIF4B. eIF4F also directly aids 43S complex joining via interactions between eIF4G and eIF3 bound to the 43S complex (Imataka and Sonenberg, 1997, De Gregorio *et al.*, 1999, Martineau *et al.*, 2008). 43S recruitment might also be further promoted by interactions of eIF3 with eIF4B and PAIP-1 (Martineau *et al.*, 2008). These interactions recruit the 43S complex at or near to the cap, forming a 48S complex.

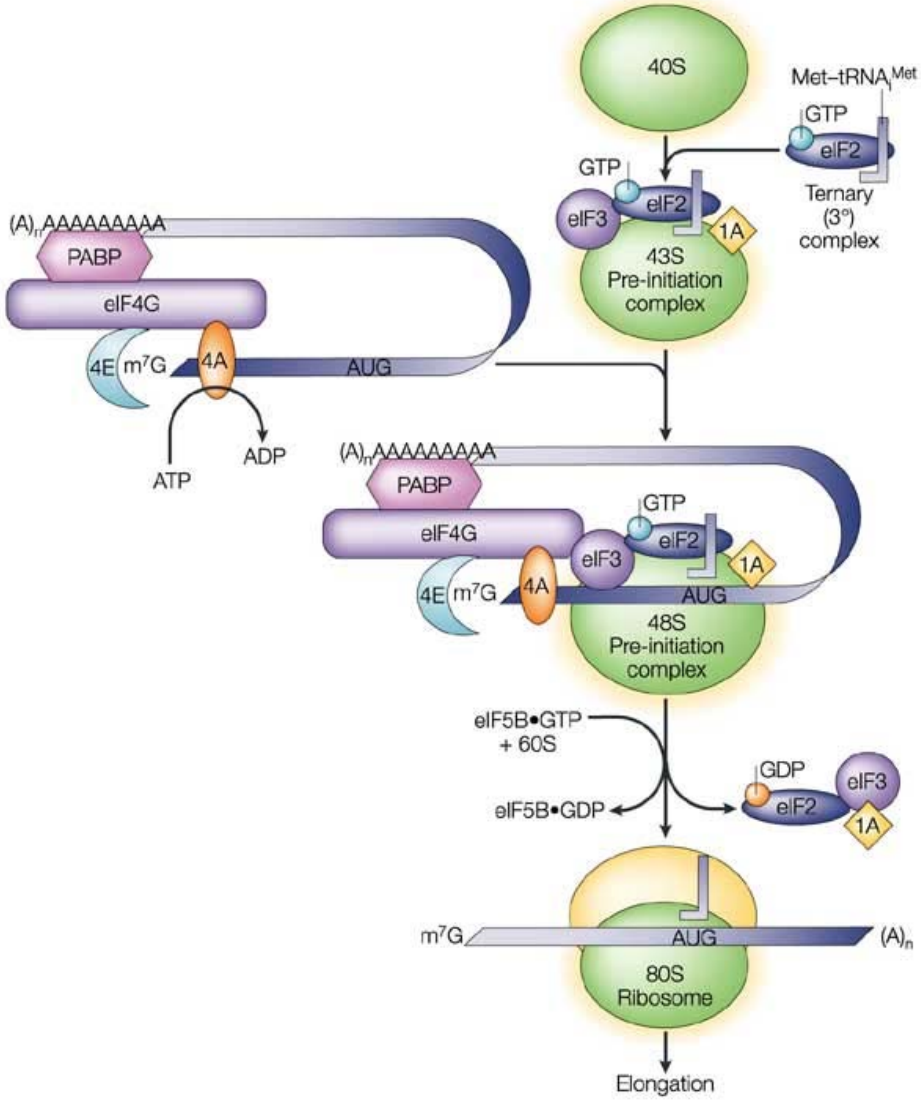


**Figure 1.9 - Translation Initiation.** Simplified diagram showing important steps in eukaryotic translation initiation (from Klann and Dever, 2004).

Surprisingly, poly(A)-binding protein (PABP) which is bound to the 3' poly(A)-tail, and mediates it's function, also promotes 43S PIC joining. By simultaneously binding eF4G, and other eIFs, at the 5'end and the poly(A)-tail at the 3'end, PABP effectively circularizes the mRNA bringing the mRNA ends into functional proximity to form a closed-loop conformation (Figure 1.23) (Kahvejian *et al.*, 2001, Kahvejian *et al.*, 2005, Pestova *et al.*, 2007b, Brook *et al.*, 2009, Sonenberg and Hinnebusch, 2009b). The role of PABPs and the closed-loop will be discussed in more detail later (section 1.3 and Figure 1.23).

Once bound to the 5'end, the 43S complex starts to move through the 5'UTR to locate a start codon (most frequently an AUG) in a process known as scanning. This process is aided by eIF1 and eIF1A (Pestova *et al.*, 1998). The start codon is normally, but not always, the first AUG encountered and recognition is influenced by the surrounding sequence or context with GCC(A/C)CCAUGG being considered optimal (Kozak, 1991b, Grunert and Jackson, 1994). AUG recognition is directed by complementarity with the Met-tRNAi anticodon and is promoted by eIF1 and eIF1A (Pestova and Kolupaeva, 2002, Fekete *et al.*, 2007). Upon codon-anticodon pairing the PIC undergoes structural rearrangements going from an "open" scanning-competent state to a "closed" scanning-arrested state, locking the ribosome to the mRNA (Maag *et al.*, 2005, Maag *et al.*, 2006, Cheung *et al.*, 2007, Passmore *et al.*, 2007). This conformation change induces the dissociation of eIF1 which prompts eIF5 to hydrolyse eIF2-bound GTP which reduces the affinity of eIF2 (eIF2-GDP) for the Met-tRNAi (Algire *et al.*, 2005, Nanda *et al.*, 2009). Finally, the interaction of eIF5B with eIF1A triggers the dissociation of initiation factors and stimulates 60S ribosomal subunit joining, forming an 80S ribosome competent to begin elongation. Figure 1.9 represents a simplified diagram of the steps involved in translation initiation.

### 1.2.3 Global translational control

Global regulation is normally mediated by changes in the activity of the basal translation factors in response to intracellular or extracellular stimuli (e.g. cell stress, viral infection or hormone levels).

Two well characterised mechanisms of global translation initiation regulation involve the initiation factors eIF2 and eIF4E. During initiation eIF2-GTP is hydrolysed to eIF2-GDP (Clemens, 1996) which must be recycled to eIF2-GTP by eIF2B for new rounds of initiation (Figure 1.10), (Clemens, 1997, Clemens and Elia, 1997, Wek *et al.*, 2006, Dever *et al.*, 2007). Importantly, eIF2 is a substrate for a variety of cellular kinases which are activated in response to diverse conditions (e.g. amino acid starvation, viral infection and ER-stress), thus eIF2 phosphorylation acts as a point of convergence for multiple pathways to regulate protein synthesis. Phosphorylated eIF2-GDP interacts with eIF2B to form a stable complex that inhibits the dissociation of eIF2B from eIF2-GDP. This sequesters eIF2B and since this factor is limiting this causes a decrease in available eIF2-GTP, resulting in a global decrease in translation initiation (Oldfield *et al.*, 1994, Clemens, 1996, Krishnamoorthy *et al.*, 2001). Translation can be recovered by dephosphorylation of eIF2 (Garcia-Bonilla *et al.*, 2007, Lee *et al.*, 2009).

Similarly, regulation of the cap-binding protein eIF4E (Figure 1.9) acts as a central control point and a major regulator of cell growth and differentiation (Morley 1997). For instance, sequestration of eIF4E by 4E-binding proteins (4E-BP1, 2 and 3) (Poulin et al., 1998), disrupts the formation of the eIF4F complex (Haghighat et al., 1995, Richter and Sonenberg, 2005) as 4E-BPs competitively bind to the same surface of eIF4E as eIF4G. The binding of 4E-BP and eIF4E is regulated by the phosphorylation status of the 4E-BP proteins, with hypophosphorylation resulting in down regulation of translation, whilst hyperphosphorylation inhibits 4E-BP interaction with eIF4E leading to increased translation (Pause et al., 1994, Gingras et al., 1999). 4E-BPs are a major target of mTOR (mammalian target of rapamycin (Gingras et al., 1998), which coordinates the responses of multiple signalling pathways to extra-cellular cues such as hormones, nutrient sensors, mitogens and growth factors (Raught and Gingras, 2007) and thus 4E-BPs play a central role in regulating cellular metabolism.

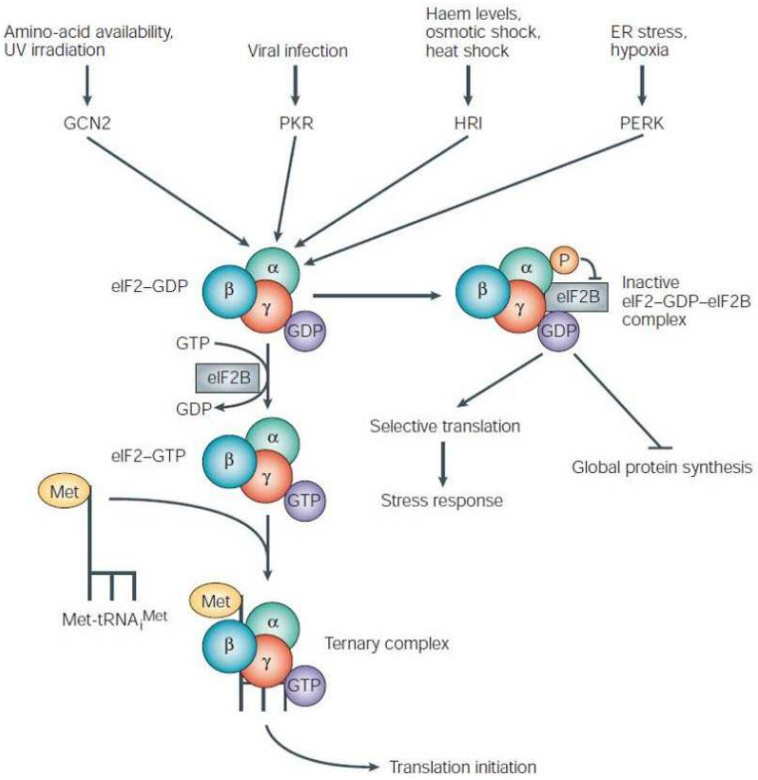


**Figure 1.10 - Formation of active ternary complex and sequestration of eIF-2B acts as a central control point.** Formation of active ternary complex requires eIF2-GTP. Following initiation, eIF2-GTP is hydrolysed to eIF2-GDP. which must be recycling by eIF2B for subsequent rounds of initiation. Multiple stimuli phosphorylate the α-subunit of eIF2, which blocks dissociation of eIF2B. As eIF2B is limiting its sequestration results in availbale eIF2-GTP. Adapted from (Holcik and Sonenberg, 2005).

Interestingly, both eIF2 phosphorylation and sequestration of eIF4E by mRNA-specific binding proteins can also modulate specific mRNA translation, in some cases switching on the translation of specific mRNAs during global translational arrest (see section 1.2.4.1).

## 1.2.4 Specific control of translation

Together with global translation control cells can regulate translation of specific subsets of mRNA. Specific regulation is most frequently rendered by *cis*-acting control elements within the 5' and the 3' UTRs some of which serve as

binding sites for positive and negative *trans*-acting factors (Figure 1.11) (reviewed in (Gray, 1998, Lackner and Bahler, 2008)).

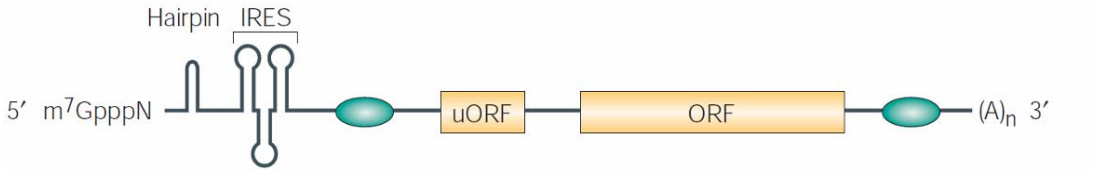


**Figure 1.11 - Translation control elements.** The m7G (m7GpppN) cap and poly(A) tail (An) are primary determinants of translation efficiency. Secondary structures (hairpin) generally impede translation and can serve as sequence-specific binding sites for trans-acting factors, although binding sites can also be unstructured (green ovals). Upstream open reading frames (uORFs) and uAUG codons (not shown) reduce translation by competing with the main ORF for the translational machinery. Internal ribosome entry sequences (IRES) mediate initiation independently of cap function. From (Gebauer and Hentze, 2004)

#### 1.2.4.1 5' UTR translation control elements

Upstream open reading frames (uORFs) and upstream AUGs (uAUGs) are 5' *cis*-acting elements that usually inhibit translation by acting as initiation sites and sequestering ribosomes from the main ORF. As a result uORFs that do not overlap with the main ORF can be less inhibitory than uAUGs as they provide the possibility for re-initiation, although this process is inefficient (reviewed in (Morris and Geballe, 2000). Although most uORFs have an inhibitory effect on translation, they can also facilitate translation of specific mRNAs under certain circumstances. This is exemplified by GCN4, a yeast transcription factor, which contains multiple uORFs within its 5'UTR and is translated during amino acid starvation when eIF2 is phosphorylated. eIF2 phosphorylation retards ternary complex recycling after translation of the initial uORF and therefore a new ternary complex is not recruited in time to re-initiate at downstream uORFs but only at the main ORF (reviewed in (Gebauer and Hentze, 2004, Hinnebusch *et al.*, 2007).

Secondary structure such as stable stem-loops located within the 5'UTR are also inhibitory to initiation since they interfere with 43S PIC joining or ribosomal subunit scanning depending on their position with respect to the cap ((Kozak, 1989, Kozak, 1991c, Kozak, 1991a, Kozak, 1991b) reviewed in (Day and Tuite, 1998)).

Stem-loops can also act as binding sites for mRNA-specific repressor proteins such as iron regulatory protein which allow for regulated steric interference with 43S PIC joining or scanning (Stripecke and Hentze, 1992, Gray and Hentze, 1994, Muckenthaler *et al.*, 1998, Paraskeva *et al.*, 1999).

Counter-intuitively, hairpins can occasionally enhance translation. For instance, when positioned immediately downstream of a start codon they can slow scanning, allowing more time for AUG recognition (Kozak, 1990). Secondary structures can also act as internal ribosome entry sites (IRES) which allow an alternative form of initiation that is cap-independent and therefore does not require all the canonical initiation factors (reviewed in (Spriggs *et al.*, 2008). This provides cells with a mechanism to translate specific mRNAs (e.g. fibroblast growth factor 2; (Bonnal *et al.*, 2005) under conditions (e.g. cell stress) when the activity of key eIFs (e.g. eIF4E) is impaired (reviewed in (Spriggs *et al.*, 2008)).

#### 1.2.4.2 3' UTR–mediated translational control regulated changes in poly(A)-tail length

As mentioned, the poly(A)-tail is a primary determinant of translation efficiency (Munroe and Jacobson, 1990, Gallie, 1991) and is progressively shortened until full degradation of the message is induced. However, poly(A)-tail length can be subject to dynamic control, with regulated deadenylation leading to translation silencing and/or degradation (reviewed in (Garneau *et al.*, 2007)) and with cytoplasmic polyadenylation leading to translation activation (reviewed in (Richter, 2007)). The latter is best studied in oocytes, where many maternal mRNAs are rapidly deadenylated upon leaving the nucleus and are stored in a translational silenced state until they undergo cytoplasmic polyadenylation and translation activation e.g. during oocyte maturation or early embryogenesis (Fox *et al.*, 1992, Sheets *et al.*, 1995, de Moor and Richter, 1999).

The dynamic regulation of poly(A)-tail length of mRNAs in oocytes is driven by balancing the functions of a cytoplasmic poly(A) polymerase Gld2 and poly(A) ribonuclease (PARN). This requires the hexanucleotide $A_2UA_3$ which is bound by CPSF (Cleavage and polyadenylation specificity factor) and is also required for

nuclear polyadenylation (Mendez and Richter, 2001). In addition other regulatory elements are required. The best characterised of these is the cytoplasmic polyadenylation element (CPE) which has the consensus sequence $U_5$[A/U]U, and is bound by CPE-binding protein (CPEB) (Tay and Richter, 2001, Racki and Richter, 2006) (Figure 1.12). CPEB is present in complexes with the scaffolding protein symplekin, CPSF, Gld2 but also PARN which antagonistically shortens poly(A)-tails. Because PARN activity overrides Gdl2 this maintains the mRNA in a deadenylated translationally silent state (Kim and Richter, 2006). Upon oocyte maturation, kinase Aurora A is activated and phosphorylates CPEB which promotes PARN dissociation (Sarkissian *et al.*, 2004), enabling Gld2 action to elongate the poly(A) tail.

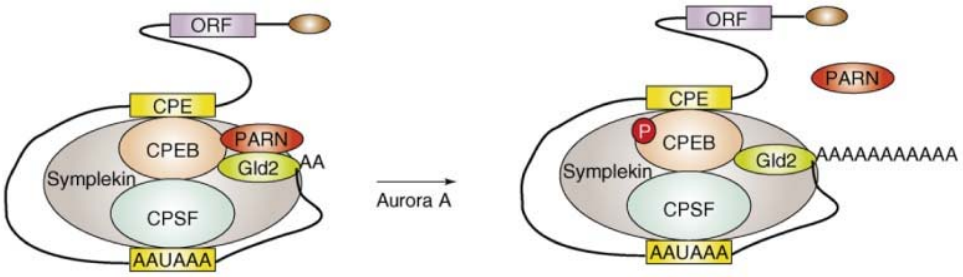


**Figure 1.12 - Cytoplasmic polyadenylation by CPEB in *X. laevis* oocytes.** CPE containing mRNAs are bound by a complex containing CPEB, CPSF, PARN, Gld2 and symplekin. The simultaneous activity of PARN and Gld2 results in controlled deadenylation. Upon oocyte maturation PARN dissociates due to CPEB phosphorylation, changing this equilibrium, resulting in polyadenylation. From (Richter, 2007)

#### 1.2.4.2.1 CPE-mediated cytoplasmic polyadenylation and oogenesis

It is now clear that the translation of many oocyte mRNAs is activated in a strict temporal order through cytoplasmic polyadenylation. Indeed bioinformatic analysis suggests that more than 30% of mouse and human mRNAs involved in oogenesis are regulated by CPE-mediated polyadenylation alone (Pique *et al.*, 2008, Brook *et al.*, 2009). The timing and extent of polyadenylation is determined, in part, by the number and position of CPEs (Pique *et al.*, 2008).

The physiological importance of cytoplasmic polyadenylation for oocyte maturation was shown in seminal studies in *X. laevis* examining the translational

activation of endogenous *c-mos* mRNA (Sheets *et al.*, 1994). Selective removal of its 3'UTR prevented both its cytoplasmic adenylation and oocyte maturation and could be rescued by injection of a "prosthetic" 3'UTR containing CPEs. c-mos mRNA in mouse and human oocytes is also under CPE-mediated cytoplasmic polyadenylation (Figure 1.13), showing the conservation of this regulation across species (Gebauer *et al.*, 1994, Racki and Richter, 2006, Prasad *et al.*, 2008).

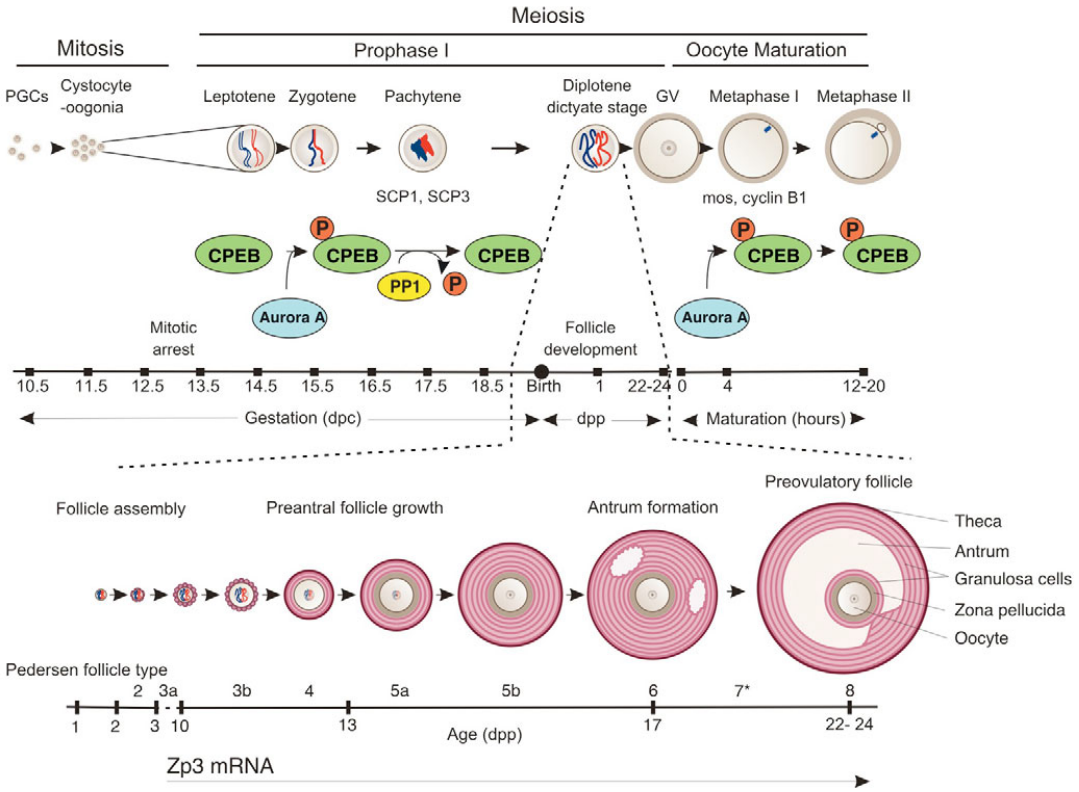


**Figure 1.13 - CPEB1 regulates the translation of mRNAs at multiple stages of oogenesis.** CPEB is required at pacyhtene for the cytoplasmic polyadenylation of mRNAs including Sycp1 and Sycp3. CPEB is phosphorylated by Aurora A, at pachytene and dephosphorylated by PP1 (protein phosphatase 1) prior to dicytate arrest (Tay *et al.*, 2003). Although CPEB1 action is required to promote the translation of mRNAs necessary for oocyte growth and folliculogenesis e.g. Gdf9, its phosphorylation status at this stage is unknown. CPEB1 is once again phosphorylated by Aurora A in pre-ovulatory follicles and is required for oocyte maturation where it promotes the translation of mRNAs including c-*mos* (mos) and cyclin B1 (Gebauer *et al.*, 1994, Tay *et al.*, 2000, Hodgman *et al.*, 2001). From (Racki and Richter, 2006)

In mice, CPEB-mediated control is not only important during oocyte maturation (Gebauer and Richter, 1997, Gebauer and Hentze, 2001, Gebauer and Hentze, 2004), as both male and female knock-out mice arrest at meiotic prophase I

(Tay and Richter, 2001). This may be due in part to reduced translation of synaptonemal complex proteins (Sycp) 1 and 3 (Tay and Richter, 2001, Brook *et al.*, 2009), which are required for the formation of the synaptonemal complex. Similarly, short interfering (si)RNA knockdown of Cpeb in growing dictyate oocytes revealed its importance for oocyte growth and folliculogenesis (Racki and Richter, 2006) as phenotypes including abnormal spindles, detachment from granulosa cells, increased granulosa cell apoptosis and oocyte atresia, precocious follicle activation, premature oocyte maturation and parthenogenesis were all observed. Amongst the CPEB-bound mRNAs identified during these stages was *Gdf9*, which encodes a growth factor that coordinates oocyte-follicle development (Matzuk *et al.*, 2002, Racki and Richter, 2006), whose poly(A)-tail was considerably shorter in the transgenic animals confirming it as a target of CPEB-mediated polyadenylation (Racki and Richter, 2006).

#### 1.2.4.3 Poly(A)-independent stimulation of translation of specific mRNAs

Not all mRNAs that are activated during oocyte maturation require changes in their poly(A)-tail length. One well characterised example of this is metazoan replication-dependent histone mRNAs which lack a poly(A) tail and end in a conserved stem-loop structure (Martin *et al.*, 1997). This 3' stem-loop is bound by stem-loop binding protein (SLBP) which activates translation (Ling *et al.*, 2002, Cakmakci *et al.*, 2008) by formation an alternative closed-loop that does not utilise PABP (Gorgoni *et al.*, 2005). This closed-loop results from a concomitant interaction of the SLBP-interacting protein 1 (SLIP1) with the SLBP bound to the 3'UTR and eIF4G bound to the 5'end (reviewed in (Marzluff *et al.*, 2008)).

Although these non-adenylated histone mRNAs represent unique cellular mRNAs, several viruses have mRNAs that lack a poly(A) tail. For instance, rotaviruses have capped non-adenylated mRNAs, which contain a 3'UTR element that is bound by non-structural protein 3 (NSP3) (Figure 1.14.). NSP3 interacts directly with eIF4G conferring a poly(A)-tail and PABP independent closed-loop confirmation (Vende *et al.*, 2000, Mazumder *et al.*, 2003). However, knockdown of

NSP3 does not abrogate viral mRNA translation, suggesting that they may also utilise an NSP3-independent translation mechanism (Montero *et al.*, 2006).

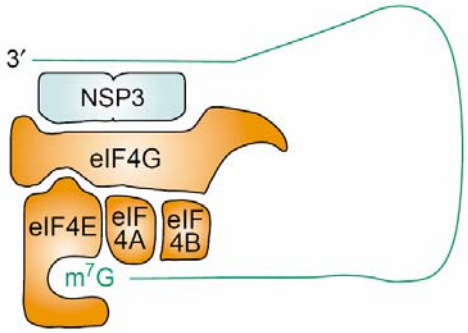


**Figure 1.14 - Poly(A)-independent rotavirus translation.** NSP3 binds an element at the 3'end and simultaneously binds the eIF4G promoting a closed loop conformation. From (Mazumder *et al.*, 2003)

Interestingly, translation of Dengue virus (DV) mRNA which also lack a poly(A)-tail still appears to require PABP, as their translation in cell-free extracts is sensitivity to PABP-interacting protein 2 (PAIP-2), a negative regulator that sequesters PABP (Polacek *et al.*, 2009a, Polacek *et al.*, 2009b). PABP was found to be recruited to these mRNAs via at least two PABP binding sequences located within its 3' UTR (Figure 1.15).

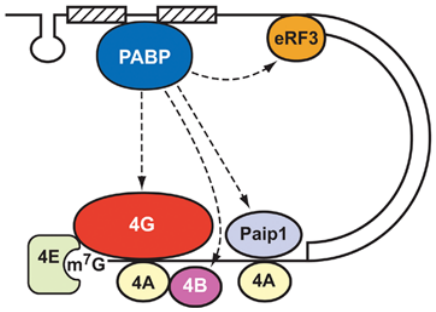


**Figure 1.15 - Dengue virus mRNA translation.** PABP binds specific 3' UTR elements (hatched boxes) within non-adenylated DV mRNAs, likely promoting translation in a manner analogous to poly(A)-bound PABP. Dotted arrows represent predicted protein-protein interactions. From (Smith and Gray, 2010).

### 1.2.4.4 3'UTR-mediated translational repression

Translation can also be regulated by 3'UTR-bound repressor proteins, many of which function in multi-protein complexes. For example, CPE-binding protein (CPEB) which promotes cytoplasmic polyadenylation can also mediate translational repression when in an appropriate context. In *X. laevis*, CPEB achieves this by

interacting with maskin, a eIF4E interacting protein that shares eIF4E-binding motifs with eIF4G and 4E-BPs. Analogous to 4E-BPs, the CPEB-maskin interaction inhibits the eIF4E-eIF4G interaction, repressing translation but only of the mRNAs to which they are bound via CPEB (Figure 1.16) (Stebbins-Boaz *et al.*, 1999, Richter and Sonenberg, 2005). mRNA-specific translational repression by proteins that bind eIF4E and block its interaction with eIF4G has also been described in invertebrates, e.g. *Drosophila* Cup which interacts with 3'UTR-bound Bruno to repress oskar mRNA (Figure 1.17) (Nakamura *et al.*, 2004) and in mammals e.g. CYFIP1 which interacts with FMRP to regulate target mRNAs (Napoli *et al.*, 2008). Assembly of the eIF4F complex at the cap is a key regulatory step and can also be targeted by proteins that directly interact with the cap rather than with eIF4E. For instance, *X. laevis* Pumilio-2 simultaneously interacts with the $m^7G$ cap and pumilio-binding elements (PBEs) in the 3'UTR of RINGO mRNA, inhibiting eIF4E binding to the cap (Cao *et al.*, 2010).

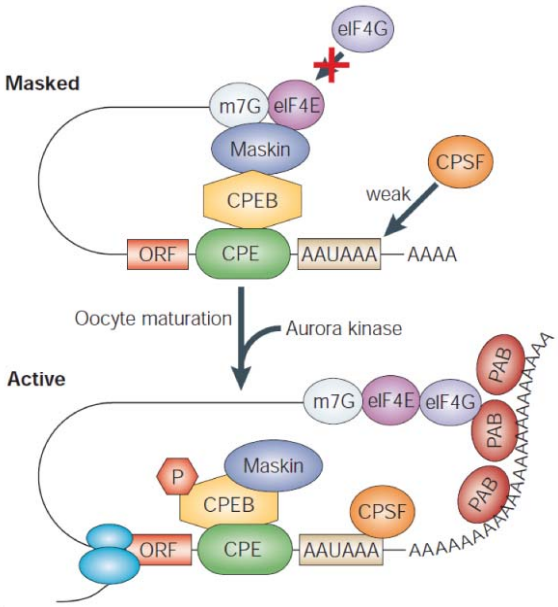


**Figure 1.16 - Maskin-mediated translation repression.** During *X. laevis* oocyte development, a subset of mRNAs containing CPEs can be translationally repressed by CPEB-maskin complexes, which compete with eIF4G for binding of eIF4E. Upon maturation, Aurora kinase 1 phosphorylates CPEB dissociating maskin from eIF4E and facilitating CPSF binding, which in turn recruits poly(A) polymerase resulting in polyadenylation. PABP binds the newly synthesised poly(A)-tail and eIF4G, which is bound to the newly liberated eIF4E. The formation of the closed-loop promotes 43S complex recruitment and translation initiation. From (Kuersten and Goodwin, 2003)

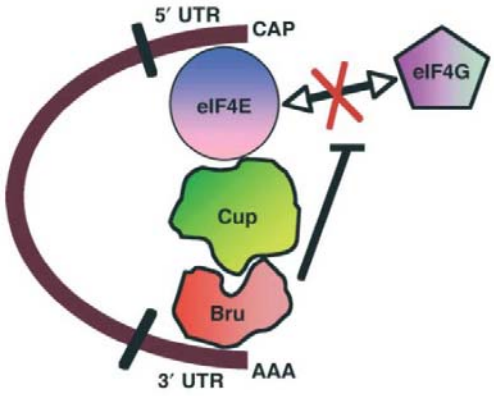


**Figure 1.17 - Translational repression of oskar by bruno.** Bruno interacts with specific elements in the oskar 3'UTR and with cup. By directly interacting with eIF4E, cup prevents eIF4G-binding. Inhibition of the eIF4E-eIF4G results in decreased translation. Brown curved line represents oskar mRNA. From (Dasgupta and Ladd, 2012).

#### 1.2.4.4.1 MicroRNA-mediated repression

3'UTR-mediated repression can also be achieved by the binding of microRNAs (miRNAs) as well as protein factors to the 3'UTR. miRNAs are small non-coding RNA molecules of approximately 22 nucleotides which inhibit translation and frequently also induce mRNA degradation. Bioinformatic approaches estimate that up to 60% of mammalian messages may be modulated by this mechanism (Friedman *et al.*, 2009) with most regulated mRNAs containing multiple miRNA-binding sites.

miRNAs associate with proteins to form functional miRNA-containing RNA-induced silencing complexes (miRISC). Many different models have been proposed for miRNA function, most focusing on translation initiation. These suggest that miRISC complexes disrupt cap binding by eIF4E (Humphreys *et al.*, 2005, Pillai *et al.*, 2005), or that TNRC6, a PABP-binding component of the RISC complex, disrupts PABP1-eIF4G interactions and/or induce deadenylation, since TNRC6 can also recruit deadenylases (this will be developed further in section 1.3.2.4) ((Walters *et al.*, 2010) reviewed in (Brook and Gray, 2012)). However, it has also been reported that miRNAs cause ribosomal dissociation during translation elongation (Petersen *et al.*, 2006).

### 1.2.4.5 5'- 3' end mediated regulation.

As previously mentioned, the same proteins can participate in different regulatory events. Their function on individual mRNAs depends on the position of their binding site within the mRNA and/or the protein partners with which they collaborate. This multi-functionality allows for the co-ordinated regulation of mRNAs. For instance, IRP (iron regulatory protein) can block 43S complex recruitment (Gray and Hentze, 1994) or scanning (Paraskeva *et al.*, 1999) depending on its position with the 5'UTR but can also regulate mRNA stability when bound to the 3'UTR. The latter is achieved by steric inhibition of an endonuclease cleavage site (Rouault, 2006, Wang and Pantopoulos, 2011). Thus IRP can simultaneously repress the translation of iron storage proteins (i.e. ferritin) and enhance the stability of mRNAs (e.g. transferrin receptor) that encode proteins which mediate cellular iron uptake (Figure 1.18). As the RNA-binding capacity of IRP is regulated by intracellular iron concentrations, this allows the maintenance of cellular iron homeostasis.

The 5' and 3'UTRs of the same mRNA can also be bound by the same RNA-binding protein to achieve regulation by distinct UTR-specific molecular mechanisms. This has been described for the regulation of *Drosophila* male-specific lethal-2 (msl-2) which functions in X-chromosome dosage compensation in males (Bashaw and Baker, 1997). In females, msl-2 is not expressed due to the action of a female specific RNA-binding protein sex-lethal (SXL) (Kelley *et al.*, 1997). When bound to the 3'UTR of msl-2 mRNA, SXL collaborates with a co-repressor UNR (upstream of N-ras) to inhibit 43S recruitment (Figure 1.19) (Duncan *et al.*, 2009). However, SXL also binds to the 5' UTR of msl-2, where it blocks the scanning of any 43S complexes that have escaped the 43S-binding block (Beckmann *et al.*, 2005, Duncan *et al.*, 2006, Duncan *et al.*, 2009). Together these two regulatory mechanisms act as a "fail-safe" to prevent toxic expression of msl-2 in female cells.

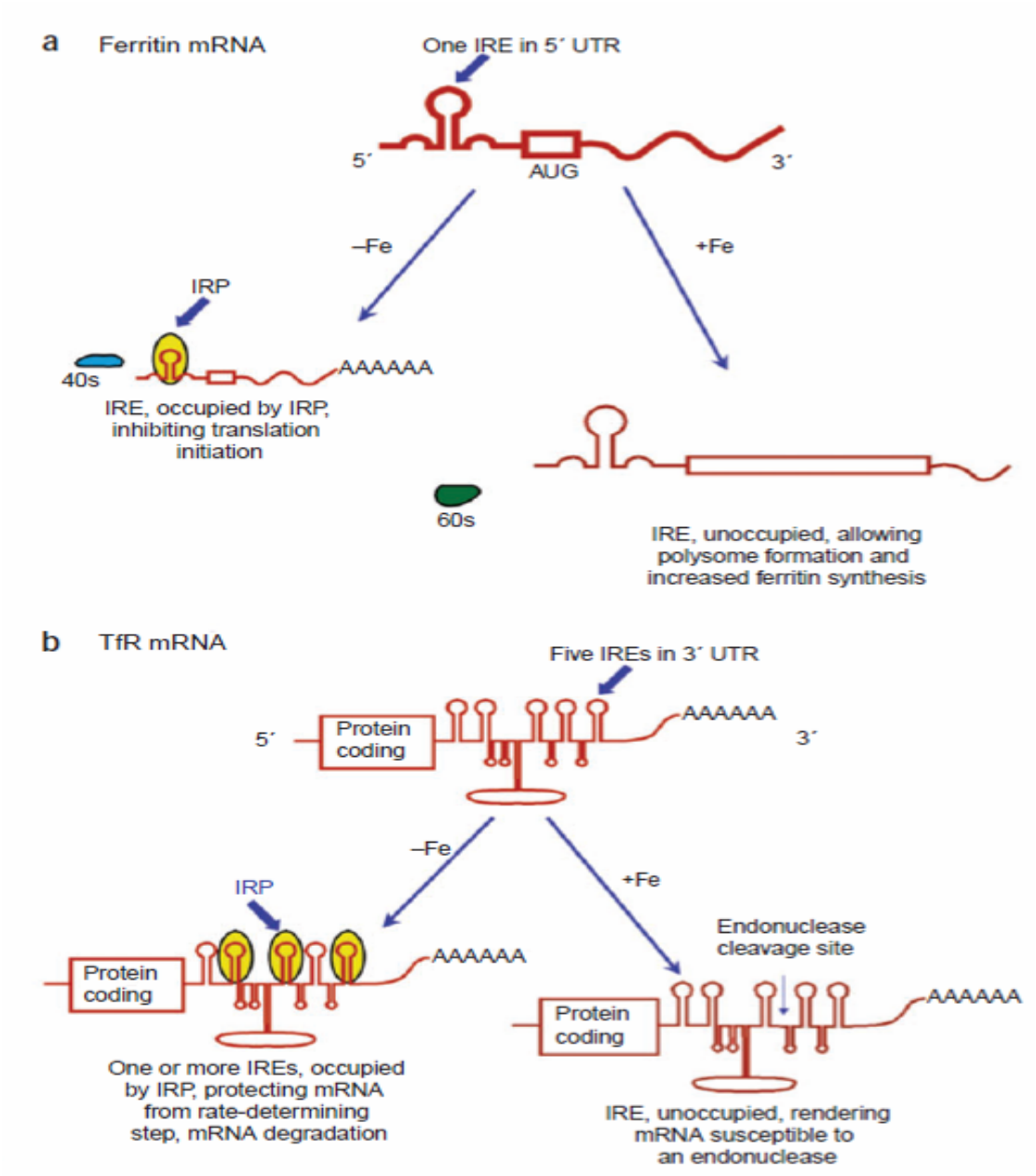


**Figure 1.18 - IRP function is regulated by the location of its binding sites.** Iron regulatory proteins (IRPs), modulate cellular iron homeostasis. Ferritin mRNA contains IRP binding sites, known as iron responsive elements (IREs) within its 5' UTR, whilst transferring receptor (TfR) mRNA contains multiple IREs within its 3' UTR. Binding of IRP to these mRNAs results translational repression and protection from endonucleases action, respectively. From (Rouault, 2006).

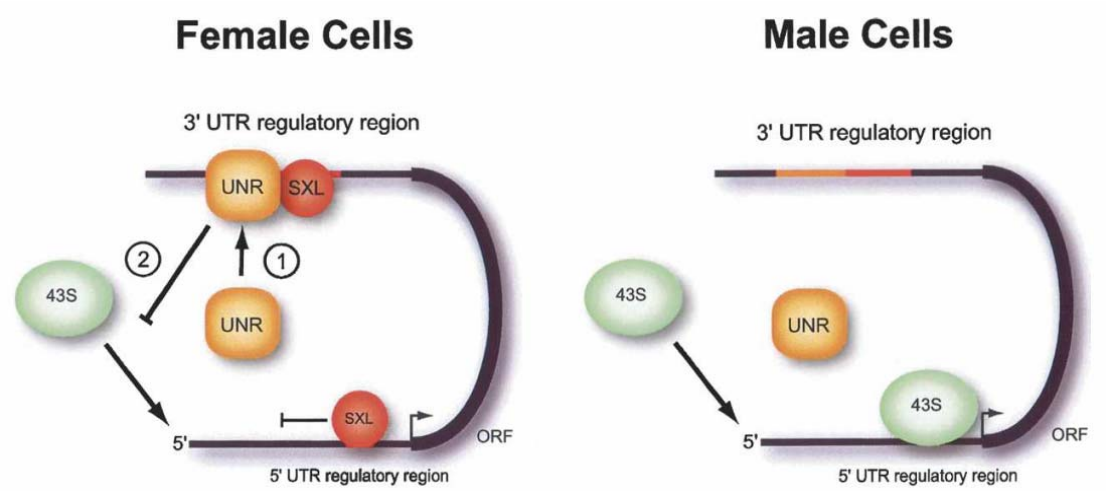


**Figure 1.19 - Male specific lethal 2 mRNA (msl-2) translational repression by sex-lethal protein (SXL).** In female *Drosophila* cells, SXL recruits UNR to the 3'UTR of msl-2 mRNA (1), which represses 43S recruitment (2). SXL also binds the 5' UTR of msl-2 RNA and blocks 43S scanning. From (Duncan *et al.*, 2006)

### 1.2.5 mRNA stability and localisation are often intimately linked to mRNA translation

mRNA translation and turnover are often intimately linked. In part this results from the closed-loop conformation that promotes initiation also protecting the ends of the mRNA from deadenylases (i.e. PAN2/3, CCR4-NOT and PARN) and decapping (i.e. DCP1/DCP2), events which precede the degradation of the mRNA body (Figure 1.20). Thus translational repression frequently results in reduced mRNA stability as the ends become more accessible to these activities (Schwartz and Parker, 2000). However, their relationships are complex and extend far beyond this correlation. For instance, active translation can disrupt mRNP complexes that stabilise specific mRNAs leading to their turnover (Grosset *et al.*, 2000) and limiting their lifetime.

Translation and mRNA localisation can also be intimately linked. This allows for the localised synthesis of proteins that need to be spatially regulated. Thus, mechanisms have evolved to repress the translation of mRNAs, avoiding mis-localised protein expression, and to activate their efficient translation when localised at specific sites. For instance, early embryonic development in *Drosophila* requires protein gradients of oskar (osk), gurken (grk), nanos (nos) and bicoid (bcd) for the

formation of anterior-posterior and dorsal-ventral axes (Gavis *et al.*, 2007). These mRNAs are synthesised during oogenesis and are transported to specific localisations within the oocyte and are only activated later in development. The localisation and translational repression and activation of these mRNAs are regulated by a variety of mRNP complexes. For instance, osk mRNA translation is repressed by Cup-Bruno (Figure 1.17) (Nakamura *et al.*, 2004), with Cup also participating in its transport by inducing its oligomerisation (Chekulaeva *et al.*, 2006).

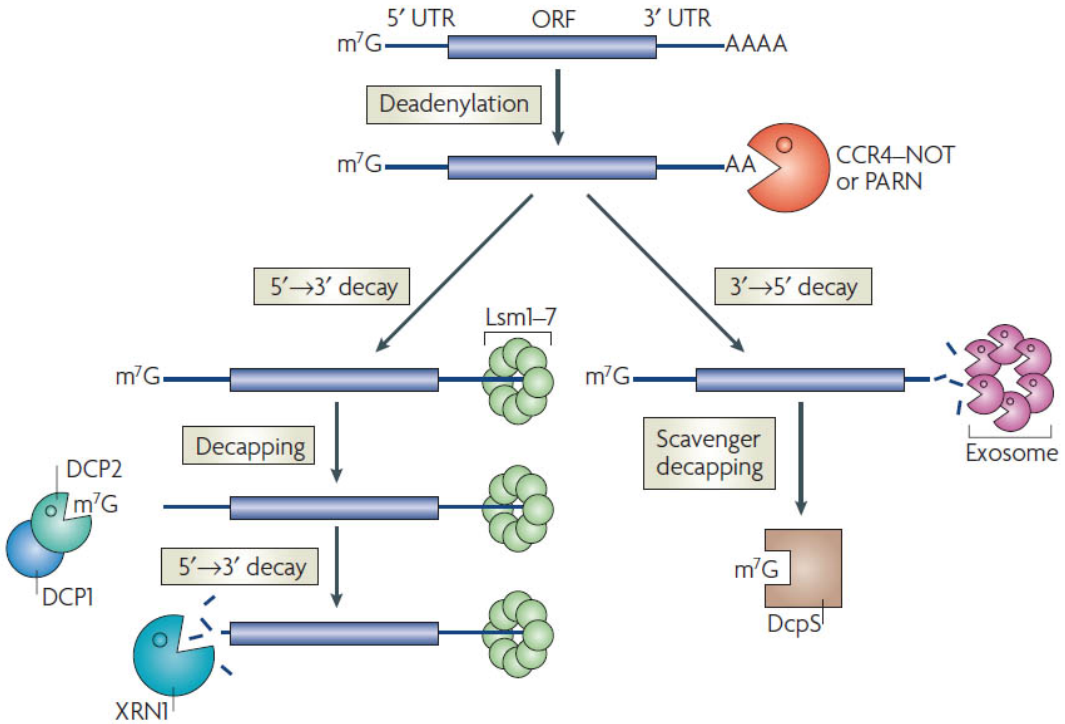


**Figure 1.20 - Deadenylation is an initial and rate limiting step in mRNA degradation.** Following PAN2/3 (not shown), CCR4-NOT or PARN deadenylation, mRNAs undergo decapping and then 5' to 3' degradation promoted by Xrn1 or 3 to 5' degradation by exosome activity. Lsm1-7 promotes mRNA degradation from 3' to 5'. (Garneau *et al.*, 2007).

## 1.3 Poly(A) binding proteins (PABPs)

The poly(A)-tail is a primary determinant of translational efficiency and is bound by poly(A)-binding proteins (PABPs), which were first described in mouse L cells and rat hepatocytes (Blobel, 1973). Subsequent work has shown the important role of PABPs in driving translation initiation from yeast to mammals (reviewed in (Mangus *et al.*, 2003, Gorgoni and Gray, 2004). Moreover, tethering experiments using unadenylated reporter mRNAs established that PABPs can functionally replace the poly(A)-tail, indicating that they merely serves as a scaffold for PABP-binding (Gray *et al.*, 2000), although poly(A)-binding *per se* is thought to enhance PABP function in some species (Tarun and Sachs, 1996, Le *et al.*, 1997, Wei *et al.*, 1998). PABPs also have complex roles in basal and regulated mRNA turnover, which are outside the scope of this thesis, but are discussed briefly in section 1.3.2.4 and have been reviewed in detail recently (Brook and Gray, 2012). Whilst *S. cerevisiae* encodes only a single PABP (Pab-1), vertebrates encode three cytoplasmic PABPs (PABP1, PABP4 and ePABP) with two further homologues (tPABP and PABP5) being present in mammals (Figure 1.21). Most species also encode a nuclear PABP protein (PABPN1) which bears little sequence resemblance to cytoplasmic PABPs and vertebrates also possess ePABP2, which is most closely related to PABPN1 but appears predominantly cytoplasmic in mouse and *X. laevis* oocytes and in *X. laevis* early embryos (Cosson *et al.*, 2004, Good *et al.*, 2004). The categorisation of the PABP family members is based on structural similarities, sub-cellular distribution and function, although both cytoplasmic PABPs and nuclear PABP shuttle (Afonina *et al.*, 1998, Calado *et al.*, 2000, Burgess *et al.*, 2011). As the function of nuclear PABP, and most likely ePABP2, are distinct from those of the cytoplasmic PABPs these proteins will not be discussed further, although a nuclear PABP homologue in Drosophila has been reported to modulate polyadenylation of oskar and cyclin B mRNAs in the cytoplasm (Benoit *et al.*, 2005) (reviewed in (Gorgoni and Gray, 2004).

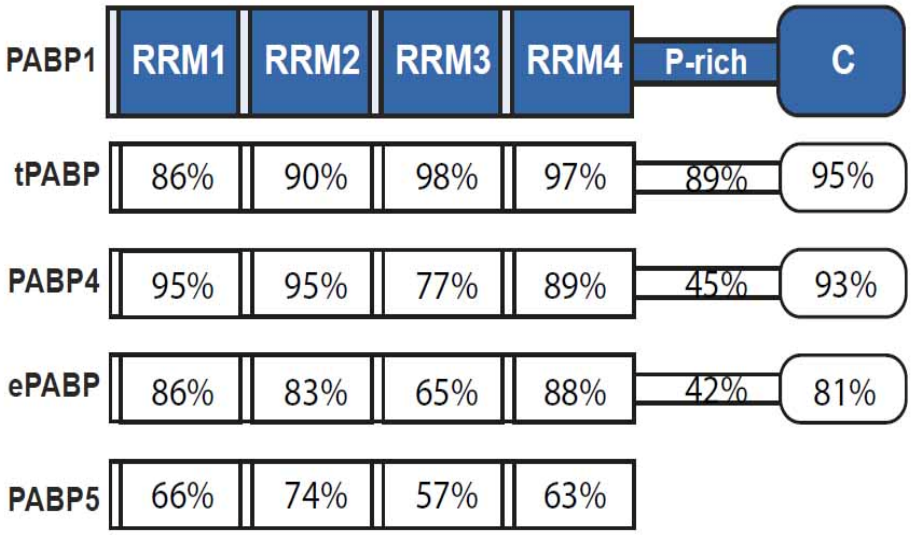


**Figure 1.21 - Human cytoplasmic poly(A) binding proteins.** PABP1 (also known as PABPC1), tPABP (PABPC2/PABPC3), PABP4 (iPABP, PABPC4) and ePABP (ePAB, PABP1L) share a common domain organisation with four non-identical RNA recognition motifs (RRMs) and a globular C-terminal domain (PABC), linked by an unstructured proline-rich region (P-rich). PABP5 lacks the proline rich-region and the PABC domain. PABP1, tPABP, PABP4 and ePABP have predicted molecular weights of 70 kDa and PABP5 of 43 kDa. Percentage identity for each functional domain is shown; PABP4-002 and ePABP PABPC1L-201 isoforms were used for homology comparison. Adapted from (Burgess and Gray, 2010).

### 1.3.1 PABP domain organisation

Cytoplasmic PABPs have four N-terminal non-identical RNA recognition motifs (RRM) and with the exception of PABP5, a globular PABC domain at the C-terminus, connected to the RRMs by a highly variable proline-rich region (Figure 1.21) (Blanco *et al.*, 2001, Kuhn and Wahle, 2004). Analysis of the domains of PABP1 has shown that the RRMs can bind both RNA and protein, with the structure of RRMs 1-2 bound to poly(A) showing how the other face is available for protein-protein interactions (Deo *et al.*, 1999). The C-terminal region (Ct) is comprised of a proline-rich region and the PABC domain. The PABC domain of PABP1 mediates multiple protein-protein interactions including those with proteins that contain a PABP-interacting motif 2 (PAM2) (Kozlov *et al.*, 2001, Roy *et al.*, 2002, Albrecht and Lengauer, 2004). The proline-rich region is the least conserved between PABPs

but contributes to the ability of PABP1 to self associate, which is important for ordered high affinity binding to poly(A) (Kuhn and Pieler, 1996, Melo *et al.*, 2003).

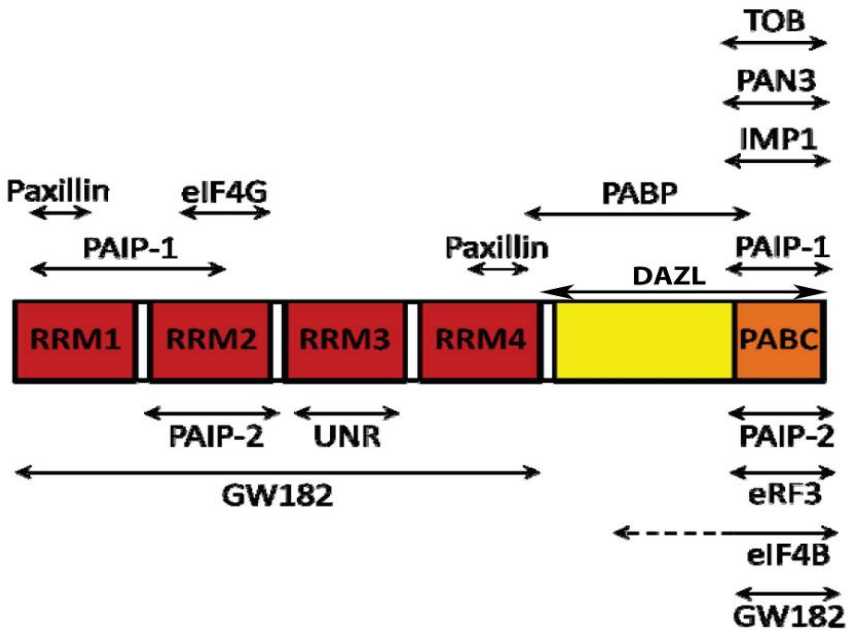


**Figure 1.22 - PABP1 interacting proteins.** The prototypical PABP, PABP1 has been demonstrated to have multiple protein partners. Interactions: TOB (Ezzeddine *et al.*, 2007); PAN (Siddiqui *et al.*, 2007); IMP1 (Patel and Bag, 2006); PABP (Melo *et al.*, 2003); eIF4G (Imataka *et al.*, 1998); Paxillin (Woods *et al.*, 2005); DAZL (Collier *et al.*, 2005b); UNR (Chang *et al.*, 2004); eIF4B (Bushell *et al.*, 2001); eRF3 (Cosson *et al.*, 2002a); PAIP-1 (Roy *et al.*, 2002); PAIP-2 (Khaleghpour *et al.*, 2001); GW182 (Zekri *et al.*, 2009, Jinek *et al.*, 2010). Lines represent the currently defined minimal binding sites. The N-terminal border of the eIF4B binding site remains unknown. Adapted from (Anderson, 2010). The references given are those describing the first report of a particular interaction.

## 1.3.2 PABP1

PABP1 (PABPC1, PABP, PAB), the prototypical PABP, is conserved across eukaryotes (Table 1.2) and is by far the best characterised family member. As a result it is often generically referred to as PABP, with many authors not taking account of additional family members that may also be present in their assays. PABP1 is essential in *Saccharomyces cerevisiae* (*S. cerevisiae*), *Drosophila melanogaster* (Drosophila) and in *X. laevis* (Sachs *et al.*, 1987, Sigrist *et al.*, 2000, Gorgoni *et al.*, 2011). It is a multi-functional protein with roles in translation initiation, positive and negative translational regulation of specific mRNAs, miRNA

mediated regulation, global and mRNA specific regulation of mRNA turnover/stability and nonsense-mediated decay. Consistent with this multi-functionality PABP1 has a plethora of protein partners (Figure 1.22).

| Organism | PABPs | PABP1 homology with hPABP1 |
|---|---|---|
| *Saccharomyces cerevisiae* | Pab1p | 46% |
| *Drosophila melanogaster* | pAbp | 58% |
| *Caenorhabditis elegans* | Pab-1, Pab-2 | 52% |
| *Xenopus laevis* | PABP1,ePABP, PABP4 | 93% |
| *Mus musculus* | Pabp1, tPabp, ePabp, Pabp4, Pabp5 | 99% |
| *Homo sapiens* | PABP1, tPABP, ePABP, PABP4, PABP5 | - |

**Table 1.2 - Cytoplasmic PABPs are conserved in eukaryotes.** PABP proteins are conserved throughout eukaryotes. The percentage identity of PABP1 proteins from different species to human PABP1 (hPABP1) is given.

#### 1.3.2.1 PABP1 mRNA poly(A) binding activity

PABP1 performs most of its functions bound to the poly(A)-tail, but can also bind to poly(U) and poly(G) substrates but to a lesser extent (Nietfeld *et al.*, 1990, Gorlach *et al.*, 1994, Kuhn and Pieler, 1996, Deardorff and Sachs, 1997, Sladic *et al.*, 2004). RNA-binding is conferred by the RRMs with two RRMs binding more efficiently than one (Burd *et al.*, 1991, Kuhn and Pieler, 1996).

Poly(A)-binding is achieved by RRMs 1-2 which require a minimum of 10-12 adenosines to bind (Sachs *et al.*, 1986, Burd *et al.*, 1991, Kuhn and Pieler, 1996, Deo *et al.*, 1999). RRMs 3-4 also have some affinity for poly(A), with mutagenesis experiments suggesting that these regions also contribute to poly(A) binding (Deardorff and Sachs, 1997). However, the specificity of RRMs 3-4 is less clear but it has been suggested that they may mediate binding to A-U rich sequences (Burd *et al.*, 1991, Kuhn and Pieler, 1996, Sladic *et al.*, 2004).

PABP1 has been shown to bind poly(A) in an ordered repeated manner, with multiple PABP1s oligomerising along the same mRNA poly(A)-tail (Baer and Kornberg, 1983, Gorlach *et al.*, 1994, Kuhn and Pieler, 1996). This is promoted by

PABP1 ability to self-associate, and leads to cooperative high affinity binding (Kuhn and Pieler, 1996, Melo *et al.*, 2003). PABP1 self-association is dependent on the proline rich linker region, since it has been demonstrated *in vitro* that the C-terminal region, but not PABC domain, is required for this function (Melo *et al.*, 2003).

PABP1 has also been shown to bind mRNAs independent of the poly(A)-tail. This mRNA-specific binding will be discussed in the relevant sections (see 1.2.4.3, 1.3.2.3, 1.3.2.4)

#### 1.3.2.2 Stimulation of translation initiation by PABP1

The best characterised function of PABP1 is its basal role in stimulating translation initiation when bound to the poly(A)-tail. An important insight into how PABP1 achieves this function came from the observation that yeast Pab-1 interacts with eIF4G (Tarun and Sachs, 1996)**.** This led to a model in which the simultaneous interaction of eIF4G with poly(A)-bound PABP and cap-bound eIF4E brings the ends of mRNAs into functional proximity by inducing a closed-loop conformation (Figure 1.23). Such functional interactions between the cap and the poly(A) tail would account for their synergistic effects on translation (Gallie, 1991, Tarun and Sachs, 1995, Michel *et al.*, 2000).

In support of this hypothesis, mutations that disrupt the Pab-1-eIF4G interaction inhibit translation (Tarun and Sachs, 1996, Amrani *et al.*, 2008) and atomic force microscopy showed that purified recombinant eIF4G, eIF4E and Pab-1 bound to RNA can form a diamond ring like structure (Wells *et al.*, 1998), where the multi-protein complex bound to the mRNA ends is the diamond and the looped out RNA, the ring. Subsequent work has shown that this interaction is highly conserved being present in plants (Le *et al.*, 1997), vertebrates e.g. *X. laevis* (Gray *et al.*, 2000) and mammals e.g. humans (Imataka *et al.*, 1998).

Although the closed-loop model is central to models of translational regulation by 3'UTR-binding proteins, an understanding of how PABP stimulates initiation is still incomplete, although analysis of initiation intermediates has shown that it mainly acts by enhancing small ribosomal subunit recruitment (Tarun and Sachs, 1995).

Insights into how the PABP1-eIF4G interaction may enhance small subunit joining have predominantly come from studies in cell-free translation systems from a variety of organisms. Studies of plant PABP showed that interaction with eIF4G, increased the affinity of PABP for poly(A) (Le *et al.*, 1997) and eIF4E for the cap (Wei *et al.*, 1998). Effects of mammalian PABP1 on cap binding have subsequently been observed (Borman *et al.*, 2000). Recently, efficient eIF4E binding to the cap was shown to be dependent on eIF4G binding to RNA (Yanagiya *et al.*, 2009), providing a potential explanation for how the PABP-eIF4G interaction may enhance cap-binding. However, a demonstration that PABP-eIF4G interactions actually enhance the binding of eIF4G to RNA is still required.

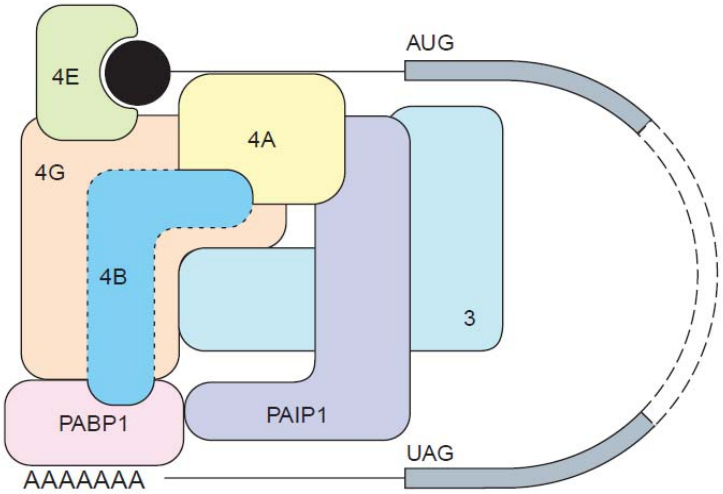


**Figure 1.23 - Simplified "closed-loop" model showing how PABP stimulates translation initiation by bringing together the 5' and 3'UTRs.** Interaction of PABP1 with eIF4G which also binds eIF4E brings the ends of the mRNA into functional proximity. Additional interactions of PABP1 with Paip1, and perhaps eIF4B (shown with a dotted outline), further stabilise this closed-loop conformation, which is proposed to enhance PABP, eIF4G and eIF4E-binding, increasing the recruitment of 43S PIC complexes (not shown). From (Brook *et al.*, 2009)

However, it is clear that PABP-eIF4G interactions are not able to fully account for the effects of PABP1 on initiation (Gray *et al.*, 2000, Kahvejian *et al.*, 2005) Indeed, multiple additional interactions, including those of PABP1 with other factors, appear to stabilise the closed-loop conformation (Figure 1.23, see also Figure 1.22

for a summary of protein binding sites within PABP). For instance, PABP1 in vertebrates interacts with the positive effector of translation, poly(A)-interacting protein (PAIP) 1 (Craig *et al.*, 1998, Gray *et al.*, 2000), which also interacts with eIF4A and eIF3 (Craig *et al.*, 1998, Martineau *et al.*, 2008). PABP1 can also interact with eIF4B (Le *et al.*, 1997, Bushell *et al.*, 2001), although functional evidence for a role of this interaction has only been presented in plants. In plants, the interaction of PABP with eIF4B and eIF4G (both of which enhance eIF4A action), has a positive effect on the ATPase and RNA helicase activity of eIF4A-eIF4B-eIF4G complexes. eIF4A mediates the unwinding of secondary structures within the 5'UTR (Bi and Goss, 2000) and thus these interactions should enhance small subunit recruitment, similar to increased recruitment of the cap-binding complex.

PABP1 has also been suggested to enhance steps downstream of small ribosomal subunit recruitment, as depleting PABP1 in Kreb-2 cell extracts decreases both 48S and 80S complex formation (Kahvejian *et al.*, 2005). An involvement of PABP1 in 60S recruitment was also inferred from early experiments examining the formation of initiation complexes on polyadenylated and unadenylated mRNAs (Munroe and Jacobson, 1990). However, the mechanism by which PABP1 affects 60S joining this effect remains unknown.

Moreover, interaction of PABP1 with a translation termination factor (eRF) 3 (Hoshino *et al.*, 1999, Cosson *et al.*, 2002a, Cosson *et al.*, 2002b, Uchida *et al.*, 2002) has also been suggested to enhance translation by promoting efficient termination, allowing ribosomal subunits to be recycled for new rounds of translation (Uchida *et al.*, 2002). This interaction is also important in PABPs role in nonsense-mediated decay and may serve to link mRNA translation and deadenylation mRNA turnover, as discussed in section 1.2.9 (Hosoda *et al.*, 2003, Singh *et al.*, 2008)

#### 1.3.2.3 Role of PABP1 in mRNA-specific translational activation

PABP has been implicated in the translation of unadenylated viral mRNAs (Figure 1.15) but also in relieving repression of a specific cellular mRNA to promote its translation. Y-box-binding protein 1 (YB-1) is a multi-function RNA-binding

protein that regulates global translation but also represses its own translation by binding to an element within its 3'UTR (Skabkina *et al.*, 2005). PABP also binds to this 3'UTR and depletion of PABP or removal of the 3'UTR sequence required to bind PABP ablates the repression of an YB-1 reporter. Similarly, titration of PABP overcomes YB-1 mediated repression (Figure 1.24). PABP1 was found to interact with a poly(A) stretch that overlaps the YB-1 binding site and to compete YB-1 binding to this 3'UTR, suggesting that it relieves YB-1 repression by interfering with YB-1 binding (Skabkina *et al.*, 2003, Lyabin *et al.*, 2011). PABP also has a more direct role in mRNA-specific translational activation by the cellular protein DAZL that will be discussed in section 1.4.4.1.

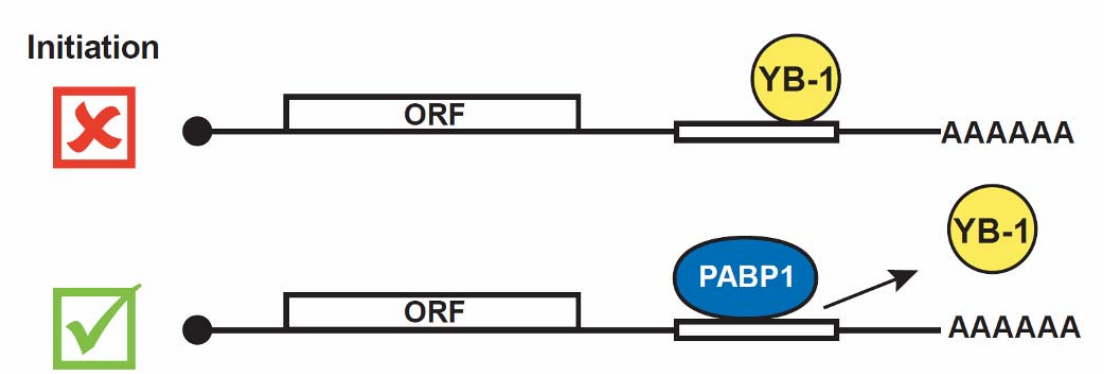


**Figure 1.24 - YB-1 mRNA translation regulation.** PABP1 and YB-1 compete for overlapping binding sites in the 3'UTR of YB-1 mRNA. Binding by YB-1 repress translation. This is blocked by binding of PABP1 allowing translation. From (Burgess and Gray, 2010)

### 1.3.2.4 Other functions of PABP1

As highlighted already in sections 1.2.4.3 (DV translation - Figure 1.15) and 1.4.2.3 (YB-1 translation - Figure 1.24) PABP has mRNA specific roles in translation, with additional examples being discussed in sections 1.4.2.5 (auto-regulation) and 1.4.4.1 (Dazl-mediated translation).

As introduced in section 1.2.4.4.1, the miRISC complex also interacts with PABP1. The interaction between PABP1 and GW182 (TNRC6) is required for miRNA directed translational silencing and turnover (Figure 1.25). This interaction may compete with the PABP1-eIF4G interaction (see Figure 1.22 for binding site) to inhibit the closed loop conformation repressing translation and thereby making the

poly(A) tail more susceptible to deadenylase action (Figure 1.20) (Zekri *et al.*, 2009). Alternatively, it may bring GW182-bound deadenylases into the proximity of the poly(A).


**Figure 1.25 - Regulation by miRNA requires PABP1.** Argonaute (Ago) recruits GW182. GW182 interacts with PABP1 and may inhibit, by competitive binding, its interaction with eIF4G (4G), breaking the closed-loop and weakening its interaction with the poly(A)-tail allowing access of deadenylases. The GW182-PABP1 interaction may also serve to bring GW182 bound-deadenylases into proximity with the poly(A) tail. From (Burgess and Gray, 2010)

In addition to regulating translation, PABP1 has a number of additional and often related roles in regulating mRNA turnover and quality. Firstly, PABP1 protects messages from degradation: reporter mRNAs are turned over ten times faster in cell-free extracts lacking PABP1 (Bernstein *et al.*, 1989). This effect is due to PABP1 precluding the access of deadenylases to the poly(A)-tail (reviewed in (Mangus *et al.*, 2003)). Deadenylation is the initial and main rate limiting step in mRNA turnover (Figure 1.20). Moreover, PABP1 is also thought to inhibit decapping by the stabilising the closed-loop conformation maintaining eIF4E on the cap (Gorgoni and Gray, 2004, Kuhn and Wahle, 2004, Brook and Gray, 2012).

Paradoxically PABP1 can also recruit two deadenylation complexes, Caf1-CCR4 indirectly via TOBs (transducer of ErbB2) and PAN2-PAN3 (Funakoshi *et al.*, 2007, Siddiqui *et al.*, 2007) and stimulate deadenylation (Uchida *et al.*, 2004, Funakoshi *et al.*, 2007). These opposing functions in protecting from and stimulating deadenylases may be coordinated by mutually exclusive interactions of the PABC domain with eRF3, TOB1/2 and PAN3, with eRF3 preventing interaction with the

deadenylases until translation termination. In addition to this global role in controlling mRNA turnover, PABP1 also functions mRNA-specifically. For instance, it protects α-globin mRNA from endonucleolytic cleavage (Wang and Kiledjian, 2000) and is part of a multi-protein complex that directs translationally coupled deadenylation of c-fos mRNA (Chang *et al.*, 2004).

Nonsense-mediated decay (NMD) induces degradation of mRNAs with premature termination codons (PTCs) (reviewed in (Brook and Gray, 2012). Selection of mRNAs for NMD is believed to be, in part, the result of competitive binding between PABP1 and the NMD machinery component UPF1 (up-stream frame shift 1) for eRF3 which distinguishes between "normal" and "premature" termination (Ivanov *et al.*, 2008, Singh *et al.*, 2008). At a natural stop codon PABP1 interacts with eRF3 to induce efficient termination, at a PTC the absence of this interaction allows UPF1 to interact with eRF3 and recruit further NMD factors including endonucleases ((Singh *et al.*, 2008) reviewed in (Schoenberg and Maquat, 2012)).

#### 1.3.2.5 PABP1 Expression

Despite the extensive work on PABP1 function, virtually nothing is known about its expression pattern. However, poly(A)-tails are an almost universal feature of eukaryotic mRNAs, Pab-1 is essential in yeast and PABP1 appears to be present in all characterised mammalian cell lines (Burgess *et al.*, 2011). This led to a widely held belief that PABP1 is ubiquitously expressed. In keeping with this idea, PABP1 mRNA is present but to varying extents in all mice and human tissues analysed by Northern blotting (Kleene *et al.*, 1994, Yang *et al.*, 1995, Feral *et al.*, 2001).

RNA analysis of enriched germ cell populations from dissociated mouse testes, revealed that PABP1 mRNAs was abundant in pachytene spermatocytes and round but not elongating spermatids (Kleene *et al.*, 1994). RNA expression in these cell types was confirmed by *in situ* hybridisation of human testes (Feral *et al.*, 2001). However, extrapolation from mRNA to protein expression is complicated by the tight regulation of PABP1 mRNA by at least two 5' UTR independent mechanisms: via an A-rich auto-regulatory sequence (ARS) (Figure 1.26) (de Melo Neto *et al.*, 1995) and a terminal oligopyrimidine tract (TOP) motif (Hornstein *et al.*, 1999).

Consistent with this, western blotting of multiple mouse tissues revealed that PABP1 was undetectable in a number of tissues (Hannah Burgess, personal communication.) which had been shown to contain significant levels of PABP1 mRNA (Yang *et al.*, 1995). Taken together these findings suggest that PABP1 may not be ubiquitously expressed and emphasises the importance of measuring protein rather than RNA levels.

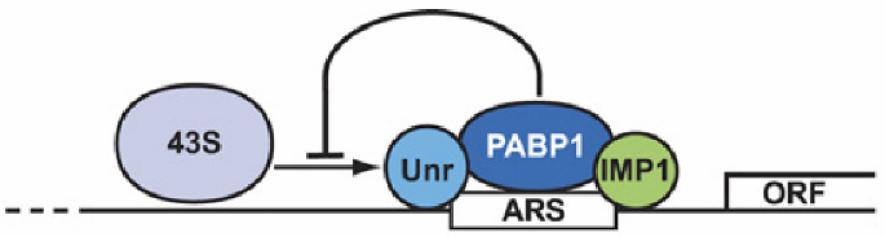


**Figure 1.26 - PABP1 auto-regulation.** PABP1 binds its own 5'UTR at an A-rich auto-regulatory sequence (ARS) as a complex with URN and IMP1. This inhibits PABP1 translation most likely by blocking 43S complex scanning. From (Burgess and Gray, 2010).

## 1.3.3 Other PABP family members

Higher eukaryotes express multiple PABP family members that share an identical domain structure and considerable protein sequence identity (Figure 1.21 and Table 1.3). With the exception of PABP5, which has a variant domain structure, all the other PABPs have been shown to bind poly(A) (Kleene *et al.*, 1994, Yang *et al.*, 1995, Feral *et al.*, 2001, Voeltz *et al.*, 2001), suggesting they may share at least some of the functions of PABP1.

| | tPABP | ePABP | PABP4 | PABP5 |
|---|---|---|---|---|
| PABP1 | 92 % | 69 % | 75 % | 62 % |
| tPABP | | 65 % | 70 % | 59 % |
| ePABP | | | 65 % | 56 % |
| PABP4 | | | | 63 % |

**Table 1.3 - Percentage identity between human PABP family members.** PABP5 homology was analysed only against the conserved RRMs since this lacks the proline-rich region and the PABC domain. ePABP - PABPC1L-001; PABP4 – PABP4.002.

In *C. elegans,* which encodes two PABPs, RNA interference (RNAi) of Pab-1 and Pab-2 result in high and low penetrance sterility respectively (Maciejowski *et al.*, 2005). Since depletion of both Pab-1 and Pab-2 results in additional soma defects, this suggests that they function redundantly in soma but have a specific germline requirement for Pab-1 (Ciosk *et al.*, 2004). In vertebrates morpholino knockdown in *X. laevis* embryos showed that PABP1, ePABP and PABP4 are all important for development, since their individual ablation resulted in lethality at different stages (Gorgoni *et al.*, 2011). Cross-rescue experiments with expression constructs with identical 5' and 3'UTRs to achieve identical expression showed that neither ePABP nor PABP4 are able to fully rescue the PABP1 phenotype revealing that they are not functionally equivalent (Gorgoni *et al.*, 2011). Since this study also showed that they share a similar mechanistic role in promoting global translation, this suggested that these PABPs may have distinct functions in mRNA-specific translation or mRNA decay(Gorgoni *et al.*, 2011). C-terminal domain swaps showed that some of these distinct functions must be mediated by protein-protein interactions (Gorgoni *et al.*, 2011), most likely those associated with the variable proline-rich region.

#### 1.3.3.1 Testis PABP (tPABP)

Testis PABP (tPABP, Pabpc2 in mice and PABPc3in humans) shares a high degree of identity with PABP1 (92%) is intron-less and believed to have originated from a PABP1 retro-transposition event in mammals (Kleene *et al.*, 1998). Its mRNA appears restricted to testes in mouse being present in late pachytene spermatids and increasing in haploid round spermatids (Kleene *et al.*, 1994) where it is also detected in human testes (Feral *et al.*, 2001). Recently, immunofluorescence using tPABP-specific antibodies confirmed the presence of tPABP in haploid spermatids (Kimura *et al.*, 2009). In keeping with this, analysis of testis extracts during the first wave of spermatogenesis suggested that appearance of tPABP mRNA and protein coincides with the first spermatids at day 18 dpp (Kimura *et al.*, 2009).

The function of tPABP has not been extensively characterised but the high degree of homology between both proteins suggests that tPABP is likely to retain PABP1 functions. Consistent with this, human tPABP binds poly(A) with the similar affinity as PABP1 (Feral *et al.*, 2001), can modestly stimulate translation of reporter

mRNAs in non poly(A)-dependent rabbit reticulocyte lysates (RRL) (Kimura *et al.*, 2009), and can interact *in vitro* with the PABP1 interacting proteins eIF4G, PAIP1 and PAIP2 (Kimura *et al.*, 2009). Intriguingly however, unlike PABP1, tPABP is not well represented in the polyribosome fractions of testicular extracts and appears to be present within distinct cytoplasmic foci in round spermatids which have been suggested to be chromatoid bodies (Kimura *et al.*, 2009). These latter observations indicate that tPABP may have a different role in mRNA regulation to that of PABP1, despite their similarities.

#### 1.3.3.2 Embryonic PABP (ePABP)

Embryonic PABP (ePABP, ePAB) was initially identified in *X. laevis* as the predominant PABP present during the later stages of oogenesis and early embryogenesis, where it essentially replaces PABP1 (Voeltz *et al.*, 2001, Cosson *et al.*, 2002c, Wilkie *et al.*, 2005). Consistent with this, ePABP is critical for both *X. laevis* oocyte maturation (Friend *et al.*, 2012) and early development (Gorgoni *et al.*, 2011). ePABP mRNA shows a similarly restricted pattern in mouse (Seli *et al.*, 2005, Wilkie *et al.*, 2005, Guzeloglu-Kayisli *et al.*, 2012) where it is also essential for oocyte maturation (Seli *et al.*, 2005, Guzeloglu-Kayisli *et al.*, 2012) but has slighter wider distribution in humans (Guzeloglu-Kayisli *et al.*, 2008).

Analysed aspects of ePABP function appear to highly resemble that of PABP1. ePABP has been shown to bind poly(A) (Cosson *et al.*, 2002c, Gorgoni *et al.*, 2011) and to stimulate translation to a similar level as PABP1 in tethering assays in *X. laevis* oocytes (Wilkie *et al.*, 2005). Their mechanisms of action may also be similar as ePABP interacts with eIF4G, PAIP2, eRF3, PAIP1 (Wilkie *et al.*, 2005, Kim and Richter, 2007, Gorgoni *et al.*, 2011) and the cap complex (Cosson *et al.*, 2002c). *X. laevis* ePABP has also been shown to protect mRNA from deadenylation and both mouse and *X. laevis* ePABP can promote cytoplasmic polyadenylation (Seli *et al.*, 2005, Kim and Richter, 2006, Friend *et al.*, 2012, Guzeloglu-Kayisli *et al.*, 2012). However, despite these similarities, ePABP is unable to fully rescue PABP1 phenotypes in *X laevis* embryos, indicating that these proteins are not functionally redundant (Gorgoni *et al.*, 2011).

#### 1.3.3.3 PABP4

PABP4 (PABPC4) was firstly described in 1995 under the name of inducible PABP (iPABP) since it was described as an mRNA that could be upregulated in activated human T-cells (Yang *et al.*, 1995). Like PABP1, PABP4 mRNA appears to be present at different levels in a range of human tissues (Yang *et al.*, 1995).

Human PABP4 has been shown to bind poly(A) (Yang *et al.*, 1995, Houng *et al.*, 1997), although with lower affinity than PABP1 (Sladic *et al.*, 2004), a property that is shared with *X. laevis* PABP4 (Gorgoni *et al.*, 2011). Both *X. laevis* and mammalian PABP4 associate with polysomes indicating it may stimulate translation (Gorgoni *et al.*, 2011, Burgess and Gray 2012). Consistent with this idea, *X. laevis* PABP4 stimulates translation in tether assays (Gorgoni *et al.*, 2011) and mammalian PABP4 can stimulate the translation of a luciferase reporter with the interleukin-2 (IL-2) 3'UTR *in vitro* (Okochi *et al.*, 2005). PABP4 has also been reported to interact with a number of PABP1 partners including eIF4G, PAIP1, PAIP2, eRF3 (Cosson *et al.*, 2002a, Gorgoni *et al.*, 2011) and TOB (Okochi *et al.*, 2005), suggesting it may retain critical functions in turnover as well as translation.

PABP4 has been found to be critical for normal vertebrate development, with morpholino mediated knockdown in *X. laevis* embryos resulting in anterior defects and embryonic lethality (Gorgoni *et al.*, 2011). However, as mentioned, PABP4 is unable to completely rescue PABP1 lethality (Gorgoni *et al.*, 2011), showing that despite the functional similarities discussed above, their functions must be partly distinct.

#### 1.3.3.4 PABP5

The least characterised member of the PABP family member is PABP5 which is mammalian specific. PABP5 transcripts can be detected at low level by RT-PCR in human fetal brain and various adult tissues (Blanco *et al.*, 2001).

As, PABP5 lacks the PABC domain, responsible for many PABP protein interactions, and the proline-rich region (Figure 1.21), and is more diverse in terms of its primary sequence, it is unclear whether it shares any of the functions of PABP1.

# 1.4 DAZ family proteins

Studies of micro-deletions within the Y-chromosomes of men with non-obstructive azoospermia (i.e. no sperm in the semen, (Reijo *et al.*, 1995)) led to the description of three azoospermia factor (AZF) regions (Vogt *et al.*, 1995, Reijo *et al.*, 1996a). Further studies led to the identification of a putative RNA-binding protein, Deleted in AZoospermia (DAZ), present as multiple copies within the AZFc region (Yen *et al.*, 1997). DAZ genes contain an RNA recognition motif (RRM) and up to fifteen copies of a 24 amino acid sequence known as the DAZ motif which is unique to this family (Saxena *et al.*, 1996). Two autosomal family members, Dazl (deleted in azoospermia-like) and Boule were subsequently described and share these features, although they contain only a single DAZ repeat (Figure 1.27), (Cooke *et al.*, 1996, Reijo *et al.*, 1996b, Yen *et al.*, 1996, Xu *et al.*, 2001). This family has a conserved essential role in gametogenesis from worms to humans (Section 1.4.4).

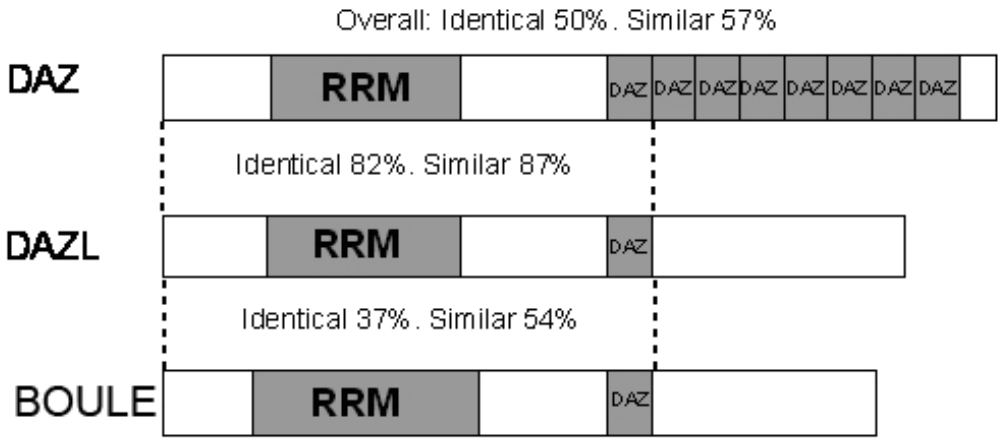


**Figure 1.27 - Human DAZ family.** Domain structure of the human DAZ family with corresponding percentages of amino acid homology shown for the N-terminal region up to and including the first DAZ repeat. From (Smith, 2007).

## 1.4.1 Evolution of DAZ family

Despite being the first DAZ family member to be identified, phylogenetic studies have shown that DAZ is actually the most recently evolved of the three family members (Xu *et al.*, 2001).

Boule is thought to be the ancestral family member and orthologues of Boule have been found in *C. elegans*, Drosophila, mouse and humans (Eberhart *et al.*, 1996,

Karashima *et al.*, 2000, Xu *et al.*, 2001, Shah *et al.*, 2010), but are not in fungi and plants (Shah *et al.*, 2010) (Figure 1.28).

DAZL orthologues are only found in vertebrates (Yen, 2004) and are believed to have arisen during the early stages of vertebrate radiation (Xu *et al.*, 2001, Shah *et al.*, 2010, VanGompel and Xu, 2011) by a duplication of the ancestor Boule gene followed by autosomal transposition.

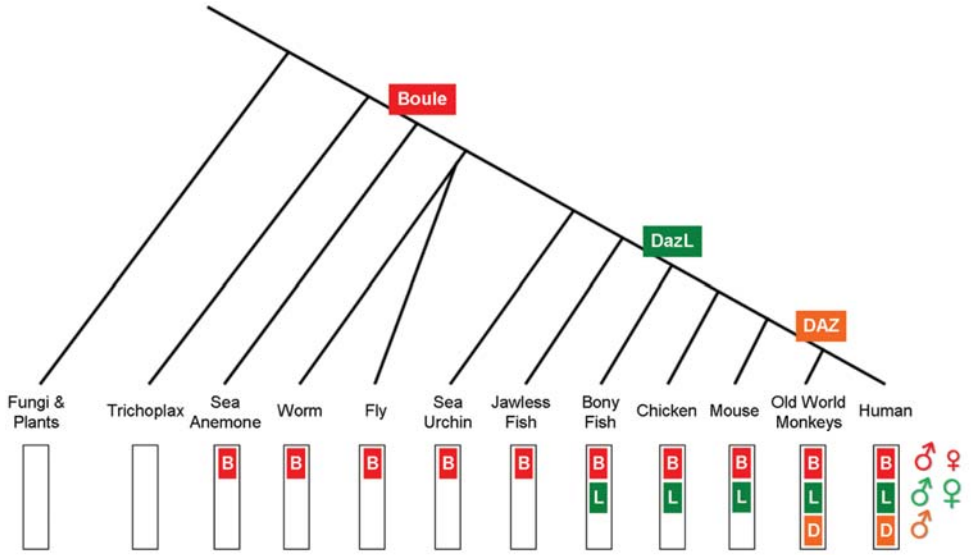


**Figure 1.28 - Distribution and sex specific expression of the DAZ family.** The DAZ family ancestor Boule (B) is present from worms to humans whilst DAZL (L) arose by duplication early in vertebrate evolution. Interestingly, DAZ (D) arose from an autosome to Y chromosome duplication-transposition of the DAZL gene during simian evolution. Boule is mainly associated with male gametogenesis (excluding fly) whilst DAZL is important in both sexes. DAZ is testis specific. From (VanGompel and Xu, 2011).

DAZ itself is believed to have originated during simiiformes evolution, since it is only present in the parvorder catarrhini which includes old world monkeys, apes and humans. It is believed to have arisen from a duplication of the autosomal DAZL gene followed by translocation to the Y chromosome meaning that is only present in males (Cooke *et al.*, 1996, Venables *et al.*, 2001). Repeated amplification resulted in variable numbers of DAZ genes in the human male population, with the reference sequence having four copies, but approximately 2 % of fertile men only carrying two copies (Repping *et al.*, 2003). The multiple copies are not always identical varying in the number of RRMs and DAZ repeats (Yen *et al.*, 1996, Saxena *et al.*, 2000). Nonetheless, western blot analysis of human testes extracts only detects a single

protein band for DAZ, suggesting that not all DAZ genes may be translated (Slee *et al.*, 1999, Reijo *et al.*, 2000). As a consequence of this, nucleotide sequence divergence is greater between DAZ genes, diverging as much as 10.9 % (Xu *et al.*, 2001) in humans and cynomologus whereas divergence between DAZL orthologues is roughly 1.5 %.

## 1.4.2 Expression pattern of the DAZ family

The differential expression of DAZ family members is an important determinant of the different phenotypes observed upon their loss of function.

### 1.4.2.1 Invertebrates

Invertebrates only encode the ancestor member of the DAZ family, Boule, which is confusingly referred to as daz-1 in *C. elegans* (Karashima *et al.*, 2000). During *C. elegans* larval development daz-1 mRNA can be detected in the mitotic germ cells within the distal area of the gonad and increases with progression into the meiotic transition, peaking at the proximal pachytene region of the gonad but being absent in mature sperm within the spermatheca. In adults, daz-1 transcripts were restricted to the female germ cell developmental (Karashima *et al.*, 2000, Maruyama *et al.*, 2005).

In Drosophila boule is not expressed in the female germ line but can be detected in pre-meiotic and meiotic spermatocytes and in post-meiotic spermatids by immunoblotting and immunohistochemistry (Cheng *et al.*, 1998). An isoform of *boule* is also present in nervous cells of Drosophila (Joiner and Wu, 2004, Hoopfer *et al.*, 2008) where it works as a negative regulator of axon pruning, suggesting that at least in flies the function of this family member is not restricted to germ cells (Hoopfer *et al.*, 2008).

Curiously flatworms (*Macrostomum lignano* (*M. lignano*)) express three different orthologues of boule, with macbol1 and 2 being specific for testes and macbol3 being restricted to ovaries and developing eggs (Kuales *et al.*, 2011).

#### 1.4.2.2 Zebrafish and X. laevis

Northern blot analysis of adult gonads in zebrafish detected *zDazl transcripts* in both sexes, with *in situ* hybridisation revealing their presence in oocytes (Maegawa *et al.*, 1999), spermatogonia and early spermatocytes (Maegawa *et al.*, 2002) but not in late spermatocytes, spermatids or mature sperm (Maegawa *et al.*, 2002). In the early embryo maternal *zDazl* mRNA was detected at the vegetal pole by *in situ* hybridation and migrated towards the blastomeres, with zDazl being detectable in migrating PGCs (Maegawa *et al.*, 1999, Hashimoto *et al.*, 2004) (Maegawa *et al.*, 1999).

Xdazl has been described in all stages of male and female germ cell development in adult *X. laevis*, with the exception of the mature spermatozoa (Mita and Yamashita, 2000). Consistent with its localisation in the germ plasm of oocytes, maternally inherited Xdazl was detected in the germ plasm of blastula embryos (Houston and King, 2000). Xdazl can also be detected in PGCs until the early tailbud stage (Houston *et al.*, 1998, Houston and King, 2000). Thus both *zDazl* mRNA and xDazl appear restricted to the germ line.

#### 1.4.2.3 Mice

Mice encode two members of the DAZ family, Boule (mBoule) and Dazl (mDazl) although to date most work has focused on Dazl.

Northern blot analysis has shown that *Dazl* expression in mice is restricted to the gonads of both males and females (Cooke *et al.*, 1996, Reijo *et al.*, 1996b, Yen *et al.*, 1996). In contrast, *Dazl* was not detected in Northern blots from two mouse lines ( $XX^{SXRA}$, white spotted or steel gene mutated) that lacked germ cells (Cooke *et al.*, 1996, Reijo *et al.*, 1996b) nor was it detected in a Sertoli cell line (TM4) (Reijo *et al.*, 1996b), suggesting that *Dazl* mRNA is germ cell specific.

During fetal development mDazl transcripts have been reported by *in situ* hybridisation in testes from 11.5 c dpc (Lin and Page, 2005) and by northern blot in ovaries at 14.5 dpc (Seligman and Page, 1998), the earliest points examined for both sexes. In both sexes, northern blotting detected mDazl mRNA up until 18.5 dpc, the last fetal gonad stage analysed (Seligman and Page, 1998). Notwithstanding, the data

provided show a peak of *Dazl* expression at 14.5 dpc for both males and females, when the first oogonia enter meiosis. At 16.5 dpc there is an abrupt decrease in *Dazl* expression in both sexes which is maintained in the developing testes at 18.5 dpc although Dazl mRNA levels increase considerably in ovaries. These differences may indicate a sexual specific requirement for Dazl during fetal development, or just a difference in number of germ cells in both sexes (Seligman and Page, 1998).

Northern blots from postpartum males detect Dazl as early as 1 day postpartum (dpp), although its level increase with the appearance of the first spermatogonia at 6 dpp and plateau by 10 dpp when the first spermatogenic cells enter meiosis (Reijo *et al.*, 1996b). Although, a different report suggested that it peaks later at 20 dpp coinciding with the appearance of the first round spermatids (Cooke *et al.*, 1996). *In situ* hybridisation showed expression of Dazl transcripts in spermatogonia at stages IV-VI, with a peak of expression in the intermediate to B spermatogonia passage, just before meiotic initiation, consistent with northern blots (Niederberger *et al.*, 1997). No Dazl RNA was reported in spermatocytes or spermatids.

Dazl protein is expressed in type B spermatogonia, preleptotene, zygotene and pachytene spermatocytes (stage I-VIII) (Ruggiu *et al.*, 1997) and has also been examined in females where it is highly expressed in the cytoplasm of pachytene oocytes at 17.5 dpc and at lower levels after birth in the cytoplasm of primordial and growing follicles (Ruggiu *et al.*, 1997, McNeilly *et al.*, 2011). Interestingly, Dazl has also been detected by IHC in the cytoplasm of granulosa cells of growing follicles (Ruggiu *et al.*, 1997) although *in situ* hybridisation data is not available to confirm whether Dazl mRNA is present in these somatic cells.

Northern blotting only detected Boule mRNA in male gonads (Xu *et al.*, 2001) with IHC showing expression in a subset of male germ cells; Boule is present in late spermatocytes with a peak of expression just before metaphase, decreases during meiotic division, but increases again in round spermatids where it can be detected until round spermatid-5. Boule mRNA was described as absent from mouse ovaries, although the report failed to present the data (Xu *et al.*, 2001). Nevertheless this would be consistent with the lack of a phenotype in female knockout mice (VanGompel and Xu, 2010).

#### 1.4.2.4 Human

In first trimester ovaries and testes, DAZL was present in the nucleus of OCT4 positive germ cells. In the second trimester DAZL is only expressed in the more cortical OCT3/4 negative germ cells located within germ cell clusters (Anderson *et al.*, 2007), where it is cytoplasmic. In the developing testes at the second trimester DAZL expression was uniformly spread through all germ cells within the gonad and remains predominantly nuclear (Dorfman *et al.*, 1999, Brekhman *et al.*, 2000, Anderson *et al.*, 2007). No data is available for DAZL expression in the last trimester of human gestation.

In adults DAZL is expressed in the oocyte cytoplasm of primordial and secondary follicles (Dorfman *et al.*, 1999). As reported for mice, DAZL has also controversially been detected in the cytoplasm of the lutein cells of the corpus luteum (Dorfman *et al.*, 1999, Pan *et al.*, 2002, Pan *et al.*, 2009). In adult testes DAZL protein is present in spermatogonia, early and late spermatocytes (Reijo *et al.*, 2000) but not in no expression has been observed in any of the later stages of spermatogenesis including round and elongating spermatids (Reijo *et al.*, 2000).

BOULE and DAZ proteins are considerably less characterised than DAZL. Boule can be detected in spermatocytes and early spermatids by IHC, but not in spermatogonia or late spermatids (Xu *et al.*, 2001, Luetjens *et al.*, 2004). Expression of Boule in ovaries has not been examined since its mRNA is undetectable in this tissue (Xu *et al.*, 2001). Analysis of DAZ expression is complicated by the existence of four DAZ genes (Huang *et al.*, 2008) but DAZ was only detected in the cytoplasm of spermatogonia in adult testes samples (Huang *et al.*, 2008). Another report suggested that DAZ was also present in spermatogonia and early spermatocytes, but the antibody utilised also detects DAZL, suggesting that this difference may be due to cross-reaction (Reijo *et al.*, 2000).

#### 1.4.2.5 Sub-cellular expression

Despite being predominantly cytoplasmic, at specific germ cell stages, DAZ family members can also be nuclear. This was first reported in flies where boule is nuclear in spermatocytes and only transits to the cytoplasm before the onset of

metaphase (Shah *et al.*, 2010). However, Boule may not function in this compartment as blocking its nuclear localisation results in no obvious phenotype (Cheng *et al.*, 1998). In humans, DAZL has been detected in the nucleus of gonocytes during fetal developmental but is reported to relocate to the cytoplasm of spermatogonia and spermatocytes after birth (Ruggiu *et al.*, 2000). In females, DAZL translocates to the cytoplasm of oogonia in the second trimester (Anderson *et al.*, 2007)

## 1.4.3 DAZ family phenotypes

Loss of function studies have been performed in both non-mammalian and mammalian species and both result in compromised gametogenesis in one or both sexes.

### 1.4.3.1 Invertebrates and non-mammalian vertebrates

Transposon-induced ablation of boule in *Drosophila* results in a meiosis I arrest at pachytene spermatocytes (Eberhart *et al.*, 1996). In contrast, RNAi of boule (daz-1) results in a lack of oocytes in hermaphroditic worms, with *C. elegans* showing a pachytene arrest during oogenesis (Karashima *et al.*, 2000) and *C. Briggsae* a block in the sperm-oocyte transition (Otori *et al.*, 2006). RNAi of the three Boule orthologues in *M. lignano* results in different phenotypes: the male specific macbol2 show no germ cell defects but the other male specific boule, macbol1 blocks spermatocyte differentiation. In females RNAi knockdown of macbol3 impairs egg maturation resulting in sterility (Kuales *et al.*, 2011).

In vertebrates, morpholino mediated knockdown of maternal Xdazl mRNA results in a loss of both male and female germ cells in *X. laevis*, due to defects in PGC proliferation and migration during their transit from ventral to dorsal endoderm (Houston and King, 2000).

### 1.4.3.2 Mice

In mice, Dazl-knockout (*Dazla*$^{Tm1Hgu}$/*Dazla*$^{Tm1Hgu}$ *(Ruggiu et al., 1997))* (Dazl-KO) results in loss of germ cells in both males and females, with the onset of

the phenotype varying according to sex and being influenced by the genetic background.

In a C57Bl6 Dazl-KO outbred strain no significant differences are observed in fetal gonads at 15.5 dpc (Ruggiu *et al.*, 1997, Saunders *et al.*, 2003). However, in females a substantial decrease in germ cells is observed by 17.5 dpc, suggesting a meiotic progression phenotype (Saunders *et al.*, 2003), with no follicles having being formed by birth (McNeilly *et al.*, 2000), and a complete absence of germ cells by 4 dpp (Ruggiu *et al.*, 1997, Saunders *et al.*, 2003). In males, a decrease in germ cell number can be observed by 19.5 dpc (Ruggiu *et al.*, 1997, Saunders *et al.*, 2003). Since male gonocytes have not entered meiosis at this stage, this phenotype appears to be associated with mitotic rather than meiotic progression (Saunders *et al.*, 2003). However, the most striking male phenotype is observed during the first wave of spermatogenesis, where pachytene spermatocytes can be observed, albeit in reduced numbers, but show clear signs of atresia suggesting a leptotene-zygotene arrest due to impaired synaptonemal formation, indicating a role for Dazl in meiotic progression during spermatogenesis (Saunders *et al.*, 2003). Spermatogonial differentiation also appears to be impaired in prepubertal Dazl-KO mice as $A_s$ and $A_{pr}$ spermatogonia are present but fail to differentiate into $A_{al}$ (Schrans-Stassen *et al.*, 2001).

Analysis of inbreed C57Bl6 Dazl-KO strain has suggested additional roles since atretic germ cells can be observed as early 15.5 dpc in both male and female mice (Lin and Page, 2005, Lin *et al.*, 2008). These female mice also show abnormal expression of meiotic markers (γH2AX and Sycp3) at 15.5 dpc suggesting impaired meiotic progression. More recently the same group has described an additional phenotype as PGCs fail to undergo sexual differentiation (Gill *et al.*, 2011). This indicates that Dazl may play an even earlier role in allowing germ cells to respond to sexual differentiation cues from the developing gonad.

Moreover, the imprinting status of sex specific genes appears to be affected in inbred C57Bl6 Dazl-KO mice. Imprinting at the H19 locus of paternal genomes is normally lost by 13.5 dpc and re-established by 16.5 dpc. In Dazl-KO mice erasure of this male specific imprinting is delayed and is not re-established by 16.5 dpc (Haston *et al.*, 2009).

Most recently, morpholino-mediated Dazl knockdown in oocytes showed that Dazl is also a major regulator of meiotic oocyte maturation. Dazl depleted oocytes show reduced completion of meiosis I and disruption of the transition into MII as they display impaired spindle formation, aberrant chromosome segregation, and a comparatively high rate of aneuploidy (Chen *et al.*, 2011). Interestingly, knock-down in early zygotes blocks embryonic cleavage revealing an unexpected post-fertilisation role (Chen *et al.*, 2011).

In contrast, Boule-KO females have no oogenesis phenotype and produce viable offspring (VanGompel and Xu, 2010). Boule deficient males progress through meiosis I and II apparently normally but arrest at round spermatid-6. This suggests a role for Boule in spermatid differentiation contrasting with its phenotype in both worms and flies, which show a pachytene arrest (Eberhart *et al.*, 1996, Karashima *et al.*, 2000, VanGompel and Xu, 2010).

#### 1.4.3.3 Humans

To date, causality between loss of DAZ family function and impaired fertility has not been established in humans. Although, DAZ gene deletions are present in men with reduced sperm number (Reijo *et al.*, 1995), some men harbouring DAZ deletions still produce low levels of sperm (Reijo *et al.*, 1996a) suggesting it is not essential. Moreover, a possible role in sperm maturation has also been suggested due to the success of ISCI (intracytoplasmic sperm injection) in men carrying DAZ deletions with severely reduced spermatogenesis (Kamischke *et al.*, 1999, Mau Kai *et al.*, 2008).

Histological analysis of men with meiotic spermatogenic arrest showed no BOULE expression (Luetjens *et al.*, 2004), but to date no mutations have been identified in Boule in males with reproductive phenotypes.

In humans, several putative mutations in DAZL have been described in patients with either premature ovarian failure, early onset menopause and azoospermia (Tung 2006). However, the effect of these amino acid substitutions on DAZL function remains to be determined.

#### 1.4.3.4 DAZ family redundancy

The ability of family members to at least partially cross-rescue loss of function phenotypes from different species suggests that they share closely related molecular functions and interactions. For instance, the meiotic phenotype of *Drosophila* Boule can be rescued by the flatworm macbol1 (Kuales *et al.*, 2011) although the resulting sperm show abnormal morphology and do not produce offspring (Kuales *et al.*, 2011). Similarly, this phenotype can also be partially rescued with *X. laevis* dazl (Houston *et al.*, 1998) and human BOULE (Xu *et al.*, 2003). Moreover, the mouse Dazl phenotype was partially rescued with human DAZL (Vogel *et al.*, 2002) and human DAZ (Slee *et al.*, 1999), indicating that different family members share common functional properties. In keeping with this, all three family members can enhance differentiation of ESCs into germ cells with spermatid features *in vitro* (Kee *et al.*, 2009), although ESCs *in vivo* only appear to express Dazl. These observations suggest their differential expression is likely to be an important contributory factor to phenotype development in species which possess multiple family members.

### 1.4.4 DAZ family functions

Clinical, genetic and molecular studies have demonstrated the importance of DAZ family members in gametogenesis but to date the mechanisms by which they achieve these functions are not completely understood. The existence of different family members, sex and species specific phenotypes together with major temporal and spatial differences in gametogenesis between sexes all add to the complexity of analysing their function.

Nonetheless several functions have been proposed based on their predominantly cytoplasmic localisation, ability to bind RNA (Tsui *et al.*, 2000a, Venables *et al.*, 2001) and interacting proteins (Figure 1.30 for summary of protein interactions) focusing on potential roles in regulating mRNAs within this sub-cellular compartment (Figure 1.31). In some cases, most notably for translational activation of mRNAs, direct experimental support for the role of DAZ family members in these processes is available.

#### 1.4.4.1 Translation initiation regulation by DAZ family

Post-transcriptional regulation of cytoplasmic mRNAs is critical for gametogenesis (reviewed in (Nguyen-Chi and Morello, 2011, Idler and Yan, 2012)). The first evidence suggesting a potential role in translational regulation for this family came from seminal studies in Drosophila, which showed that boule null flies had impaired meiotic progression, similar to the phenotype observed in twine null flies (Maines and Wasserman, 1999). Importantly, they found that the level of twine transcripts was unchanged in boule mutants, although levels of twine protein was significantly reduced compared to WT (Maines and Wasserman, 1999), suggesting either a direct or indirect effect on twine mRNA translation.

Potential roles in translation in vertebrates was first highlighted by the association of mouse Dazl (mDazl) and zebrafish Dazl (zDazl) with actively translating polysomes (Tsui *et al.*, 2000b, Maegawa *et al.*, 2002). Reporter mRNA assays in micro-injected *X. laevis* oocytes directly established the ability of *X. laevis*, mouse and human DAZL and also human DAZ and BOULE to robustly stimulate the translation of mRNAs to which they were bound, revealing that they shared a conserved function as mRNA-specific translational activators (Collier *et al.*, 2005b). These observations were in keeping with subtle effects of zDazl on the translation of reporter mRNAs in transfected somatic cells (Maegawa *et al.*, 2002). Subsequently, this function has been verified *in vivo* for mouse Dazl and *C. elegans* Daz-1 by the identification and verification of mRNAs that they translationally activate (Reynolds *et al.*, 2005, Otori *et al.*, 2006, Reynolds *et al.*, 2007, Chen *et al.*, 2011) (Section 1.4.4.2).

Insights into the mechanism by which DAZ family members stimulate translation was provided by analysis of the step at which it acts, which revealed that Dazl promotes the initiation phase of translation (Collier *et al.*, 2005b). A Y2H screen of initiation factors revealed that Xdazl interacted with PABP1 but not other canonical initiation factors (eIF1, eIF1A, eIF2, eIF2B, eIF3, eIF4A, eIF4E, eIF4G, eIG4H, eIF5, eIF5A and eIF5B). Interaction with endogenous *X. laevis* PABP1 and ePABP was confirmed by co-immunoprecipitation. Mammalian DAZ family members that were able to stimulate translation in *X. laevis* oocytes showed a

conserved ability to interact with *X. laevis* PABPs, suggesting this interaction may be functionally important (Collier *et al.*, 2005b). To probe whether this interaction was required for the ability of mDazl to stimulate translation, a series of deletion mutants were made. Importantly, deletion of the minimal PABP-binding region but not other regions of mDazl abrogated its ability to stimulate translation (Collier *et al.*, 2005b) indicating that this interaction was functionally required (Collier *et al.*, 2005b). As mDazl efficiently stimulates the translation of unadenylated reporter mRNAs (Collier *et al.*, 2005b), this suggests that this interaction is sufficient to allow the direct poly(A)-independent recruitment of PABPs to mRNAs via protein-proteins interaction, providing an mechanism of activating germ cell that is distinct from cytoplasmic polyadenylation (Collier *et al.*, 2005b, Pique *et al.*, 2008).

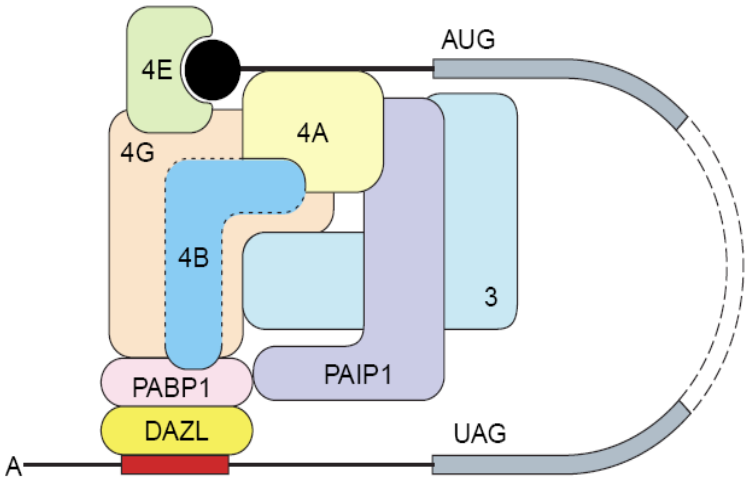


**Figure 1.29 - DAZL-PABP Closed-loop conformation**. By working as an interacting scaffold, DAZL enables PABP to bring together the 5' and the 3' ends of the mRNA via protein-protein interactions, leading to enhanced translation initiation. The outline of eIF4B is broken, as although suggested to be a PABP-binding protein in mammalian cell free extracts (Bushell JBC 2001), this report awaits verification (from Brook *et al*, 2009).

Together these studies provide the basis for the DAZL-PABP model, in which DAZ proteins bound to the 3'UTR of specific mRNAs recruit PABPs, which in turn interacts with the 5'end factors (i.e. eIF4G and PAIP1), promoting an alternative closed-loop conformation (Figure 1.29) (Collier *et al.*, 2005b, Brook *et al.*, 2009). As would be predicted from this model, mDazl was found to stimulate the translation of adenylated reporter mRNAs to a lesser extent that that of unadenylated mRNAs

(Collier *et al.*, 2005b), as the former have the capacity to bind PABP independently of Dazl.

Whilst genetic evidence to support this model is absent in vertebrates, pab-1 deficient *C. elegans* show an early meiotic block in female oogenesis, similar to that observed in daz-1 deficient *C. elegans* (Maciejowski *et al.*, 2005, Maruyama *et al.*, 2005). However, verification of this model in genetically accessible mammalian models remains an important goal.

#### 1.4.4.2 Translational targets of the DAZ family

Initial studies of the RNA-binding capacity of this family revealed a general affinity for poly(U) and to a lesser extent, poly(G) homopolymers (Tsui *et al.*, 2000a) with mutation or deletion of the RRM in mDazl and hDAZL respectively confirming the importance of this region in RNA-binding (Ruggiu and Cooke, 2000, Tsui *et al.*, 2000a). SELEX and yeast-three hybrid screens suggested that Dazl may bind U-rich sequences interrupted by G or Cs (Venables *et al.*, 2001). Recently, the structure of mouse Dazl bound to RNA has been solved showing that the RRM of mDazl has high affinity towards GUU[U/C] in different sequence contexts (Jenkins *et al.*, 2011).

Although Drosophila *twine* was not shown to be a direct target of Drosophila boule (Maines and Wasserman, 1999), it was subsequently shown that reporter mRNAs containing this 3'UTR could be stimulated by zDazl in transfected CV-1 cells, an effect that was dependent on a GUUC sequence (Maegawa *et al.*, 2002). Despite the human homologue, CDC25A, being proposed as a target for human family members, no evidence to support this has been provided, although testes sections lacking BOULE also lack CDC25A protein (Luetjens *et al.*, 2004).

In mammals, several studies have aimed to identify mRNA targets, most involving the isolation of mRNA from testes extracts with purified proteins, but very few targets have been validated *in vivo*. A pull-down of mRNAs from testes extracts using GST-mDazl identified potential mouse Dazl targets (Jiao *et al.*, 2002) including Tpx-1, a testicular cell adhesion protein that modulates spermatogenesis progression, Grsf-1, a RNA-binding protein that regulates translation, and the

transcription factor Trf-2. Another screen using the same approach (Zeng *et al.*, 2008), re-isolated Tpx-1 (Jiao *et al.*, 2002) and a new variety of potential targets including testis-specific serine kinase 2 (Tssk2) which is a member of a family of Ser/Thr protein kinases implicated in male germ cell development (Kueng *et al.*, 1997). TSSK2 binding to mDazl was confirmed by electrophoretic mobility shift assay (EMSA) (Zeng *et al.*, 2008) and human DAZL was found to be able to pull-down human TSSK1, TSSK2, TSSK4 and TSSK5. A similar screen using hDAZL and mRNA from human testes isolated over 60 possible targets, with SDAD1, a homolog of the yeast severe depolymerastion of actin (sda1) gene being confirmed as a potential binding mRNA by immunoprecipitation of human testes mRNA with purified hDAZL protein (Fox *et al.*, 2005). However, none of these potential targets have been shown to be regulated by DAZ family members *in vitro*, in cell culture or *in vivo*.

Potential targets were also isolated from rodent testes extracts by RNA-IP using antibodies against endogenous Dazl and hybridised to microarrays. Comparison to mRNAs isolated by another RNA-binding protein and in the presence of peptide control resulted in the identification of 15 potential targets of mDazl (Maratou *et al.*, 2004, Reynolds *et al.*, 2005). Comparisons of the 3'UTR of these mRNAs led to the proposed consensus $U_{2\text{-}10}$[G-C]$U_{2\text{-}10}$ (Reynolds *et al.*, 2005), similar to the motif present in mRNAs from previous screens (Jiao *et al.*, 2002) and consistent with the solved structure of Dazl-bound to RNA (Jenkins *et al.*, 2011). Importantly, two of potential targets, mouse vasa homologue (Mvh) and the synaptonemal complex protein 3 (Sycp3) mRNAs, were validated in a series of assays (Reynolds *et al.*, 2005, Reynolds *et al.*, 2007). mDazl was shown to bind the 3'UTR of both transcripts and reporter mRNAs carrying these 3'UTRs were shown to be translationally activated by mDazl in microinjected *X. laevis* oocytes (Reynolds *et al.*, 2005, Reynolds *et al.*, 2007). Importantly, mutations within these 3'UTRs that abrogated Dazl binding *in vitro* also prevented their translational activation in these assays (Reynolds *et al.*, 2007). The phenotypes of both the Mvh (Tanaka *et al.*, 2000) and Sycp3 (Yuan *et al.*, 2000) KO mice resemble the outbred Dazl-KO phenotype (Saunders *et al.*, 2003). Specifically Mvh-KO males have a leptotene to zygotene block at meiosis I (Tanaka *et al.*, 2000) and Sycp3 KO males have a meiotic arrest at

prophase I (Yuan *et al.*, 2000). Critically, the levels of both proteins was decreased in Dazl-KO mice compared to WT (Reynolds *et al.*, 2005, Reynolds *et al.*, 2007), which combined with evidence that they can be bound and translationally activated by Dazl provides strong evidence that they are *bona fide* target mRNAs. The residual levels of Mvh and Sycp3 observed in Dazl KO mice is consistent with Dazl stimulating, rather than being essential for, their basal translation (Collier *et al.*, 2005b).

Recently, potential Dazl target mRNAs in female mice have been identified and in some cases validated in a genome-wide study to identify mRNAs involved in progression through oocyte maturation (Chen *et al.*, 2011). Polysome profiling, in which mRNAs are recovered from the translating ribosomes, was performed GV, MI and MII matured oocytes. This showed that many of the RNAs that moved onto polysomes during maturation contained CPEs ($U_4A[A/U]U$) and/or DAZL ($U_{2\text{-}10}[G\text{-}C]U_{2\text{-}10}$) binding sites. Consistent with the idea that Dazl may be regulating the translation of mRNAs critical for this process, morpholino-mediated knock-down of Dazl impaired meiotic maturation (Chen *et al.*, 2011). The translation of reporter mRNAs containing the 3'UTR of three of the putative Dazl regulated mRNAs, Dazl, Tex19.1 and Tpx2 was investigated in morpholino injected oocytes. This confirmed that their translational recruitment during maturation was Dazl-dependent, and in the case of Tex-19 this effect was shown to require the Dazl binding sites (Chen *et al.*, 2011). Tex-19.1 was previously identified as a potential target mRNA in mouse testis (Reynolds *et al.*, 2005) although the results here were in contrast with those in zebrafish embryos injected with mDazl where a subtle repression of a Tex-19 reporter was observed (Zeng *et al.*, 2009). Tpx2 has been previously shown to regulate spindle formation and activation of Aurora A (Eyers and Maller, 2004). siRNA depletion of Tpx2 from mouse oocytes results in meiotic progression defects with progression from meiosis I and oocyte maturation severally impaired (Brunet *et al.*, 2008), as it was also observed in Dazl MO-depleted oocytes (Chen *et al.*, 2011).

### 1.4.4.3 Other molecular functions of the DAZ family

An interaction between the C-terminal region of mDazl and the transporter protein dynein light chain (Figures 1.30 and 13.1), a component of the dynein-dynactin motor complex, suggested that mDazl may be involved in mRNA transport and localisation (Lee *et al.*, 2006). In support of this, Dazl-bound mRNAs were shown to aggregate in sub-cellular foci in some transfected somatic cells (Lee *et al.*, 2006). The presence of TIA-1 in these foci suggested they may represent stress granules, sites of mRNA storage that can be induced by cellular stress or the over expression of RNA-binding proteins (reviewed in (Anderson and Kedersha, 2009, Buchan and Parker, 2009)). Interestingly, heat shock was recently shown to induce Dazl positive stress granules in early spermatocytes (Kim *et al.*, 2012), the formation of which was reduced in Dazl-KO animals, suggesting that DAZL may play a role in stress granule formation as well as the transport of mRNAs to such foci (Kim *et al.*, 2012).

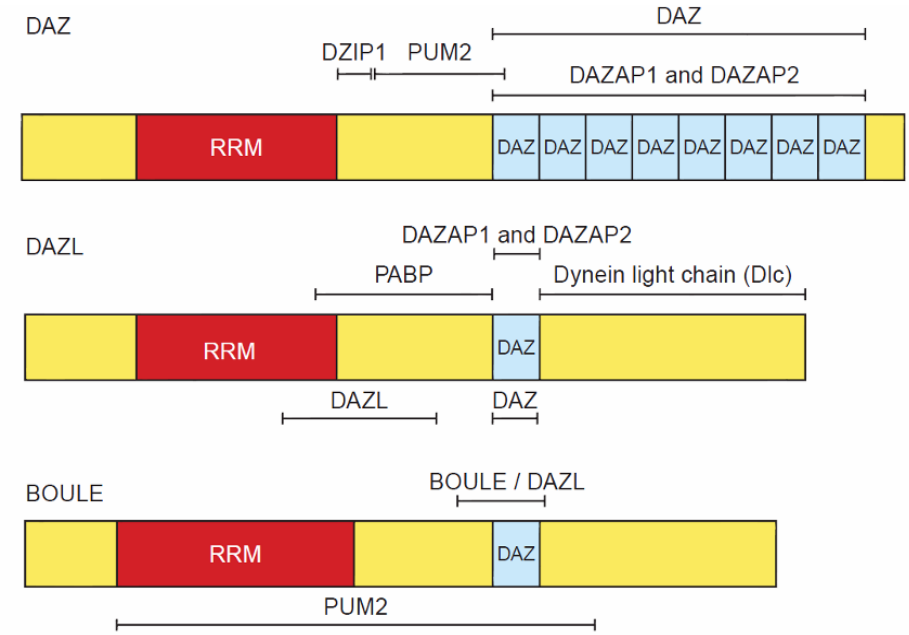


**Figure 1.30 - DAZ family interacting proteins.** Schematic representation of DAZ family domains structure depicting interactions described in vertebrate models. From (Brook *et al.*, 2009).

DAZ family members also interact with PUMILIO-2 (PUM-2) (Moore *et al.*, 2003, Urano *et al.*, 2005) and for human DAZ this interaction is mapped to the region that bridges the RRMs and the DAZ motif (Figures 1.30 and 13.1) (Moore *et al.*, 2003). Pumilio proteins have well characterised roles in translation as part of multi-protein repressor complexes ((Wickens *et al.*, 2002, Urano *et al.*, 2005) reviewed in (Quenault *et al.*, 2011)), suggesting that DAZ proteins may function to repress mRNAs in germ cells. Alternatively, interaction with PUM-2 may repress the ability of DAZ family members to stimulate translation, as the region bound by PUM-2 overlaps with the PABP-binding site in mDazl. Consistent with this latter hypothesis Ringo mRNA is translational repressed in fully grown *X. laevis* oocytes and is bound by Pum-2, Xdazl and ePABP and becomes translational active when Pum-2 dissociates during maturation. However, whilst it is clear that Pum-2 represses Ringo mRNA translation, it remains unclear whether its subsequent translation requires Dazl (Padmanabhan and Richter, 2006).

Another translation regulator DAZAP-1 (DAZ associated protein-1) has been shown to interact with both human DAZ and DAZL protein. This widely expressed protein (Dai *et al.*, 2001) was first shown to interact in a Y2H screen using DAZ as a bait protein (Tsui *et al.*, 2000a). The *X. laevis* homolog of DAZAP-1, proline-rich RNA binding protein (Prrp), has been implicated in mRNA localisation (Zhao *et al.*, 2001) and both the *X. laevis* and human homologues can stimulate translation of reporter mRNAs in tethering assays (Smith *et al.*, 2011). Interestingly, translational stimulation by DAZAP-1, like that of DAZL, is sensitive to poly(A) tail length raising the possibility that DAZAP-1 may contribute to the ability of DAZL to stimulate translation. In keeping with this idea deletion of the DAZAP-1 binding site reduces the ability of Dazl to stimulate translation (Collier *et al.*, 2005b) and to bind polysomes (Tsui *et al.*, 2000b), however this deletion also impacts PABP1 binding (Collier *et al.*, 2005b). Thus the role, if any, of DAZAP-1 in promoting the ability of Dazl to stimulate translation or to localise mRNAs awaits clarification.

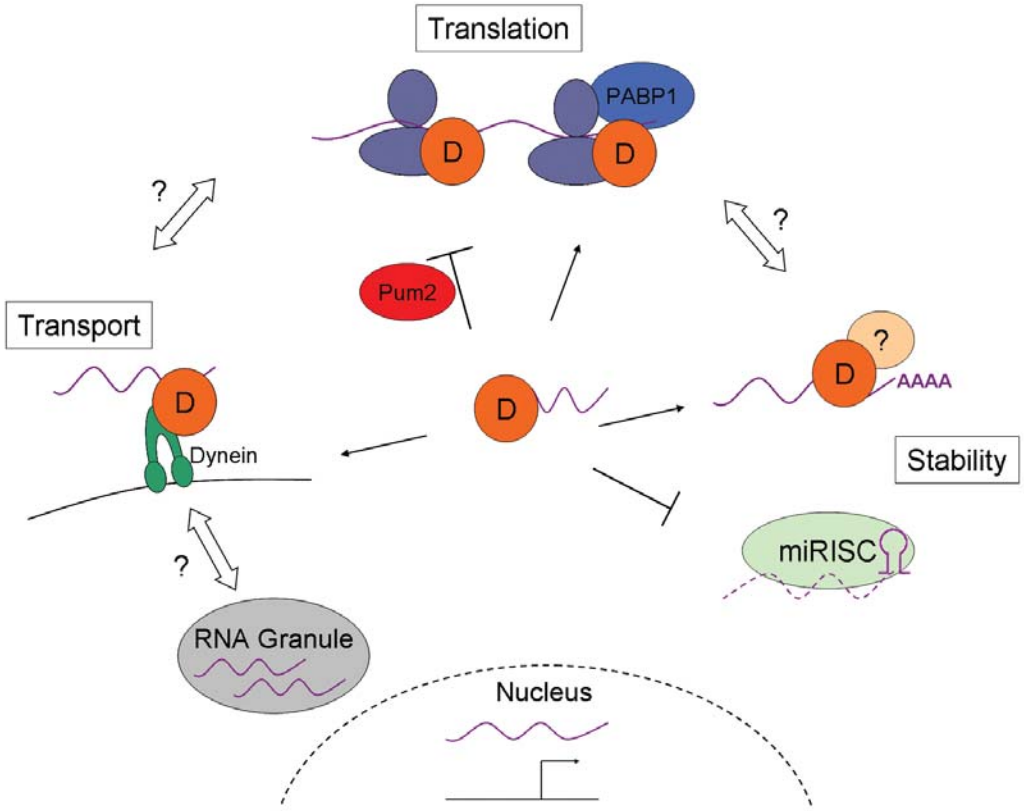


**Figure 1.31 - DAZ family functions in gametogenesis.** Schematic representation of proposed DAZ (orange circle represents generic DAZ family member) family functions in the cytoplasm. The multiple functions proposed for DAZ family are likely to be dependent on protein partners with which they interact in different multi-protein complexes, a common functional feature of 3'UTR binding proteins. DAZ proteins can activate the translation of specific mRNAs a function that appears to require interaction with PABP. Interaction with dynein has been proposed to promote mRNA transport and pumilio-2 (Pum2) repression of mRNAs bound by this family. Family members have also been associated with relief of miRNA mediated degradation (miRISC) and with regulating poly(A) tail length. In *C. elegans* the latter may involve interaction with CPEB3. From (VanGompel and Xu, 2011). Purple line depict mRNA molecule.

Zebrafish DAZL has recently been shown to abrogate micro RNA (miRNA) mediated degradation of reporter mRNAs by miR-430 when injected into somatic cells (Takeda *et al.*, 2009). These reporter mRNAs contained the 3'UTRs of *nanos1* and *tdrd7* which are only expressed in PGCs, in part due to their degradation in somatic cells by miR-430, suggesting that Dazl may permit their expression in PGCs by relieving miR-430 action. Whilst the mechanism of de-repression remains unclear, the authors noted that binding of zDazl induced polyadenylation of reporter mRNAs independently of miR-430 action. Whether this reflects protection of poly(A) tail by DAZL recruited PABP remains to be determined but *C. elegans* daz-1 was shown to interact with the CPEB homolog, Cpb-3, suggesting the potential for a more direct role in cytoplasmic polyadenylation (Hasegawa *et al.*, 2006). Such a role is supported by their partially overlapping expression patterns during worm meiotic progression although the subcellular distribution of Dazl and, at least, CPEB1 does not significantly overlap in mouse spermatocytes and these protein do not appear to interact (Reynolds *et al.*, 2007). In keeping with this lack of interaction in mice, CPEs and Dazl binding sites overlap in target mRNAs such as Sycp3 (Reynolds *et al.*, 2007) suggesting these proteins are not simultaneously bound and CPEB1-mediated activation of target mRNAs (i.e. Dazl mRNA) in mouse oocytes has been shown to occur prior to their Dazl-mediated activation (Chen *et al.*, 2011).

Other interacting partners such as DAZAP-2 (Tsui *et al.*, 2000a) and DAZ interacting protein-1 (DZIP-1) and DZIP-2 have been demonstrated to interact with both human DAZ and DAZL proteins (Moore *et al.*, 2003, Moore *et al.*, 2004a). However no information exists regarding the functionality or possible roles of these interactions but as DZIP1 and DZIP2 are not RNA binding proteins the functions of DAZ proteins could extend beyond RNA biology.

# 1.5 – Aims

Understanding the molecular mechanisms involved in mammalian germ cell development would progress our knowledge of clinically relevant research areas such as sub-fertility, infertility, aneuploidy, embryo development, and germ cell cancers.

The identification of the DAZ family in patients with spermatogenic defects, together with the data from animal models provides evidence that this family plays important roles in gametogenesis. Previous work in the laboratory has shown that DAZL fulfils this critical role at least in part by regulating the translation of specific mRNAs and has provided a molecular model for DAZL function showing that it acts, at least in *X. laevis* oocytes, by recruiting PABP, a translation initiation factor. This allows formation of an alternative closed-loop mRNA conformation which brings the ends of the mRNA into functional proximity and drives efficient recruitment of ribosomes (Collier *et al.*, 2005b).

However, mammals encode additional members of both DAZ and PABP families, suggesting the potential for an additional layer of complexity. With this in mind, it was hypothesised that DAZL recruits one or more PABP family member for its function in promoting the translation of specific mRNAs during mammalian gametogenesis. To investigate this hypothesis three main questions were addressed:

1 – What is the expression pattern of Pabp1 and Pabp4 in mouse gonads and are they co-expressed with Dazl during male and/or female mouse gametogenesis. If so, at what stages does co-expression occur and does this correspond to times associated with Dazl phenotypes?

2 - Do the members of the PABP family that are present alongside Dazl at specific germ cell stages in mouse also retain the ability to interact with Dazl?

3 – Do putative mutations in human DAZL associated with reproductive phenotypes affect the function of DAZL in activating translation, and if so, do these affect its ability to interact with proteins that are required for this function?

# Chapter 2
# Materials and Methods

**Notes:**

Unless otherwise stated:

1 – Oligonucleotides were purchased from Eurogentec.

2 – Centrifugations:

- Up to 2 ml volumes were performed in an Eppendorf 5417R - fixed angle rotor centrifuge.

- Over 2ml volume were performed in a Sigma-Aldrich 6K15 – swing out bucket rotor centrifuge.

3 – Overnight incubation is considered approximately 16hrs.

# 2.1 Suppliers

| Company | Location | Country |
|---|---|---|
| Abcam | Cambridge | UK |
| Adobe Systems Europe Ltd | Maidenhead | UK |
| Ambion | Austin, TX | USA |
| Biotium | Hayward, CA | USA |
| Applied Biosystems | Carlsbad | USA |
| BD Biosciences | Oxford | UK |
| Bio-Rad | Hemel Hempstead | UK |
| Carl Zeiss Ltd | Welwyn Garden | UK |
| Cell Path | Hemel Hempstead | UK |
| Clontech | Guilford | UK |
| Clontech | Mountain View | USA |
| CovaLAB | Cambridge | UK |
| EmbiTech | San Diego, CA | USA |
| Eppendorf | Cambridge | UK |
| Eurogentec | Seraing | Belgium |
| Finnzymes | Espoo | Finland |
| GE Healthcare | Amersham | UK |
| Harvard Apparatus | Kent | UK |
| Hoefer | Holliston, MA | USA |
| Invitrogen | Paisley | UK |
| Melford | Ipswich | UK |
| Merk | Hertfordshire | UK |
| Millipore | Billerica | USA |
| MP Biomedicals UK | Cambridge | UK |
| Nanodrop Technologies Inc | Wilmington | USA |
| Narishige | London | UK |
| New England Biolabs | Hitchin | UK |
| Novagen | Nottingham | UK |
| Pang UK | Suffolk | UK |
| Perkin-Elmer | Beaconsfield | UK |
| Pharmacia | Uppsala | Sweden |
| Photometrics Ltd | Tuscon, AZ | USA |
| Promega | Southampton | UK |
| Qiagen | Crawley | UK |
| Roche | Welwyn Garden | UK |
| Sigma-Aldrich | Gillingham | UK |
| Vector Laboratories | Peterborough | UK |
| Stratagene | Cedar Creek | USA |

**Table 2.1 - Suppliers.**

# 2.2 Buffers and solutions

## 2.2.1 DNA/RNA techniques

6 x DNA loading buffer

-0.03% bromophenol blue

-0.03% xylene cyanol FF

-30% glycerol

-60 mM EDTA

-10 mM Tris-HCl (pH 7.6)

TAE agarose gel running buffer

-90 mM Tris-HCl (pH 8.3)

-90 mM acetic acid

-2 mM EDTA

## 2.2.2 Protein techniques

NuPAGE Transfer buffer (pH 7.4)

-25 mM Tris-base

-200 mM glycine

-20% methanol

PBS (Phosphate buffered saline) (pH 7.4)

-137 mM NaCl

-6.5 mM $Na_2HPO_4$

-2.7 mM KCl

-1.5 mM $KH_2PO_4$

PBS-T (PBS-Tween-20) (pH 7.4)

-PBS (pH 7.4)

-0.1% Tween-20

Phospho co-Immunoprecipitation (co-IP) buffer (pH 7.4)

-20 mM Hepes (pH 7.6)

-10 mM KCl

-1.5 mM $MgCl_2$

-150 mM NaCl

-0.5% Triton-X-100

-10 mM sodium pyrophosphate

-1 mM (Dithiothreitol) DTT

-1 protease inhibitor cocktail tablet (Roche)

-10 nM Calyculin A

Phospho-Radio-Immunoprecipitation Assay (RIPA) buffer (pH 7.4)

-50 mM Tris-base

-150 mM NaCl

-1 mM EDTA

-1% NP40

-0.2% SDS

-10 mM sodium pyrophosphate

-25 mM β-glycerophosphate

-0.5% sodium deoxycholate

-100 mM sodium orthovanadate

-5 mM sodium fluoride

-1 mM DTT

-1 complete protease inhibitor cocktail tablet (Roche)

-10 nM Calyculin A

Protein binding buffer

-50 mM Tris (pH 8)

-1.5 mM $MgCl_2$

-150 mM NaCl

-0.5 mM DTT

-0.05% Triton-X-100

Pull-down wash buffer

-50 mM Tris (pH 8)

-1.5 mM $MgCl_2$

-200 mM NaCl

-0.5 mM DTT

-0.1% Triton-X-100

Protein purification lysis buffer (on ice)

-20 mM Tris-HCl (pH 8)

-150 mM NaCl

-10 mM Imidazole

-1 complete protease inhibitor cocktail tablet, EDTA free (Roche)

-1 x BugBuster solution (Novagen)

-1 mM DTT

-25 units/ml benzonase

-1000 units/ml lysozyme

His-column protein purification wash buffer (on ice)

-300 mM NaCl

-50 mM Tris-HCl (pH 8)

-20 mM Imidazole

-1 mM DTT

-1 complete protease inhibitor cocktail tablet, EDTA free (Roche)

His-column protein purification elution buffer (on ice)

-300 mM NaCl

-50 mM Tris-HCl (pH 8)

-250 mM Imidazole

-1 mM DTT

-1 complete protease inhibitor cocktail tablet, EDTA free (Roche)

Strep-column protein purification wash buffer (on ice)

-300 mM NaCl

-50 mM Tris-HCl (pH 8)

-1 mM DTT

-1 complete protease inhibitor cocktail tablet, EDTA free (Roche)

Strep-column protein purification elution buffer (on ice)

-150 mM NaCl

-50 mM Tris-HCl (pH 8)

-1.5 mM $MgCl_2$

-30% glycerol

-2.5 mM D-desthiobiotin

-1 mM DTT

-1 complete protease inhibitor cocktail tablet, EDTA free (Roche)

4 x Sample Loading Buffer

-20% Glycerol

-200 mM 2-mercaptoethanol

-4% SDS

-0.2% Bromophenol blue

-100 mM Tris-HCl (pH 6.8)

Sodium dodecyl sulphate polyacrylamide gel electrophoresis (SDS-PAGE) running buffer (pH 8.8)

-25 mM Tris-base

-250 mM Glycine

-0.1% SDS

20 x SSC (Sodium Chloride / Sodium Citrate buffer) (pH 7.0)

-3 M NaCl

-0.3 M $Na_3C_6H_5O_7.2H_2O$

TBS (Tris-buffered saline) (pH 7.4)

-10 mM Tris-base

-137 mM NaCl

TBS-T

-TBS

-0.1% Tween-20

Tris-HEPES Running Buffer (pH 8)

-100 mM Tris-base

-100 mM Hepes (pH 7.6)

-3.5 mM SDS

## 2.2.3 Bacterial Techniques

Luria Broth (LB)

-10 g/l NaCl

-10 g/l Bacto-tryptone

-5 g/l Yeast extract

Luria Broth (LB) agar

-10 g/l NaCl

-10 g/l Bacto-tryptone

-5 g/l Yeast extract

-15 g/l Difco agar

TE (pH 7.5)

-10 mM Tris-HCl

-1 mM EDTA

LiOAc/1x TE

-50 ml 10 x TE

-50 ml 10x (1M) LiOAc

40% PEG/ 0.1 M LiOAc/1xTE/ (50 ml)

-40 ml of 50% Polyethylene glycol (PEG) 3350

-5 ml 10x TE

-5 ml 10x (1M) LiOAc

## 2.2.4 Yeast techniques

Z Buffer

-60 mM $Na_2HPO_4$

-40 mM $NaH_2PO_4.H_2O$

-10 mM KCl

-1 mM $MgSO_4.7H_2O$

-39 mM 2-mercaptoethanol

Minimal Yeast Plates (pH 5.8) 1L

-6.7 g Yeast nitrogen base without amino acids

-20 g Agar

-100 ml of the appropriate sterile 10X amino acid dropout solution

-5% Glucose

- 200 mg arginine HCl
- 300 mg isoleucine
- 300 mg lysine HCl
- 200 mg methionine
- 500 mg phenylalanine
- 2000 mg threonine
- 300 mg tyrosine
- 200 mg uracil
- 1500 mg valine

*Add appropriate selection markers (below)

L-Adenine hemisulfate salt 100 mg/ 50ml

L-Histidine HCl monohydrate 100 mg/ 50ml

L-Leucine 500 mg/ 50ml

L-Tryptophan 100 mg/ 50ml

YPD medium

20 g/L Difco peptone

10 g/L Yeast extract

20 g/L Agar (for plates only)

### 2.2.5 Xenopus techniques

Marc's Modified Ringers (MMR) buffer

-100 mM NaCl

-2 mM KCl

-5 mM HEPES

-1 mM $MgCl_2$

-2 mM $CaCl_2$

-0.1% penicillin streptomycin

## 2.3 Bacterial work

### 2.3.1 Bacterial strains

The following strains of chemically competent *Escherichia coli* (*E. coli*) were utilised.

| Function | Strain | Genotype | Supplier |
|---|---|---|---|
| Plasmid propagation | XL1-Blue | *recA1 endA1 gyrA96 thi-1 hsdR17 supE44 relA1 lac [F´ proAB lacIqZΔM15 Tn10 (Tetr)]* | Stratagene |
| Recombinant protein expression | BL21(LysS) | *E. coli B, F-, dcm, ompT, hsdS(rB-mB-), gal(DE3) [pLysS Camr]* | Invitrogen |

**Table 2.2 - *E. coli* strains used.**

### 2.3.2 Bacterial growth

Bacteria were grown in Luria Bertani (LB) agar plates containing the appropriate antibiotics at 37ºC. Liquid cultures were grown in LB medium in a shaking incubator (250 rpm) at 37ºC. Plates were stored at 4ºC.

| Antibiotic | | Final concentration |
|---|---|---|
| Ampicillin | (Amp) | 100 µg/ml |
| Kanamycin | (Km) | 25 µg/ml |
| Chloramphenicol | (Chp) | 34 µg/ml |

**Table 2.3 - Antibiotic concentrations.**

### 2.3.1.1 Quick transformations

Chemical competent *E. coli* cells, prepared by Bill Richardson, were stored at -80ºC and thawed on ice. Per transformation 50-100 ng of plasmid DNA was added to 10 µl of cells, and incubated at 4ºC (on ice) for 2 minutes. The transformation mix was heat shocked for 45 seconds at 42ºC, and then incubated on ice for 2 further minutes. 250 µl of LB medium was added to the transformation mix prior to incubation at 37ºC for 60 minutes. 100 µl of the transformation mix was plated in LB agar plates containing the appropriate selection antibody ( Table 2.3). Plates were incubated overnight at 37ºC.

In all transformations a no plasmid DNA control was performed in parallel to test the antibiotic selection.

### 2.3.1.2 Standard transformations

Transformation of chemical competent *E. coli* cells with ligation products followed the same principal as quick transformations apart from the following; 5-10 ng of DNA was added to 50 µl of cells and incubated for 30 minutes on ice, before a 45 second heat shock at 42ºC and then incubated on ice for 2 further minutes. 450 µl of LB medium was added to the transformation mix prior to incubating the cells at 37ºC for 60 minutes. 100µl and 400µl were plated onto LB agar plates containing the appropriate selection antibody (Table 2.3).

# 2.4 General nucleic acid techniques

## 2.4.1 Plasmid DNA propagation and purification

Plasmid DNA was propagated in *Escherichia coli* (*E. coli)* (see 2.5), and purified using mini, midi or maxi QIAquick Prep kits (Qiagen) according to manufacturer's instructions.

## 2.4.2 Restriction digestion of DNA

Restriction digests were performed with restriction enzymes from Roche, New England BioLabs or Promega using appropriate buffers and according to the manufacturer's instructions. The final volume of enzyme never comprised more than 10% of the reaction volume. Digests were carried out to linearise DNA to confirm authenticity of plasmids after purification (see 2.4.1), for cloning (see 2.4.6), or *in vitro* transcription (see 2.4.14).

## 2.4.3 Agarose gel electrophoresis

1-2% agarose gels were routinely used for DNA/RNA visualisation. Agarose was dissolved in TAE by heating in a microwave until boiling, after cooling down, Gel-Red (Biotium) was added to a final concentration of 1/10 000. 6 x DNA loading buffer (see 2.2.1) was added to samples before loading. Gels were run at 25-100 volts in TAE buffer and visualized using a trans-illuminator (Geneflash). DNA band sizes were determined using a 100bp or 1kb DNA bench-top ladder (Promega), following manufacturer's instructions.

## 2.4.4 Gel purification of DNA fragments

Linearised DNA fragments from restriction digests (see 2.4.2), were run on 1-2% agarose gels (see 2.4.3). Following identification by UV light, the desired fragments were extracted with a sterile razor blade and purified using a QIAquick Gel Purification Kit (Qiagen) according to the manufacturer's instructions.

## 2.4.5 Purification of PCR products

Polymerase chain reaction products (PCR) (see 2.5) were purified using a QIAquick PCR product purification kit (Qiagen) according to manufacturer's instructions.

## 2.4.6 Plasmid de-phosphorylation

When performing DNA cloning, after restriction digest (see 2.4.2), linearised DNA fragments from the vector backbone plasmids were de-phosphorylated, to prevent self-ligation, using Shrimp Alkaline Phosphatase (Fermentas) according to manufacturer's instructions. The enzyme was heat inactivated at 65°C for 10 minutes before ligation with insert DNA (see 2.7)

## 2.4.7 DNA ligations

Ligation of DNA fragments, after gel purification (see 2.4.3.1), was performed at room temperature for 2 hours, for compatible ends or overnight at 16°C for blunt ends, using a T4 DNA ligase (Stratagene) according to manufacturer's instructions. Different molar ratios of vector back-bone to insert (1:1; 1:3 and 1:5) were utilised. Two controls were performed: one with no insert and another with no ligase.

## 2.4.8 Quantification of nucleic acids

DNA and RNA was quantified by measuring its absorbance at 260nm using a Nanodrop ND-1000 (Nanodrop Technologies Inc.) spectrophotometer.

## 2.4.9 DNA phenol/chloroform extraction

Plasmid DNA was purified by adding an equal volume of phenol:chloroform:isoamyl alcohol (25:24:1; pH 7.8), followed by vortexing and centrifugation (14,000 rpm, 2 minutes). The aqueous phase (top layer) was collected. The same procedure was repeated and the final supernatant ethanol precipitated (see 2.4.1.3).

## 2.4.10 Ethanol precipitation of DNA

DNA was mixed with 0.1 volumes of 3 M NaOAc (pH 5.2) and 2.5 volumes of 100% ethanol (ice cold), vortexed and incubated for 30 minutes at -20°C. The DNA was spun down at 14,000 rpm for 30 minutes at 4°C and the supernatant removed. The DNA pellet was washed twice with 80% ethanol (ice cold) and spun down at 14,000 rpm for 10 minutes. The supernatant was removed and the resultant pellet left to dry at room temperature for 10 minutes followed by resuspension in distilled water.

## 2.4.11 DNA sequencing

All plasmids used were sequenced at the technical services facility in the MRC Human Genetics Unit, Edinburgh. Results were analysed using the program vector NTI (Invitrogen) or BioEdit 7.0.0 (Ibis Therapeutics).

## 2.4.12 RNA extraction

RNA was extracted from tissues and cells using Tri-Reagent (Ambion) following manufacturer's instructions.

## 2.4.13 Ethanol precipitation of RNA

RNA was precipitated by mixing with 0.05 volumes of 3 M NaOAc (pH 5.2) and 2.5 volumes of 100% ethanol. This solution was vortexed and incubated at -20°C for 1 hour. RNA was pelleted by centrifugation at 14,000 rpm for 30 minutes at 4°C and the supernatant removed. The pellet was then washed twice with 80% ice cold ethanol, left to dry at room temperature for 2 minutes, followed by resuspension in nuclease-free water.

## 2.4.14 *In vitro* transcription

mRNAs for micro-injections or cell-free translation were transcribed *in vitro*. Prior to transcription, plasmids were linearised by restriction enzyme digestion (see 2.4.2) at the 3' end of the template sequence and purified using the QIAquick PCR kit (Qiagen) (see 2.4.5).

50µl Reaction Mix:

-1x transcription buffer (Stratagene)

-30 mM DTT

-1 mM ATP

-1 mM CTP

-1 mM UTP

-7 mM $m^7G$ cap analogue (New England Biolabs)

-100 units RNasin (Promega)

-0.5 - 2 µg/µl linearised DNA template

-4 units T7 or SP6 RNA polymerase (Stratagene)

Transcription reactions were incubated at 37°C for 5 minutes in the absence of GTP to allow optimal capping of transcripts, followed by addition of 1 mM of GTP and a further incubation of 120 minutes at 37°C. In order to destroy the original DNA template 2.5 units of RQ1 RNase-free DNase (Promega) was added to the reaction mix and incubated for 30 minutes at 37°C.

Following two acid phenol:chloroform:isoamylalcohol (25:24:1) (Ambion) extractions (see 2.4.7), the purified RNA was passed over a Chroma Spin-100 DEPC-$H_20$ column (Clontech) to remove unincorporated cap analogue, nucleotides and partially transcribed RNA products. Finally the RNA was ethanol precipitated (section 2.4.8) and resuspended in nuclease-free water (Ambion).

# 2.5 Polymerase chain reaction (PCR)

## 2.5.1 Polymerase chain reaction (PCR)

Unless otherwise stated PCR reactions were carried out with a Bio-X-Act Long High-Fidelity polymerase (Bioline).

50 µl Reaction Mix:

-50 ng of DNA template

-1x PCR reaction buffer (Bioline)

-5 mM $MgCl_2$

-1 mM dNTPs

-5 pM forward primer

-5 pM reverse primer

-3 units of Bio-X-Act long high-fidelity polymerase (Bioline)

Reactions were incubated in a Dyad PCR machine (Bio-Rad) using the following program:

1) 5 minutes 95°C
2) 1 minute 95°C
3) 30 seconds 50-65°C (according to the Tm of the primer +3º)
4) 1 minute (per kb) 68°C
   *2-4 repeated 24 times
5) 10 minutes 68°C

## 2.5.2 Reverse transcription PCR (RT-PCR)

cDNA was prepared from RNA retrieved from tissues (see 2.4.10) using a First Strand cDNA Synthesis AMV Kit (Roche) with Poly(dT) and random primers according to manufacturer's instructions. Intron-spanning gene specific primers (see Table 2.9) were used in a PCR reaction (see 2.5) to detect and amplify desired transcripts.

25 µl Reaction Mix:

-1-2 µg of RNA

-5 µl 5 x Reaction Buffer

-2.5µl 40 mM sodium pyrophosphate

-2.5 µl dNTP mix

-0.5 µg primer/µg RNA of poly(dT) primer

-0.5 µg primer/µg RNA of random primer

-40 units RNasin® Ribonuclease Inhibitor

-30 units AMV RT

Reactions were incubated in a Dyad PCR machine (Bio-Rad) using the following program:

1) 10 minutes 25°C
2) 60 minutes 42°C
3) 5 minutes 99°C

cDNA samples were then subjected to PCR (previous section).

### 2.5.3 Site directed mutagenesis

Specific mutations were created in DNA templates using a QuikChange® II XL Site-Directed Mutagenesis Kit (Stratagene), following manufacturer instructions. Briefly, two oligonucleotide primers containing the desired mutation, each complementary to opposite strands of the original DNA vector, were extended by PCR with a Pfu Turbo DNA polymerase. The final PCR product contained parental template and the newly synthesised mutated plasmid containing staggered nicks. This was then subjected to Dpn I endonuclease treatment (target sequence: 5´-Gm6ATC-3´), which specifically targets methylated and hemimethylated DNA and digested the parental DNA template. The DNA vector containing the desired mutations was then transformed into competent *E. Coli.* The mutagenesis technique will be discuss further in Chapter 5.

## 2.6 Yeast work

### 2.6.1 Yeast strains used

Yeast-two hybrid assays were performed with *Saccharomyces cerevisiae (S. cerevisiae)* strain L40ura$^-$ *(MATa,ura3-52, leu2-3,112, his3, trpΔ1, ade2, Δgal4, lys:(lexAop)-HIS3, ura3:(lexAop)-LacZ)* (Zhang *et al.*, 1999).

### 2.6.2 Growth of yeast strains

Yeast was grown in YPD agar plates or YPD medium at 30°C. Yeast transformed with plasmids were grown at 30°C on minimal media supplemented with amino acids apart from those used for selection.

### 2.6.3 Yeast transformations

A single colony of L40ura$^-$ was used to inoculate 5 ml of YPD media and incubated overnight at 30°C with shaking at 250 rpm. The following morning 50 ml of YPD media was inoculated with 1 ml of the overnight culture and incubated with

shaking at 30°C until $OD_{600}$ was between 0.4-0.6. A transformation mix was prepared with 50 µl 0.1 M LiOAc/1 x TE and 6 µl of salmon sperm carrier DNA (Clontech) with 1 µg of each plasmid to be transformed. 1 ml of yeast culture was used per transformation. This was prepared by spinning down the yeast culture in a 1.5 ml Eppendorf at 7,000 rpm. The supernatant was removed and the yeast pellet washed with 1 ml of water followed by 1 ml of 0.1 M LiOAc/1xTE. The transformation mix was added to the washed pellet together with 300 µl of 40% PEG/0.1 M LiOAc/1 x TE and incubated at 30°C for 30 minutes, prior to heat shock at 42°C for 15 minutes. Finally the transformed yeast was pelleted at 7,000 rpm, resuspended in 400 ul of distilled water and 200 ul plated onto selective media YPD plates. Plates were incubated for 3 days at 30°C.

### 2.6.4 β-galactosidase assay

Two-hybrid protein-protein interactions were detected by β-galactosidase assay. Colonies from transformed yeast were streaked onto 2 mm Whatman filter paper, placed on a selective media plate and grown over night at 30°C. The filter papers were removed from the plates and fast frozen twice in liquid nitrogen for 15 seconds and thawed at room temperature. These were then placed into Petri dishes containing two Whatman filter papers soaked with Z-buffer (see 2.2.4) supplemented with 100 µg/ml X-gal. The Petri dish was sealed with parafilm and incubated at 30°C and colour changes monitored.

## 2.7 General protein work

### 2.7.1 Protein extraction

All protein samples were prepared with phospho-RIPA buffer (pH 7.4) (see 2.2.2), apart from samples used for co-immunoprecipitation, which were prepared in co-IP buffer (see 2.2.2). All the procedures were conducted on ice to minimise protease activity.

#### 2.7.1.1 From tissues

Mouse organs were snap frozen in cryovials using liquid nitrogen immediately upon collection. Tissues were homogenised in phospho-RIPA buffer, using the minimal volume required to submerge the tissue, using a Qiagen TissueLyser homogeniser (Qiagen) (25Hz, 2 minutes) followed by 10 minute incubation on ice. The homogenised solutions were then centrifuged at 14,000 rpm for 10 minutes at 4°C to pellet debris. The supernatant was collected and stored at -20°C for future applications.

#### 2.7.1.2 From cultured mammalian cells

Cultured cells were washed twice with 0.5 ml/ $cm^2$ of ice cold PBS and collected in 0.5-1 ml of ice cold PBS using a cell scrapper. Cells were pelleted at 1000g for 5 minutes at 4°C. The cell pellet was then re-suspended in phospho-RIPA buffer followed by "aggressive pipetting". Cells were left on ice for an extra 5 minutes to allow complete cell lysis. The homogenised solution was then centrifuged at 14,000 rpm for 10 minutes at 4°C. The supernatant was recovered and stored at -20°C for future applications.

### 2.7.2 Bradford assay

Protein concentrations were quantified using Bradford Protein Assay Reagent (Bio-Rad). 1 µl of protein sample was added to 99 µl of water and 900 µl of Bradford Reagent in a spectrophotometer microcuvette. Using a Genequant Pro spectrophotometer (GE Healthcare) the 595 nm absorbance was read and the concentration of the sample calculated using a standard curve generated with bovine serum albumin (0-20 µg).

### 2.7.3 Polyacrylamide gel electrophoresis (PAGE)

SDS-polyacrylamide gel electrophoresis was performed using 10% acrylamide, 4-12% NuPAGE MOPS (Invitrogen), or 8-16% Tri-HEPES-SDS gels (ThermoScientific). Samples were mixed with 4 x sample loading buffer (see 2.2.2)

and boiled at 95°C for 10 minutes before loading alongside pre-stained or unstained protein Benchmark ladders (Invitrogen). Gels were run until the loading dye reached the bottom of the gel.

#### 2.7.3.1 10% acrylamide gels

The separating gel (0.375 M Tris, 3.5 mM SDS, 10-12% [v/v] acrylamide/bisacrylamide [29:1], 4.4 mM ammonium persulphate APS, 6.7 mM TEMED, pH 8.8) was poured into the apparatus and allowed to polymerise before addition of the stacking gel (0.125 M Tris, 3.5 mM SDS, 4% acrylamide/bisacrylamide [29:1], 4.4 mM APS, 6.7 mM TEMED, pH 6.8) with an appropriate comb to form the desired number/size of wells. Gels were run in SDS-PAGE running buffer (25 mM Tris, 250 mM glycine, 0.1% SDS; pH 8.8) at 100-150V.

#### 2.7.3.2 4-12% NuPAGE Invitrogen gels

Pre-cast gels purchased from Invitrogen were run using NuPAGE MOPS SDS Running Buffer (50 mM MOPS, 50 mM Tris, 0.1% SDS, 1 mM EDTA; pH 7.7) (Invitrogen) at 100-200V.

#### 2.7.3.3 8-16% Tris-HEPES-SDS ThermoScientific gels

Pre-cast gels bought from ThermoScientific were run with Tris-HEPES Running Buffer (100 mM Tris-Base, 100 mM Hepes, 3.5 mM SDS; pH 8) at 150-200V.

### 2.7.4 Staining protein gels

Proteins resolved by SDS-PAGE were visualised using GelCode Blue (ThermoScientific). Following electrophoresis, gels were washed three times for 10 minutes in 150 ml of water then incubated overnight in sufficient GelCode Blue stain to give full immersion at 4°C on a rocking platform. Excess stain was removed the following day by repeated 20 minute washes in 200 ml water at room temperature on a rocking platform.

## 2.7.5 Western blotting

In the following section, all manipulations were performed with the minimal volume required to submerge the gel or the membrane. Washes were performed in an abundant volume of TBS-T at room temperature on a rocking platform.

### 2.7.5.1 Transfer

After electrophoresis the gel was incubated in 100 ml of NuPAGE transfer buffer (see 2.2.2) for 10 minutes. The gel, together with an Immobilon-P membrane, previously hydrated in 25 ml of 100% methanol and incubated for 10 minutes in 100 ml of NuPAGE transfer buffer (Millipore), was "sandwiched" between 6 sheets of Whatman filter paper soaked in NuPAGE Transfer Buffer. Proteins were transferred at 100 mA for 60 minutes using a V20-SDB semi-dry blotter (SCIE-PLAS).

### 2.7.5.2 Blocking, antibody incubation and detection

Unless otherwise stated, the membrane was blocked in 5 % (w/v) skimmed milk in TBS-T for 1 hour at room temperature on a rocker.

Primary antibodies were diluted (see 2.15.2 Table 2.7) in 5 % (w/v) skimmed milk in TBS-T and incubated for 1 hour at room temperature or overnight at 4°C on a rocking platform. After primary antibody incubation, the membrane was washed 3 times for 5 minutes in TBS-T. The membrane was then incubated for 1 hour at room temperature with secondary antibody conjugated to HRP diluted (see 2.15.2 Table 2.8) in 5 % skimmed milk in TBS-T. The membrane was washed 3 times in TBS-T for 10 minutes and incubated in enhanced chemiluminescence solution (ECL) (GE Healthcare) according to manufacture's instructions. Finally membranes were blotted dry and exposed to ECL Hyperfilm (GE Healthcare) and developed using Exograph compact x4 X-ray processor (XoGraph Imaging Systems).

## 2.7.6 Immunoprecipitation (IP)

100 µl of 50 % protein G sepharose beads slurry (GE Healthcare) was washed 3 times in 1 ml of ice cold phospho-RIPA buffer (beads were pelleted at 2,500 rpm, 1

minute at 4°C between washes). This slurry was then added to 1 mg of protein lysate in a final volume of 1ml made up with phospho-RIPA buffer containing 1 µg of the relevant antibody and tumbled overnight at 4°C on a rotor. Antibody bound beads were washed 5 times with 1 ml of ice cold phospho-RIPA buffer (beads were pelleted at 2,500 rpm, 1 minute at 4°C between washes). The stringency of the washes was varied by adjusting the NaCl concentration (150 mM-600 mM) according to the antibody used and is explained in detail in the appropriate results sections. The beads were collected using a Pierce spin cup (ThermoFisher) (2,500 rpm, 1 minute at 4°C), and eluted in sample loading buffer (see 2.2.2) by heating to 75°C for 10 minutes. Beads were pelleted at 14,000 rpm for 1 minute and the supernatants run on a SDS-PAGE gel and submitted to western blot analysis.

## 2.7.7 In vitro translation using cell free extracts

In vitro synthesis of proteins in cell-free extracts was used to verify the size of protein products from plasmid constructs.

### 2.7.7.1 Rabbit reticulocyte lysate

Nuclease treated rabbit reticulocyte lysate (RRL) (Promega) is a commonly utilised *in vitro* translation system that is favoured due to its ability to synthesise relatively large proteins and its low background due to absence of endogenous mRNAs. The RRL system was used according to manufacturer's instructions with 90 minute incubations at 30°C.

50 µl RRL reaction mix:

-2 µg of RNA

-1 µl amino acid mixture minus methionine (1 mM)

-2 µl of [$^{35}$S]-methionine (1,200 Ci/mmol at 10 mCi/ml) (MP Biomedical)

-35 µl of rabbit reticulocyte lysate (Promega)

-Nuclease free water to a final volume of 50 µl

$^{35}$S-labelled proteins were run at 150V on NuPAGE 4-12 % Bis-Tris pre-cast gels (see 2.7.3.) with a pre-stained protein ladder (BioLabs). For non-radiolaballed

proteins to test antibody specificity, the amino acid mixture minus methionine and the [$^{35}$S]-methionine was substituted with 1 ul of complete amino acid mixture (1 mM).

#### 2.7.7.2 Transcription and Translation (TnT)

TnT is a modified rabbit reticulocyte lysate that contains a bacteriophage polymerase, providing a one step system that both transcribes and translates mRNAs. TnT reactions were performed with the T7 Quick TNT system (Promega) according to manufacturer's instruction.

50 µl TnT reaction mix:

-1 µg of DNA plasmid

-1 µl of 1 mM [$^{35}$S]-methionine at 10 mCi/ml

–40 µl TnT® T7 Quick Master Mix.

-Nuclease free water to a final volume of 50 µl

TnT expressed proteins were run at 150V on NuPAGE 4- 12% Bis-Tris pre-cast gels (Invitrogen) with a pre-stained protein ladder (BioLabs) as described in section 2.7.3.2.

## 2.8 Recombinant protein generation

### 2.8.1 His-Strep recombinant protein induction and purification

Single transformed *E. coli* colonies (section 2.3.3) were used to inoculate 5 ml LB liquid cultures containing the appropriate antibiotic and grown overnight at 37ºC. 0.5 ml of the overnight culture was used to inoculate 200 ml of fresh LB media with appropriate antibiotics and was grown at 37ºC (aerated at 250 rpm) until $OD_{600}$ ~ 0.4. Recombinant protein induction was achieved by addition of 200 µl of 1 M iopropyl-β-D-thio-galactoside (IPTG) for 4 hours at 22°C. Cells were collected by centrifugation at 4,700 rpm for 30 minutes at 4ºC. Cell pellets were lysed by addition of 10 ml of protein purification lysis buffer (see 2.2.2) and incubated at room

temperature on a turn-wheel for 30 minutes prior to removal of cell debris by centrifugation at 4,700 rpm for 20 minutes at 4ºC.

1 ml of Ni-NTA agarose beads (Qiagen) was added to a Bio-Rad Poly-Prep chromatography column and washed twice by addition 10 ml of His-column protein purification wash buffer (see 2.2.2) and allowed to drain by gravity flow. The cleared lysate was passed over the column containing the washed beads. The flow through was collected and passed over the column for a second time. The column was washed three times with 10 ml His-column protein purification wash buffer and bound proteins eluted with 10 ml of His-column protein purification elution buffer (see 2.2.2).

Bio-Rad Poly-Prep chromatography columns containing 1 ml of Strep-Tactin Superflow agarose beads (Novagen) were washed twice with 10 ml of Strep-column protein purification wash buffer (2.2.2) and allowed to drain by gravity flow. The eluate from the Ni-column was passed over the pre-washed Strep-column with the flow-through being reapplied. The column was washed three times by addition of 10 ml of Strep-column protein purification wash buffer. Prior to elution, columns were capped to allow a 5 minute incubation (at 4ºC) with 1 ml of Strep-column elution buffer (see 2.2.2). Eluates were collected by gravity flow in 0.5 ml volume fractions. Following each 0.5 ml collection, an extra 0.5 ml of Strep-column protein purification elution buffer was added to the column, up to a total of 4 ml (8 samples of 0.5 ml). Samples were quantified (section 2.8.2) and stored at -80ºC.

## 2.8.2 Quantification of induced purified proteins

Two different dilutions of each eluate and four different concentrations of a BSA standard (250-1000ng/µl) were run on a SDS-PAGE gel and stained with SYPRO Ruby (Invitrogen) following manufacturer's instructions. Protein concentrations were calculated using ImageQuant software (GE Healthcare) after scanning the gel with a 488 nm excitation laser (Typhoon Variable Mode Imager), by comparison with the known BSA concentrations.

## 2.9 Pull-down assays

50 µl of glutathione sepharose 4B beads (GE Healthcare) were washed twice in 1 ml of binding buffer (see 2.2.2), followed by an incubation with 1 ml of 1 µg/µl BSA for 30 minutes at room temperature on a rotating wheel. Beads were pelleted at 2,500 rpm at 4ºC for 1 minute and washed two times in 1 ml of binding buffer. 3 pmol of GST proteins (GST and GST-hDAZL (Abnova #H00001618-P01)) were added to the beads and the volume increased to 1 ml with binding buffer (see 2.2.2) before incubation for 1 hour at 4ºC on a rotating wheel. Beads were spun down at 2,500 rpm at 4ºC for 1 minute and the supernatant containing unbound proteins removed. 30 pmol of purified His-PABP-Strep proteins (see 2.8.1) in binding buffer (see 2.2.2) was added to the beads in a total volume of 1 ml. The samples were tumbled for 1 hour at 4ºC on a rotating wheel. Finally, beads were transferred to a Pierce SpinCup (ThermoFisher) and washed five times with 1 ml of pull-down wash buffer (see 2.2.2), pelleting at 2,500 rpm for 1 minute at 4$^{o}$C between washes. 30 µl of sample loading buffer was added to the samples before heating at 75°C for 5 minutes and eluates collected by spinning the columns at 14,000 rpm for 1 minute. The recovered samples were run on a SDS-PAGE gel and subject to western blot analysis.

## 2.10 Histological analysis

### 2.10.1 Fixation, embedding and sectioning

Tissues were fixed either in Bouin's or 4% NBF in 20x the volume of the tissue. After fixation, tissues were washed twice with, and stored in, 70% ethanol until being processed. Tissues were embedded in paraffin wax by the histology core facility in the CRH on a Leica TP1050 processor (Leica Microsystems).

Paraffin embedded tissues were sectioned (5 µm) using a Leica RM2135 microtome. Sections were floated on a 50°C water bath and mounted on electrostatic charged glass slides (Merck - BDH #406/0179/00) and dried overnight at 50°.

### 2.10.2 De-waxing and re-hydration

Paraffin fixed tissues mounted on slides were subject to de-waxing and re-hydration. Slides were de-waxed by two 5 minutes washes in a xylene bath and then re-hydrated in baths with decreasing concentrations of ethanol starting at 100%, 95% and finally 70% for 20 seconds each. Slides were then washed in running tap water for 30 seconds. At this point the sections were ready for staining or immunohistochemical (IHC) analysis.

### 2.10.3 Haematoxylin and eosin staining of tissues

In serial sections of tissues, every tenth section was submitted to H&E to assess tissue and cell morphology. The in between sections were used for IHC if the histology was satisfactory.

Following de-waxing and re-hydration (see 2.10.2), sections were immersed in a haematoxylin bath for 5 minutes to stain the nuclei of cells blue. The slides were then washed in running tap water for 30 seconds and immersed on 1% acid alcohol (1 % HCl, 70 % ethanol) for 5 seconds to remove non-specific cytoplasmic staining. Slides were washed in running tap water followed by a 30 second immersion in Scott's tap water bath (20 mM $KCl_2$; 160 mM $MgSO_4$) and washed again in running tap water. In order to stain the cytoplasm, the slides were immersed in Eosin bath for 30 seconds, giving the cytoplasm a distinct pink colour. After washing the slides one last time in tap water, they were dehydrated by immersion in a series of increasing concentrations of ethanol (70 %, 80 %, 95 % 2x 100 %) for 20 seconds each. Finally the slides were incubated twice for 5 minutes in xylene and mounted in Pertex (Cell Path) with a glass cover slip.

### 2.10.4 Immunohistochemistry

#### 2.10.4.1 General principle

Immunohistochemistry was used to visualise the expression of proteins in tissues using antibodies specific for target proteins. Detection is achieved by a second antibody conjugated to HRP (chromogenic DAB detection) or fluorescent

detection tag (Immunofluorescence) (Figure 2.1).

All the IHC was carried out following the following steps:

-Antigen retrieval (not applicable for PABP1)

-Blocking of non specific interaction

-Primary antibody

-Secondary antibody

-Detection

-Counter-staining

-Dehydration and xylene wash

-Mounting with cover slip

Two separate washes of 5 minutes were performed between each one of the previous steps in 400 ml of TBS on a rocking platform at room temperature.

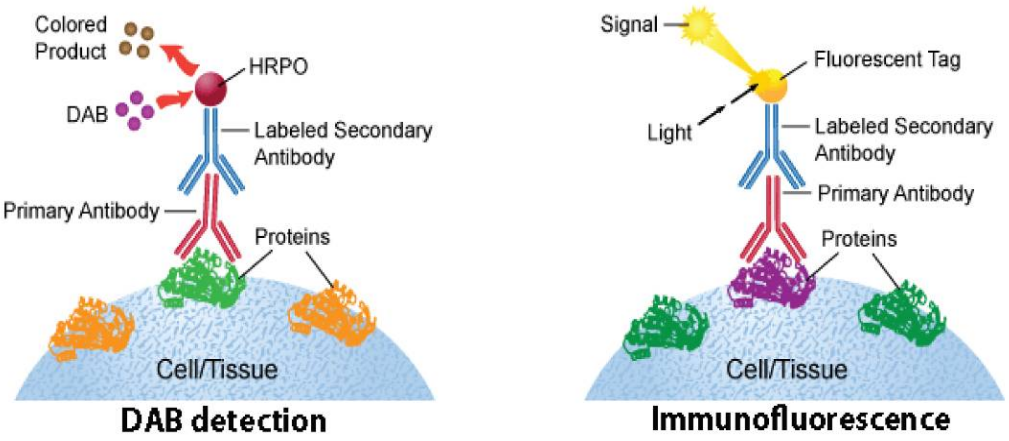


**Figure 2.1 - IHC detection systems. Illustration of DAB and immunofluorescence detection systems for Immunohistochemistry (IHC).** Adapted from - http://www.leinco.com/immunohistochemistry

Dewaxed and de-hydrated sections (see 2.10.2) were submitted to an antigen retrieval step, with the exception of PABP1 antibody which did not require an antigen retrieval step. Antigen retrieval uncovers possible hidden antigen sites by breaking cross-links between proteins formed due to formalin fixation. For this, the slides were boiled for 5 minutes in 0.01 M citrate buffer (pH 6.0) in a pressure cooker and then left to stand in the citrate buffer for 20 minutes. Subsequently slides were incubated in 30 % hydrogen peroxide in methanol bath on a rocking platform for 30 minutes to block any endogenous peroxidase present in the tissues (this step

was only applied for the chromogenic and the tyramide fluorescence detection systems). The slides were washed in tap water followed by two washes with TBS. Samples were then incubated with 100 µl blocking solution (5 % v/v serum from the animal species used to raise secondary antibody, 5 % w/v BSA in TBS) for 1 hour at room temperature. This minimizes the non-specific binding of the antibodies to the tissue. After blocking, sections were incubated with the primary antibody diluted in blocking solution (see 2.15.2 Table 2.7) and incubated over night at 4°C. The following morning slides were washed twice with TBS and incubated with the secondary antibody (see 2.15.2 Table 2.8) diluted in blocking solution for one hour at room temperature. The slides were then washed twice for in TBS. The following steps were dependent on the detection system used.

### 2.10.4.2 Chromogenic DAB detection

In this detection system, the secondary antibody is conjugated to biotin, which binds streptavidin conjugated to horseradish peroxidase (HRP) that when catalyses the 3, 3'diaminobenzidinetrahydrochloride (DAB) substrate and gives a brown colour.

After the secondary antibody incubation and subsequent TBS washes (see 2.10.4.1), the slides were incubated with 100 µl of 1 µg/ml streptavidin-HRP (Dako Labs) for 30 minutes at room temperature. Slides were washed two times for 5 minutes in a TBS bath. DAB solution was diluted in the provided buffer (ImmPACT DAB kit - Vector Lab) according to manufacturer's instructions. 100 µl of DAB solution was added to the tissue section. Incubation periods with DAB solution vary depending on the antibody and the tissue, therefore each slide was prepared individually and colour change monitored under a light microscope for between 30 seconds to 1 minute. DAB reaction was stopped by washing slides in tap water. The tissue sections were then counter-stained with haematoxylin, dehydrated and mounted (see 2.10.3).

Sections were examined on a Provis AX70 (Olympus Optical) light microscope fitted with a Canon DS6031 camera (Canon Europe) and images analysed using Adobe Photoshop CS2 (Adobe Systems Europe Ltd) and AxioVS40 v4.8 (Carl Zeiss

Ltd).

### 2.10.4.3 Immunofluorescence

#### 2.10.4.3.1 Direct detection

In this detection system the secondary antibody is conjugated with a fluorescent marker (see Figure 2.1), thus following incubation with the secondary antibody the slides were washed twice in 400 ml bath of TBS-T for 5 minutes in a rocking platform at room temperature, and counter-stain applied (see DAPI counter staining 2.10.4.3.3).

#### 2.10.4.3.2 Tyramide signal amplification detection

The tyramide signal amplification (TSA) system (Perkin Elmer) is used to enhance detection in IHC. Tyramide is a phenolic compound activated by HRP that works as an amplification reagent, by covalently binding to tyrosine residues of adjacent proteins. Activation only occurs immediately adjacent to sites at which HRP is bound (Figure 2.2).

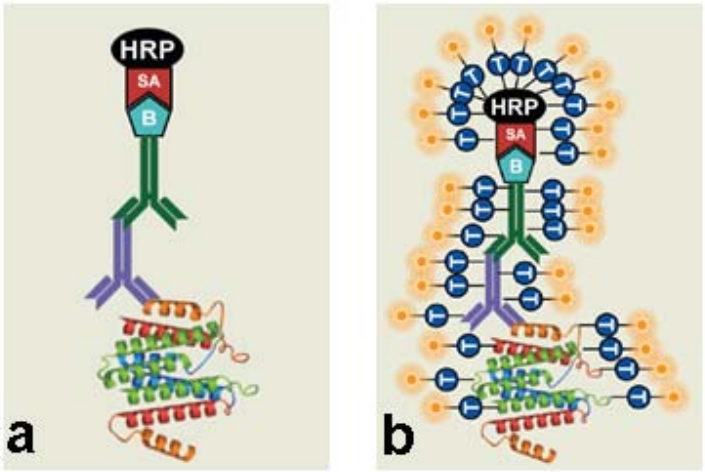


**Figure 2.2 - Tyramide signal amplification (TSA) diagram.** Illustration of TSA; a – standard HRP conjugated detection; b – TSA. B – biotin label; SA – streptavidin; HRP Horseradish peroxidase; T – tyramide. Adapted from - http://www.perkinelmer.com/pages/020/staticpages/tsasystems.xhtml

Following incubation with the appropriate peroxidase-conjugated secondary antibody (see 2.10.4.1), slides were washed twice for 5 minutes in a TBS bath. Slides

were then incubated for 10 minutes at room temperature with the fluorescein tyramide signal amplification (TSA) diluted 1:50 in the TSA buffer provided with the TSA Kit (Perkin Elmer). Slides were finally washed in TBS-T for 5 minutes and counter-staining with DAPI.

#### 2.10.4.3.3 Fluorescent counter-staining with DAPI

Following direct or TSA immunofluorescence detection nuclei were visualised by DAPI fluorescent stain. After washing slides in TBS-T, sections were stained by a 10 minute incubation at room temperature in 100 µl of DAPI (diamidino-2-phenylindole) (Sigma) diluted 1:1000 in TBS. The slides were then washed in a TBS-T bath for 1 minute and mounted using PermaFluor (ThermoScientific) and a glass cover slip.

Fluorescent images were captured using a Zeiss LSM 710 Meta Axiovert 100M confocal microscope (Carl Zeiss Ltd). DAPI signal was detected with a laser emission at 409-480 nm and excitation at 405 nm. Alexa-488 was obtained with emission at 490-539 nm and excitation at 488 nm. Finally alexa-546 was obtained with emission at 549-670 nm and excitation at 546 nm.

All images were analysed in Adobe Photoshop CS2 (Adobe Systems Europe Ltd).

## 2.11 In situ proximity ligation assay

This technique allows the detection of endogenous protein interactions in tissue samples prepared for microscopy. Briefly, target proteins are detected with primary antibodies (raised in different species) which are themselves detected with oligonucleotide labelled secondary antibodies (PLA probes). The PLA probes are ligated through the addition of complementary oligonucleotides and amplified by rolling-circle amplification. Ligation only occurs when the two PLA probes are in close proximity of less than 40 nm. The result is a several hundred-fold increase in the number of oligonucleotides which are detectable through hybridization of fluorescence labelled oligonucleotides complementary to the amplified sequence. As each amplified PLA signal can be visualised as an individual fluorescent dot, this

allows the localization of specific protein-protein interactions, within tissues and cells (Soderberg *et al.*, 2006).

Until the addition of the PLA probed secondary antibodies, the PLA procedure follows the same protocol as previously described for IHC (see 2.10.4.1). All solutions, buffers and enzymes describe hereafter are provided as part of a PLA kit (OLink biosciences) and were used following manufactures instruction. All described TBS-T washes represent two 400 ml bath washes in TBS-T for 5 minutes at room temperature on a rocking platform. Each incubation was performed in 100 µl volumes, covering the entire tissue at 37°C on a humidity incubator.

After primary antibody incubation and the following TBS-T washes, the sections were incubated with secondary antibodies, PLA probes for 2 hours. The slides were then washed twice in TBS-T followed by incubation with the hybridization solution for 15 minutes. After a 1 minute wash with TBS-T, slides were incubated with the Duolink ligation solution for 15 minutes, and washed twice for two minutes in TBS-T. Sections were then incubated with the PLA polymerase enzyme solution for 90 minutes. After two washes with TBS-T, the slides were incubated with Duolink detection solution for 60 minutes, washed for 2 minutes in TBS-T and incubated with DAPI (see 2.10.4.3.3) for 10 minutes at room temperature. Finally, slides were prepared for mounting by a serial bath washes in solutions of decreasing concentration of SSC (2 x SCC; 1 x SSC; 0.2 x SSC and 0.02 x SSC) for 2 minutes each. Slides were then mounted using PermaFluor (ThermoScientific) and a glass cover slip.

Fluorescent images were captured using a Zeiss LSM 710 Meta Axiovert 100M confocal microscope (Carl Zeiss Ltd). Confocal microscopy specifications are explained in further detail in the “Fluorescent counter-staining with DAPI” section (see 2.10.4.3.3).

# 2.12 Cell culture techniques

## 2.12.1 Cell culture

HeLa (human cervical carcinoma) cells were kept at 37°C in 5% $CO_2$ in Dulbecco's Modified Eagle Medium (DMEM) (Invitrogen) supplemented with 10% fetal calf serum (FCS) (Perbio). Cells were "passaged" by washing twice with PBS and incubation with 1 ml/$cm^2$ 10% trypsin-PBS (Sigma) to detach cells from the flask. Trypsinised cells were collected and vigorously pippeted to declump cells. A small number of cells, 1.5 x $10^4$ per $cm^2$ was used to seed new cultures.

Cell counting was performed in a 0.1 mm depth, 1/400 $mm^2$ Neubauer haemocytometer (Hawksley Crystallite). 10 µl of trypsonised cells suspension was applied into the Neubauer haemocytometer. The number of cell per ml was calculated by averaging the number of cells in four different 1 $mm^2$ squares multiplied by $10^4$.

## 2.12.2 DNA transfection

Cells were split in a 1.8 x $10^4$/$cm^2$ ratio, 16 hours prior transfection to achieve 70% confluency at the point of transfection. Lipofectamine™ 2000 Transfection Reagent (Invitrogen) was used to transfect cells, according to manufacturer instructions. Briefly, for a 6 well plate (9.4$cm^2$/well), 2 µg of plasmid DNA was incubated with 1.5 ml of serum-free DMEM (Invitrogen) and mixed with a solution of 1.5 ml DMEM with 10 µl of Lipofectamine. This mix was incubated for 20 minutes at room temperature to allow formation of transfection complexes and added to the cells, prior to incubation for 6 hours. The medium was then changed to DMEM supplemented with 10% FCS and cells incubated overnight. The following morning cells were subject to for microscopy analysis, or cell extracts made for western blot analysis or immunoprecipitation.

## 2.12.3 siRNA transfection

1.2 x $10^5$ cells were seeded per well in 12 well-plates and grown over night in DMEM supplemented with 10% FCS. The following morning, cells were transfected

with 5 nM of the required siRNAs (Qiagen) (Table 2.4) using Hiperfect reagent (Qiagen) according to manufacturer instructions (Burgess *et al.*, 2011). Cells were incubated in OPTIMEM (Invitrogen) for 48 hours after which they were collected in 1 ml of ice cold PBS and stored at -80°C until required.

| siRNA | Catalogue No | Target sequence |
|---|---|---|
| Hs_PABPC1_4 | SI00676662 | CGGGCTCGGAACACACATTA |
| Hs_PABPC4_8 | SI04179861 | AGGGAAGGCCTCCATATTATA |

**Table 2.4 - siRNA; sequences of human PABPs siRNAs.** (Burgess *et al.*, 2011).

# 2.13 Xenopus laevis oocyte techniques

Animals were housed at the QMRI *Xenopus laevis (X. laevis)* facility in a 12 hour light/dark regime with water temperature between 15-18°C. All procedures followed the regulations imposed by the UK Home Office (Animal Act, 1986 [Scientific Procedures]).

## 2.13.1 Oocyte preparation

a 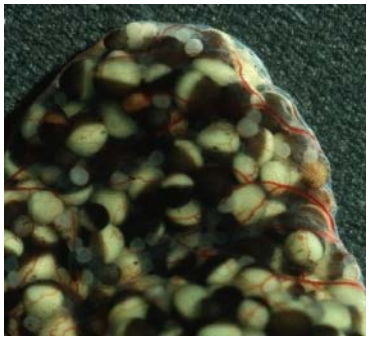 b 

**Figure 2.3 - *Xenopus laevis* oocytes.** a - *Xenopus laevis* ovary containing oocytes at varied stages of development wrapped in connective tissue, containing blood vessels. From - http://ibmmsrvlakitu.unibe.ch/sigel/xenopus.html; b - *Xenopus laevis* oocytes. Animal pole, dark brown hemisphere; and the vegetal pole, cream colour. From - http://www.xenopus.com/links.htm

Oocytes for micro-injections were collected from adult female *X. laevis*. Animals were culled by submersion in a lethal dose of anaesthetic (500 ml 8g/L of 4-aminobenzoic acid (Sigma) for 30 minutes). Once the animal failed in the

responsiveness test (failed to right when turned over), an intra-cardiac injection of 0.4 ml Phenobarbital was given. Death was confirmed by decapitation and exsanguination by removing the heart. The ovary lobes (Figure 2.3-a) were removed and washed several times in 20 ml of MMR (see 2.2.5), until the MMR remained clear. Oocytes were collected manually by "scrapping", or by collagenase treating the ovary.

#### 2.13.1.1 Oocyte "scraping"

To release oocytes from the ovary, the ovaries were gently pulled open with scissors, and with the aid of a metallic bacterial inoculation loop, oocytes were carefully scrapped off the connective tissue under a Leica MZ6 (Leica) dissecting microscope.

#### 2.13.1.2 Collagenase treatment

Ovaries were gently opened and incubated twice for 1 hour at room temperature in 25 ml of 2.5 mg/ml collagenase B (Roche) in 1x MMR on a turn-wheel. In between incubations, oocytes were washed 5 times in 1x MMR. Finally the oocytes were allowed to recover in 1x MMR solution at 18ºC overnight, before being injected in the following morning.

### 2.13.2 Oocyte micro-injection

Oocytes were sorted under a Leica MZ6 (Leica) dissecting microscope and stage VI oocytes selected for micro-injection based on size (1200–1300 μm) and appearance (Figure 2.3-b) and kept in 1x MMR solution at 18ºC. Stage VI *X. laevis* oocytes were micro-injected using a PLI-100 Harvard Apparatus micro-injector and a Narishige Micromanipulator under a Leica MZ6 dissecting microscope. Between 30 and 50 oocytes were selected per experimental point, depending on the condition of the oocytes. RNA was injected at the mid-line to avoid nuclear damage, and each injection delivered approximately 50 nl of *in vitro* transcribed RNA (see 2.412). Oocytes were incubated at 18°C in 1x MMR until harvested (Figure 2.4).

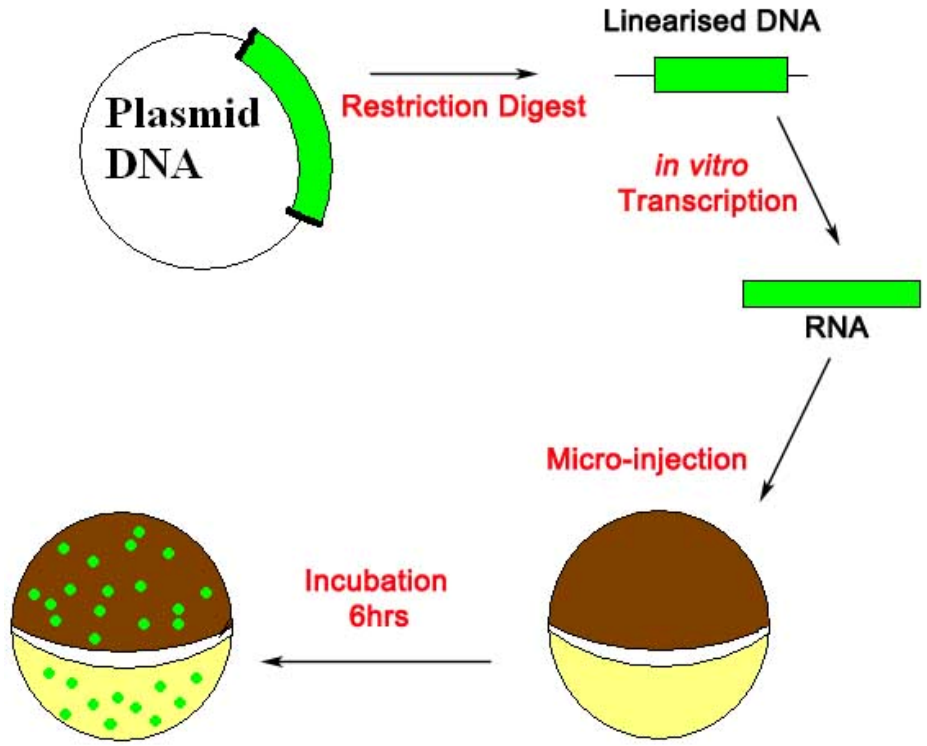


**Figure 2.4 - Micro-injections.** Schematic representation of the micro-injection strategy. Plasmid DNA linearised and transcribed *in vitro*. mRNAs were micro-injected into stage VI oocytes to produce proteins and/or measure translation rates.

### 2.13.3 Tethered function assays

Oocytes were initially injected with 50 nl of RNA encoding MS2-fusion proteins at a concentration of 1 µg/µl, and incubated at 18°C in MMR for 6 hours. Each oocyte was then injected with a solution containing luciferase (5 ng/µl) and β-galactosidase (20 ng/µl) reporter mRNAs and incubated overnight at 18°C in 1x MMR (Figure 2.5). The following morning, before collecting the oocytes, any necrotic or unhealthy oocytes were discarded. The remaining oocytes were pooled in groups of 5, to reduce the effect of variation between individual oocytes, and homogenised in 200 µl of lysis buffer (Tropix). Both assays, luciferase and β-galactosidase, were performed in duplicate for each pool of 5 oocytes and were done using a Monolight 3010 Luminometer (Pharmingen). For the luciferase assay 100 µl of luciferase assay reagent (Promega) was added to 5 µl of oocyte extract and assayed immediately. β-galactosidase activity was assayed using 2.5 µl of oocyte lysate and 100 µl of a 1/100 dilution of Galacton-Plus (Tropix) in Galacto Reaction

Buffer Diluent (Tropix). Samples were incubated at room temperature in the dark for 45 minutes before mixing with 100 µl of Accelerator II Reaction Substrate (Tropix) and assay.

Luciferase values were normalised against β-galactosidase activity which acted as a co-injection control.

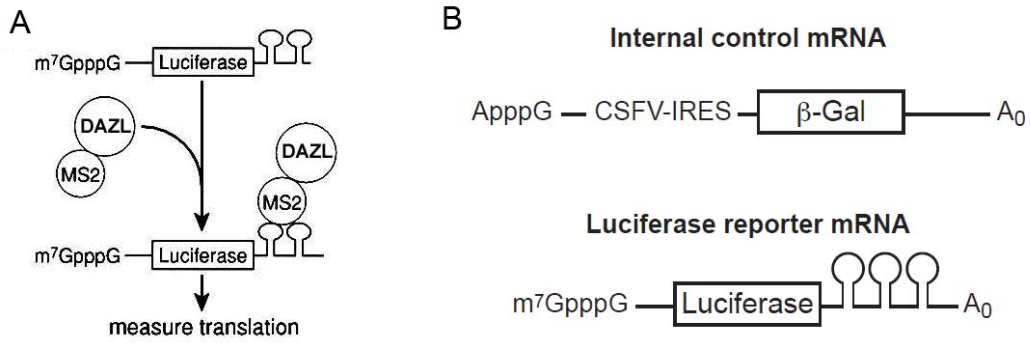


**Figure 2.5 - Tethered function assay.** A- Schematic representation of the tethered function assay. A fusion between the MS2 coat protein and human DAZL (MS2-DAZL), binds the MS2 binding sites within the 3'UTR of a luciferase reporter mRNA (Luc-MS2), tethering DAZL to the RNA. The effects of DAZL on translation are measured by luciferase assay. B– Cartoon of the reporters used for the tethered function assay. β-galactosidase reporter mRNA is used as an co-injected control. *Adapted from (Gray *et al.*, 2000).

### 2.13.4 Radio-labelling of newly synthesised proteins in oocytes

In order to assess the expression of MS2-fusion in a sub-population (circa 5) of injected oocytes (see 2.13.2) they were incubated overnight in 10 µl/ml of *in vitro* labelling grade $^{35}$[S]-methionine (50 mCi/µl) (GE Healthcare). After 16 hours, oocytes were collected and washed in 1x MMR to remove any non-internalised $^{35}$[S]-methionine. Oocytes were lysed in 10 µl of TE per oocytes. 10 ml of TE was supplemented *a priori* with a protease inhibitor cocktail tablet (Roche). Lysates were cleared twice by centrifugation at 14,000 rpm at 4°C for 5 minutes with the supernatant collected to a new 1.5 ml tube. 10 µl of cleared supernatant, the equivalent to 1 oocyte, was mixed with 10 µl 2 x sample loading buffer (see 2.2.2) and boiled for 5 minutes at 95°C, cooled for 5 minutes on ice and run at 150 V on a

NuPAGE 4- 12 % Bis-Tris pre-cast gel (Invitrogen) with a pre-stained protein ladder (BioLabs).

The gel was fixed by being submerged three times for 10 minutes in fixing solution (40 % methanol, 10 % acetic acid) followed by a 30 minute incubation in 5 % glycerol Enlightening solution (Perkin-Elmer). The gel was dried for 2 hours at 80°C in a Bio-Rad 583 Gel Drier and then placed on an exposing cassette with a Kodak BioMax MR film overnight at -80°C. The following morning the cassette was placed vertically for 30 minutes at room temperature to thaw, and the film processed in an Exograph compact X4 X-ray processor (XoGraph Imaging Systems).

## 2.14 Mouse work

### 2.14.1 Mouse husbandry and welfare

Animals were maintained in the Biomedical Research Facility at Little France, University of Edinburgh on a 12 hour light/dark regime, with humidity maintained at 55% and temperature between 20 and 25°C as specified in the Animal Act, 1986 (Scientific Procedures). Food and water were available *ad libitum*. All procedures were undertaken according to the UK Home Office regulations. Animals were culled by inhalation of rising concentration of carbon dioxide and subsequent cervical dislocation (Schedule 1 method). Setting up of timed matings (see 2.14.2) was carried out under my direction by facility staff. Neonates were culled by decapitation (Schedule 1 method). Unless otherwise stated, mice were wild-type C57BL/6.

### 2.14.2 Time matings

To assess fetal gonad development timed matings with individual pairs were set up. Females were examined for post-copulatory vaginal plugs with the morning of discovery being designated as 0.5 days post-coitum (0.5dpc), since mice mate during the middle of their dark period (overnight). Following Schedule 1 culling pregnant dams were placed in a supine position to allow removal of the intact uterus through the abdomen. Embryos were removed from the amniotic sacs, decapitated and immersed in PBS. Up to 13.5dpc the entire embryo was fixed. For embryos older

than 13.5dpc the fetal gonads were removed, washed once in 1 ml of ice cold PBS, and fixed.

### 2.14.2.1 Sex genotyping

To determine the sex of the fetus, DNA was prepared from the head (11.5dpc and 13.5dpc) or tail (15.5dpc) which was snap frozen and stored at -80°C upon collection. The tissue was processed by immersion in 25 µl of TE-T (TE with 1% Tween -20) and 2 µl of 10 mg/ml proteinase K (Sigma) for 2 hours at 55°C to allow proteinase activity. Proteinase K was then denatured by boiling the sample at 95°C for 10 minutes. The digested tissue was spun at 7,000 rpm for 5 minutes at 4°C and the supernatant transferred into a fresh 1.5 ml tube. 10 µl of supernatant was diluted in 90 µl of distilled water and used for PCR.

PCR Mix:

-2 µl of the DNA

-10 µl of Biomix Red Mix (Bioline)

-0.2 µl of 100 mM each forward primer (Table 2.5)

-0.2 µl of 100 mM each reverse primer (Table 2.5)

Reactions were run in a Dyad PCR machine (Bio-Rad) using the following program:

| | |
|---|---|
| 1) 3 minutes | 94°C |
| 2) 45 seconds | 94°C |
| 3) 50 seconds | 63°C |
| 4) 1 minute | 72°C |
| *2-4 repeated 40 times | |
| 5) 5 minutes | 72°C |

PCR products were run on a 2% agarose gel with a 100 bp ladder (NEB). Male fetuses generate 2 bands (225 and 370bp) and females, a single band (370bp).

| Name | Location | 5’ primer | 3’ primer | size |
|---|---|---|---|---|
| Zfy | Y | 5'TGGCATCTGTCTCCTGACT | 3'GCCACATGCTTCTTGAGTTC | 225bp |
| Xist | X | 5'T GCTCCACTTGAGACGGAAC | 3'TCGGCCACTACTATGAGCAG | 370bp |

**Table 2.5 - Primers for sex genotyping.** Location refers to the chromosome encoding the amplified sequence.

# 2.15 Antibodies

## 2.15.1 In-house antibodies

Two different polyclonal antibodies specific for mouse PABP1 (PABP1) were raised in rabbits using two different peptides (Marshal – AQKAVNSATGVPTV; VINPY - PVINPYQPAPPSGY).

One PABP4 antibody was raised in rabbits immunised against a peptide sequence present in both mouse and human PABP4 (KKEAAQKVGTVAAATS). Antibodies were raised by Covalab lab.

Polyclonal sera from immunised rabbits was affinity purified by other members of the laboratory before use and stocks stored at -20°C in 20% glycerol PBS solution with 0.05% sodium azide.

Concentrations of the affinity purified antibodies were calculated by Bradford assay (see 2.7.2).

| Antibody | Concentration |
|---|---|
| Marshal | 112.6 µg/µl |
| VINPY | 56.3 ng/µl |
| Anti-PABP4 | 240 ng/µl |

**Table 2.6 - In-house antibody concentrations.**

## 2.15.2 Commercial antibodies

Several commercial antibodies were used in this project. Details on the suppliers, species raised in and dilutions for specific assays are detailed in Table 2.7 – Primary antibodies and Table 2.8 – Secondary antibodies.

| Protein | Raised in | Supplier | TSA | DAB | IF | WB |
|---|---|---|---|---|---|---|
| α - LH subunit (R20 – GSU) | Rabbit | McNeilly Lab*1 | | | 1/1000 | |
| β - LH subunit (518 B7) | Mouse | Dr. J. F. Roser*1 | | | 1/5000 | |
| DAZL | Mouse | Serotec – MCA2336 | | 1/250 | 1/20 | 1/200 |
| DAZL | Goat | Everest – EB06857 | | Not Specific | | |
| DAZL | Abcam | No longer available | | 1/100 | | |
| GAPDH-HRP | Mouse | Abcam -Ab9484 | | | | 1/1,000 |
| GST | Goat | Abcam – ab6613 | | | | 1/1,000 |
| IgG | Mouse | Sigma - I5381 | | | | |
| IgG | Rabbit | Sigma - I5006 | | | | |
| IgG | Goat | Perbio – 31402 | | | | |
| His-6 | Mouse | Sigma – H1029 | | | | 1/1,000 |
| PABP1 (VINPY) | Rabbit | Gray Lab [*2] | | 1/1000 | | 1/5,000 |
| PABP1 (Marshal) | Rabbit | Gray Lab | 1/10,000 | 1/5,000 | 1/500 | 1/10,000 |
| PABP4 | Rabbit | Gray Lab [*2] | 1/7,500 | 1/2,000 | 1/1,000 | 1/2,500 |
| PABP4 | Rabbit | Abnova – 8761-D01P | | Not Specific | | |
| PABP4 | Rabbit | Bethyl – IHC-00561 | | 1/250 | | 1/1,000 |
| Strep-Tag | Mouse | Novagen – 71590-3 | | | | 1/1,000 |
| T7-Tag | Mouse | Novagen – 69522-3 | | | | 1/10,000 |

**Table 2.7 - Primary antibodies.** *1 - (Pope *et al.*, 2006) *2 - (Burgess *et al.*, 2011); TSA –tyramide signal amplification; IF – Immunofluorescence; WB – Western blot.

| Anti-Species | Raised in | Conjugated | Supplier | IHC | Western blot |
|---|---|---|---|---|---|
| Goat | Chicken | Biotin | SantaCruz - sc2984 | 1/500 | |
| Goat | Chicken | HRP | SantaCruz - sc2953 | | 1/20,000 |
| Mouse | Donkey | Alexa-488 | Invitrogen - A21202 | 1/200 | |
| Mouse | Goat | Biotin | Vector - E0433 | 1/500 | |
| Mouse | Goat | HRP | Pierce - 31444 | | 1/20,000 |
| Rabbit | Goat | Alexa-546 | Invitrogen - A11035 | 1/200 | |
| Rabbit | Goat | Biotin | Vector - E0432 | 1/500 | |
| Rabbit | Goat | HRP | Sigma - A0545 | | 1/150,000 |

**Table 2.8 - Secondary antibodies.**

## 2.15.3 Oligonucleotides

| Oligo | Sequence | Restriction sites |
|---|---|---|
| l.P1-F1 | CAT GCA GAA TTC ATC AAC CCC TAC CAG CCA GCA CC | EcoRI |
| l.P1-R1 | CAT GCA CAT ATG TTA GAC AGT TGG AAC ACC AGT GGC AC | NdeI |
| l.tP-F1 | CAT GCA GAA TTC AAC CCC TAC CAA CCA GCA TCT TCC | EcoRI |
| l.tP-R1 | CAT GCA CAT ATG TTA AAC AGT TGG GAC ACC AGA GGT ACT GC | NdeI |
| l.P4-F1 | CAT GCA GAA TTC GCC ATC TTA AAT CAG TTC CAG CCT GC | EcoRI |
| l.P4-R1 | CAT GCA CAT ATG TTA AGA GGT AGC AGC AGC AAC AGT GCC C | NdeI |
| mB-F2 | ATG GAG ACC GAG TCC CGG GCG C | |
| mB-R2c | TCA AAA TAA ACT CCT TAC TTT AAT TGG CTC AGG C | |
| mB-F2RE | CAT GCA GGA TCC CAT GGA GAC CGA GTC CCG GGC GC | BamHI |
| mB-R2cRE | CATGCACTCGAGTCAAAATAAACTCCTTACTTTAATTGGCTCAGGC | XhoI |
| c85a-F | CTCGAGTCTACTGCAAATCATGAAACTCCAAACTCAACC | |
| c85a-R | GGTTGAGTTTGGAGTTTCATGATTTGCAGTAGACTCGAG | |
| a97t_c98g-F | CTGCAAATCCTGAAACTCCAATGTCAACCATCTCCAGAGA | |
| a97t_c98g-R | TCTCTGGAGATGGTTGACATTGGAGTTTCAGGATTTGCAG | |
| a178g_t179c-F | CCAAGGCTATATTTTACCAGAAGGCAAAGCCATGCCAAACACTGTTTTT | |
| a178g_t179c-R | AAAAACAGTGTTTGGCATGGCTTTGCCTTCTGGTAAAATATAGCCTTGG | |
| a412g-F | AGCTGGGCCCTGCAATCGGGAAACAAAATTTATGTG | |
| a412g-R | CACATAAATTTTGTTTCCCGATTGCAGGGCCCAGCT | |
| hD+t –F | GAATTCGATTTAGCCTCGATGTCTACTGCAAATCCTGAA | |
| hD+t – R | TTCAGGATTTGCAGTAGACATCGAGGCTAAATCGAATTC | |
| hD.P6H+T-F | GGA ATT CGA TTT AGC CTC GAT GTC TAC TGC AAA TCA TGA AA | |
| hD.P6H+T-R | TTT CAT GAT TTG CAG TAG ACA TCG AGG CTA AAT CGA ATT CC | |
| 3G9xD-F | CCTTGAGTGATTTTTCCCCTTTTCATAGGAGTC | |
| 3G9xD-R | GGAACTCACTAAAAAGGGGAAAAGTATCCTCAG | |
| MmPABP1CDS-F | GTG CCA CTG GTG TTC CAA CTG TCG TCG AC | SalI |
| MmPABP1CDS-R | GGA TCC TAT GAA CCC CAG CGC CCC CAG CTA CCC | BamHI |
| MmPABP4CDS-F | TGT ACA TAT GAA CGC TGC AGC CAG CAG C | BsrGI |
| MmPABP4CDS-R | GCA CTG TTG CTG CTG CTA CCT CTG TCG AC | SalI |
| MmPABP5CDS-F | GGA TCC TAT GAG TGG GGA GCC TAA TAC TGC | BamHI |
| MmPABP5CDS-R | GGC AAG CTA GGC ACA GGT GGG TCG AC | SalI |
| hDexp.F | CAT GCA TCT AGA ATG TCT ACT GC AAA TCC TG | XbaI |
| HDexp.R | CAT GCA GGA TCC TCA AAC AGA TTT AAG CAT TGC CCG | BamHI |

**Table 2.9 - Oligonucleotides.** Name, corresponding sequence and restriction digest site (when existent).

## 2.16 Plasmids

All plasmids were sequence verified (see 2.4.9). The primers involved in the generation of these plasmids are described in Table 2.9.

| Plasmids | |
|---|---|
| **pGEM** | |
| pGEM-T-easy-mPabp1c * | pGEM-T-easy-hDAZL-N10C (no ATG) * |
| pGEM-T-easy-mtPabpc * | pGEM-T-easy-hDAZL-I37A (no ATG) * |
| pGEM-T-easy-mPabp4.001c * | pGEM-T-easy-hDAZL-R115G(no ATG) * |
| pGEM-T-easy-mPabp4.002c * | pGEM-T-easy-hDAZL (ATG) * |
| pGEM-T-easy-mPabp4.003c * | pGEM-T-easy-hDAZL-P6H * |
| pGEM-T-easy-mPabp4.004c * | pGEM-T-easy-hDAZL-N10C * |
| pGEM-T-easy-mPabp5 | pGEM-T-easy-hDAZL-I37A * |
| pGEM-T-easy-mBoll * | pGEM-T-easy-hDAZL-R115G * |
| pGEM-hDAZL | pGEM-hGDF9 |
| pGEM-T-easy-hDAZL-P6H (no ATG) | pGEM-T-easy-xATG-hDAZL |
| **YEAST TWO-HYBRID** | |
| pACT-hDAZL | BTM-mPabp1 (RRM 1-4) |
| pGAD-hDAZL | BTM-xPabp1c |
| pGAD-hDAZ | BTM-hPABP1c |
| pACT-mDazl | BTM-mtPabpc |
| pGAD-xDazl | BTM-htPABPc |
| pGAD-hBOLL | BTM-mPabp5 |
| pACT-mBoll * | BTM-mPabp4.001c * |
| pACT-IRP | BTM-mPabp4.002c * |
| BTM-KnDB | BTM-mPabp4.003c * |
| BTM-mPabp1c | BTM-mPabp4.004c * |
| pACT-hPAIP | BTM.xPabp4c |
| plexA-MS2 | BTM-hDAZL |
| **PROTEIN EXPRESSION** | |
| pET52b(+)-mPabp1 * | pET52b(+)-mPabp5 * |
| pET52b(+)-mPabp4.001 * | pGEX |
| pET52b(+)-mPabp4.002 * | pCGN |
| pET52b(+)-mPabp4.003 * | pCG.hDAZL * |
| pET52b(+)-mPabp4.004 * | pEGFP-C1 |
| **REPORTER ASSAY** | |
| pMSPN | pLG.MS2 |
| pMS2-hDAZL | pMS2.U1A |
| pMS2-hDAZL-P6H (no ATG) * | pLuc.hGDF9.3'UTR |
| pMS2-hDAZL-N10C (no ATG) * | pLuc.hGDF9.3'UTR.ΔhDAZL * |
| pMS2-hDAZL-I37A (no ATG) * | pCSFV-lacZ |
| pMS2-hDAZL-R115G (no ATG) * | |

**Table 2.10 - Plasmids.** *- marks plasmids generated for this work.

### 2.16.1 pGEM constructs

All pGEM-T-easy clones represent intermediate cloning steps, unless otherwise stated.

pGEM-T-easy-mPabp1c was obtained by PCR generation of a fragment containing the C-terminal region of mouse Pabp1 open reading frame (ORF) (mPABP1c, amino acids 396-633) from the IMAGE clone (#6816124), using the oligonucleotide primers I.P1-F1 and I.P1-R1 (see Table 2.9). The resulting fragment and pGEM-T-easy were digested with EcoRI and NdeI prior to ligation.

pGEM-T-easy-mtPabpc containing the C-terminal region of mouse tPabp ORF (mtPABPc, amino acids 396-628) was generated following the strategy described for pGEM.Teasy-mPabp1c, but from the IMAGE clone #6704229 and using the primers I.tP-F1 and I.tP-R1.

pGEM-T-easy-mPabp4 isoforms (001-004) containing the C-terminal region of the mouse Pabp4 splice variants (mPabp4c, starting at amino acid 395 until the end of the ORF), numbered according to the ENSEMBL predictions. These fragments were generated by RT-PCR from day 15 mouse testes RNA (see 2.4.2) using primers I.P4-F1 and I.P4-R1. The resulting PCR fragments were cloned into pGEM-T-easy using EcoRI and NdeI.

pGEM-T-easy-mPabp5 which contains the complete ORF of mouse PABP5. Gift from Ross Anderson (University of Edinburgh, unpublished).

pGEM-T-easy-mBoll contains the ORF of mouse Boule obtained by RT-PCR (see 2.4.1) with primers mB-F2 and mB-R2c from day 15 mouse testes RNA (see 2.4.2). This PCR fragment was cloned into pGEM-T-easy using BamHI and XhoI.

pGEM-hDAZL containing the hDAZL ORF minus the endogenous start codon has been previously described (Collier *et al.*, 2005b).

pGEM-T-easy-hDAZL-P6H (no ATG) contains the hDAZL mutant P6H ORF minus the endogenous start codon and was generated using the XL site directed mutagenesis kit (Stratagene) following manufacturer's instructions. pGEM- hDAZL was used as a PCR template with the mutation oligonucleotides c85a-F and c85a-R..
pGEM-T-easy-hDAZL-N10C (no ATG) contains the hDAZL mutant N10C ORF minus the endogenous start codon and was generated as described for pGEM-T-easy-hDAZL-P6H (no ATG) but using the oligonucleotides a97t_c98g-F and a97t_c98g-R.

pGEM-T-easy-hDAZL-I37A (no ATG) contains the hDAZL mutant I37A ORF minus the endogenous start codon and was generated as described for pGEM-T-easy-hDAZL-P6H (no ATG) but using the oligonucleotides a178g_t179c-F and a178g_t179c-R.

pGEM-T-easy-hDAZL-R115G (no ATG) contains the hDAZL mutant R115G ORF minus the endogenous start codon and was generated as described for pGEM-T-easy-hDAZL-P6H (no ATG) but using the oligonucleotides a412g-F and a412g-R.

pGEM-T-easy-hDAZL (ATG) contains the hDAZL ORF and was generated as described for pGEM-T-easy-hDAZL-P6H (no ATG) but using the oligonucleotides hD+t-F and hD+t-R, to introduce a functional start codon.

pGEM-T-easy-xATG-hDAZL contains the hDAZL ORF with a functional start codon. It was generated by digesting pGEM-T-easy-hDAZL (ATG) with EcoRI to liberate the hDAZL ORF which was ligated into EcoRI digested ATG-pGEM (Gorgoni *et al.*, 2011), a pGEM-T.easy plasmid with mutated upstream ATGs. This plasmid was used for target reporter assays (see chapter 5).

pGEM-T-easy-hDAZL-P6H contains the hDAZL P6H mutant ORF with a functional start codon. It was generated following the same principle as pGEM-T-easy-hDAZL-P6H (no ATG) but using the oligonucleotides hD.P6H+T-F and hD.P6H+T-R. The

resulting PCR product was digested with EcoRI and cloned into ATG-pGEM (Gorgoni *et al.*, 2011) with mutated upstream ATGs, previously digested with EcoRI. This plasmid was used for target reporter assays (see chapter 5).

pGEM-T-easy-hDAZL-N10C contains the hDAZL N10C mutant ORF with a functional start codon cloned into ATG-pGEM (Gorgoni *et al.*, 2011). It was generated following the procedure described for pGEM-T-easy-hDAZL (ATG) from the initial template pGEM-T-easy-hDAZL-N10C (no ATG). The result of this PCR and ATG-pGEM were digested with EcoRI and ligated. This plasmid was used for target reporter assays (see chapter 5).

pGEM-T-easy-hDAZL-I37A contains the hDAZL I37A mutant ORF with a functional start codon in ATG-pGEM (Gorgoni *et al.*, 2011). It was generated following the procedure described for pGEM-T-easy-hDAZL (ATG) from the initial template pGEM-T-easy-hDAZL-I37A (no ATG). The result of this PCR and ATG-pGEM were digested with EcoRI and ligated. This plasmid was used for target reporter assays (see chapter 5).

pGEM-T-easy-hDAZL-R115G contains the hDAZL R115G mutant ORF with a functional start codon in ATG-pGEM (Gorgoni *et al.*, 2011). It was generated following the procedure described for pGEM-T-easy-hDAZL (ATG) from the initial template pGEM-T-easy-hDAZL-R115G (no ATG). The result of this PCR and ATG-pGEM were digested with EcoRI and ligated. This plasmid was used for target reporter assays (see chapter 5).

pGEM-hGDF9 containing the human GDF9 3'UTR was obtained by PCR amplification from the IMAGE clone #2978938 with primers 5'hGDF9 and 3'hGDF9, and blunt cloned into pGEM-T-easy (SP6 promoter). This unpublished plasmid was a gift from Dr B. Collier (MRC Human Genetics Unit, Edinburgh).

### 2.16.2 Y2H vectors

pACT.mBoll containing the complete ORF of mBoll fused to the activation domain of GAL4 was obtained by retrieving the complete ORF of mBoll from pGEM-T-easy-mBoll, using the restriction sites BamHI and XhoI. The mBoll ORF was cloned into the pACT backbone obtained from pACT.hDAZL (Ruggiu and Cooke, 2000)previously digested with the same enzymes. Sequence analysis showed that the construct was out of frame. To correct this, the plasmid was digested with BamHI and then "filled in" with Klenow and religated.

BTM-KnDB containing the lexA DNA binding domain was a gift from D. Bernstein, University of Wisconsin-Madison.

BTM-mPabp1c containing the C-terminal region of mouse Pabp1 (mPABP1c, amino acids 396-633) fused to the lexA DNA binding domain was generated by digesting pGEM-T-easy-mPabp1c with EcoRI and NdeI. The fragment corresponding to mPabp1c was then cloned into BTM-KnDB (gift from D. Bernstein, University of Wisconsin) previously digested with the same restriction enzymes.

BTM-mtPabpc containing the C-terminal region of mouse tPabp (mtPABPc, amino acids 396-628) fused to the lexA DNA binding domain was generated as described for BTM-mPabp1c but starting with pGEM-T-easy-mtPabpc.

BTM-mPabp4.001c containing the C terminal region of mouse Pabp4.001 (mPabp4c, amino acid 395 – 660) fused to the lexA DNA binding domain was generated as described for BTM-mPabp1c but starting with pGEM-T-easy-mPabp4.001c.

BTM-mPabp4.002c containing the C terminal region of mouse Pabp4.002 (mPabp4c, amino acid 395 – 615) fused to the lexA DNA binding domain was generated as described for BTM-mPabp1c but starting with pGEM-T-easy-mPabp4.002c.

BTM-mPabp4.003c containing the C terminal region of mouse Pabp4.003 (mPabp4c, amino acid 395 – 631) fused to the lexA DNA binding domain was generated as described for BTM-mPabp1c but starting with pGEM-T-easy-mPabp4.003c.

BTM-mPabp4.004c containing the C terminal region of mouse Pabp4.004 (mPabp4c, amino acid 395 – 644) fused to the lexA DNA binding domain was generated as described for BTM-mPabp1c but starting with pGEM-T-easy-mPabp4.004c.

BTM-hDAZL containing the complete ORF of hDAZL fused to the lexA DNA binding domain was generated by digesting pGEM-T-easy-hDAZL(ATG) with EcoRI and BamHI. The resulting fragment was then cloned into BTM-KnDB (gift from D. Bernstein, University of Wisconsin), previously digested with the same restriction enzymes.

pACT-hDAZL, and pACT-mDazl containing the ORFs of mouse and human DAZL fused to the GAL4 activation domain have been previously described (Ruggiu and Cooke, 2000).

pGAD.hBOULE, pGAD-xDazl (Collier *et al.*, 2005b) and pACT.IRP (SenGupta *et al.*, 1996) containing respectively the complete ORF of human BOLL, *X. laevis* Dazl and IRP fused to the activation domain of GAL4 have been previously described.

BTM-Ct contains the C-terminal region of *X. laevis* PABP1 and has been previously described (Gray *et al.*, 2000) BTM-hCt and BTM-tCt contain C-terminal region of human PABP1 and tPABP respectively fused to the LexA DNA binding domain and were a gift from Joel Smith (University of Edinburgh).

lexA.MS2 containing the ORF of the MS2 coat protein fused to the DNA binding domain of lexA has been previously described (SenGupta *et al.*, 1996).

pACT.hPAIP contains the ORF of human PAIP1 fused to the GAL4 activation domain and has been previously described (Gray *et al.*, 2000).

pGAD.hDAZL, pGAD.hDAZ contains the ORFs of human DAZL and DAZ fused to the activation domain of GAL4 and were a gift from Joel Smith (University of Edinburgh, unpublished).

BTM-PABP4Ct containing the C-terminal region of *X. laevis* PABP4 fused to the lexA DNA binding domain, has been previously described (Gorgoni *et al.*, 2011).

BTM-mPabp1(RRM1-4) and BTM-mPABP5 contains RMM1-RRM4 of mouse Pabp1 and the ORF of mouse Pabp5, respectively, fused to the lexA DNA binding domain, and were gifts from Ross Anderson (University of Edinburgh, unpublished).

### 2.16.3 Expression plasmids

pCGN is a mammalian expression vector that produces N-terminal T7 tagged proteins and has been previously described (Tanaka and Herr, 1990).

pEGFP-C1 is a commercial plasmid (Clontech), containing a GFP mut1 variant (Cormack *et al.*, 1996) followed by a multiple cloning site.

pET52b(+) is a commercial plasmid (Merckmillipore), used for expression of proteins with an N-terminal Strep•Tag II and a 10X•His•Tag at the C-terminus.

pET52b(+)-mPabp1 is a bacterial expression vector containing the ORF of mPabp1 with a N-terminal Strep•Tag II and a 10X•His•Tag at the C-terminus. It was created by PCR of the mPabp1 ORF from the IMAGE clone (#6816124), using the oligonucleotides MmPABP1CDS-F and MmPABP1CDS-R. The PCR product and pET52b(+), were digested with BamHI and SalI prior to ligation.

pET52b(+)-mPabp4.002 is a bacterial expression vector containing the ORF of mPabp4.002 with an N-terminal Strep•Tag II and a 10X•His•Tag at the C-terminus. It was created by PCR generation of a fragment from the IMAGE clone #277091,

using the oligonucleotides MmPABP4CDS-F and MmPABP4CDS-R. The PCR product and pET52b(+) were digested with BsrGI and SalI prior to ligation.

pET52b(+)-mPabp4.001 is a bacterial expression vector containing the ORF of mPabp4.001 with an N-terminal Strep•Tag II and a 10X•His•Tag at the C-terminus. It was created by digesting the fragment containing the splice variant region of mPabp4.001 from the plasmid pGEM-Teasy-mPabp4.001c using the enzymes NsiI and StuI. This fragment was cloned into the pET52b(+)-mPabp4.002 that was previously digested with the same enzymes (to replace the corresponding fragment from mPabp4.002).

pET52b(+)-mPabp4.003 is a bacterial expression vector containing the ORF of mPabp4.003 with an N-terminal Strep•Tag II and a 10X•His•Tag at the C-terminus. It was generated as described for pET52b(+)-mPabp4.001 but using pGEM-T-easy-mPabp4.003c as a template.

pET52b(+)-mPabp4.004 is a bacterial expression vector containing the ORF of mPabp4.004 with an N-terminal Strep•Tag II and a 10X•His•Tag at the C-terminus. It was generated as described for pET52b(+)-mPabp4.001 but using pGEM-T-easy-mPabp4.004c as a template.

pET52b(+)-mPabp5 is a bacterial expression vector containing the complete ORF of mPabp5 with an N-terminal Strep•Tag II and a 10X•His•Tag at the C-terminus. It was generated as described for pET52b(+)-mPabp1 but using the IMAGE clone #125979 as a template and the oligonucleotides MmPABP5CDS-F and MmPABP5CDS-R.

pCG.hDAZL is a mammalian expression vector containing the ORF of hDAZL with an N-terminal T7 tag. It was created by PCR of the hDAZL ORF from the pGEM-T-easy-hDAZL(ATG) using oligonucleotides hDexp.F and h.Dexp.R, which introduce XbaI and BamHI restriction sites. The PCR product and pGCN was digested with XbaI and BamHI prior to ligation.

pGEX is a bacterial expression vector containing the glutathione S-transferase, provided by GE Healthcare.

### 2.16.4 Reporter assay plasmids

pLG-MS2 containing the luciferase ORF reporter with 3 MS2 binding sites on its 3'UTR has been previously described (Gray *et al.*, 2000).

pMSPN containing the ORF of the MS2 bacteriophage coat protein has been previously described (Wilkie *et al.*, 2005).
pCSFV-lacZ containing the lacZ gene with the classical swine fever virus IRES has been previously described (Smith *et al.*, 2011).

pMS2-U1A containing the ORF of the MS2 bacteriophage coat protein fused to the U1A ORF has been previously described (Gray *et al.*, 2000).

pMS2-hDAZL has been previously described (Collier *et al.*, 2005a). This plasmid contains the MS2 coat protein fused to the hDAZL in which the hDAZL ATG is absent. This plasmid was used in tethered function assays.

pMS2-hDAZL-P6H containing the MS2 coat protein fused to the hDAZL mutant P6H was generated by liberating the ORF of hDAZL-P6H from pGEM-T-easy-hDAZL-P6H(no ATG) using XhoI and BamHI. This fragment was cloned to pMSPN, previously digested with the same enzymes. This plasmid was used in tethered function assays.

pMS2-hDAZL-N10C containing the MS2 coat protein fused to the hDAZL mutant N10C was generated as described for pMS2-hDAZL-P6H but using pGEM.Teasy-hDAZL-N10C(no ATG) as a template. This plasmid was used in tethered function assays.

pMS2-hDAZL-hDAZL-I37A containing the MS2 coat protein fused to the hDAZL mutant I37A was generated as described for pMS2-hDAZL-P6H but using pGEM-T-easy-hDAZL-I37A(no ATG) as a template. This plasmid was used in tethered function assays.

pMS2-hDAZL-R115G containing the MS2 coat protein fused to the hDAZL mutant R115G was generated as described for pMS2-hDAZL-P6H but using pGEM-T-easy-hDAZL-R115G (no ATG) as a template. This plasmid was used in tethered function assays.

pLuc.hGDF9.3'UTR containing the luciferase reporter gene fused to the 3'UTR of hGDF9 was a gift from Dr Collier (MRC Human Genetics Unit, Edinburgh, unpublished). hGDF9 3'UTR was digested from pGEM- hGDF9 with SalI and PstI and cloned into pUC19Luc (Reynolds *et al.*, 2007), previously digested with the same enzymes.

pLuc.hGDF9.3'UTR.ΔhDAZL contains the luciferase reporter gene fused with the 3'UTR of hGDF9 in which the most striking DAZL binding site has been mutated using the XL site directed mutagenesis kit (Stratagene) following manufacturer's instructions. pLuc.hGDF9.3'UTR was used as a template with the mutation oligonucleotides 3G9xD-F and 3G9xD-R.

## 2.17 Statistical analysis

Statistical analysis was performed using GraphPad (GraphPad Software Inc). Detailed statistical tests are described in the appropriate sections.

# Chapter 3

# Investigating potential interactions between mammalian DAZL and PABP1

# 3.1 Introduction

During gametogenesis, gene expression is highly dependent on post-transcriptional regulation, in part due to long intervals of transcriptional quiescence. Therefore an important mechanism of gene regulation in germ cells is the activation of stored silent mRNAs by RNA-binding proteins (Seydoux and Braun, 2006, Kimble and Crittenden, 2007, Paronetto and Sette, 2009). In many cases such mRNAs are stored with short poly(A) tails.

Reports from several labs have shown that DAZL family members, which are crucial for germ cell development, are mRNA-specific regulators of translation (Maines and Wasserman, 1999, Maegawa *et al.*, 2002, Collier *et al.*, 2005b, Reynolds *et al.*, 2005, VanGompel and Xu, 2011). Two models have been proposed for their ability to stimulate translation. Collier *et al.* in 2005 presented a model based on work in *Xenopus laevis (X. laevis)* oocytes in which Dazl proteins act by directly recruiting PABP proteins to mRNAs circumventing the requirement for a long poly(A) tail in promoting the closed–loop conformation. An alternative model emerged from work in zebrafish suggesting that DAZL enhances mRNA translation and stability by suppressing micro RNA (miRNA) induced deadenylation (Takeda *et al.*, 2009).

Interestingly, both mouse and human DAZL can stimulate the translation of reporter mRNAs in *X. laevis* oocytes and show a conserved ability to interact with *X. laevis* PABP proteins, suggesting that this mechanism may be utilised in mammals. However, mammals encode additional members of both the DAZ and PABP families, adding to the complexity of possible DAZL-PABP interactions that may drive mRNA-specific translational activation during mammalian gametogenesis (Kleene *et al.*, 1994, Saxena *et al.*, 1996, Reijo *et al.*, 2000, Saxena *et al.*, 2000, Blanco *et al.*, 2001, Feral *et al.*, 2001, Kimura *et al.*, 2009), necessitating an understanding of their relative expression patterns.

Previous work has provided insight into the expression of Dazl in mouse gonads. At 12.5 days post coitum (12.5dpc), prior to germ cell sex differentiation, Dazl transcripts can already be observed. In oogonia, these increase by 14.5dpc, coinciding with the time that the first this initiates meiosis (13.5-14.5dpc) (Seligman

and Page, 1998). Dazl protein is present in the cytoplasm of oocytes throughout oogenesis increasing during oocyte maturation (Ruggiu *et al.*, 1997, Chen *et al.*, 2011). In male germ cells, Dazl protein can be observed from fetal prospermatogonia through primary spermatocytes (Ruggiu *et al.*, 1997, Reijo *et al.*, 2000, Anderson *et al.*, 2007). However, despite this reasonably comprehensive characterisation, important information on Dazl expression is still missing for both sexes during specific phases of mammalian germ cell proliferation and differentiation.

Characterisation of PABP1 (the prototypical PABP) expression is in contrast surprisingly sparse in part due to a lack of PABP-specific antibodies. However in adult mouse testes, where it has been most intensely characterised, northern blot analysis on single cell suspensions from seminiferous tubules has shown that Pabp1 mRNA is restricted to the pachytene spermatocytes and round spermatids (Kleene *et al.*, 1994).

This chapter explores the possibility that mammalian DAZL proteins regulate translation initiation by interacting with the translation initiation factor PABP1, as in proposed to occur in *X. laevis* (Collier *et al.*, 2005b). Hence, their precise expression patterns in mammalian gonads, the extent of their colocalisation within developing germ cells and their ability to interact will be determined.

# 3.2 Results

## 3.2.1 Dazl in mouse adult testes

12 tubule stages (I-XII) have been identified by Russel *et al.* (Figure 3.1) in adult testis, but Dazl expression has only been examined in stages III-IV, VII and X (Ruggiu *et al.*, 1997). Therefore, information on important phases such as the mitosis to meiosis transition in stage V –VII tubules, and the zygotene progression in stages XI-XII is missing. Hence, to gain a more comprehensive characterisation of Dazl expression, an anti-DAZL antibody was optimised for fixed tissue (Appendix 1) and applied to adult mouse testes sections with the 12 tubule stages of spermatogenesis being identified based on cell phase and morphology. The 12 stages represent the developmental progression and differentiation that occurs during adult spermatogenesis, starting with spermatogonia which are germ cell stem cells

committed to a male differentiation pathway, through mitosis and meiosis until 16th-phase haploid spermatids are released into the lumen of the seminiferous tubules.

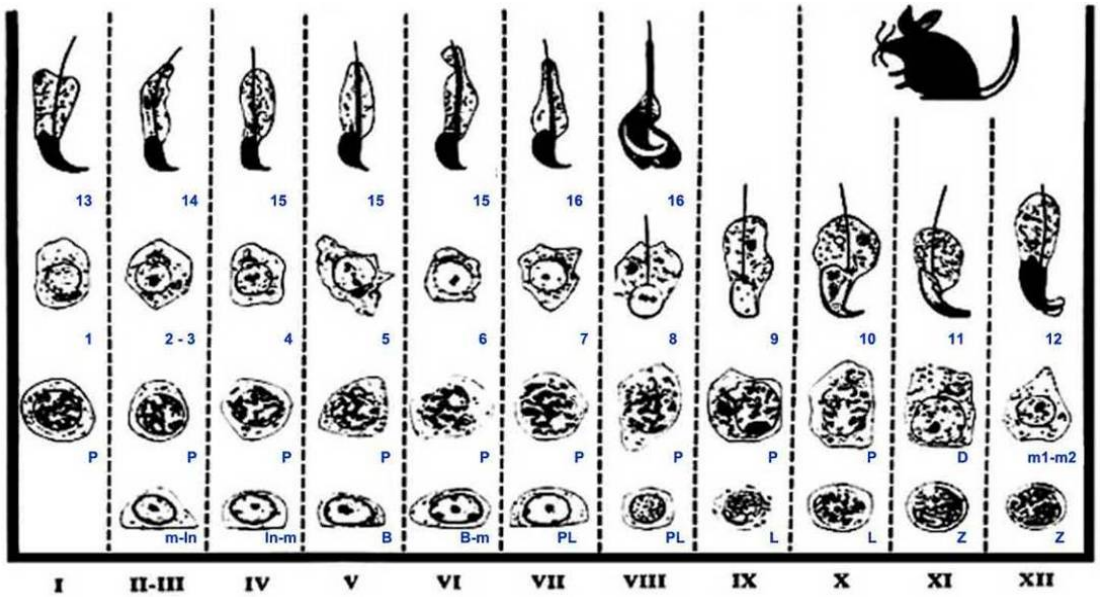


**Figure 3.1 - Staging diagram for mouse spermatogenesis.** Diagram depicting the different phases of spermatogenesis in adult mouse. Tubule stages are described in roman numerals I-XII. The progression of germ cell types within these tubules is described by letters or numbers. m-In – mitotic A spermatogonium into intermediate spermatogonium; In-m - mitotic intermediate spermatogonium into B spermatogonium; B – B spermatogonium; B-m – mitotic B spermatogonium into preleptotene spermatocyte; PL – preletotene spermatocyte; L – leptotene spermatocyte; Z – zygotene spermatocyte; P – pachytene spermatocyte; D – diplotene spermatocyte; m1-m2 – transition between meiosis I and II; 1-16 – stages of spermatids, 1-8 round spermatids, 9-16 elongating spermatids (Lahn *et al.*, 2002), although stages 7-9 can be considered transitional stages. Stage II and III are grouped together due to an inability to precisely distinguishing them by light microscopy. From Russel et al. 1990.

Figures 3.2 to 3.5 show the results of the Dazl immunostaining in the 12 different developmental stages, with the last panel in Figure 3.5 showing a no primary antibody negative control.

Dazl expression was detected in A spermatogonia (Figure 3.4 – stage X), intermediate spermatogonia (Figure 3.2 – stage II/III), B spermatogonia (Figures 3.2 and 3.3 – Stages IV and VI) and preleptotene spermatocytes (Figures 3.3 and 3.4 – stages VI - VIII). Surprisingly there was a clear decrease in Dazl levels in leptotene cells at stage IX (Figure 3.4). This decrease became more evident at stage X, when Dazl was essentially undetectable in leptotene cells (Figure 3.4). At Stage XI (Figure

3.5), with progression of early spermatocytes into zygotene phase, Dazl expression was restored and continued through the zygotene phase in stage XII tubules. Dazl expression was observed through the entire pachytene phase from stage I to stage X (Figures 3.2 -3.4). At diplotene phase in stage XI, there was a considerable decrease in Dazl expression (Figure 3.5). With progression of cell cycle into the meiosis I to meiosis II transition at stage XII, Dazl expression decreased even further to levels just above background (Figure 3.5). Dazl was not detected in round or elongating spermatids at any stage (Figures 3.2 to 3.5). As expected, Dazl was not detected in Sertoli cells, somatic cells within the tubules that support the developing germ cells (Cooke *et al.*, 1996). In the absence of primary antibody, immunostaining was only present in the Leydig cells between the tubules, suggesting that the observed pattern in germ cells is specific for Dazl (Figure 3.5 – Neg).

A representative montage of individual cells from each phase of development was constructed (Figure 3.6) using Adobe Photoshop and collated into a spermatogenesis developmental diagram based on the table of Russell 1990. This representation allowed periods of strong Dazl expression during mouse spermatogenesis to be clearly discerned. These results show that Dazl is present in the cytoplasm of all observed spermatogonia (A, intermediate and B) and continues through early meiotic cells including preleptotene, but decreases at leptotene in stage IX tubules and is undetectable in stage X leptotene cells. Through zygotene (stages XI and XII) Dazl expression resumes and is very robust throughout pachytene but starts to decrease again at diplotene (stage XI). Finally by anaphase of the meiosis I to meiosis II transition (m1-m2) Dazl was almost completely absent. Where observed Dazl was cytoplasmic but nuclear expression was also observed in B spermatogonia (stage V-VI), as described (Ruggiu *et al.*, 1997).

In conclusion, this detailed characterisation showed that Dazl is expressed during mitosis and meiosis, but undergoes a surprising reduction at leptotene before recovering during zygotene and is most robustly expressed during pachytene. Levels of Dazl diminish during the meiosis I to meiosis II transition and Dazl is absent from post-meiotic germ cells.

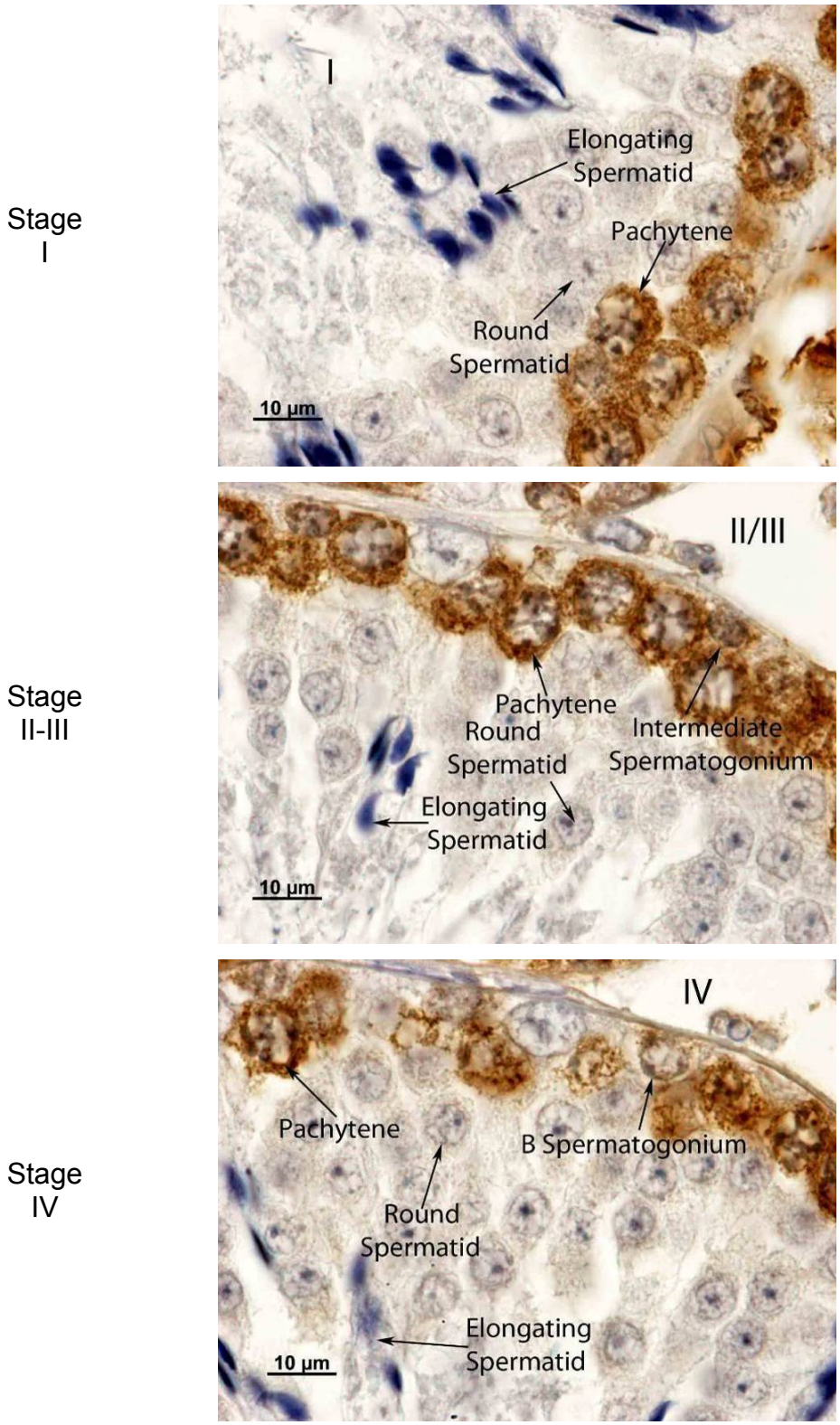


**Figure 3.2 - Dazl is expressed in mouse adult testes – stages I to IV.** IHC with DAB detection using an anti-DAZL antibody (1/250 dilution) in adult mouse testes detects Dazl expression. Germ cell types are marked. Tubule stages indicated in roman numerals. x100 magnification.

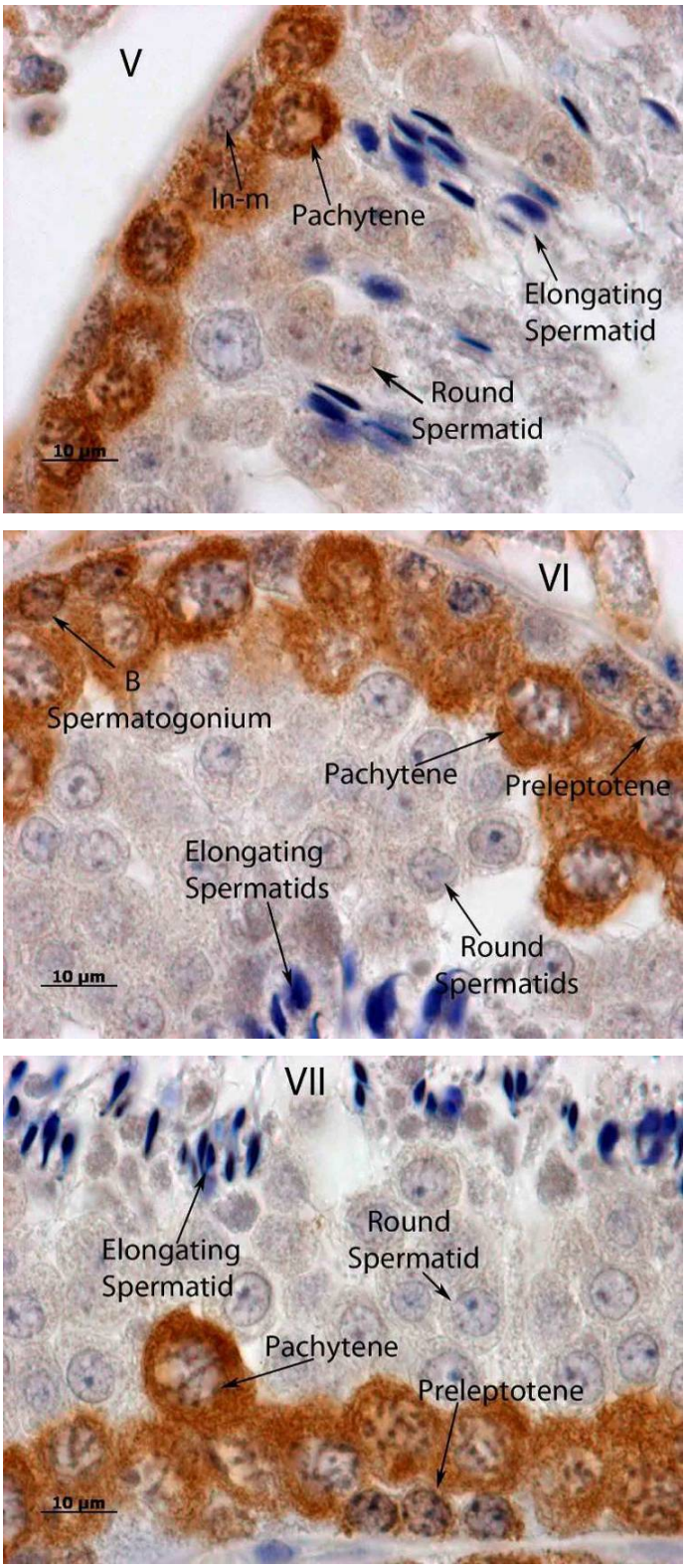


**Figure 3.3 -** Dazl is expressed in mouse adult testes – stages V to VII. **IHC with DAB detection using an anti-DAZL antibody (1/250 dilution) in adult mouse testes detects Dazl expression. Germ cell types are marked. Tubule stages indicated in roman numerals. x100 magnification.**

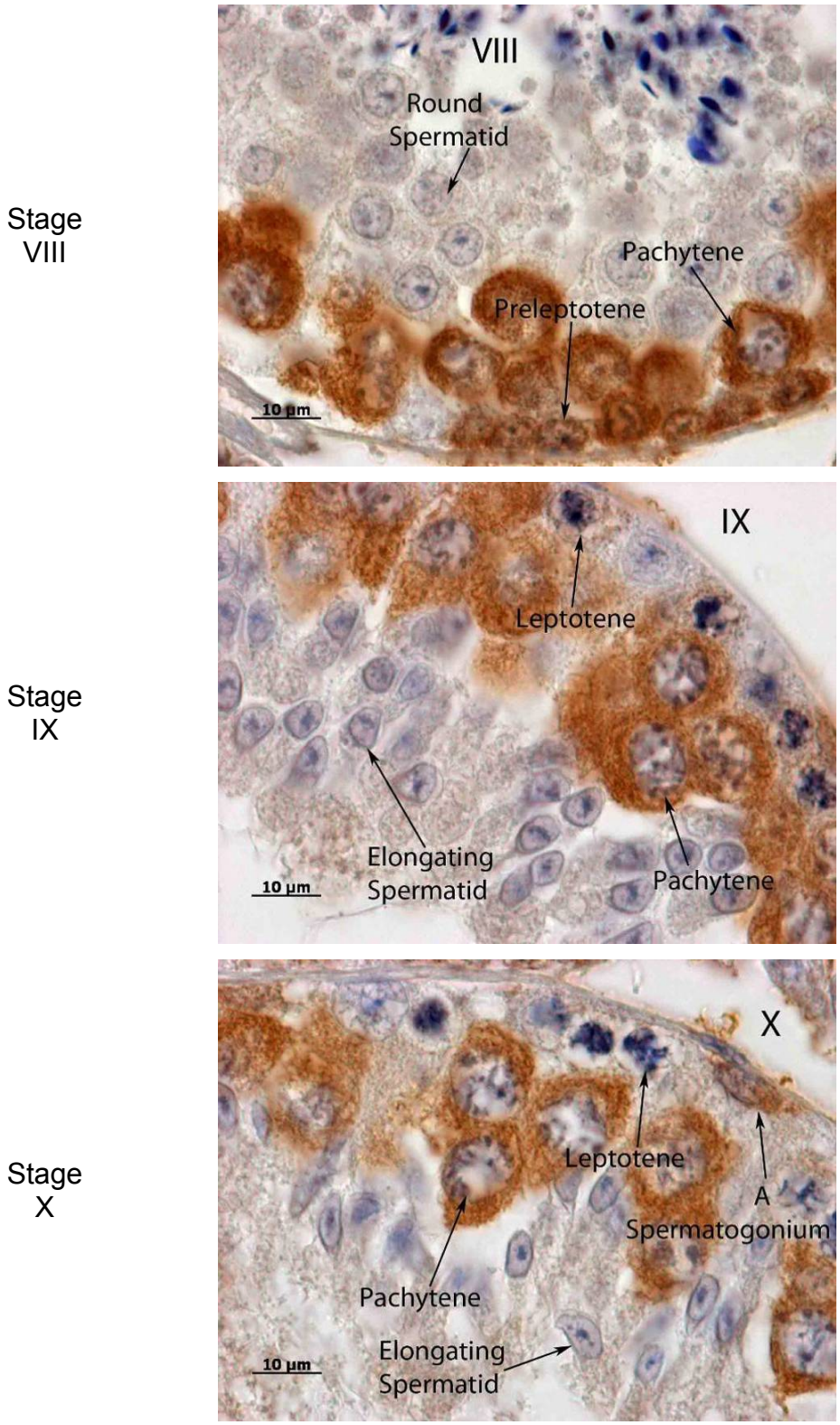


**Figure 3.4 -** Dazl is expressed in mouse adult testes – stages VIII to X. **IHC with DAB detection using an anti-DAZL antibody (1/250 dilution) in adult mouse testes detects Dazl expression. Germ cell types are marked. Tubule stages indicated in roman numerals. x100 magnification.**

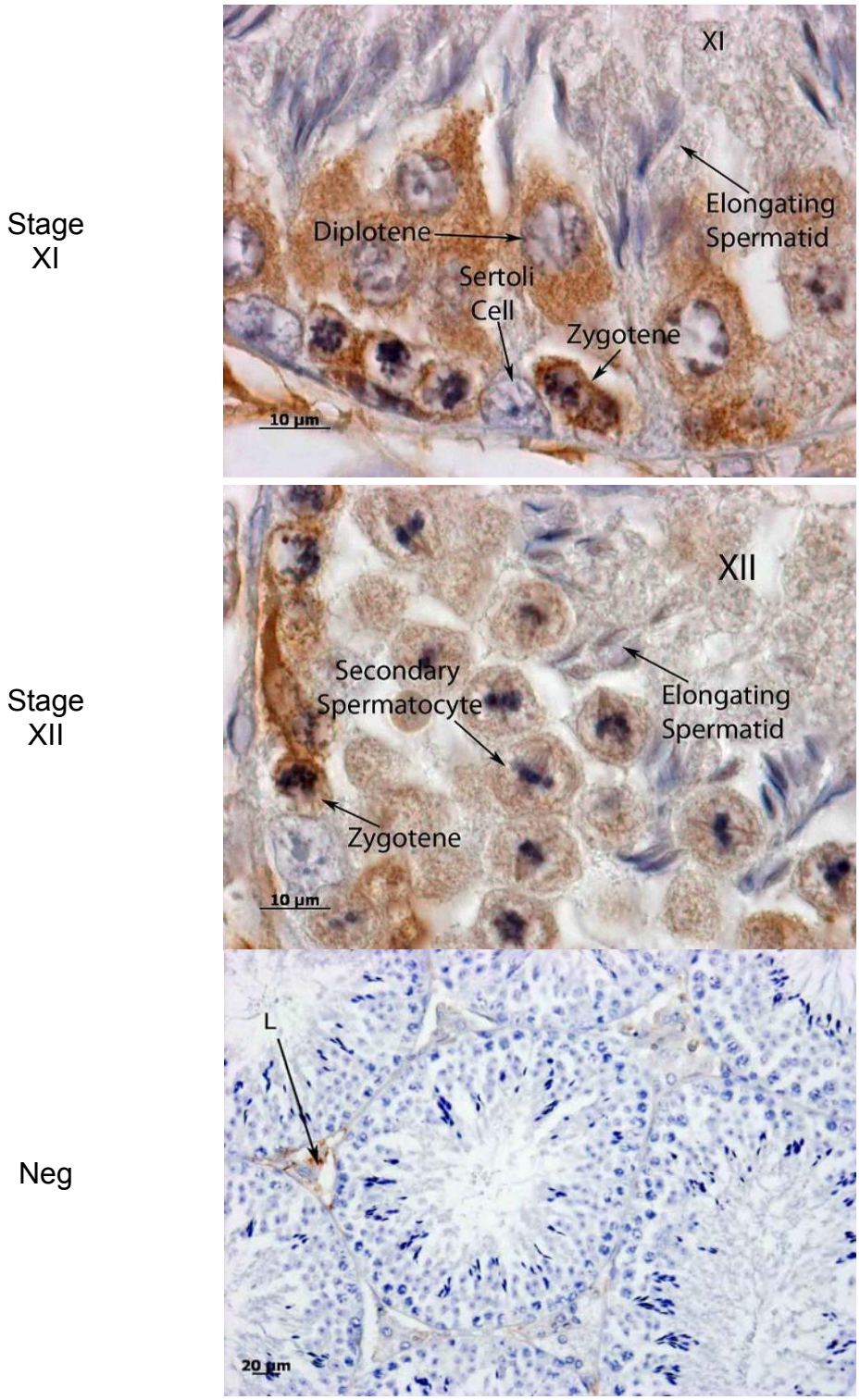


**Figure 3.5 -** Dazl is expressed in mouse adult testes – stages XI and XII. **IHC with DAB detection using an anti-DAZL antibody (1/250 dilution) in adult mouse testes detects Dazl expression. Germ cell types are marked. Tubule stages indicated in roman numerals. Stage XI and XII x100 magnification. Neg – negative control; L – Leydig cell; Neg – x40 magnification.**

**Figure 3.6 -** Montage of individual cells representing the stages of mouse spermatogenesis immunostained for Dazl. **Tubule stages indicated by roman numerals I - XII. Ais – isolated A spermatogonium; Apr – proliferating A spermatogonium; m-In - A spermatogonium into intermediate spermatogonium; In-m - intermediate spermatogonium into B spermatogonium; B – B spermatogonium; B-Im - B spermatogonium into preleptotene spermatocyte; Pl – preletotene spermatocyte; L – leptotene spermatocyte; Z – zygotene spermatocyte; P – pachytene spermatocyte; D – diplotene spermatocyte; m1-m2 – transition between meiosis I and II; 1-16 – stages of spermatids, 1-8 round spermatids, 9-16 elongating spermatids.**

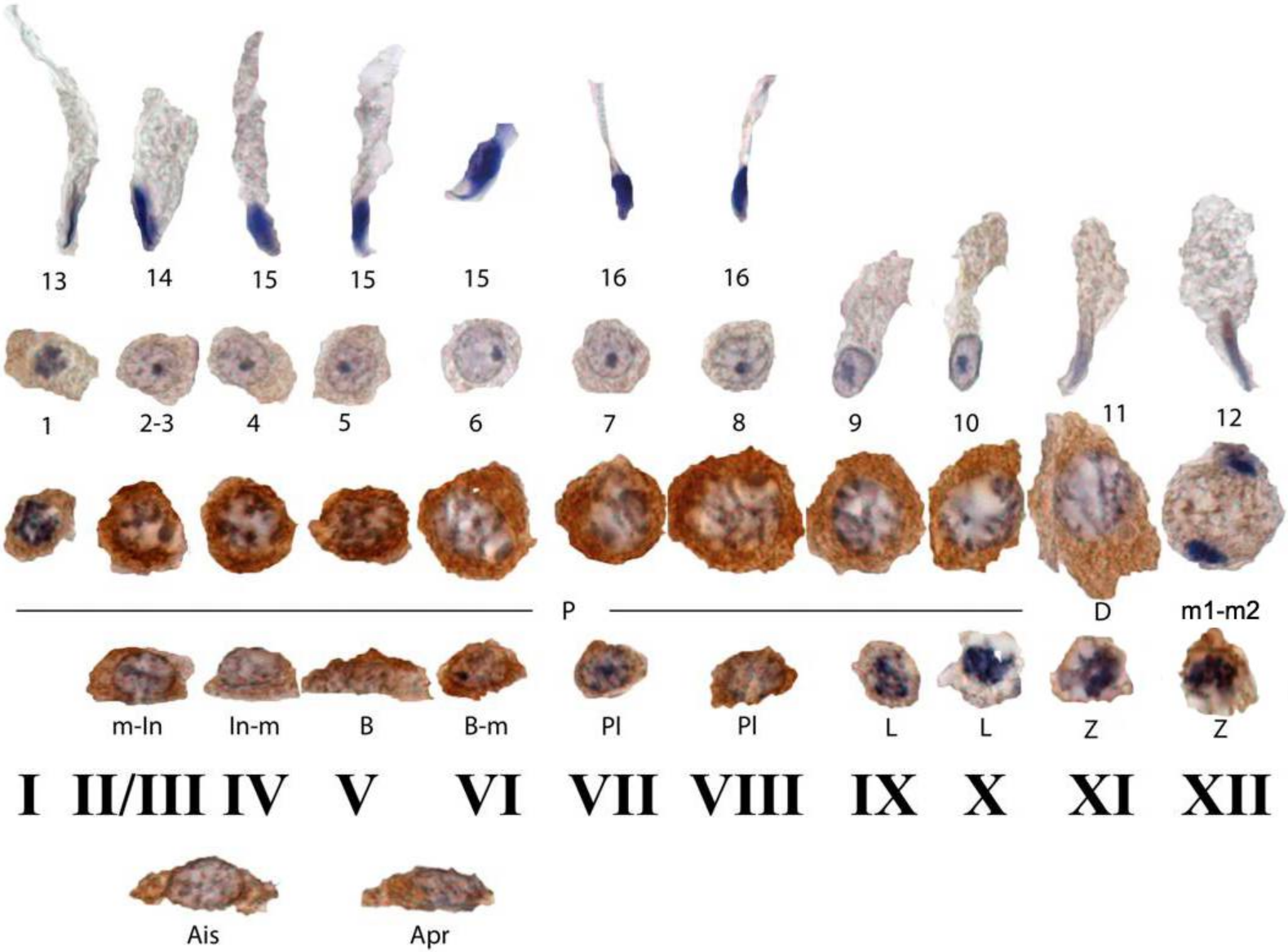
13
14
15
15
15
16
16
1
2-3
4
5
6
7
8
9
10
11
12
P
D
m1-m2
m-In
In-m
B
B-m
Pl
Pl
L
L
Z
Z
I
II/III
IV
V
VI
VII
VIII
IX
X
XI
XII
Ais
Apr

### 3.2.2 Pabp1 in mouse adult testes

Pabp1 mRNA has been shown to be present in pachytene spermatocytes and round spermatids (Kleene *et al.*, 1994, Gu *et al.*, 1995), however it is not clear to what extent this reflects the expression of Pabp1 protein, as PABP1 mRNA is subject to robust translational control. Thus, in order to gain an understanding of Pabp1 expression during mouse spermatogenesis, the efficacy of two anti-PABP1 antibodies, recently generated within the lab, for IHC was investigated (Appendix 2). One of these antibodies (Marshall) had been shown to be PABP1-specific by western blotting and immunofluorescence in cultured cell lines (Burgess *et al.*, 2011). As both antibodies gave similar results (Appendix 2), subsequent experiments were performed with Marshall, described subsequently as anti-PABP1 antibody.

Anti-PABP1 antibody was applied to adult testis sections and tubule stages identified based on cell morphology. In stage I-IV tubules (Figure 3.7), Pabp1 was present in the cytoplasm of round and elongating spermatids, but no expression was observed in pachytene spermatocytes. Pabp1 was not detected in any of the spermatogonial phases in stages I-VI (or in any other tubule stages, Figures 3.8 to 3.10). Pabp1 was also robustly expressed in round spermatids within stage V-VII tubules (Figure 3.8) and to a lesser extent in elongating spermatids at these stages. Pabp1 was absent in pachytene cells at stage V (Figure 3.8), but started to be visible in stage VI pachytene cells and was abundant in the cytoplasm of pachytene cells by stage VII. No Pabp1 expression was observed in early spermatocytes in these or any later stages, until pachytene spermatocytes in stage VI. In stages VIII-X (Figure 3.9) Pabp1 was present in all pachytene spermatocytes and spermatids (round and elongating) but not in the spermatozoa in the lumen of the tubules (stage VIII). In the last two stages, XI and XII, Pabp1 was expressed in late pachytene and diplotene spermatocytes (stage XI), secondary spermatocytes (stage XII) and elongating spermatids (stage XI and XII) but not in early zygotene spermatocytes (Figure 3.10). Pabp1 was absent from the Sertoli and Leydig cells at all stages and as the no primary antibody control (Figure 3.11) did not show immunostaining the observed pattern appeared to dependent on the PABP1 antibody. Lastly, Pabp1 was not

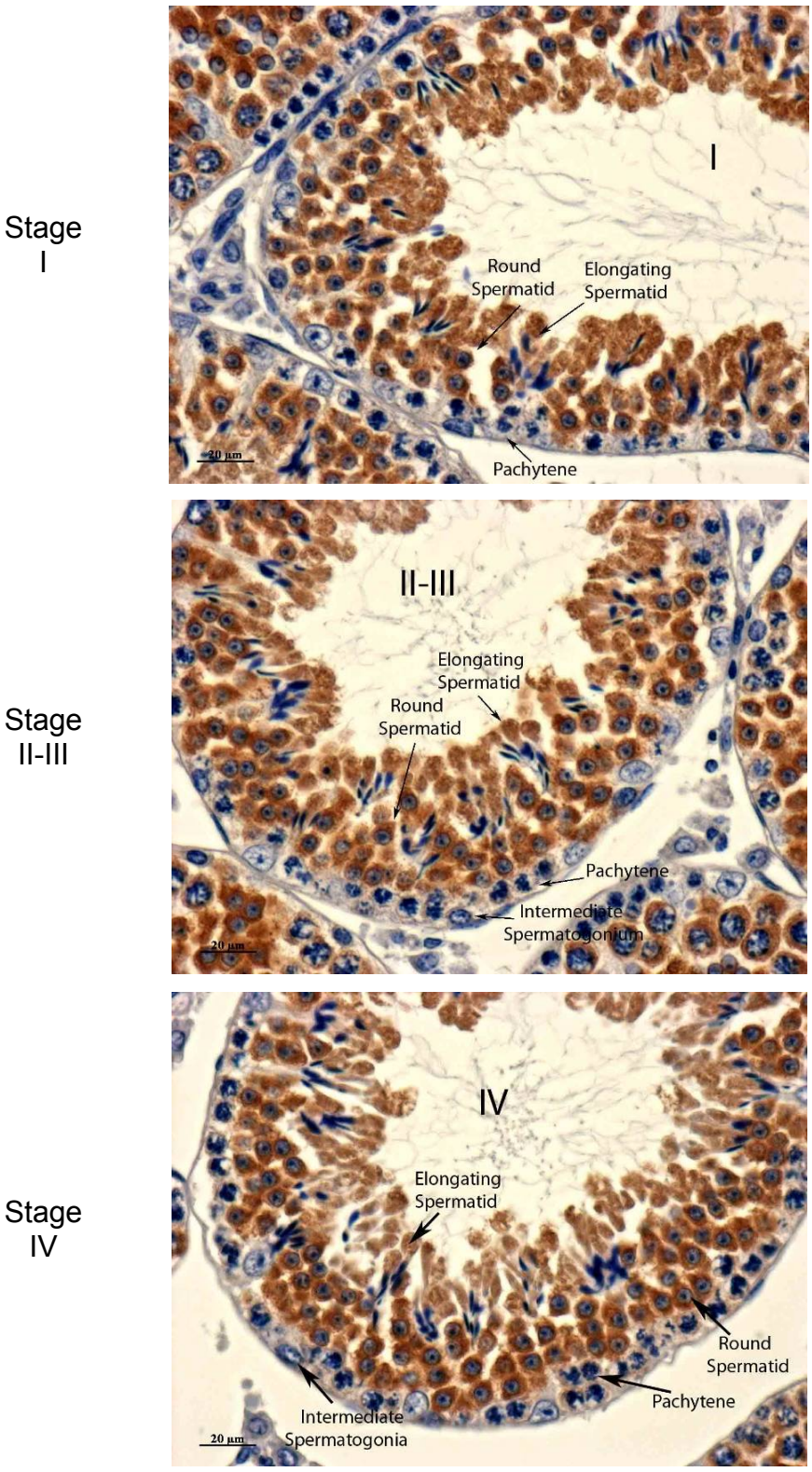


**Figure 3.7 -** Pabp1 is expressed in mouse adult testes – stages I to IV. **IHC with DAB detection using an anti-PABP1 antibody (1/5000 dilution) in adult mouse testes detects Pabp1 expression. Germ cell types are marked. Tubule stages indicated in roman numerals. x40 magnification.**

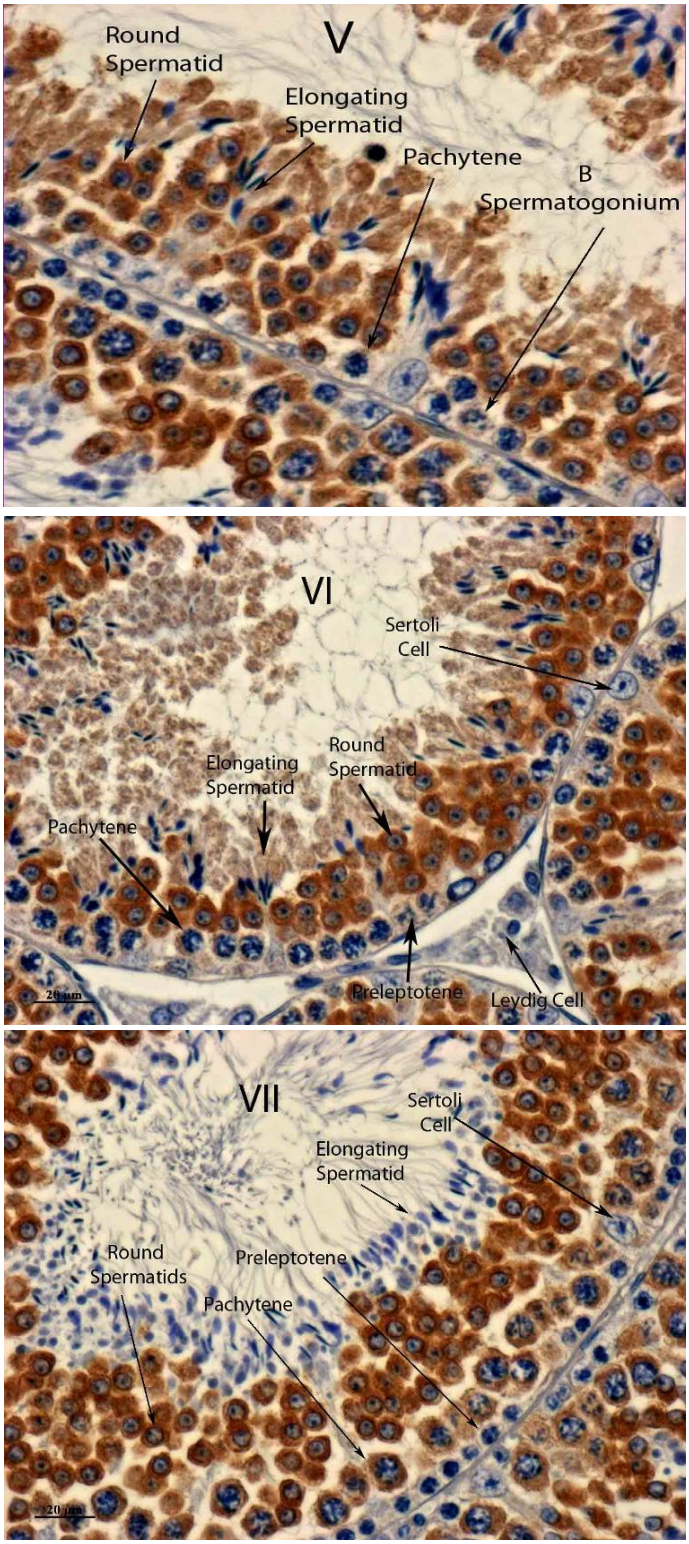


**Figure 3.8 -** Pabp1 is expressed in mouse adult testes – stages V to VII. **IHC with DAB detection using an anti-PABP1 antibody (1/5000 dilution) in adult mouse testes detects Pabp1 expression. Germ cell types are marked. Tubule stages indicated in roman numerals. x40 magnification.**

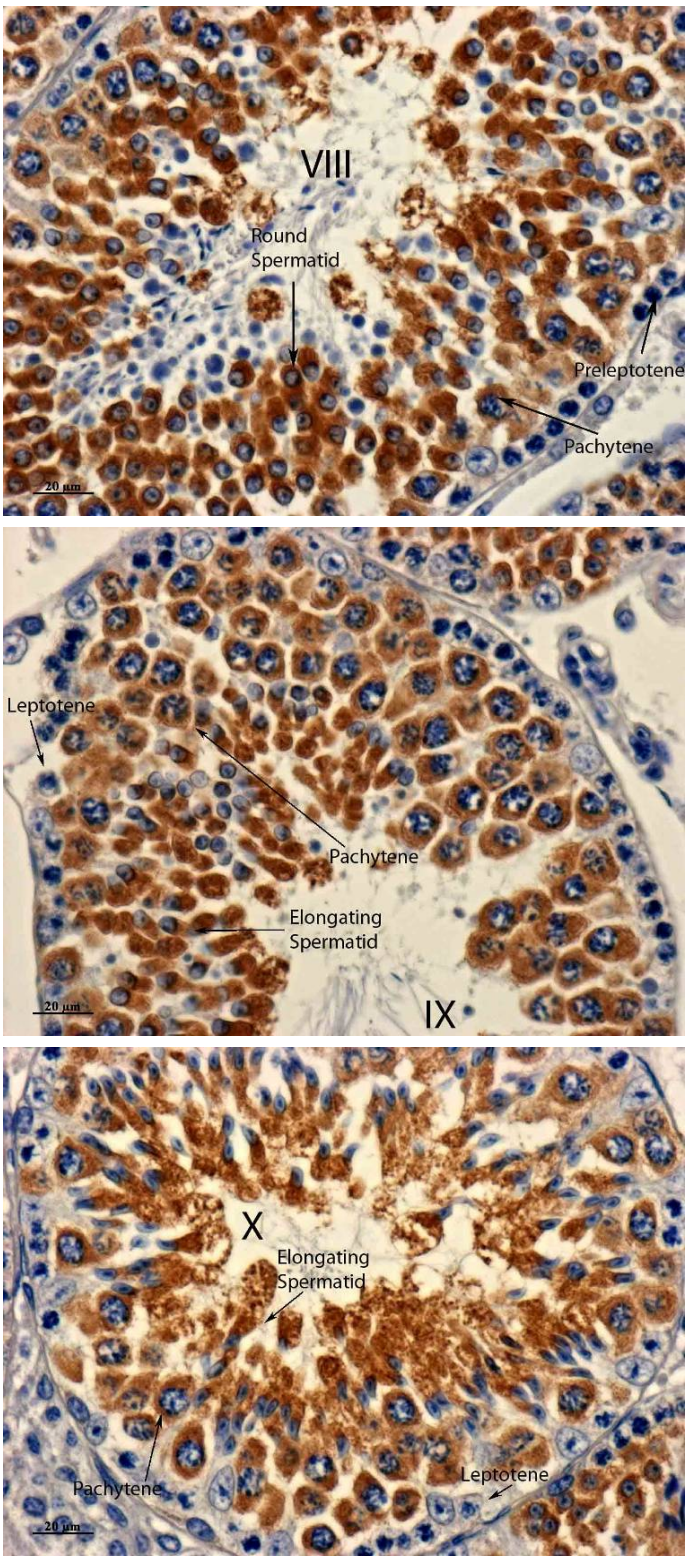


**Figure 3.9 -** Pabp1 is expressed in mouse adult testes – stages VIII to X. **IHC with DAB detection using an anti-PABP1 antibody (1/5000 dilution) in adult mouse testes detects Pabp1 expression. Germ cell types are marked. Tubule stages indicated in roman numerals. x40 magnification.**

Stage XI

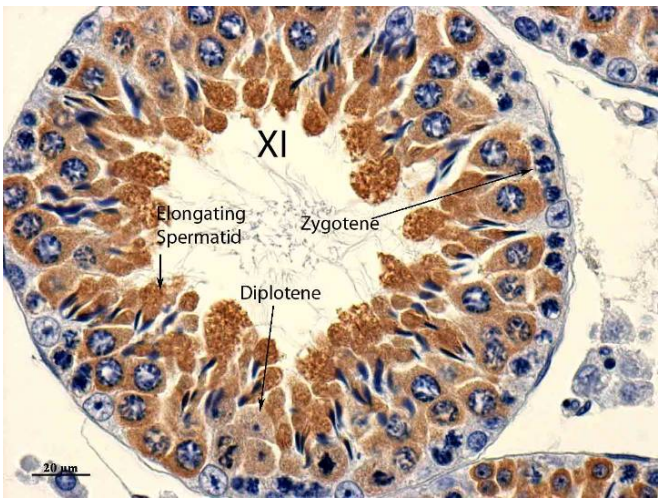


Stage XII

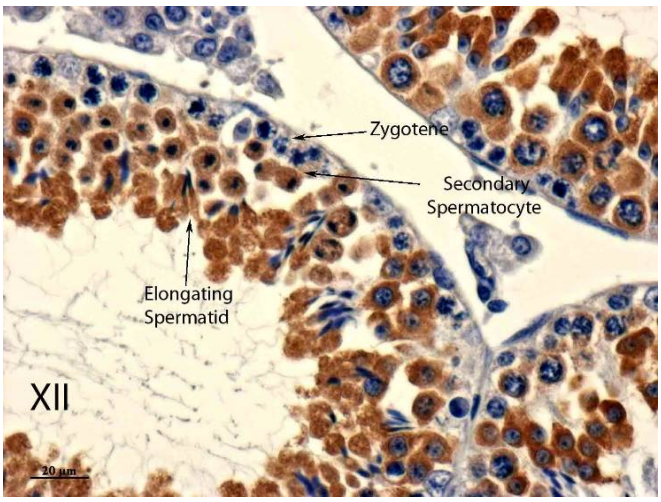


spermatozoa

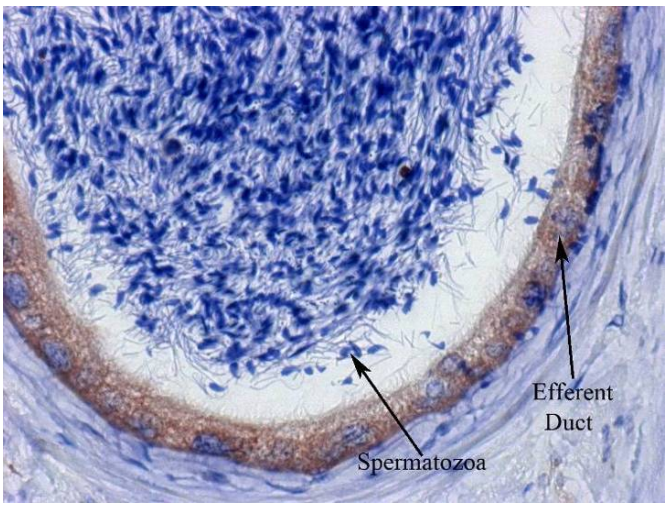


**Figure 3.10 -** Pabp1 is expressed in mouse adult testes – stages XI, XII and efferent ducts. **IHC with DAB detection using an anti-PABP1 antibody (1/5000 dilution) in adult mouse testes detects Pabp1 expression. Germ cell types are marked. Tubule stages indicated in roman numerals. x40 magnification.**

Neg

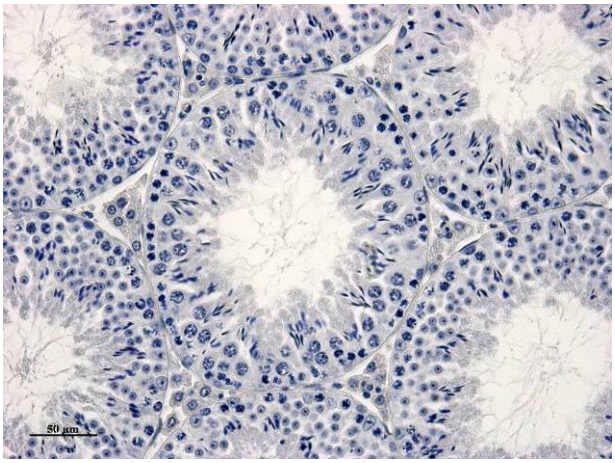


**Figure 3.11 -** Negative control for PABP1 antibody in mouse testes. **Negative control for IHC with DAB detection for the PABP1 antibody in mouse testes performed with no primary antibody.. x20 magnification.**

observed in spermatozoa within the efferent ducts (Figure 3.10), although the ciliated epithelium cells of the efferent ducts did express Pabp1, providing a positive control for immunostaining.

The twelve stages were subsequently compiled to form a Russel *et al.*-like staging diagram (Figure 3.12) (Russell *et al.*, 1990)showing that Pabp1 expression starts in the cytoplasm of germ cells at pachytene spermatocytes within stage VI-VII tubules. A peak of Pabp1 expression can be observed between phase 4 and 9 spermatids. Nonetheless, PABP1 expression appears robust from pachytene stage VII until the phase 9-10 spermatids. As the spermatids undergo nuclear elongation and condensation, Pabp1 levels diminish gradually with no Pabp1 being observed by the 16th-spermatid phase by which time they are released into the lumen of the tubules (stage VIII).

**Figure 3.12 -** Pabp1 expression during mouse spermatogenesis. **Tubule stages are described in roman numerals I-XII. A – isolated A spermatogonium; Apr – proliferating A spermatogonium; m-In – A spermatogonium into intermediate spermatogonium; In-m - intermediate spermatogonium into B spermatogonium; B – B spermatogonium; B-Im – B spermatogonium into preleptotene spermatocyte; PI – preletotene spermatocyte; L – leptotene spermatocyte; Z – zygotene spermatocyte; P – pachytene spermatocyte; D – diplotene spermatocyte; m1-m2 – transition between meiosis I and II; 1-16 – stages of spermatids, 1-8 round spermatids, 9-16 elongating spermatids.**

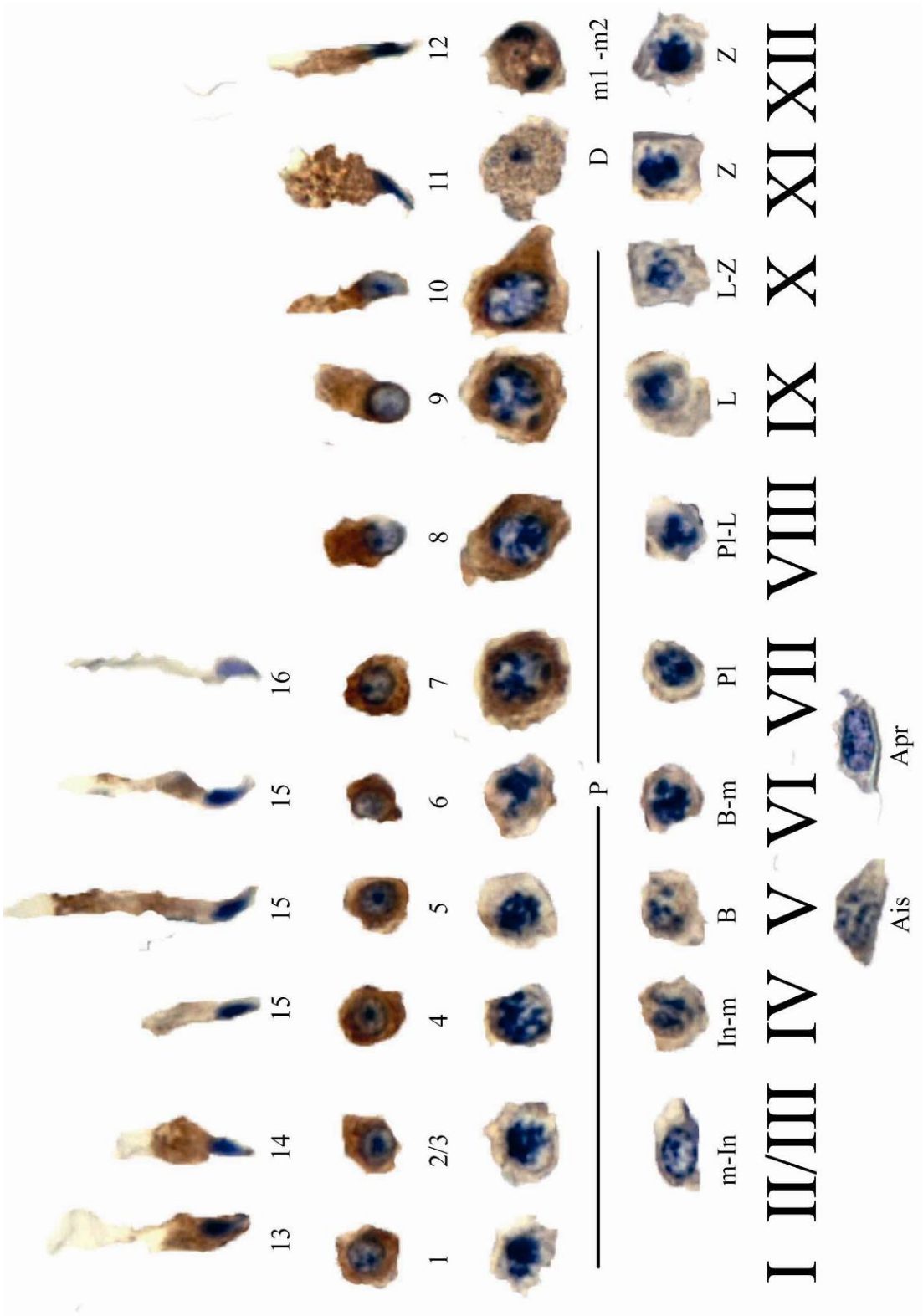
I II/III IV V VI VII VIII IX X XI XII
m-In In-m B B-m Pl Pl-L L L-Z Z Z
1 2/3 4 5 6 7 8 9 10 11 12
13 14 15 15 15 16
P
D m1 -m2
Ais Apr

### 3.2.3 Colocalisation of Dazl and Pabp1 in adult mouse testes

An *in vivo* interaction between DAZL and PABP1 in mammalian gametogenesis would require the simultaneous presence of both proteins in the cytoplasm of the same cells. The previous data (Figure 3.6, 3.12 and 3.13) show that both proteins appear to be present in the cytoplasm of pachytene spermatocytes from stage VI until the meiosis I to meiosis II transition at stage XII.

To formally verify their co-localisation, dual immunofluorescence (IF) was performed with fluorescently labeled secondary antibodies. Since previous optimization showed that anti-DAZL and anti-PABP1 antibodies work best in 4% NBF and Bouin's fixed tissues respectively (Appendix 1 – Figure A1.2 and Appendix 2 – Figure A2.2), intiatial dual IF was performed on tissues fixed with either of the fixatives (data not shown). Subsequent analysis was undertaken in 4% NBF fixed tissues. In the absence of the PABP1 primary antibody, Dazl was detected in spermatogonia and most stages of spermatocytes, including pachytene (Figure 3.14-a), consistent with previous results. Pabp1 was detected in round and elongating spermatids in all tubules but only in some pachytene stages (Figure 3.14-b), when the Dazl antibody was omitted. When both primary antibodies were present (Figure 3.14-c), merged images showed that Pabp1 and Dazl did not colocalise in stage III pachytene spermatocytes but did colocalise in the cytoplasm of pachytene spermatocytes in stage V-VI and VII tubules (Figure 3.14c). In stage VII, where both proteins are more strongly expressed, colocalisation results in a more yellow colour than in stage V-VI tubules where the pixels remain green-yellow due to weaker PABP1 expression at this stage.

These results, together with the individual DAB expression patterns (Figures 3.6, 3.12 and 3.13), support the conclusion that Dazl and Pabp1 are present together in the cytoplasm of pachytene spermatocytes from stage VI-VII (Figure 3.14) until the meiosis I to meiosis II transition at stage XII (summarized in Figure 3.15).

a)

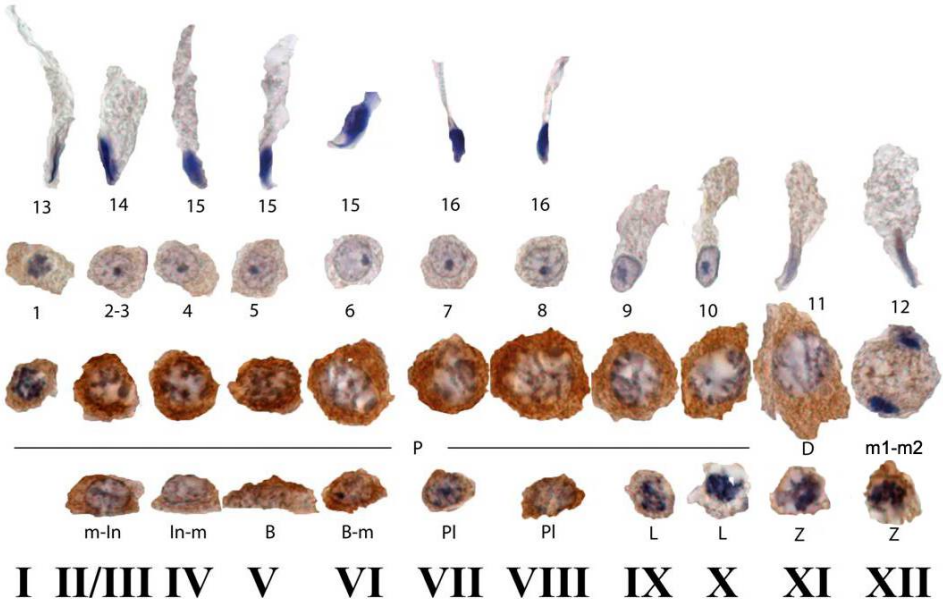


b)

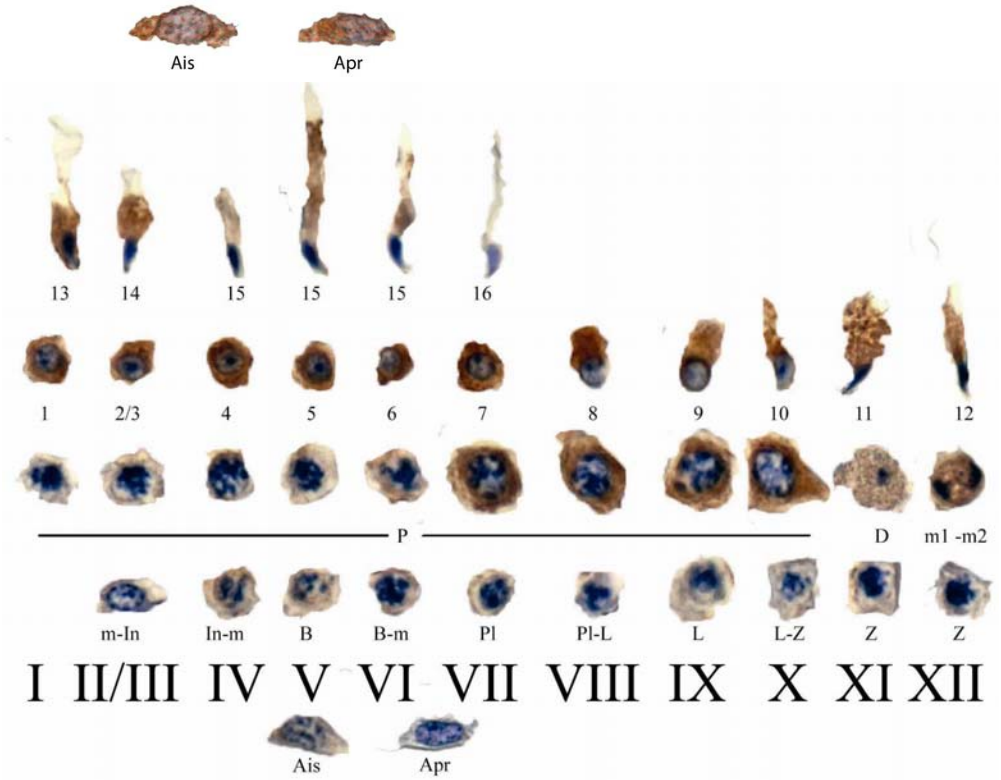


**Figure 3.13 - Dazl (a) and Pabp1 (b) are co-expressed in the cytoplasm of stage 7 pachytene spermatocytes until the meiosis 1 to meiosis 2 transition.** Diagrams of spermatogenic developmental were assembled based on the Russel et al diagram (Figure 3.1) following IHC with DAB detection with a DAZL (Figure 3.6) and PABP1 (Figure 3.12) primary antibodies. More detailed descriptions are provided in the legends of Figure 3.6 and 3.12.

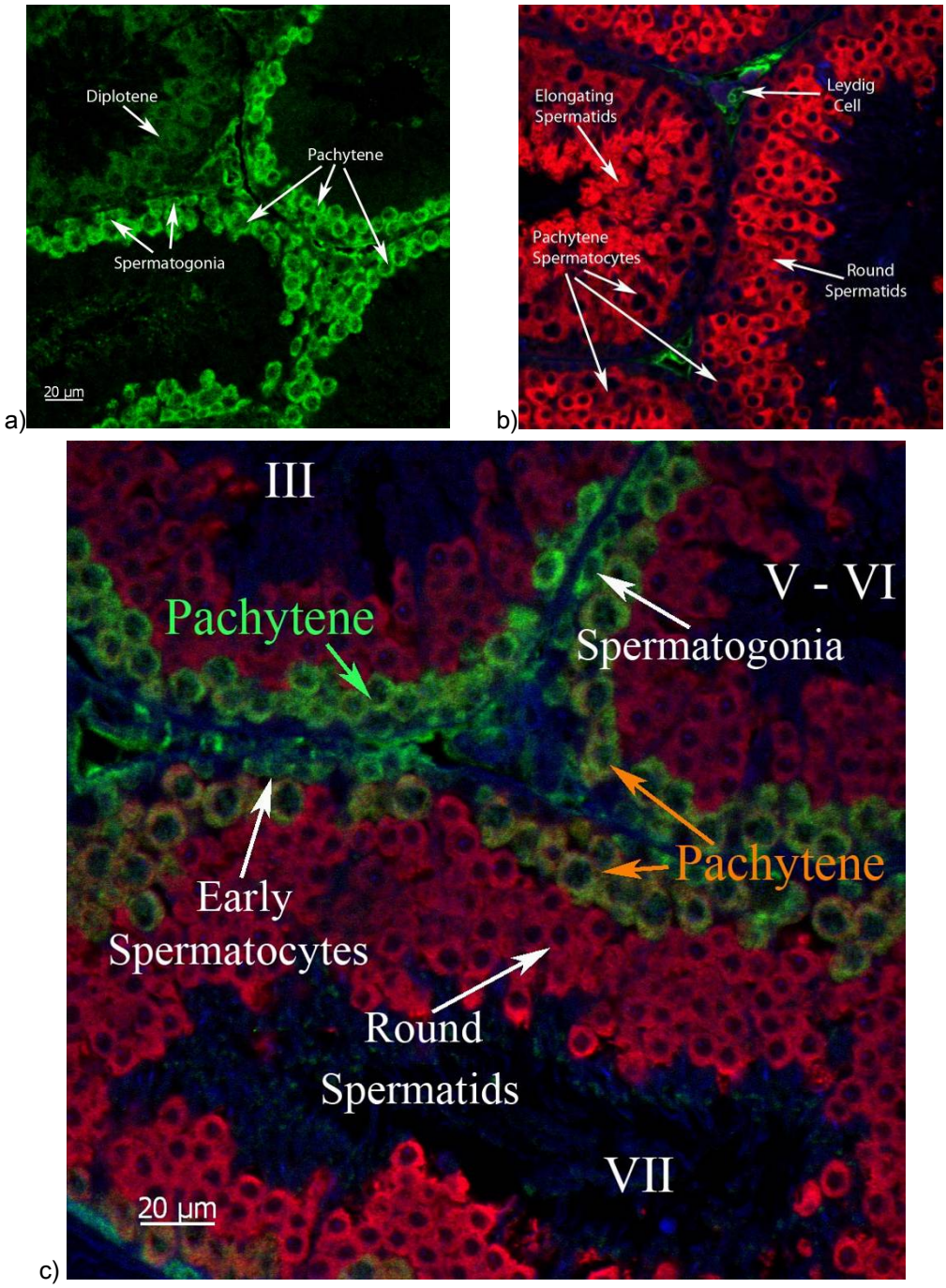


**Figure 3.14 -** Stage specific Dazl and Pabp1 colocalisation. **Adult testes were used for dual-IF was used to detect co-expression of Dazl (green) and Pabp1 (red) in adult mouse testes using fluorescently labelled secondary antibodies. a and b represent negative controls, for secondary antibodies, preformed with only one primary antibody: a – Anti-DAZL primary antibody; b – Anti-PABP1 primary antibody; nuclear counterstain (DAPI) – blue. Pachytene spermatocytes showing expression of both proteins are identified by orange arrows (Stage V-VI and VII), green arrow identifies pachytene spermatocytes only expressing Dazl. Specific cell types are indicated. Tubule stage is indicated by roman numerals.**

**Figure 3.15 -** Staging diagram summarising the expression and co-expression of Dazl and Pabp1 during mouse spermatogenesis. **Adaptation of the Russel et al diagram for mouse spermatogenesis, showing periods of Dazl (green) and Pabp1 (red) expression. Ais - isolated A spermatogonium; Apr - proliferating A spermatogonium; m-In - A spermatogonium into intermediate spermatogonium; In-m - intermediate spermatogonium into B spermatogonium; B - B spermatogonium; B-lm - B spermatogonium into preleptotene spermatocyte; PL - preletotene spermatocyte; L - leptotene spermatocyte; Z – zygotene spermatocyte; P – pachytene spermatocyte; D – diplotene spermatocyte; m1-m2 – transition between meiosis I and II; 1-16 – stages of spermatids, 1-8 round spermatids, 9-16 elongating spermatids.**

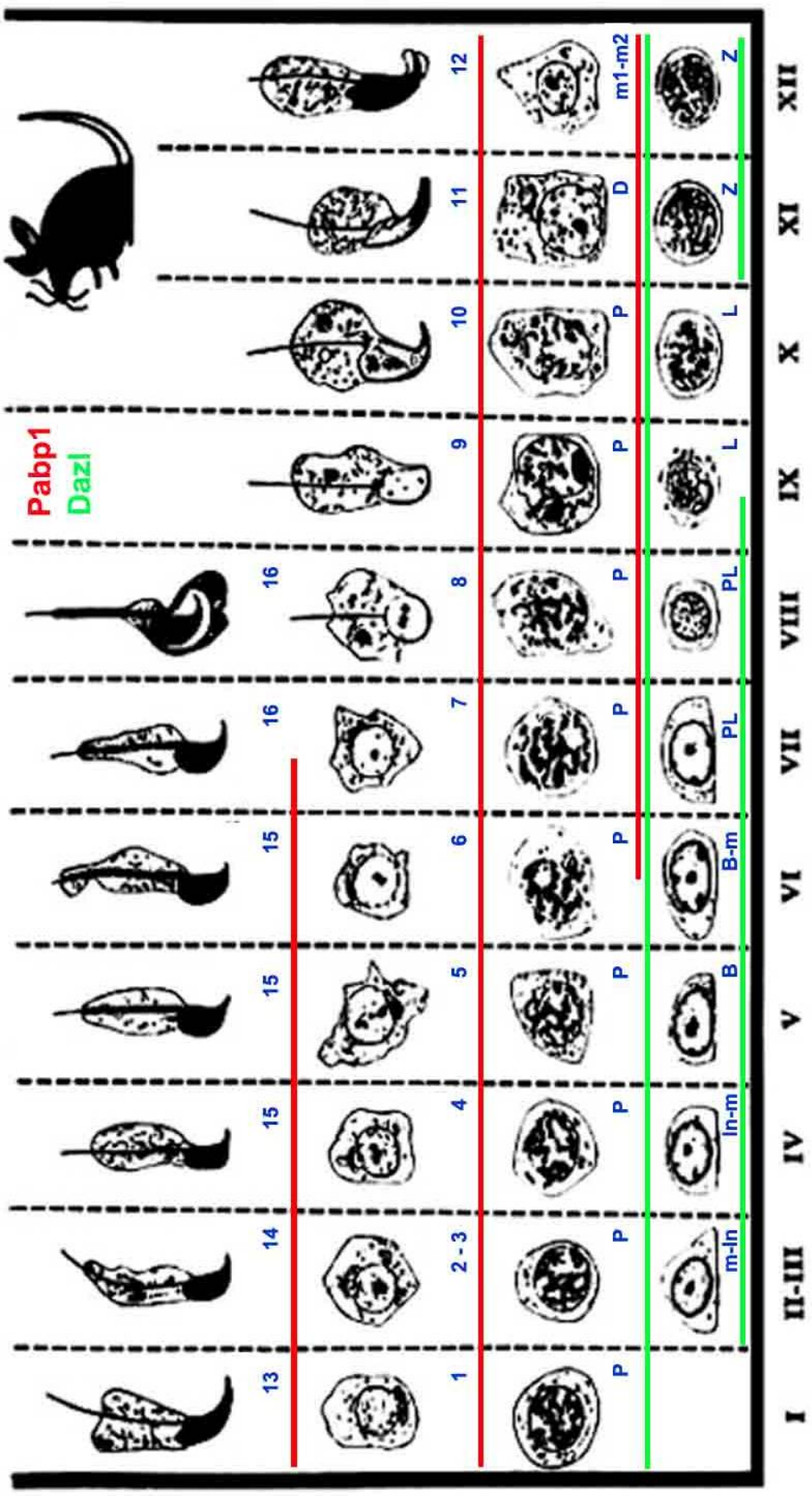
Pabp1
Dazl
I
II-III
IV
V
VI
VII
VIII
IX
X
XI
XII
P
m-ln
ln-m
B
B-m
PL
L
D
m1-m2
Z

### 3.2.4 Expression of Dazl and Pabp1 in pre-pubertal testis

Several mRNA targets have been proposed to be translationally regulated by Dazl during mammalian spermatogenesis (Venables *et al.*, 2001, Jiao *et al.*, 2002, Reynolds *et al.*, 2005, Reynolds *et al.*, 2007, Zeng *et al.*, 2008). To date only two, Mvh and Sycp3 (Reynolds *et al.*, 2005, Reynolds *et al.*, 2007), have been validated with Mvh and Sycp3 protein levels being decreased by 4-5 and 7 days post-partum (dpp) respectively in outbred Dazl knockout mice (Dazl-KO). Because this analysis was carried out during the first wave of spermatogenesis, expression of Dazl and Pabp1 was assessed during this timeframe to determine whether they are present within the same cells at times when decreased translation of target mRNAs is observed in Dazl-KO mice (Reynolds *et al.*, 2005, Reynolds *et al.*, 2007).

Three developmentally relevant time points were chosen: 3 dpp prior to the initiation of meiosis (when the only germ cells present are prospermatogonia); early meiosis (10 dpp, when spermatogonia, preleptotene and leptotene spermatocytes are present); and mid-meiosis (12 dpp when spermatogonia, preleptotene/leptotene and zygotene/pachytene spermatocytes are present) (Bellve *et al.*, 1977). Germ cells were identified by the morphology of their nuclei.

Despite significant general background within the lumen, weak Pabp1 expression can be observed in the cytoplasm of prospermatogonia at 3 dpp (Figure 3.16-a). At 10 dpp, weak Pabp1 expression can be observed in the cytoplasm of spermatogonia (Figure 3.16-b). Finally, at 12 dpp, Pabp1 expression is observed in the cytoplasm of spermatogonia and early spermatocytes (preleptotene and leptotene) (Figure 3.16-c). No immunostaining was observed in the absence of primary antibody. These results indicate that Pabp1 expression can be detected in early stages of spermatogenesis, during differentiation of spermatogonia and early spermatocytes overlapping with the period when Mvh and Sycp3 expression is reduced in the Dazl-KO mouse.

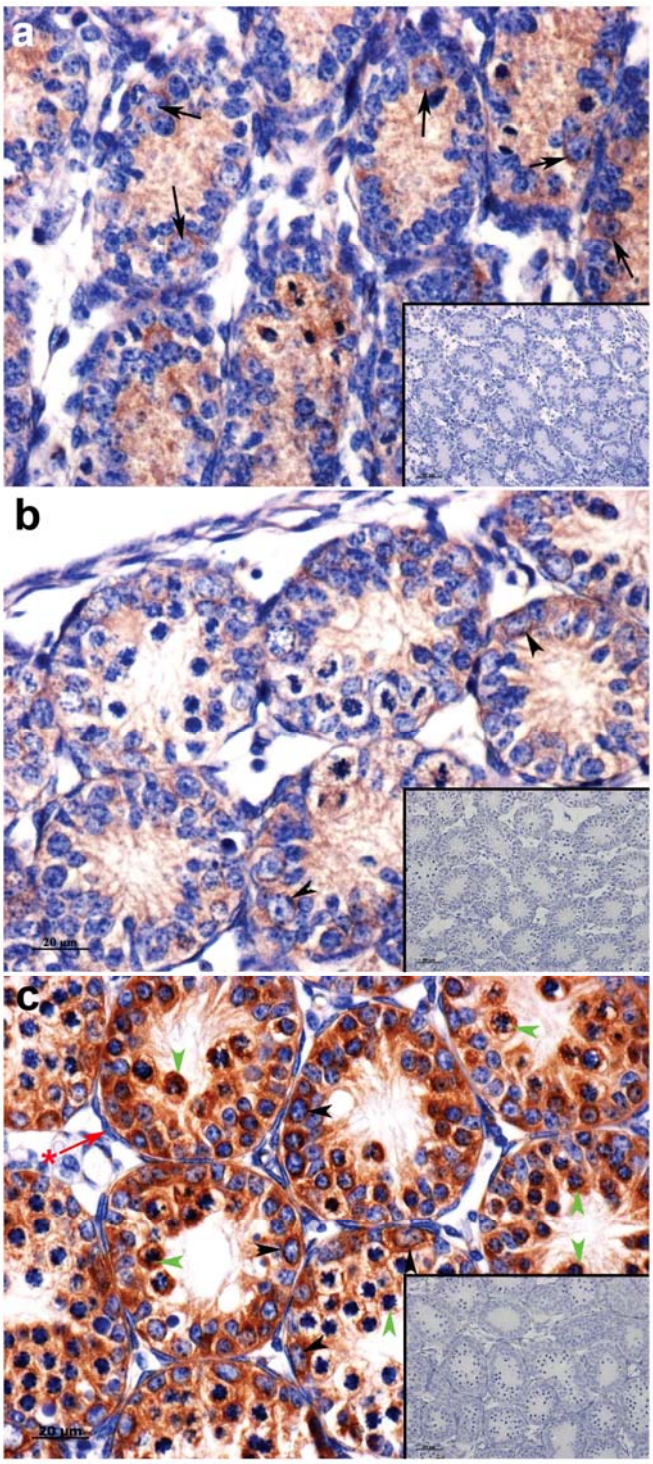


**Figure 3.16 - Pabp1 is expressed in pre-pubertal mouse testes.** IHC using a PABP1 antibody in pre-pubertal mouse testis aged a – 3 dpp; b – 10 dpp; c – 12 dpp. Black arrows indicate prospermatogonia; arrowheads indicate spermatogonia; green arrowheads indicate early meiotic germ cells. Germ cells were identified by characteristically large circular nucleus. In comparison, the somatic cells have narrow elongated nuclei. Red * - peritubular cell with no Pabp1 expression. x40 magnifications. insets – negative control with no primary antibody.

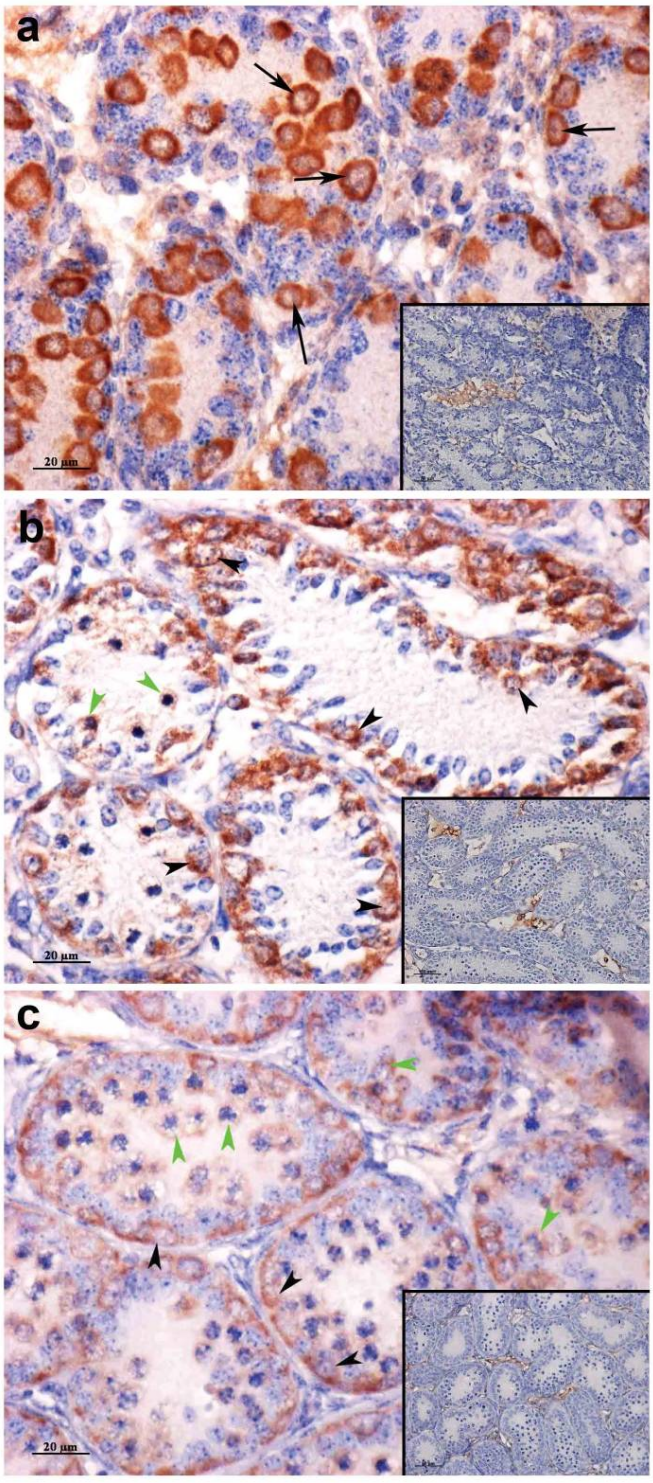


**Figure 3.17 -** Dazl is expressed in pre-pubertal mouse testes. **IHC using a DAZL antibody in pre-pubertal mouse testis aged a – 3 dpp; b – 10 dpp; c – 12 dpp. Black arrows indicate prospermatogonia; arrowheads indicate spermatogonia; green arrowheads indicate early meiotic germ cells. Germ cells were identified by characteristically large circular nucleus. In comparison, the somatic cells have narrow elongated nuclei. x40 magnifications. insets – negative control with no primary antibody.**

The presence of Dazl within these germ cells was confirmed showing that Dazl was strongly expressed at 3 dpp in prospermatogonia (Figure 3.17-a), decreasing with differentiation at 10 dpp (Figure 3.17-b) and was further reduced by 12 dpp (Figure 3.17-c). Thus, Pabp1 and Dazl are both present during germ cell development in male pre-pubertal mice, consistent with the model that DAZL may utilise PABP1 to stimulate translation of mRNAs such as Scyp3 and Mvh (Collier *et al.*, 2005b, Reynolds *et al.*, 2005, Reynolds *et al.*, 2007).

### 3.2.5 Expression of Dazl and Pabp1 during female fetal gametogenesis

In adult male mice, Dazl and Pabp1 colocalise during meiosis at the late pachytene phase. A similar colocalisation in females would occur during fetal development, as meiosis is initiated at 13.5 dpc in females concomitant with the germ cells being surrounded by somatic cells to form germ cell cysts (12.5 and 13.5 dpc) (Tam and Snow, 1981, Bendel-Stenzel *et al.*, 1998, McLaren, 2003). This event marks the beginning of germ cell sexual differentiation when they become committed to sex specific pathways and differences arise between sexes (Haston *et al.*, 2009, Kerr and Cheng, 2009). Male germ cells do not enter meiosis but undergo mitotic arrest. In keeping with this sex specific difference, meiotic progression is impaired in 15.5 dpc oogonia and germ cells are lost by 4 dpp in outbred Dazl-KO mice (Ruggiu *et al.*, 1997, Saunders *et al.*, 2003, Lin *et al.*, 2008).

Therefore the expression patterns of Dazl and Pabp1 were examined during fetal germ cell development in females both prior to and at the initiation of meiosis (12.5 dpc and 13.5 dpc respectively) and at 15.5 dpc when all germ cells have left interphase and are engaged in prophase I (Di Carlo *et al.*, 2000). Importantly, Figure 3.18-a reveals that Dazl protein is already present in the PGCs of 12.5dpc fetal ovaries. This is consistent with reports that Dazl mRNA is present as early as 14.5 dpc (Seligman and Page, 1998) and with recent reports that that PGCs in inbreed Dazl-KO C57BL/6 fail to respond to feminising or masculinising cues in developing gonads, which leads to the proposal that Dazl may serve as a so-called “licensing factor” for entry into oogenic or spermatogenic pathways (Gill *et al.*, 2011). At 13.5

dpc (Figure 3.18-b) PGCs continued to express significant levels of Dazl as they start to organize into clusters surrounded by developing granulosa cells, known as germ cell cysts (McLaren, 2003). By 15.5 dpc highly dense germ cell cysts can be observed, expressing high levels of Dazl (Figure 3.18-c).

Unfortunately, Pabp1 expression could not be assessed at 12.5 dpc due to scarcity of the tissue but was examined at 13.5 and 15.5 dpc (Figure 3.19). At 13.5 dpc, Pabp1 was expressed throughout the developing ovary, and it was possible to ascertain that this included the cytoplasm of the differentiating PGCs (Figure 3.19-a) which express Dazl (Figure 3.18-b). At 15.5dpc (Figure 3.19-b), Pabp1 remained diffusely expressed including in the cytoplasm of oogonia, although appeared less abundant than at 13.5 dpc. This reduced expression was consistently observed.

In conclusion, these results show that Dazl and Pabp1 are both present in the cytoplasm of PGCs at 13.5 dpc, the period when XX PGCs commit to a female differentiation pathway and initiate meiosis, with Pabp1 levels declining once meiosis is initiated. The presence of both proteins during this timeframe raises the possibility that the reported requirement for Dazl at this stage (Lin *et al.*, 2008, Gill *et al.*, 2011)) may reflect its role in stimulating mRNA-specific translation (Collier *et al.*, 2005b, Reynolds *et al.*, 2005, Reynolds *et al.*, 2007).

### 3.2.6 Expression of Dazl and Pabp1 in fetal male gonads

During fetal development, inbred male Dazl-KO mice develop phenotypes (Lin and Page, 2005, Lin *et al.*, 2008) and male germ cells enter into a sexual dimorphic mitotic arrest. It was of interest to determine the expression of Dazl and Pabp1 in male fetal gonads and whether their expression varies significantly to that in females.

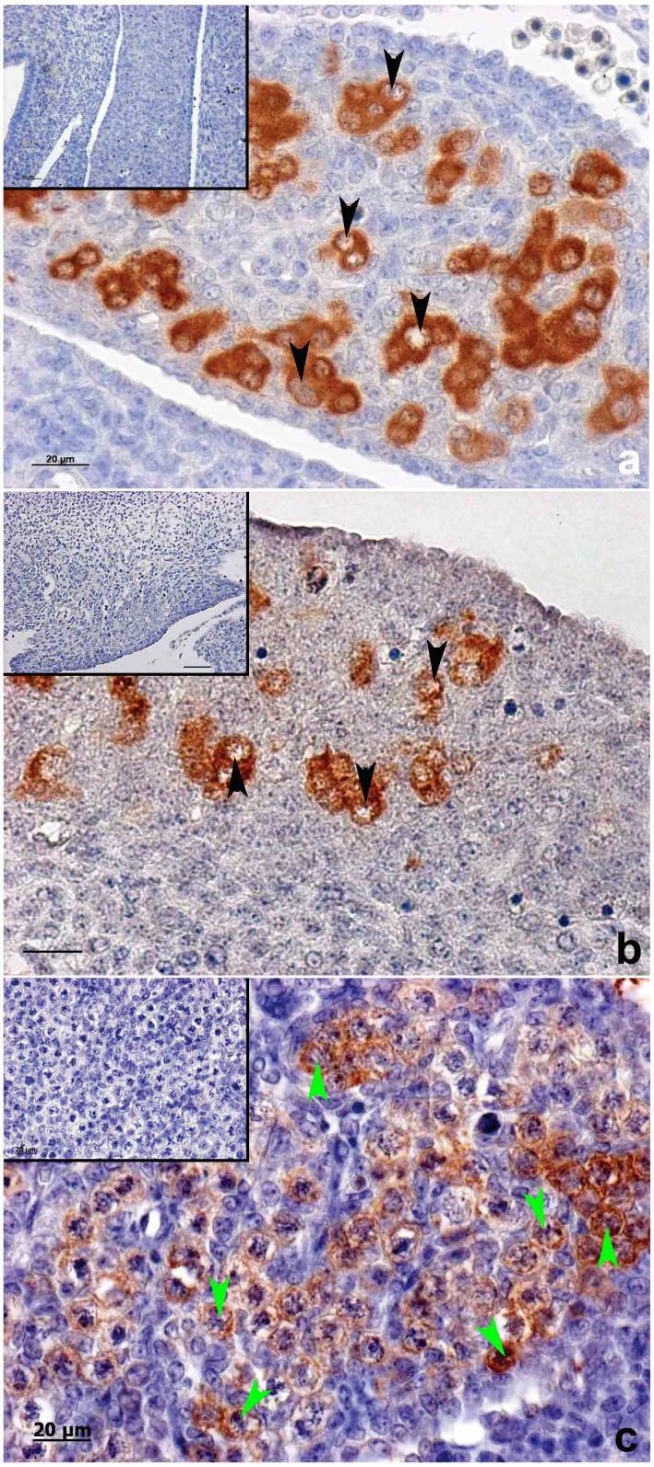


**Figure 3.18 -** Dazl is expressed in fetal female germ cells. **IHC analysis using a DAZL antibody in fetal mouse ovaries: a – 12.5 dpc; b – 13.5 dpc; c – 15.5 dpc; insets - negative control performed with no primary antibody. Arrowheads indicate germ cells which can be identified by their distinctive big round nuclei with diffuse chromatin and low nuclear to cytoplasm ratio, compared to the developing somatic cells which have smaller and more elongated nuclei: black – primordial germ cells; green - oogonia. x40 magnifications.**

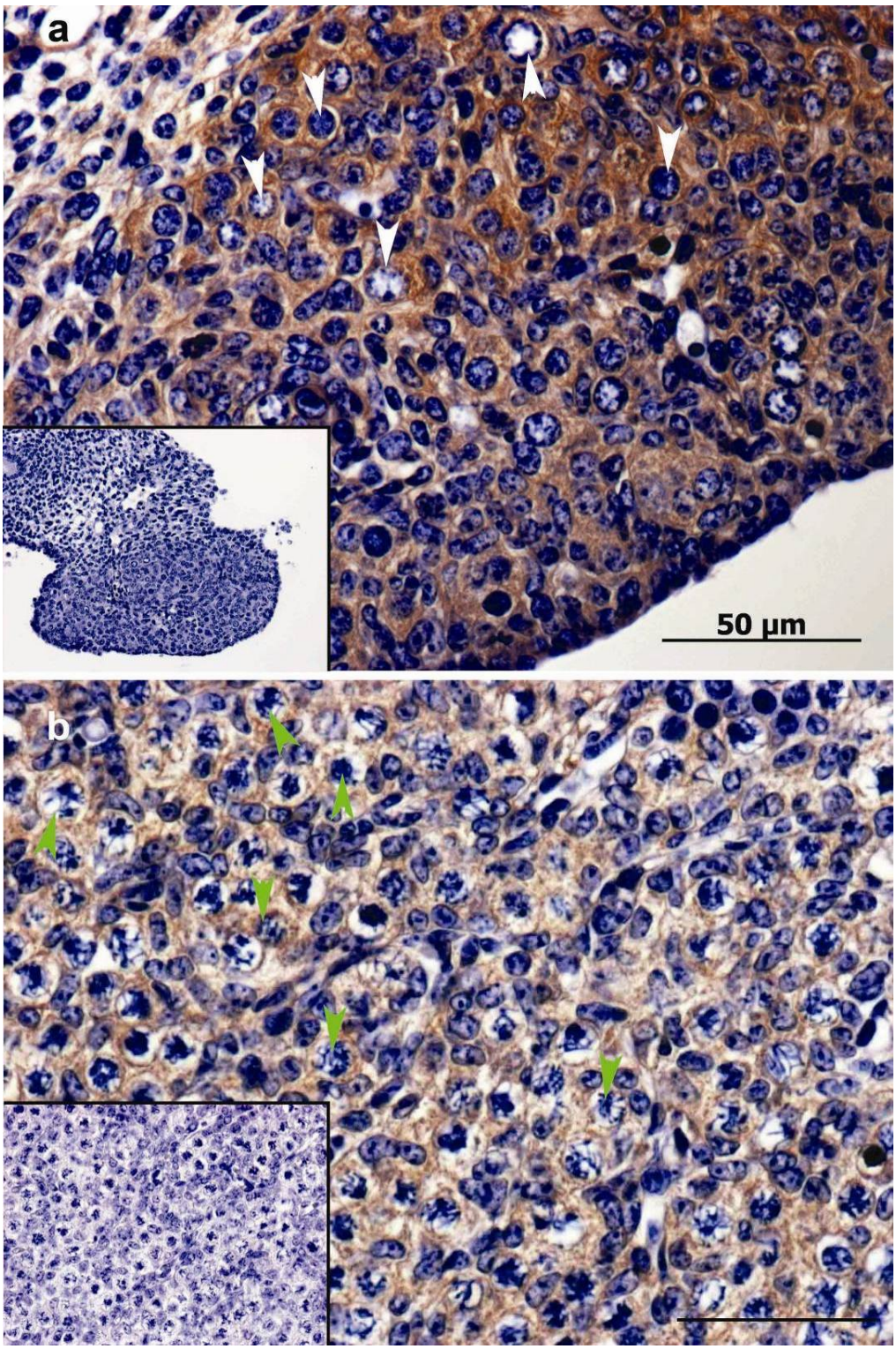


**Figure 3.19 -** Pabp1 is expressed in fetal female germ cells. **IHC analysis using a PABP1 antibody in fetal mouse ovaries: a – 13.5 dpc; b – 15.5 dpc; insets - negative control performed with no primary antibody. Arrowheads indicate germ cells which can be identified by their distinctive big round nuclei with diffuse chromatin and low nuclear to cytoplasm ratio, compared to the developing somatic cells which have smaller and more elongated nuclei: white – primordial germ cells; green - oogonia. x40 magnifications.**

Therefore, Dazl and Pabp1 expression were examined in fetal male gonads at the developmental times previously studied in females. At 12.5 dpc, similarly to females, PGCs were dispersed throughout the developing testis and robustly expressed Dazl (Figure 3.20-a). No Dazl expression was observed in the surrounding somatic cells, comprising the future Sertoli and Leydig cells. At 13.5 dpc (Figure 3.20-b), fetal testes start to show clear morphological differences compared to age-matched ovaries. At this time point PGCs are already organized within the developing seminiferous tubules and continue to express Dazl. As expected, Dazl negative cells can be also observed within the tubules, representing developing somatic Sertoli cells. At 15.5 dpc, the seminiferous tubules were highly populated with Dazl positive germ cells (Figure 3.20-c) although the more peripheral cells, likely the precursors of the somatic Sertoli cells, or somatic cells outside the tubules, were negative.

In contrast to Dazl, Pabp1 is widely expressed within the developing 13.5 dpc testes (Figure 3.21-a) including in the cytoplasm of the Dazl expressing PGCs and the surrounding somatic cells. At 15.5 dpc, Pabp1 is observed in the cytoplasm of cells including the prospermatogonia (Figure 3.21-b). This diffuse staining is dependent on primary antibody since no signal is detected in the negative controls performed with no primary antibody (Figure 3.21-insets).

In conclusion, during mouse testes development, Dazl and Pabp1 are both present within PGCs at 13.5 dpc. However, by 15.5 dpc in prospermatogonial cells, Pabp1 expression is dramatically reduced. Pabp1 levels also decline during this time in female mice but to a much lesser extent. Regarding Dazl expression no significant difference is observed between ages or sexes during the three time points analysed.

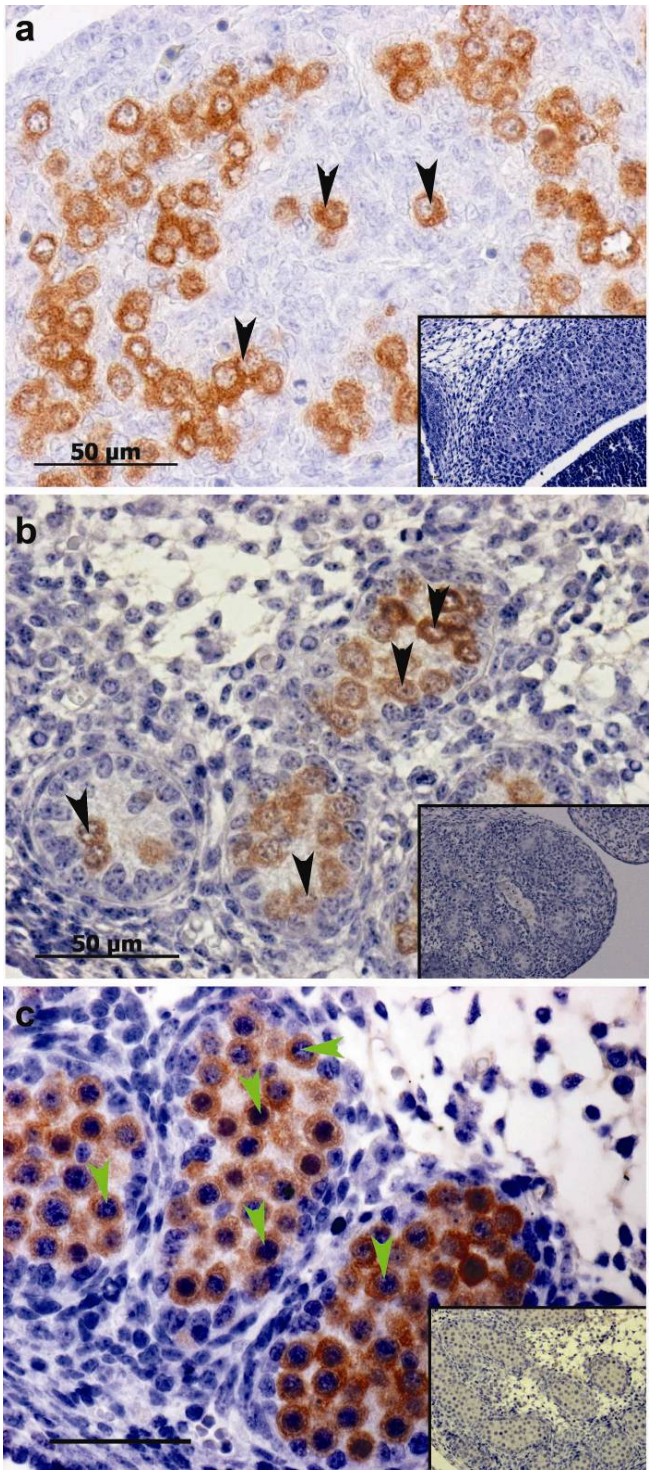


**Figure 3.20 -** Dazl is expressed in fetal male germ cells. **IHC analysis using a DAZL antibody in fetal mouse testes: a – 12.5 dpc; b – 13.5 dpc; c – 15.5 dpc; insets - negative control performed with no primary antibody. Arrowheads indicate germ cells which can be identified by their distinctive big round nuclei with diffuse chromatin and low nuclear to cytoplasm ratio, compared to the developing somatic cells which have smaller and more elongated nuclei: black – primordial germ cells; green - prospermatogonia. x40 magnifications.**

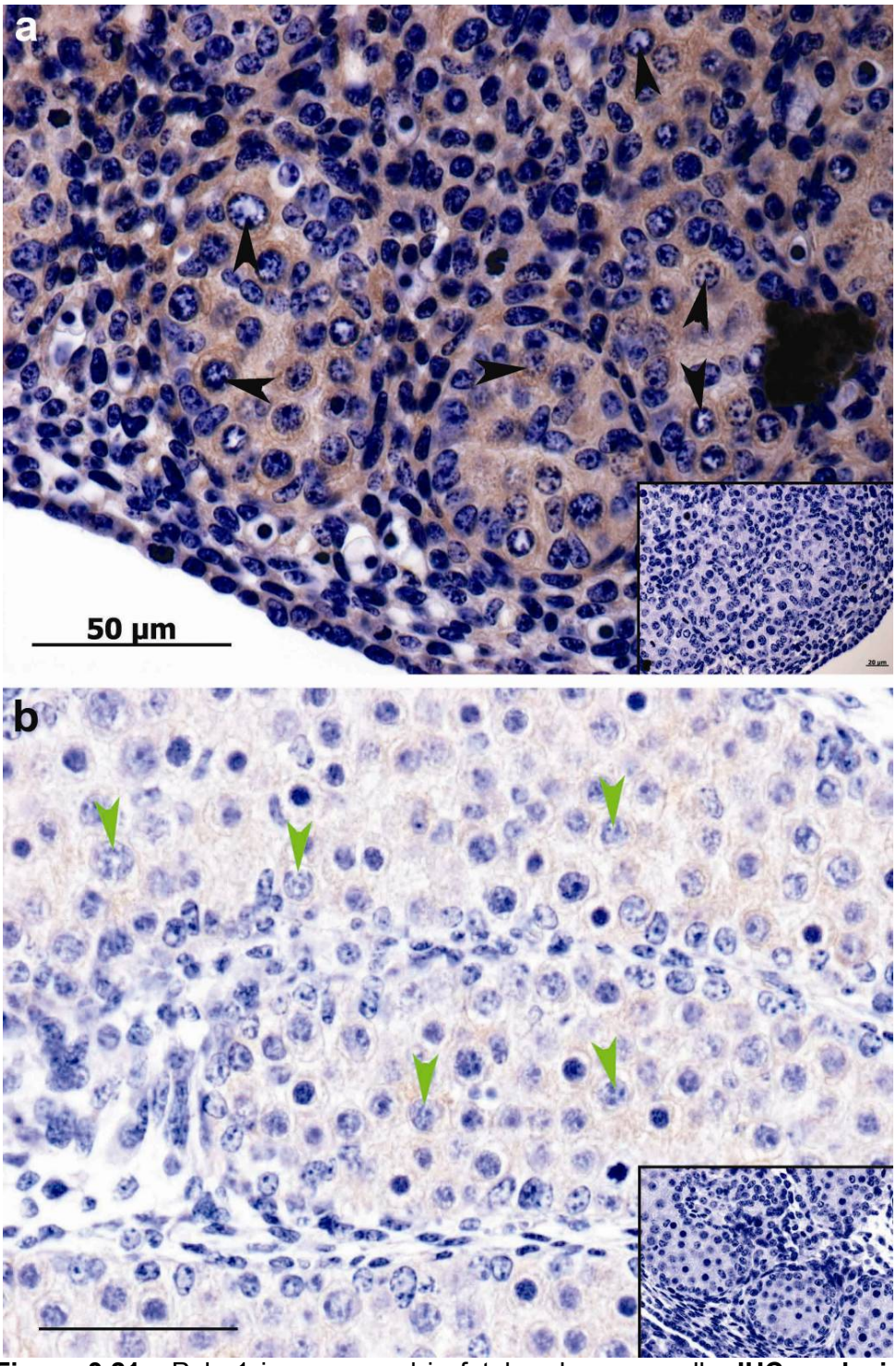


**Figure 3.21 -** Pabp1 is expressed in fetal male germ cells. **IHC analysis using a PABP1 antibody in fetal mouse testes: a – 13.5 dpc; b – 15.5 dpc; insets - negative control performed with no primary antibody. Arrowheads indicate germ cells which can be identified by their distinctive big round nuclei with diffuse chromatin and low nuclear to cytoplasm ratio, compared to the developing somatic cells which have smaller and more elongated nuclei: black – primordial germ cells; green - prospermatogonia. x40 magnifications.**

### 3.2.7 Dazl and Pabp1 expression in adult female gonads

At birth, oocytes are arrested at the diplotene stage of meiosis I, and only those surrounded by granulosa cells in primordial follicles survive atresia (Pepling, 2006). Subsequently, subpopulations of primordial follicles are activated progressing through primary, secondary and antral phases (Eppig, 2001), prior to A meiotic maturation and ovulation (Lee *et al.*, 1996, Richards, 2005).

Although the outbred Dazl-KO mice show no germ cells by 4 dpp (Saunders *et al.*, 2003), recent work using morpholino knockdown has shown that Dazl is also required for the translational activation of mRNAs during oocyte maturation (Chen *et al.*, 2011). Thus, to assess whether Dazl may utilise Pabp1 to activate translation in developing oocytes, their expression was investigated in adult mouse ovaries.

IHC analysis in adult mouse ovaries showed strong Dazl immunostaining in the cytoplasm of oocytes of primordial and primary follicles (Figure 3.22), which started to decrease in secondary follicles with antral follicles appearing to contain little Dazl. This reduction of Dazl in growing oocytes may appear at odds with its function during maturation but Chen et al. 2011 have shown that Dazl mRNA translation is activated during maturation. Dazl was also detected in the granulosa cells and the cells of the *corpus luteum,* only in the presence of primary antibody, despite being regarded as germ cell specific protein (Figure 3.22 - a and b).

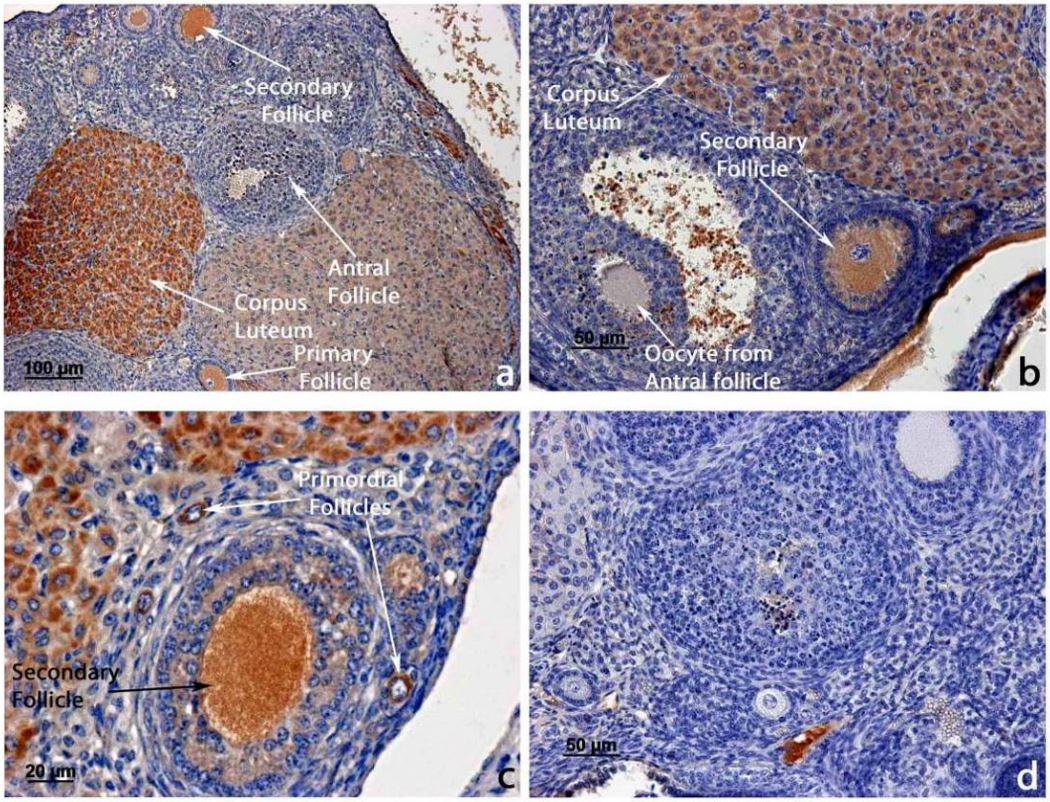


**Figure 3.22 -** Dazl is expressed in oocytes of primordial and primary follicles. **IHC analysis of Dazl expression in adult mouse ovaries using an anti-DAZL antibody. a, b and c - Dazl expression in mouse adult ovaries. d – negative control performed with no primary antibody. a – x10 magnification; b – x20 magnification; c – x40 magnification; d – x20 magnification.**

Similar investigation of Pabp1 expression (Figure 3.23) showed that it was expressed in a variety of cell types within the ovary and to varying extents. As observed for Dazl, there was significant Pabp1 expression in the cytoplasm of oocytes in primordial and primary follicles, which decreased in secondary follicles and was extremely low in the oocytes of antral follicles. Pabp1 was also robustly expressed in the granulosa cells and to a lesser extent in *corpus luteum* cells.

In summary, in adult mouse ovaries, Dazl and Pabp1 show similar temporal expression within oocytes, both peaking in the oocytes of primordial and primary follicles, and diminishing as oogenesis progresses. Due to the small window of oocyte maturation, 10-20 hours, it was not possible to assess expression in maturing oocytes within the sections. This would require super-ovulation of mice and/or *in vitro* maturation of oocytes.

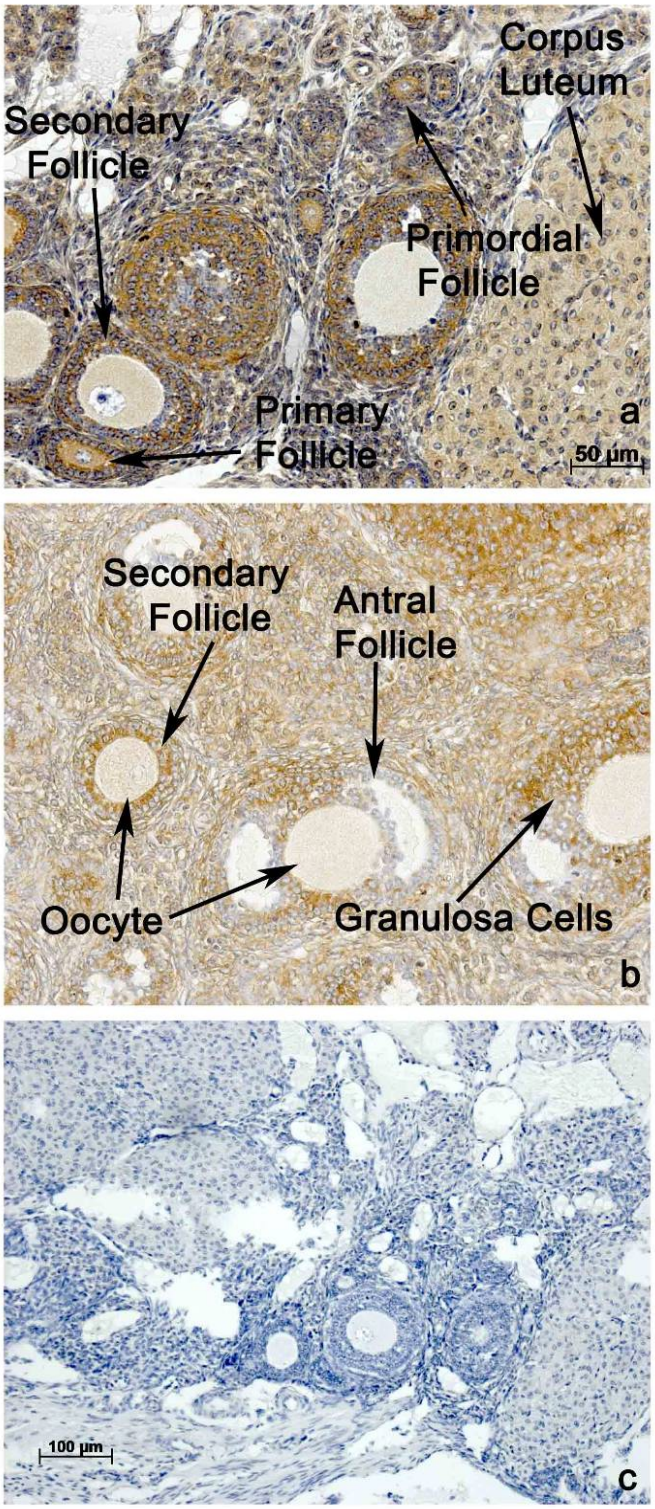


**Figure 3.23 -** Pabp1 is highly expressed in oocytes and granulosa cells of primary and primordial follicles and *corpus luteum*. **IHC analysis of Pabp1 expression in mouse adult ovaries using an anti-PABP1 antibody. a and b – expression of Pabp1 in mouse adult ovaries; c - no primary antibody control. a and b - x40 magnifications; c - x20 magnification.**

### 3.2.8 Interactions between mammalian DAZL and PABP1

Previous work within the laboratory has shown that Dazl can stimulate translation in *X. laevis* oocytes by interacting with the C-terminal portion of *X. laevis* PABP1 and/or ePABP (xPABP1 and xePABP) (Collier *et al.*, 2005b). The observation that Dazl and Pabp1 colocalise during specific stages of male and female gametogenesis in mouse suggests that this mechanism of action may be conserved in mammals. Thus the ability of murine Dazl (mDazl) and Pabp1 (mPabp1) to interact was investigated using a variety of *in vitro* and *in vivo* approaches.

### 3.2.9 *In situ* proximity ligation assay

Since colocalisation within the same cells does not establish a physical interaction, an *in situ* proximity ligation assay (PLA) was established to probe the ability of endogenous mDazl and mPabp1 to interact.

PLA technology (Soderberg *et al.*, 2006) extends the ability of FRET (reviewed in (Weibrecht *et al.*, 2010)) to study protein-protein interactions within cells by detecting those between endogenous proteins. As described in section 2.11 and in Figure 3.24, PLA uses primary antibodies (raised in different species) to detect endogenous proteins *in situ* and secondary antibodies conjugated to unique short DNA strands. When these secondary antibodies are in close proximity (0 < 40 nm) the two PLA probes can be ligated by addition of complementary oligonucleotides. Once hybridised to the PLA probes these oligonucleotides form a circle which can be amplified several-hundred fold via rolling circle amplification. The amplified sequence is then hybridized with complementary fluorescent oligonucleotide probes. This results in a high concentration of a fluorescent signal for each single molecular interaction, detectable as distinct spots by fluorescence microscopy, thus even transient or weak interactions can be detected by PLA.

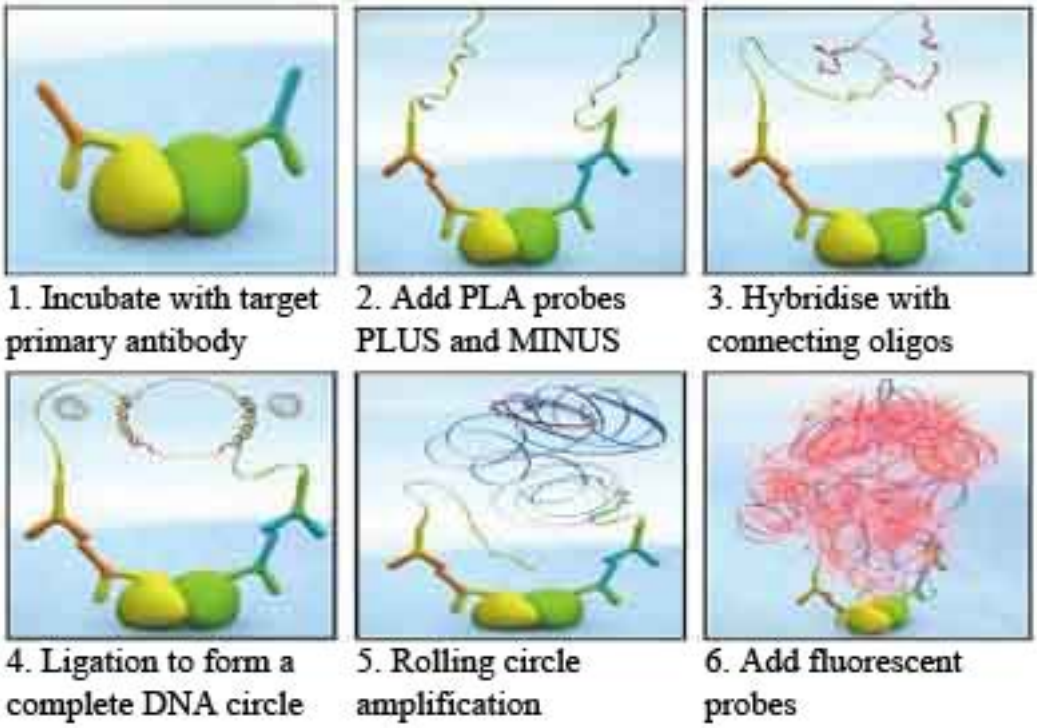


**Figure 3.24 -** *In situ* proximity ligation assay. **Schematic representation of the in situ proximity ligation assay. Adapted from** [http://www.olink.com/products-services/duolink/how-use-duolink/assay-design](http://www.olink.com/products-services/duolink/how-use-duolink/assay-design).

### 3.2.10 Optimisation of the *in situ* proximity ligation assay with anti-α and anti-β LH subunits in mouse pituitary

As PLA is a relatively new and specialised technique, validation and optimisation was performed with a well-established interaction prior to using this technique to assess potential Dazl-PABP1 interactions.

Luteinizing hormone (LH) is produced by the anterior pituitary gland and is an important regulator of reproduction both in males and females. LH is a heterodimeric glycoprotein composed of α and β subunits, which are non-covalently associated. The α and β subunits only heterodimerise in more peripheral regions of the anterior pituitary following a gonadotrophin releasing hormone (GnRH) stimulus from the hypothalamus (Pope *et al.*, 2006). These properties make this interaction within the mouse pituitary attractive for optimising PLA, as the absence of subunit interactions in the posterior pituitary, provides a negative control.

The initial steps of the PLA protocol are in common with IHC. Sections from mouse pituitary are antigen retrieved, blocked and incubated with both anti-α and anti-β LH subunit antibodies (Table 2.7) (Pope *et al.*, 2006). After this, a specific OLink *in situ* proximity ligation assay protocol is followed (described in section 2.11).

Three variations of the method were tested to optimize the assay. In the first instance, the supplied OLink protocol was followed exactly. This included a final wash with 70% ethanol (EtOH), prior to mounting the slides with the provided OLink Biosciences media containing an Alexa Fluor 488 counterstain (#80100) and sealing the cover slip with nail varnish. This (Figure 3.25-a) resulted in a very weak signal in the anterior but not posterior pituitary, with localisation of this signal suggesting it was specific. In the second, the final 70% EtOH wash was omitted enhancing the signal in the anterior pituitary (Figure 3.25-b). No fluorescence signal was observed in the posterior pituitary. Lastly, an extra incubation with DAPI 488 counterstain was introduced before the serial washes with SSC buffer (see 2.11). This was followed by a 70% EtOH final wash and mounting with a cover slip using PermaFluor solution (ThermoScientific). This change in mounting media produced a signal pattern (Figure 3.25-c) identical to the one observed with the provided OLink Biosciences mounting media and of similar strength (Figure 3.25-a); however, the use of PermaFluor made the slides more durable and avoided the poor image quality and evaporation of mounting media sometimes associated with using nail varnish as a sealant.

As including a DAPI 488 incubation and excluding the 70% EtOH wash both appeared to enhance the signal quality, a final experiment was performed with both protocol modifications (i.e. incubation with DAPI 488 counterstain; no 70% EtOH wash; cover slip mounted with PermaFluor). A montage of a mouse pituitary using this modified PLA protocol (Figure 3.26) showed a robust positive signal for LH heterodimerisation in the peripheral regions of the anterior pituitary. This pattern was not observed without anti-α LH subunit antibody (Figure 3.26 - inset) and resembles that described in the literature (Pope *et al.*, 2006), indicating that the optimised PLA protocol is a viable technique to assess *in situ* interactions between two proteins.

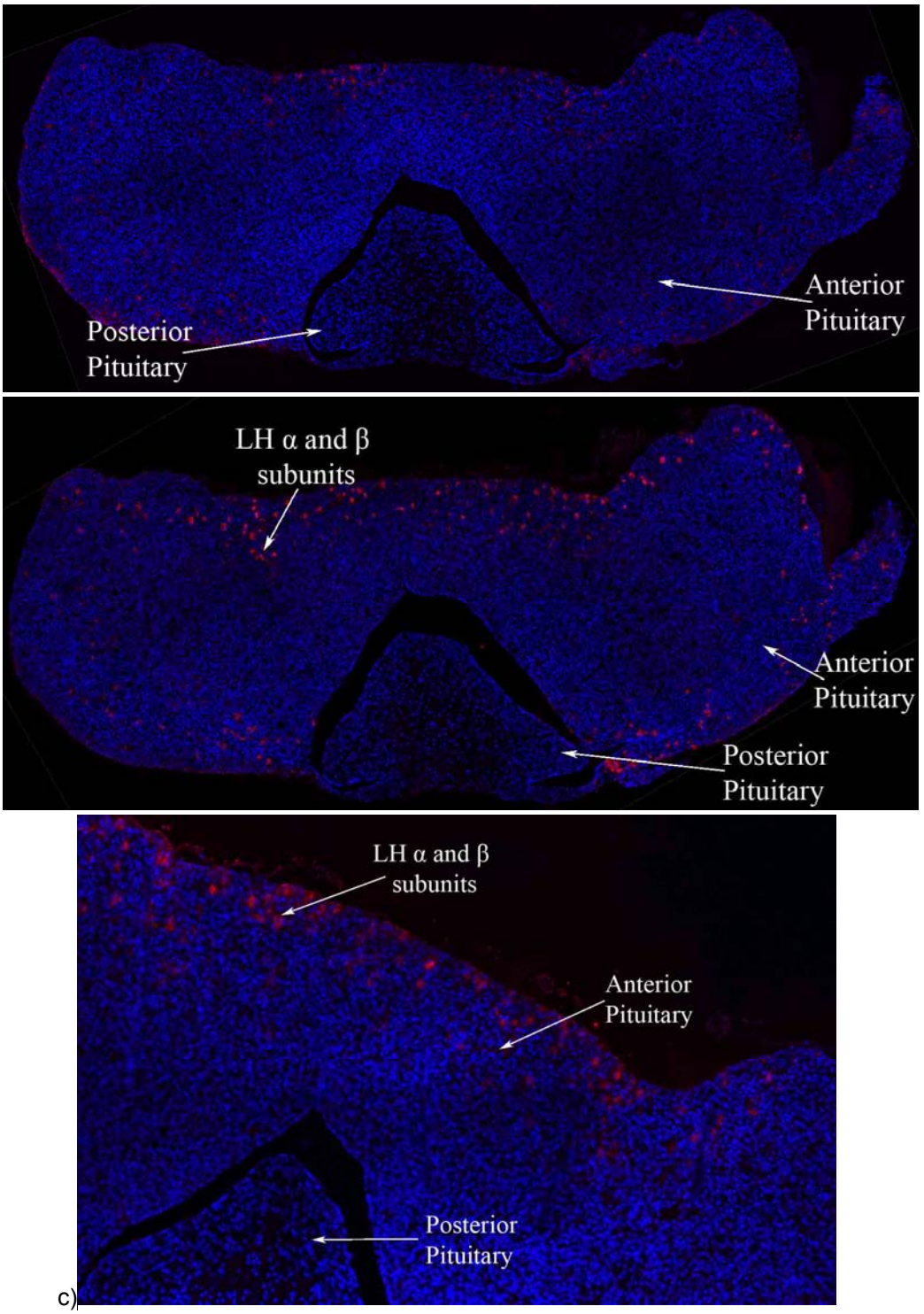


**Figure 3.25 - Optimisation of the *in situ* PLA for α and β LH subunits in mouse pituitary.** In situ PLA protocol suggested by the manufacturer was optimised for mouse pituitary fixed sections, using an anti-α (1/1000) and an anti-β (1/5000) LH sub-unit primary antibodies. Three different steps for *in situ* PLA protocol optimization: a – as per manufacturer instructions; b – no 70% EtOH wash before mounting with Olink biosciences #80100; c – slide incubated with DAPI counter staining followed by mounting with PermaFluor. Red – Interaction of α and β LH subunits. Blue – nuclear counter.

***Figure 3.26 - In situ* PLA for α and β LH subunits in mouse pituitary.** *In situ* PLA with α (1/1000) and β (1/5000) LH subunit primary antibodies performed in mouse pituitary fixed sections. Protocol followed manufacturer but including previous optimisation steps: incubated with DAPI, no 70% EtOH wash and mounted with PermaFluor. insets – negative control, in situ PLA with no α-subunit primary antibody, incubated with DAPI, no 70% EtOH wash and mounted with PermaFluor. Red – Interaction of α and β LH subunits. Blue – nuclear counter stain by DAPI.

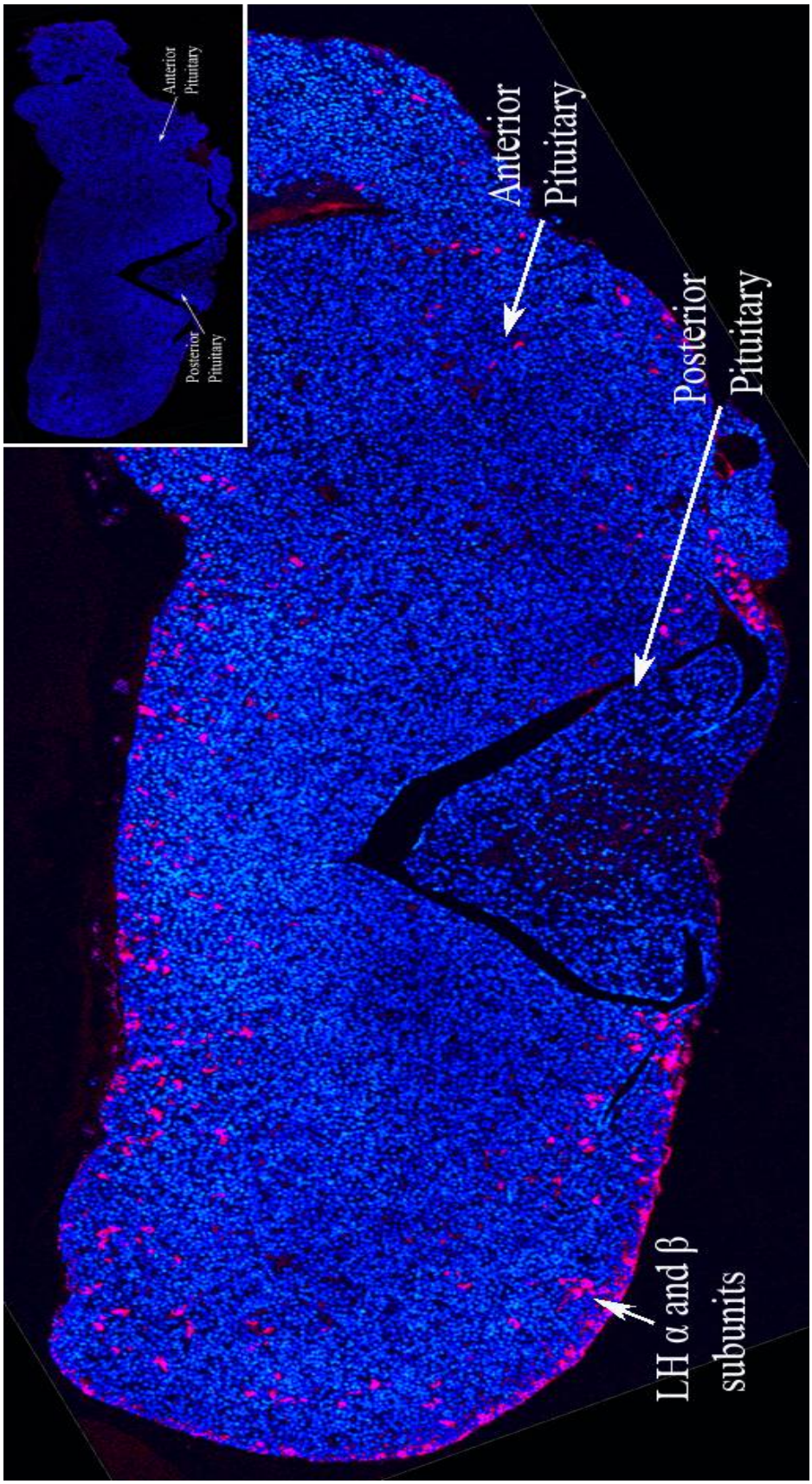
Anterior Pituitary
Posterior Pituitary
Anterior Pituitary
Posterior Pituitary
LH α and β subunits

### 3.2.11 In situ proximity ligation assay with anti-Dazl and anti-PABP1 antibodies in mouse testes

After optimisation of the PLA protocol with the LH subunits, this technique was used to assess potential interactions between Dazl and Pabp1 in mouse adult testes.

Given the expression patterns of Pabp1 and Dazl as summarised in Figure 3.13 and 3.15, any interaction in adult males is only likely to occur in the cytoplasm of spermatocytes between stage VI pachytene spermatocytes until the meiosis I to meiosis II transition (stage XII). However, PLA with anti-PABP1 (Marshall) and anti-DAZL antibodies produced a strong signal within Leydig cells and occasional weak foci in the seminiferous tubules (Figures 3.27-a). Increasing the amount of primary antibodies only diminished rather than enhanced the signal (Figure 3.27-b) and higher magnification images (Figure 3.28-a) showed that the signal obtained within the seminiferous tubules is within the early spermatocytes, a stage when Pabp1 is not expressed (see section 3.2.2), suggesting it does not represent a genuine interaction. Moreover, omitting either the anti-DAZL (Figure 3.27-c and 3.28-b) or anti-PABP1 (Figure 3.27-d) antibody confirmed the lack of specificity.

It is possible that the lack of specificity was due to cross-reaction of the secondary mouse antibody with mouse testis proteins. Therefore, a newly available anti-DAZL antibody (Everest #EB06857) raised in goat was tested to establish whether it could be used for PLA (Figure A1.5 - Appendix 1). However, the pattern observed with this antibody was not consistent with the findings described earlier in this chapter nor with previous literature on Dazl mRNA or protein expression (Niederberger *et al.*, 1997, Ruggiu *et al.*, 1997). Thus it was unsuitable for use in PLA.

In conclusion, although these results show that the proximity ligation assay proved to be a powerful technique to investigate *in situ* interaction of proteins, it could not be applied to study the DAZL-PABP1 interaction with the available antibodies.

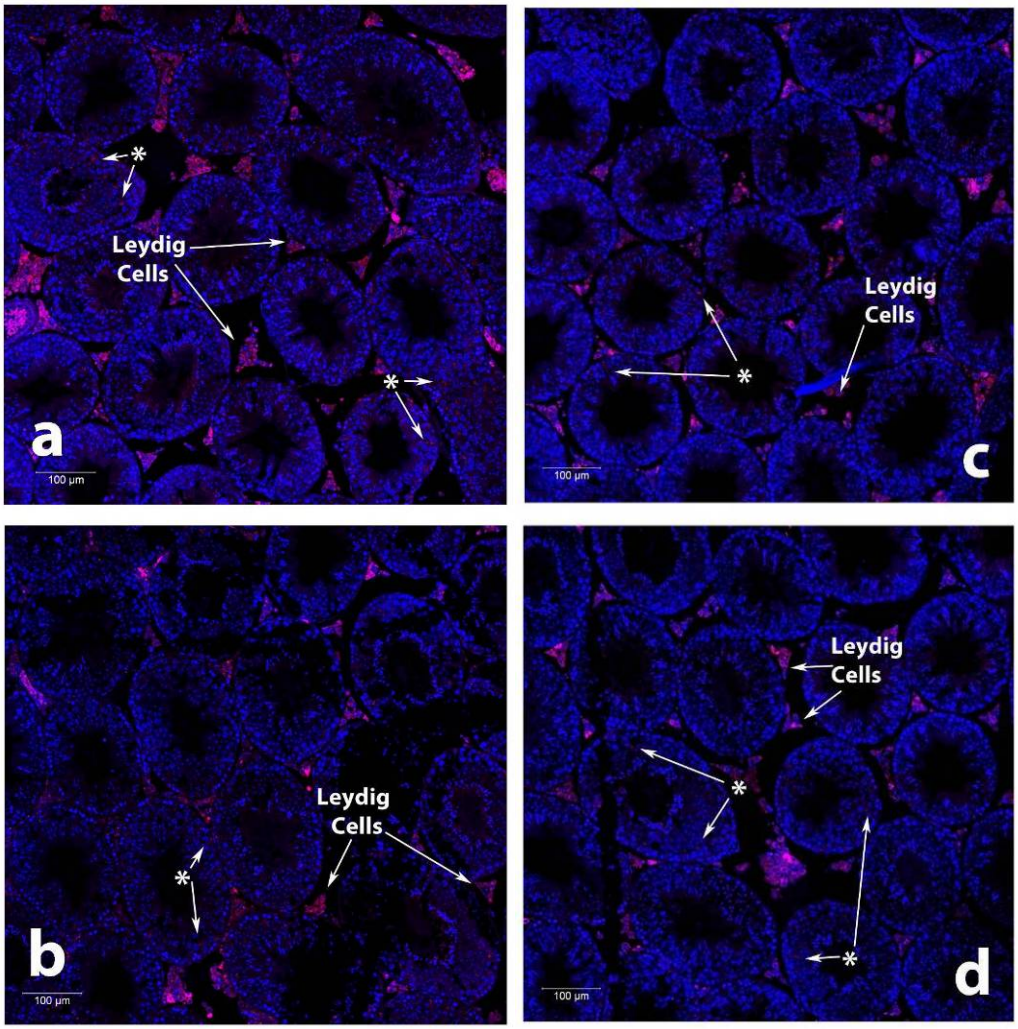


**Figure 3.27 -** *In situ* PLA in mouse testes with DAZL and PABP1 antibodies. ***In situ* PLA performed in mouse testes using an anti-DAZL and an anti-PABP1 antibody following previously optimised PLA protocol. a –anti-DAZL (1/20) and anti-PABP1 (1/500) as optimised for dual immunofluorescence; b – anti-DAZL (1/10) and anti-PABP1 (1/250); c – negative control with no DAZL primary antibody; d – negative control with no PABP1 primary antibody Red – Interaction. Blue – nuclear counterstain by DAPI. * - Fluorescent signal within the seminiferous tubules. Each image represents a 4 x 4 montage of x40 magnification images.**

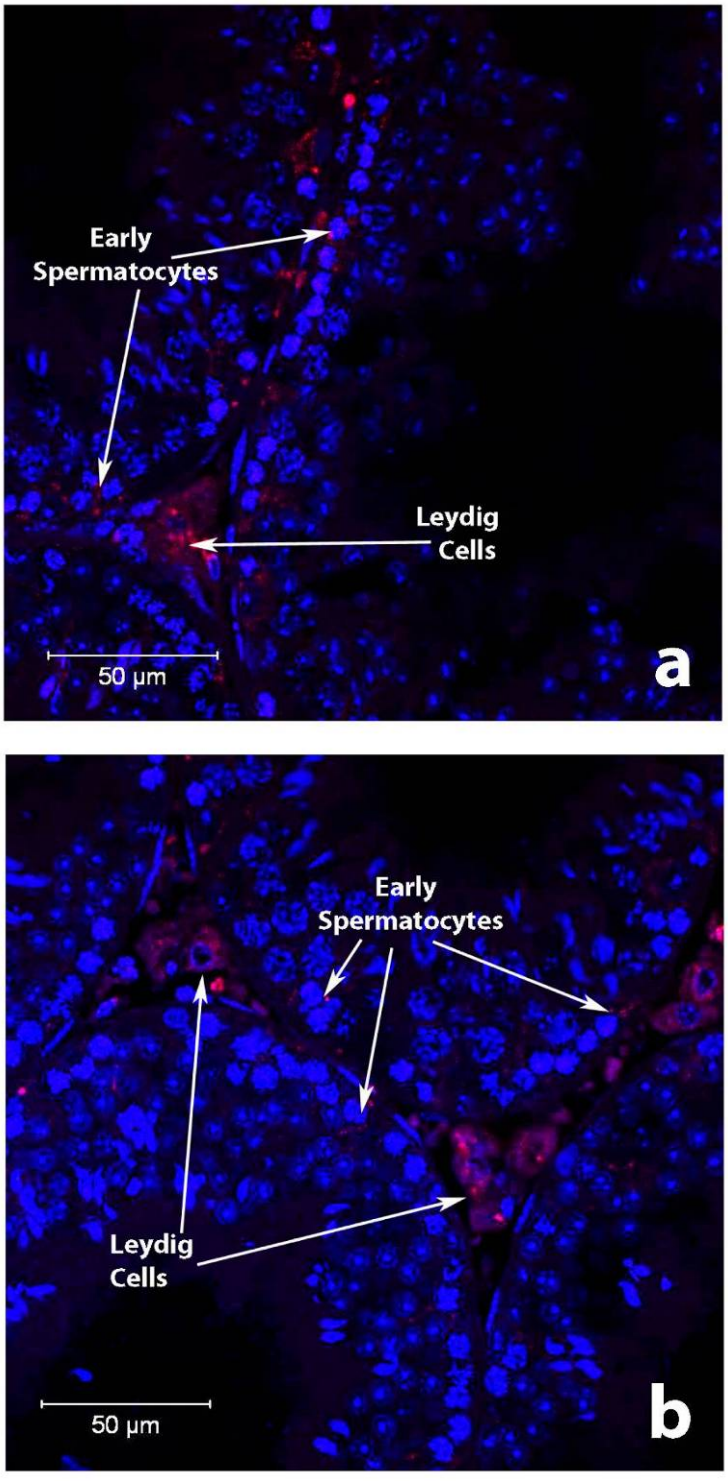


**Figure 3.28 -** *In situ* PLA in mouse testes with DAZL and PABP1 antibodies. **Magnifications of 3.26 b (3.27 – a) and c (3.27 – b) figures. a – using 1/10 dilution of anti-DAZL and anti-PABP1 (1/250) primary antibody; b – negative control with no DAZL primary antibody; Red – Interaction. Blue – nuclear counterstain by DAPI. x40 magnifications.**

## 3.2.12 *In vitro* interaction between DAZL and PABP1

The yeast-two hybrid (Y2H) assay takes advantage of the ability of the DNA binding domain and the activation domain of transcription factors to be physically separated but to function when brought into proximity. Thus by expressing these domains as fusions with other proteins, protein-protein interactions can be assessed by transcriptional activation of reporter genes (in this case LacZ; Figure 3.29; (Fields and Song, 1989). Activation of the lacZ reporter is detected by a colorimetric assay.

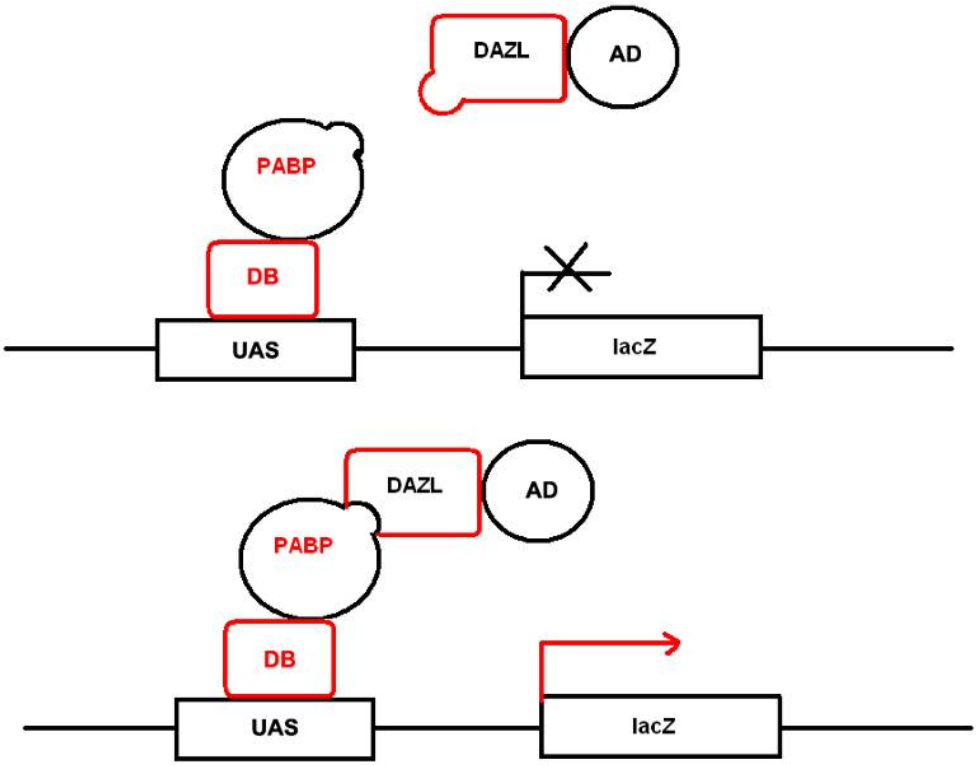


**Figure 3.29 -** Yeast two-hybrid assay schematic. **Two fusion proteins are expressed in yeast. One has a transcription factor DNA binding domain (DB) fused to a "bait" protein (PABP) whilst the other contains an transcription activation domain (AD) fused to a "prey" protein (DAZL). If the "bait" protein interacts with the "prey" protein, the AD is brought into proximity of the DB, at the upstream activation sequence (UAS) of a LacZ reporter gene inducing its transcription. LacZ encodes β-galactosidase, which cleaves the substrate X-gal producing blue-pigmented colonies. In the absence of protein interaction colonies maintain a yellow/cream colour.**

Thus, in order to assess whether mammalian DAZL and PABP1 interact, a directed Y2H approach was undertaken using the C-terminal region from mouse and

human PABP1 fused to the lexA DNA-binding domain and mouse and human DAZL genes as GAL4-activation domain fusions. The C-terminal region of *X. laevis PABP1* served as a positive control (Collier *et al.*, 2005b) and iron regulating protein (IRP) and MS2, which are RNA-binding proteins, as negative controls (Gray *et al.*, 2000).

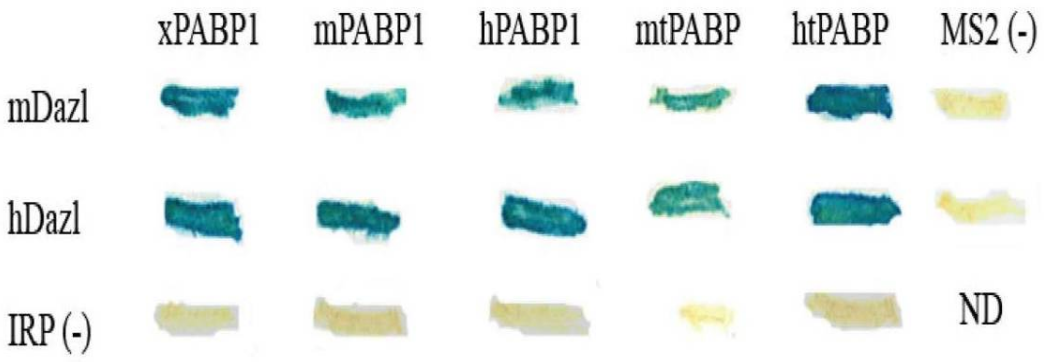


**Figure 3.30 -** DAZL-PABP interactions are conserved in mammals. **Yeast two-hybrid assay between DAZL and the C-terminus of vertebrate and mammalian PABP family members using qualitative β-Gal filter assays. IRP and MS2 represent negative controls. Blue plaques indicate a positive interaction. ND – not done.**

This showed that both the mouse and human DAZL proteins retained the ability to interact with *X. laevis*, mouse and human PABP1. No interactions were observed with the negative controls. This result indicates that the DAZL-PABP1 interaction is maintained in multiple mammals as well as non-mammalian vertebrates, with its evolutionary conservation supporting its biological relevance. Furthermore, a second mammalian specific family member, tPABP, both from mouse and human was also able to interact with Dazl (Figure 3.30). tPABP is a germ cell specific protein that is only expressed in round spermatids (Kimura *et al.*, 2009).

## 3.2.13 Human DAZL and PABP1 interact in HeLa cells

To confirm the interaction between mammalian PABP1 and DAZL by coimmunoprecipitations (co-IPs), cultured mammalian cells were transfected with a Dazl expressing plasmid because DAZL is only expressed in germ cells for which

cell lines are not available. HeLa cells were chosen as they are easily cultured and transfected and express endogenous PABP1.

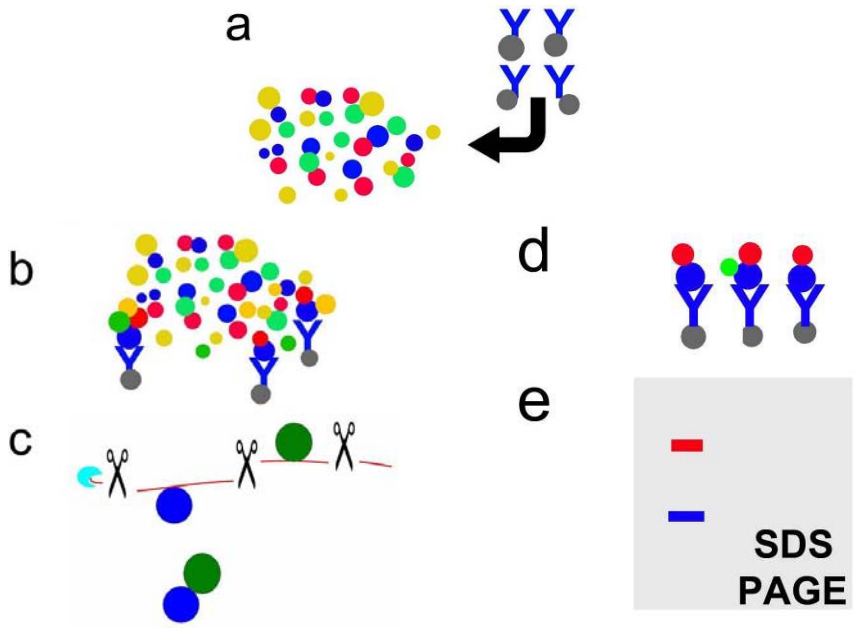


**Figure 3.31 -** Schematic representation of co-immunoprecipitation (Co-IP). **a - antibody bound to protein-A beads tumbled with cell extract, (b) in the presence of RNase1 which cleaves RNA molecules, including poly(A) sequences (c). Antibody binding to the specific protein of interest it is raised against retains this protein with the beads, and in permissive conditions its protein binding partners are also retained (d). Repeated washes remove unbound proteins. Finally bound proteins are eluted from the beads and analysed by western blot (e).**

Following optimisation of the transfection protocol (Appendix 3), HeLa cells were transfected with a vector expressing hDAZL (pCG-hDAZL). 24 hours post-transfection cell extracts were prepared and subjected to immunoprecipitation with the anti-PABP1 antibody. Since both DAZL and PABP1 are RNA-binding proteins, RNase1 which cleaves after all 4 bases, was added to the co-IP to eliminate spurious RNA-mediated interactions (Figure 3.31-c). Co-immunoprecipitating (co-IP) proteins were detected by western blotting (Figure 3.31). To reduce non-specific binding of DAZL, washes were performed with a buffer containing 450 mM NaCl. Under these high stringency conditions (Figure 3.32) DAZL could be directly immunoprecipitated and was co-precipitated by the anti-PABP1 antibody, but not by the control antibody (anti-rIgG) indicating that these proteins interact.

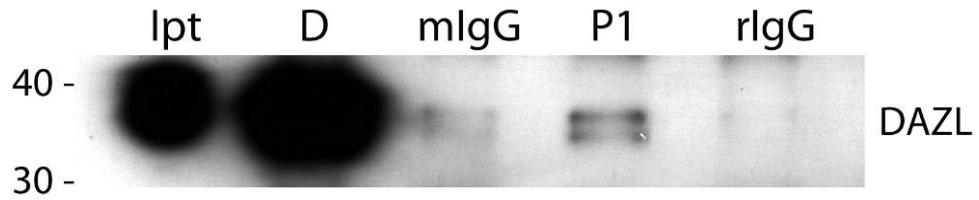


**Figure 3.32 -** DAZL-PABP1 interaction in HeLa cells. **Immunoprecipitation (IP) with anti-DAZL (D), anti-mouse IgG (mIgG), anti-PABP1 (P1) and anti-rabbit IgG (rIgG), from HeLa cell extracts transfected with hDAZL. IPs were western blotted against DAZL. Ipt represent 1% input of the material used for each IP. IPs were washed with 450mM NaCl. Mouse and rabbit IgG work as IP negative controls.**

To confirm this interaction, the reverse co-IP was also performed. At low salt concentrations PABP1 was co-immunoprecipitated by Dazl but also by the control antibody (mIgG). However, following high salt washes (600 mM NaCl) PABP1 was significantly enriched by the anti-DAZL antibody compared to the mIgG control (Figure 3.33). These results validate those obtained by Y2H providing further evidence that mammalian DAZL and PABP1 can interact.

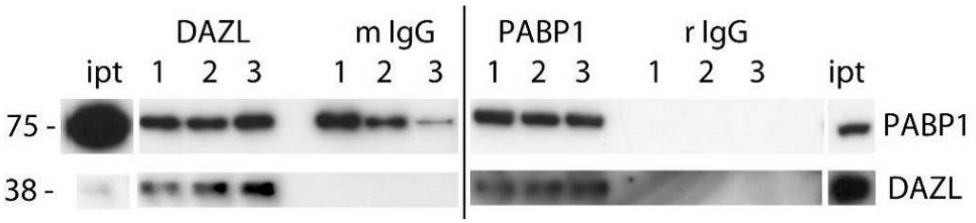


**Figure 3.33 -** Co-immunoprecipitation of PABP1 and DAZL. **Immunoprecipitation (IP) with anti-DAZL, anti-mouse IgG (mIgG), anti-PABP1 and anti-rabbit IgG (rIgG), in HeLa cell extracts transfected with hDAZL. IPs were western blotted for PABP1 and DAZL. Immunoprecipitating antibodies are shown along the top and western blotting antibodies on the side of panels Ipt represent 0.5% of the material used for each IP. Different NaCl concentrations of the washing solutions: 1 – 300mM; 2 - 450mM; 3 – 600mM. Mouse and rabbit IgG are IP negative controls.**

### 3.2.14 Interaction between endogenous Dazl and Pabp1 in adult mouse testes extracts

To test whether the DAZL-PABP1 interaction is recapitulated with the endogenously expressed mouse proteins, co-IPs were performed using adult mouse testes extracts treated with RNase1. Immunoprecipitation was conducted using the anti-PABP1 antibody or rabbit immunoglobulin G (rIgG) to control for non-specific interactions. Western blotting for Dazl demonstrated that the anti-PABP1 antibody but not rIgG efficiently co-IP murine Dazl (Figure 3.34).

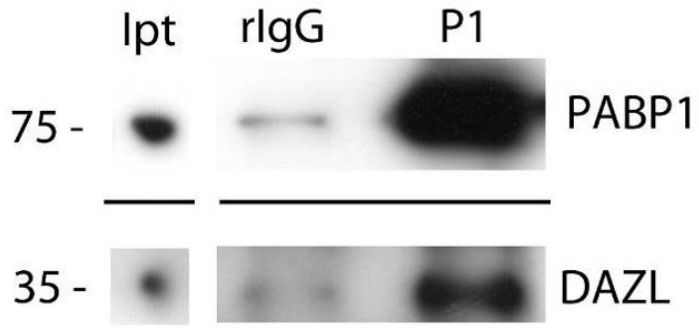


**Figure 3.34 -** Endogenous Dazl-Pabp1 interactions. **Immunoprecipitation (IP) with anti-PABP1 (P1) and anti-rabbit IgG (rIgG) as a negative control, in mouse adult testes extracts. IPs were western blotted for PABP1 and DAZL. Ipt represent 1% of the material used for each IP. IPs were washed with 200mM salt.**

These results show that endogenous mouse Dazl can interact with the translation initiation factor Pabp1. Taken together with their colocalisation in a subset of male and female germ cells, these data suggest that the Dazl-Pabp1 interaction may promote translation activation of specific mRNAs during mouse gametogenesis.

## 3.3 Discussion

This chapter examined whether DAZL may recruit PABP1 to fulfil its role in promoting mRNA-specific translation during mammalian gametogenesis. To this end the ability of these proteins to interact was established, and the extent of their colocalisation in adult and fetal male and female germ cells investigated. In so doing, this also provided insight into the expression of Pabp1 within mouse tissues and extended our understanding of the expression pattern of Dazl.

### 3.3.1 Dazl expression in adult, pre-pubertal and fetal mouse gonads

Despite the earliest phenotypes associated with loss of Dazl function occurring between 14.5 and 15.5 dpc (Lin and Page, 2005, Lin *et al.*, 2008), Dazl expression in fetal ovaries prior to 17.5 dpc or in fetal testes had not been examined, although its mRNA was known to be present as early as 11.5 dpc in developing testes (Lin and Page, 2005). Consistent with the spectrum of phenotypes that arise during fetal development and after birth, Dazl expression in germ cells was initiated prior to morphological sex differentiation (at 13.5 dpc) (Figures 3.18 and 3.20) and could still be detected at the end of meiosis I in both sexes. In females, Dazl was present till the dictyate stage of oogenesis, declining significantly after the secondary follicle stage (Figure 3.22). Dazl levels are still low in fully grown oocytes (Nishi *et al.*, 1999) but increase again during oocyte maturation (Chen *et al.*, 2011). Interestingly, Dazl levels also declined in males, but to undetectable levels, in leptotene spermatocytes (stage IX-X) but recovered by zygotene ( stages XI-XII), consistent with a recent independent report (Kim *et al.*, 2012). This indicates that Dazl may have additional functions after the described leptotene/zygotene arrest in males (Schrans-Stassen *et al.*, 2001, Saunders *et al.*, 2003) up until the meiosis I to meiosis II transition in stage XII spermatocytes (Figure 3.6) when expression ceases.

Whilst Dazl appeared restricted to the cytoplasm of female germ cells at all stages examined, it was possible to observe some apparently nuclear Dazl in mitotic spermatogonia (Figures 3.2, 3.3 and 3.6), in agreement with previous reports (Ruggiu

*et al.*, 1997, Reijo *et al.*, 2000). Consistent with this sub-cellular distribution, *Drosophila Boule* has a biphasic sub-cellular localisation translocating to cytoplasm just prior to the onset of the phenotype. However, eliminating it from the nucleus does not perturb entry into meiosis suggesting that its critical role is cytoplasmic (Cheng *et al.*, 1998). Mouse Dazl has described roles in the erasure and re-establishment of the imprinting methylation status of germ cells (Haston *et al.*, 2009, Navarro-Costa *et al.*, 2010), but these roles may well be indirect (i.e. through regulation of mRNAs required for these processes) and it is difficult to conclude with certainty from DAB stained tissues that Dazl is nuclear in the absence of additional evidence e.g. confocal analysis of cells from disaggregated testes. Nonetheless its presence within this compartment would allow for as yet undescribed functions in nuclear RNA regulation.

Although Dazl is widely accepted as a germ cell specific protein (Cooke *et al.*, 1996, Reijo *et al.*, 1996b), notably it was also detected in the cytoplasm of granulosa cells and particularly within the cells of the *corpus luteum.* Although controversial, similar somatic expression has previously been observed in mouse and humans (Ruggiu *et al.*, 1997, Pan *et al.*, 2002, Pan *et al.*, 2008), raising the question as to whether they are indeed sites of Dazl expression. In line with this, a specific form of *Drosophila* boule is expressed in the laminar cells of the fly eye (Joiner and Wu, 2004, Hoopfer *et al.*, 2008), showing that this family, at least in invertebrates, is not germ cell specific.

### 3.3.2 Pabp1 expression in mouse gonads

Surprisingly, given the large amount of biochemical information available on PABP1 function, its expression pattern in multi-cellular organisms is virtually unknown. Thus this work provides the first characterisation of Pabp1 expression, focusing on both developing and adult testes and ovary; testis is the only tissue for which information regarding its mRNA distribution within different cell types was available (Kleene *et al.*, 1994, Gu *et al.*, 1995, Kleene *et al.*, 1998) although PABP1 mRNA was known to be present in human ovary (Feral *et al.*, 2001).

In fetal gonads, Pabp1 appeared to be expressed in both the PGCs and somatic cells at 13.5 dpc (Figures 3.19 and 3.21), although markers are required to further clarify the different cell types as only some could be identified by morphology with any certainty. Interestingly, Pabp1 was almost absent in testes by 15.5 dpc whilst females showed only a small decrease in Pabp1 expression which may reflect sex specific differences at this age since female germ cells progress through meiosis whilst male germ cells enter mitotic arrest.

In adults, Pabp1 was found to be expressed in the granulosa and theca cells of the ovary but not in the Sertoli and Leydig cells of the testis, despite these being considered broadly functionally equivalent. Within the germ cells, Pabp1 was abundant in primordial and primary oocytes with a marked decreased after this stage (Figure 3.23) and in stage VI-VII pachytene until the last phase of spermatid development (Figure 3.12). However, the conclusion that round spermatids express Pabp1 is complicated by the presence of tPabp within this stage (Kleene *et al.*, 1994, Feral *et al.*, 2001, Kimura *et al.*, 2009), as the peptide used to raise the Pabp1 antibody is 75% conserved within tPabp (Appendix 2). Nevertheless, several lines of evidence argue that Pabp1 is expressed in round spermatids. Firstly, the equivalent stage in humans contains Pabp1 mRNA (Feral *et al.*, 2001) secondly, another in house Pabp1 antibody (VINPY) raised against a distinct peptide (64% identical to tPABP) also detected Pabp1 in round spermatids (Appendix 2), and thirdly, an independent Pabp1 antibody raised against an epitope with almost no homology to tPabp similarly detected Pabp1 in these cells (Kimura *et al.*, 2009).

| | hPABP1-c | mtPabp-c | htPABP-c | xPABP1-c |
|---|---|---|---|---|
| **mPabp1-c** | 99% | 69% | 90% | 89% |
| **hPABP1-c** | | 69% | 91% | 89% |
| **mtPabp-c** | | | 62% | 62% |
| **htPABP-c** | | | | 80% |

**Table 3.1 - Homology between PABP1 and tPABP C terminal regions.** A tPABP homologue is not present in *X. laevis* and percentages represent amino acid identity. hPABP-c – human PABP C terminal region; mPabp – mouse Pabp; xPabp – *X. laevis* PABP.

While the patterns obtained with our Marshall and VINPY antibodies were essentially identical (Appendix 2), they differed from that of Kimura et al., 2009 in one aspect. Neither of the in house antibodies detected Pabp1 in spermatogonia in adults, consistent with Pabp1 transcripts being restricted to late spermatocytes and round spermatids in humans (Kleene *et al.*, 1994, Feral *et al.*, 2001), but Pabp1 was apparently detected at low levels at this stage with the Kimura antibody (Kimura *et al.*, 2009). However, Kimura et al detected Pabp1 by IF but did not identify tubule stages or use markers for spermatogonia, making assessment of this claim difficult from the low magnification images (Kimura *et al.*, 2009).

Another explanation for this apparent difference arises from our comparison of PABP1 expression in adults and during the first wave of spermatogenesis, since Kimura et al do not state whether adult or pre-pubertal mice were subject to IF with PABP1 antibodies. This comparison revealed that although mitotic spermatogonia and early spermatocytes do not express Pabp1 during adult spermatogenesis it can be detected in prospermatogonia (3 dpp), spermatogonia and early spermatocytes during the first wave. While this difference could reflect the presence of cross-reacting proteins in pre-pubertal mice, northern and western blot analysis of 5 dpp testes, in which the only germ cells are prospermatogonia, both detect Pabp1 (Kimura *et al.*, 2009). This indicates that Pabp1 expression is surprisingly differentially regulated during the first and subsequent waves of spermatogenesis. This unusual difference in the waves has also been noted for euchromatin epigenetic marker histone H3 acetylated at lysine 9 (acetyl H3K9) (Webster *et al.*, 2005). The physiological role of this intriguing difference in Pabp1 expression remains unclear but it could be related to differentiated spermatogonia arising directly from gonocytes during the first wave and from a spermatogonial stem cell population in subsequent waves.

### 3.3.3 Dazl may activate mRNA-specific translation during mammalian gametogenesis by PABP1 recruitment

This chapter examined the hypothesis that DAZL proteins may activate the translation of specific mammalian mRNAs by recruiting PABPs as described in *X.*

*laevis* oocytes (Collier *et al.*, 2005b). This model is dependent on the ability of Dazl to interact with PABPs. Importantly, three independent lines of evidence supported a direct RNA-independent interaction between Dazl and the prototypical family member, Pabp1, which was found to be expressed in a subset of male and female germ cells. Firstly, both murine and human DAZL interacted with PABP1 in an Y2H assay (Figure 3.30), secondly DAZL could be immunoprecipitated from transfected cell lysates with an anti-PABP1 antibody (Figure 3.32) and thirdly, endogenous Pabp1 and Dazl were reciprocally co-IPed from adult mouse testes lysates (Figure 3.34). While the latter supports the physiological relevance of this interaction, controls showing that these proteins do not also pulldown unrelated proteins, would further support the specificity of this interaction, although stringent conditions were utilised. Conservation of this interaction is consistent with the ability of mouse Dazl to interact with *X. laevis* PABPs and to stimulate the translation of reporter mRNAs in stage VI oocytes (Collier *et al.*, 2005b).

*X. laevis* oocytes do not, however, contain a tPabp homologue which is mammalian specific. The C-terminal regions of murine and human tPABP are 69 % and 91 % identical compared to their respective Pabp1 counterparts (Table 3.1). Although not verified by a second method, Y2H indicated that tPABP could interact with Dazl. However, tPABP is only expressed in round spermatids (Kleene *et al.*, 1994, Gu *et al.*, 1995, Kimura *et al.*, 2009), which appear to lack Dazl, since it is last detected during the meiosis I to meiosis II transition. Therefore it is unlikely that DAZL recruits tPABP for its function in promoting translation *in vivo*. The apparently fortuitous interaction of tPabp and Dazl, and the ability of proteins which are normally physically separated to interact following lysate preparation (Ohh *et al.*, 1998) emphasise the importance of directly visualising interacting proteins within the same cells in this study.

### 3.3.4 Dazl-KO phenotypes and Pabp1 expression

*Dazl* null mice present complex phenotypes (summarised in Figure 3.35). On an inbred background, abnormal germ cells appear in the fetal gonads of both sexes as early as 14.5-15.5dpc (Lin and Page, 2005, Lin *et al.*, 2008). Germ cell survival is greatly enhanced on an outbred background with germ cells reaching the pachytene spermatocyte phase in males, although apoptotic, leading this to being described as a leptotene-zygotene block (Schrans-Stassen *et al.*, 2001, Saunders *et al.*, 2003). In outbred females abnormal chromatin condensation is detectable by 17.5 dpc and germ cells are absent by 4 dpp (Saunders *et al.*, 2003). Importantly, Pabp1 is present within germ cells during the time frames when the various Dazl phenotypes develop (summarised in Figure 3.35), with dual IF confirming that Pabp1 and Dazl are both present, at the same time, within the cytoplasm of studied germ cells (Figures 3.13 and 3.15). Thus these results taken together with the interaction data support the hypothesis that Dazl activates the translation of specific mRNAs by recruiting Pabp1, allowing formation of a closed-loop mRNA conformation.

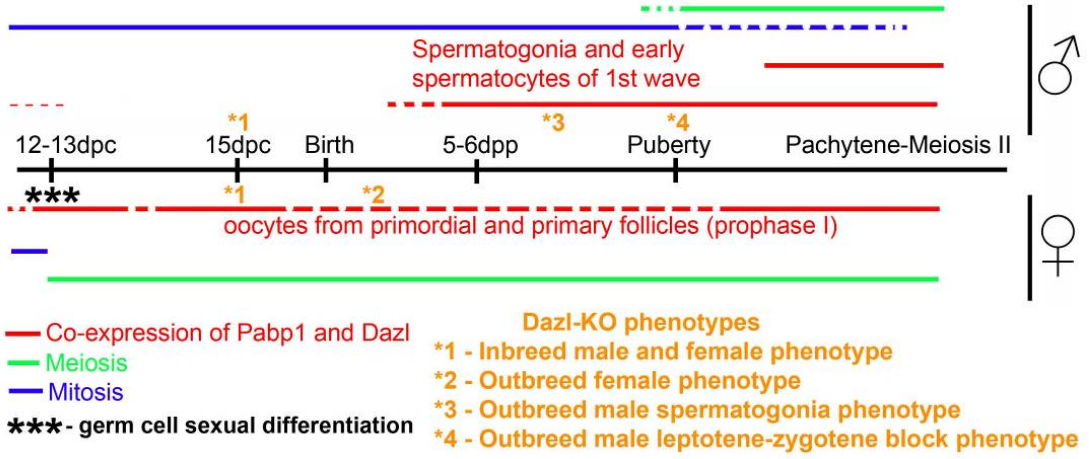


**Figure 3.35 -** Dazl and Pabp1 co-expression in mouse gametogenesis. **Dazl and Pabp1 are both expressed during stages associated with mouse Dazl-KO phenotypes. In males co-expression is depicted with two different red lines, the bottom one starting after birth until pachytene-meiosis II spermatocytes represent the first wave of spermatogenesis, the top representing subsequent waves of spermatogenesis which show co-expression only between pachytene and meiosis II. *1 - (Lin and Page, 2005, Lin *et al.*, 2008); *2 - (Saunders *et al.*, 2003); *3 - (Schrans-Stassen *et al.*, 2001); *4 - (Ruggiu *et al.*, 1997, Schrans-Stassen *et al.*, 2001, Saunders *et al.*, 2003).**

However, the translational activation of Dazl target mRNAs is likely to be complex. For instance, Pabp1 is present at 3 and 10 dpc straddling the timeframe when Dazl has been shown to function as a translational activator of verified target mRNAs, Mvh and Sycp3. In Dazl KO mice, their protein levels decrease at 4-5dpp and 7dpp respectively (Reynolds *et al.*, 2005, Reynolds *et al.*, 2007), consistent with Pabp1 playing a critical role in this process. But, in subsequent rounds of spermatogenesis, Pabp1 expression apparently follows the initial translation of Sycp3 (Dobson *et al.*, 1994, Yuan *et al.*, 2000) apparently inconsistent with this model. However, Sycp3 mRNA is also translationally activated by CPEB1 in both sexes (Tay and Richter, 2001) with Sycp3 protein levels being incompletely ablated in both Dazl and CPEB1 KO mice (Tay and Richter, 2001, Reynolds *et al.*, 2007). The CPEB1 and Dazl binding sites within Sycp3 mRNA overlap suggesting that their binding may be mutually exclusive (Tay and Richter, 2001, Reynolds *et al.*, 2007, Brook *et al.*, 2009) and interestingly in this regard recent work during oocyte maturation has shown that Dazl mRNA translation is initially activated by CPEB1 and subsequently by itself (Chen *et al.*, 2011). Thus the absence of Pabp1 when Sycp3 is initially activated during spermatogenesis in adults may reflect the temporality of translational activation by CPEB1 and Dazl, with Dazl maintaining active Sycp3 translation during late prophase I.

# Chapter 4

# Investigating potential interactions between Dazl and Pabp4

# 4.1 Introduction

PABP4 is one of the least characterised members of the PABP family. However, recent work in *X. laevis* has shown that this vertebrate specific PABP appears to activate global translation in a manner similar to PABP1 (Gorgoni *et al.*, 2011). Consistent with this, mammalian PABP4 was found to associate with polysomes in cell lines (Burgess and Gray 2012) and to activate the translation of a reporter mRNA containing the IL-2 3'UTR in cell-free extracts (Okochi *et al.*, 2005). To date, little work has been done to assess the temporospatial expression pattern of PABP4 in any species, although RT-PCR suggests it is developmentally regulated in *X. laevis* (Gorgoni *et al.*, 2011) and northern blotting suggests that PABP4 mRNA is variably expressed in a range of human tissues (Yang *et al.*, 1995). PABP1 mRNA is subject to extensive translational control (Burgess and Gray, 2010), and examination of the 5'UTR of PABP4 suggests the conservation of at least one of these control elements (NK Gray, personal communication), highlighting the importance of examining the expression of PABP4 protein directly.

As previously discussed, *X. laevis* Dazl has been shown to interact with two PABP family members, the prototypical PABP1 and embryonic PABP (ePABP). It has been shown that these interactions underlie the ability of Dazl to promote the translation of specific germ cell mRNAs (Collier *et al.*, 2005b). Chapter 3 extends these observations by showing that the interaction between PABP1 and DAZL is conserved in mammals. Although PABP4 has the C-terminal region that mediates PABP1/ePABP-DAZL interactions, the amino acid sequence of this region differs considerably between PABPs and thus it remains unclear whether DAZL can also utilise PABP4 to activate specific mRNAs. In support of a putative DAZL-PABP4 interaction, PABP4 transcripts are highly enriched in both human testis and ovary (Yang *et al.*, 1995), although it remains to be determined whether PABP4 is expressed in germ cells. Therefore, in this chapter, the possibility that Dazl fulfils its role in translation activation, in part, by interacting with PABP4 will be scrutinised. To this end, the expression pattern of murine Pabp4 within gonads will be established, to determine the extent of its colocalisation with Dazl. The ability of these proteins to interact will also be examined.

# 4.2 Results

## 4.2.1 PABP4 antibody validation

To date most work on the PABP family has revolved around the archetypical PABP1. As a result no PABP4-specific antibodies have been available, leading to a lack of information pertaining to its expression pattern.

Thus to investigate Pabp4 expression in mouse tissues an in house antibody was raised against a C-terminal peptide (KKEAAQKVGTVAAATS). This peptide is conserved in the four putative mouse Pabp4 splice variants proposed by Ensembl (Hubbard *et al.*, 2009), but differs greatly from the equivalent peptide in ePabp and, to a lesser extent, Pabp1 and tPabp (Figure 4.1).

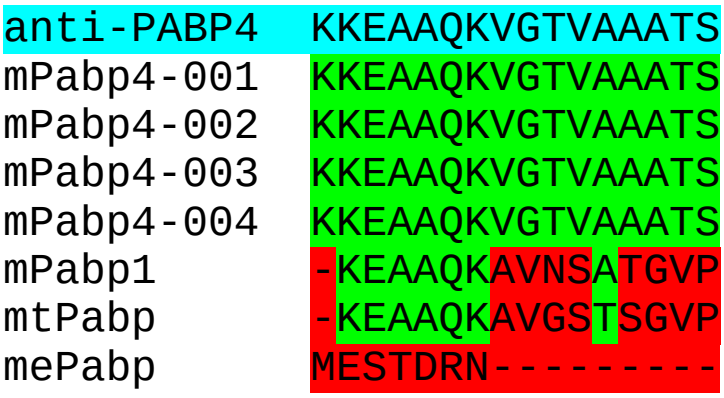


**Figure 4.1 - Peptide homology corresponding to sequence within the C terminal domain of mouse Pabp4 used to raise the anti-PABP4 antibody.** Peptide homology corresponding to the sequence within the C-terminal region of mouse Pabp4 used to raise the PABP4 antibody (blue). Green and red-amino-acids either match or vary from the peptide sequence respectively; mPabp4.001-004 – putative splice variants of mouse Pabp4 (isoforms 1 to 4); mPabp1 – mouse Pabp1; mtPabp – mouse tPabp; mePabp – mouse ePabp.

As a first step to testing the specificity of the anti-PABP4 antibody, HeLa cells, which express both PABP1 and PABP4, were transfected with siRNAs found to be effective for PABP1 or PABP4-specific knockdown (Burgess *et al.*, 2011). Western blotting of the resulting cell extracts with the anti-PABP4 antibody (Figure 4.2) showed that it appeared to be specific for PABP4 since no protein band was detected in the siPABP4 lane, but a protein of the predicted size was detected in

mock and siPABP1 transfected cell extracts (Figure 4.2 – a). GAPDH served as a loading control. Conversely, the PABP1 antibody, used in Chapter 3, failed to detect PABP1 in the siPABP1 lane (Figure 4.2 – b), supporting the specificity of both the PABP1 and PABP4 antibodies.

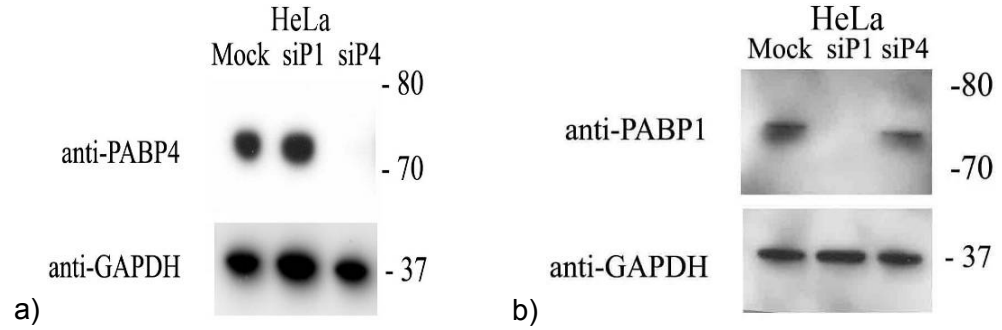


**Figure 4.2 - Anti-PABP4 antibody specifically detects PABP4 in HeLa cells.** HeLa cells were transfected with 5 nM of siPABP1 (siP1), siPABP4 (siP4) or were mock transfected and incubated for 48 hours. a – Anti-PABP4 antibody only detects PABP4 in cells transfected with siPABP1 or mock transfected. b - An anti-PABP1 antibody (Marshall) does not detect any signal following PABP1 knockdown but still detects PABP1 following PABP4 knockdown or mock transfection. GAPDH is used as a loading control.

To investigate the specificity of this antibody for IHC across a range of tissues, the PABP4 and PABP1 antibodies were applied to serial sections of whole 15.5 dpc mouse embryos, fixed in Bouin's. Interestingly, this revealed that Pabp4 was widely expressed across different mouse tissues but by no means ubiquitous (Figure 4.3). In particular Pabp4 showed significant expression in the neopalial cortex (the future cerebral cortex), heart, intercostal muscle, liver, Bowman's capsule in the developing kidney, pancreatic primordium, lining of the stomach (Fundic glands) and the lungs. Pabp1 was also found not to be ubiquitously expressed and was concentrated in several developing organs: the posterior area of the ventricular zone; mesodermic condensation (future extrinsic ocular muscle); primordial of follicles of vibrissae, Bowman's capsule in the developing kidney, ovaries, pancreatic primordium, lining of the stomach (Fundic glands) and the lungs (Figure 4.4). Importantly, while some tissues/structures showed expression of both proteins (neopalial cortex, extrinsic ocular muscle, kidney, ovary and lining of the stomach), others only showed expression of one or other of these PABPs (liver, heart, intercostals muscle, ventricular zone, whiskers).

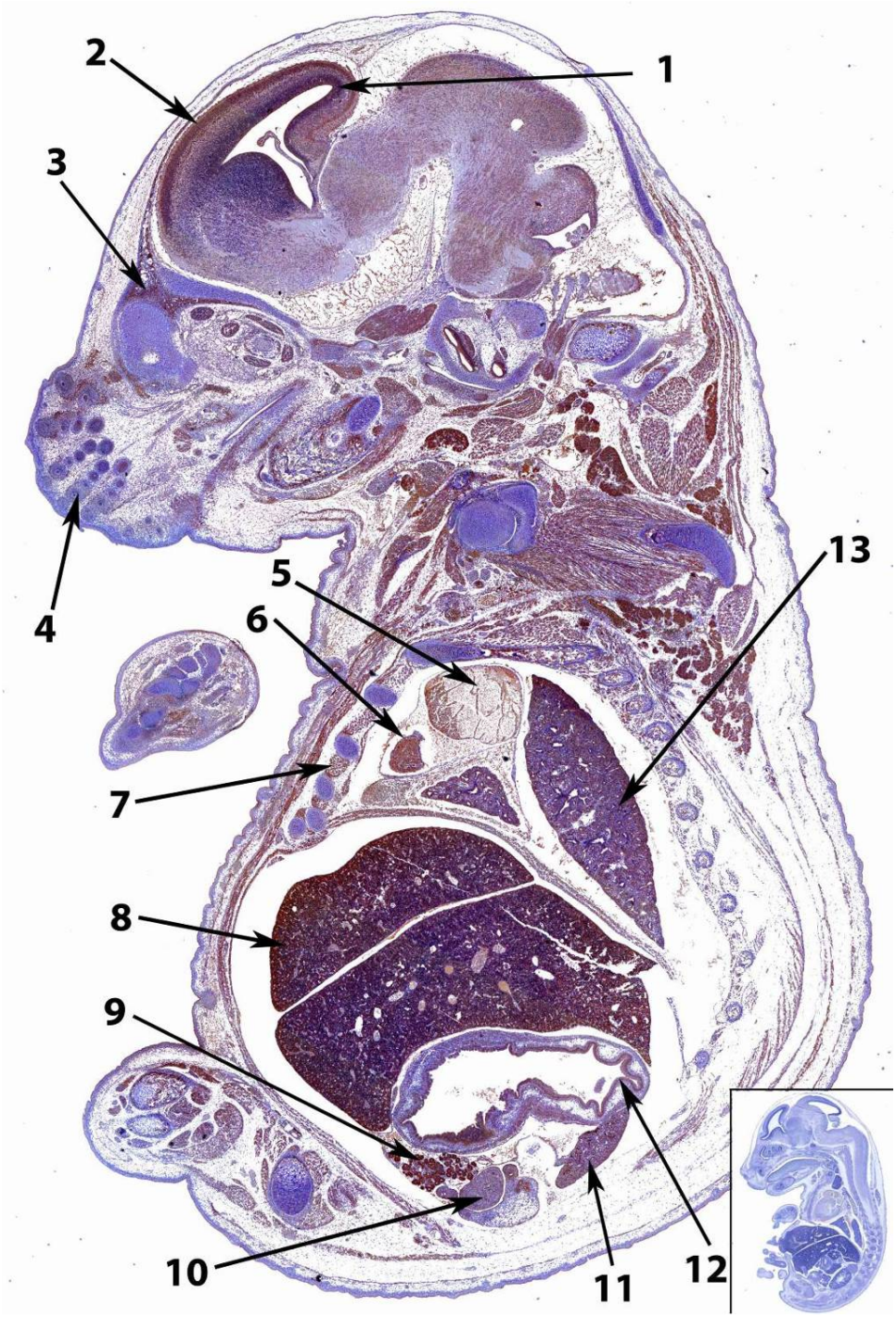


**Figure 4.3 - Pabp4 is not ubiquitously expressed during mouse fetal development.** IHC on 15.5 dpc female mouse using the anti-PABP4 antibody (1/2000 dilution). 1 – ventral zone; 2 – neopalial cortex (future cerebral cortex); 3 – mesodermal condensation (future extrinsic ocular muscle); 4 – primordial of follicles of vibrissae; 5 – atrium; 6 – ventricle; 7 – intercostal muscle; 8 – liver; 9 – kidney (Bowman's capsule); 10 – ovary; 11 – pancreatic primordium; 12 – lining of the stomach (Fundic glands); 13 – lung. Inset – negative control performed with no primary antibody.

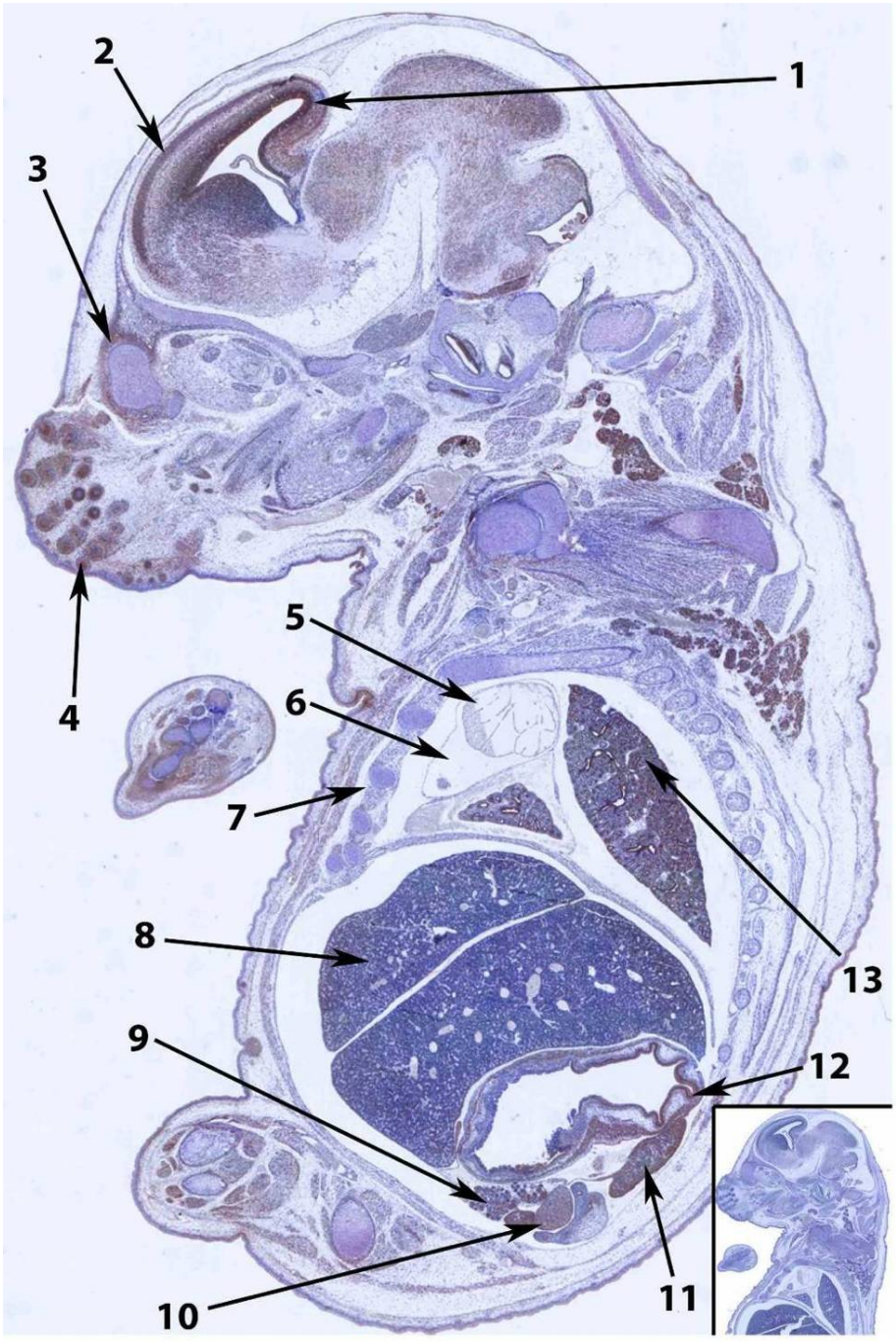


**Figure 4.4 - Pabp1 is not ubiquitously expressed during mouse fetal development and has a different expression pattern from PABP4.** IHC on 15.5 dpc female embryo using an anti-PABP1 antibody (1/5000 dilution). 1 – ventral zone; 2 – neopalial cortex (future cerebral cortex); 3 – mesodermal condensation (future extrinsic ocular muscle); 4 – primordial of follicles of vibrissae; 5 – atrium; 6 – ventricle; 7 – intercostal muscle; 8 – liver; 9 – kidney (Bowman's capsule); 10 – ovary; 11 – pancreatic primordium; 12 – lining of the stomach (Fundic glands); 13 – lung. Inset – negative control performed with no primary antibody.

These results establish that neither PABP is ubiquitously expressed during mammalian development, with sites of concomitant expression of both Pabp1 and Pabp4 and sites where they are differentially expressed.

As this data also supported the efficacy of this antibody in distinguishing between Pabp4 and Pabp1, it was optimised for further use on Bouin's fixed adult mouse testes by applying different dilutions (range 1/500 to 1/2000).

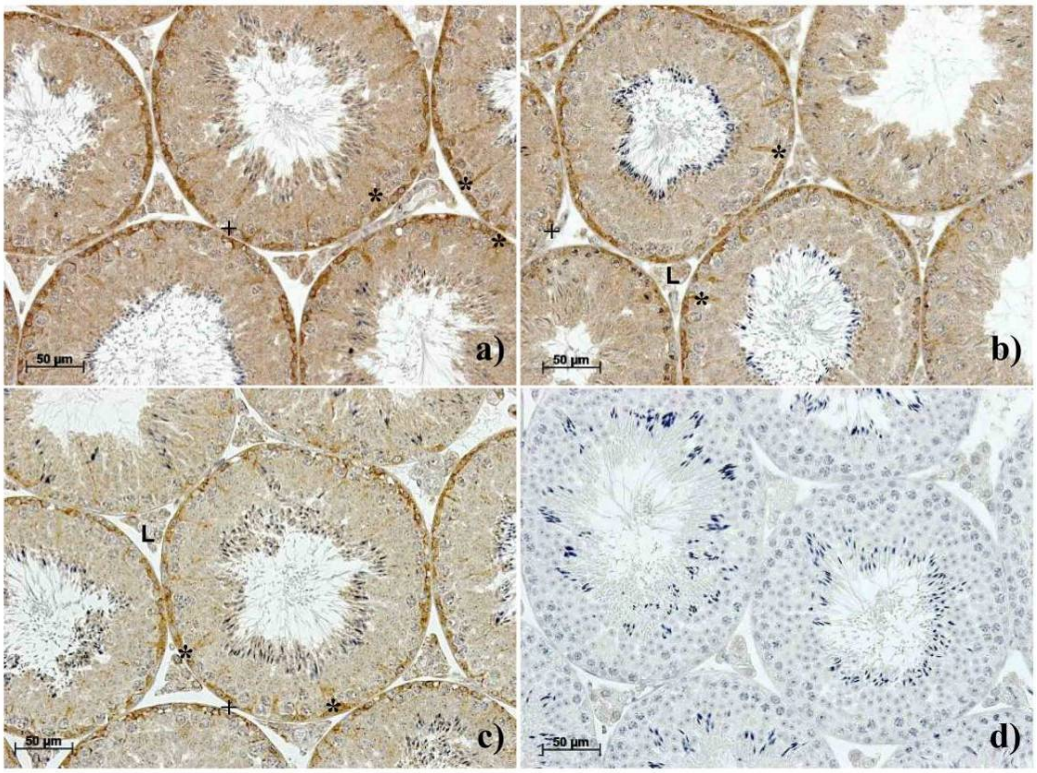


**Figure 4.5 - Optimisation of the anti-PABP4 antibody for IHC in mouse testes.** Three dilutions of the PABP4 antibody in mouse testes. a) 1/500; b) 1/1000; c) 1/2000 diluted in normal goat serum were applied to Bouin's fixed adult mouse testes. d) No primary antibody control. * - Sertoli cell cytoplasm; + - germ cells; L – Leydig cells. x20 magnifications.

All dilutions showed a similar pattern of DAB detection with cytoplasmic staining in a variety of cell types and stages (Figure 4.5). In all dilutions, Pabp4 appeared most highly expressed in the germ cells adjacent to the basement membrane (spermatogonia and early spermatocytes, a more in depth description is provided in section 4.2.2) and in the cytoplasm of the Sertoli cells. Pabp4 was also detected at lower levels, particularly at higher antibody concentrations, within later

germ cell stages excluding spermatozoa, and in the Leydig cells. In the absence of primary antibody (Figure 4.5- d) or in the presence of rabbit IgG or normal rabbit serum (Figure 4.6; Ross Anderson), immunostaining was not detected in any of these cell types suggesting that the observed pattern is dependent on the PABP4 antibody. Hereafter, the anti-PABP4 antibody was used as a 1/2000 dilution in normal serum.

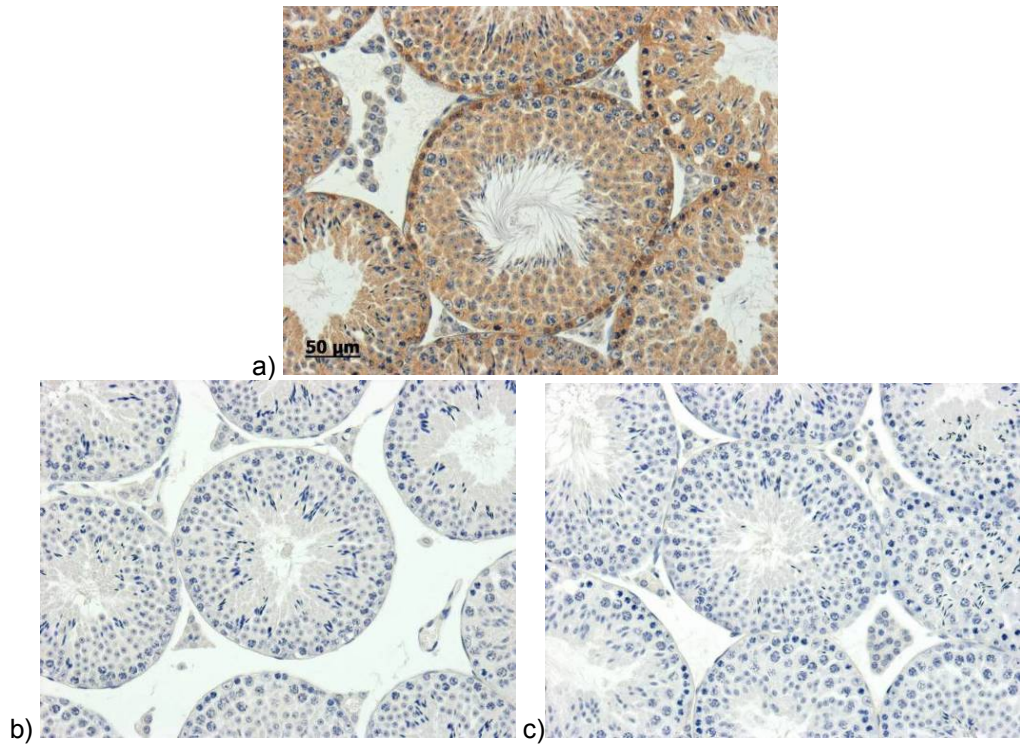


**Figure 4.6 - Additional controls further support the specificity of the anti-PABP4 antibody.** Sections of adult mouse testes immunostained for Pabp4 in parallel with additional negative controls. a – anti-PABP4 antibody; b – rabbit IgG control; c - normal rabbit serum. x20 magnification (Performed by Ross Anderson).

## 4.2.2 PABP4 expression in mammalian adult testes

Following optimisation and validation of the antibody, the cells expressing Pabp4 within the testes were analysed in greater detail. In agreement with Figure 4.5, Figure 4.7- a recapitulates the previous observed Pabp4 expression pattern with markedly stronger expression in the cells adjacent to the basement membrane Staging of different tubules according to Russell et al., 1990 (Figure 3.1) (Russell *et al.*, 1990) revealed these cells to be B-spermatogonia and early spermatocytes,

namely preleptotene, leptotene and zygotene spermatocyte cells. Pabp4 expression was significantly diminished essentially to background levels in subsequent stages (i.e. pachytene, secondary spermatocytes (spermatocyte in metaphase – Figure 4.7)) and round and elongating spermatids.

However, Pabp4 was strongly expressed in the cytoplasm of the Sertoli cells which extends from the basement membrane towards the lumen and also weakly in the Leydig cells. Its presence in these somatic cells which support germ cell development by delivering nutrients, regulating hormone levels and by secreting tubular lumen fluid (reviewed in (Russell *et al.*, 1990), reveals that Pabp4 is not restricted to the germ cells within the testis. As expected, no expression was observed in spermatozoa released into the lumen of the seminiferous tubules (stages VII-VIII) (Figure 4.7-a) or in the efferent duct, where sperm are concentrated due to testicular fluid reabsorption and undergo maturation (Hermo and Smith, 2011) (Figure 4.7- b). However, the ciliated epithelium cells of the efferent ducts express Pabp4, providing an internal control for the efficacy of the antibody. Pabp4 may contribute to the high rate of protein synthesis in these cells which produce lumicrine factors required for sperm transport and maturation (Hermo and Smith, 2011).

Comparison of the Pabp4 expression to that observed with Pabp1 and Dazl revealed that the expression of Pabp4 within the testes is almost reciprocal to that of Pabp1, and highly reminiscent of the expression of Dazl within the germ cells (see Figure 4.8 for a comparison).

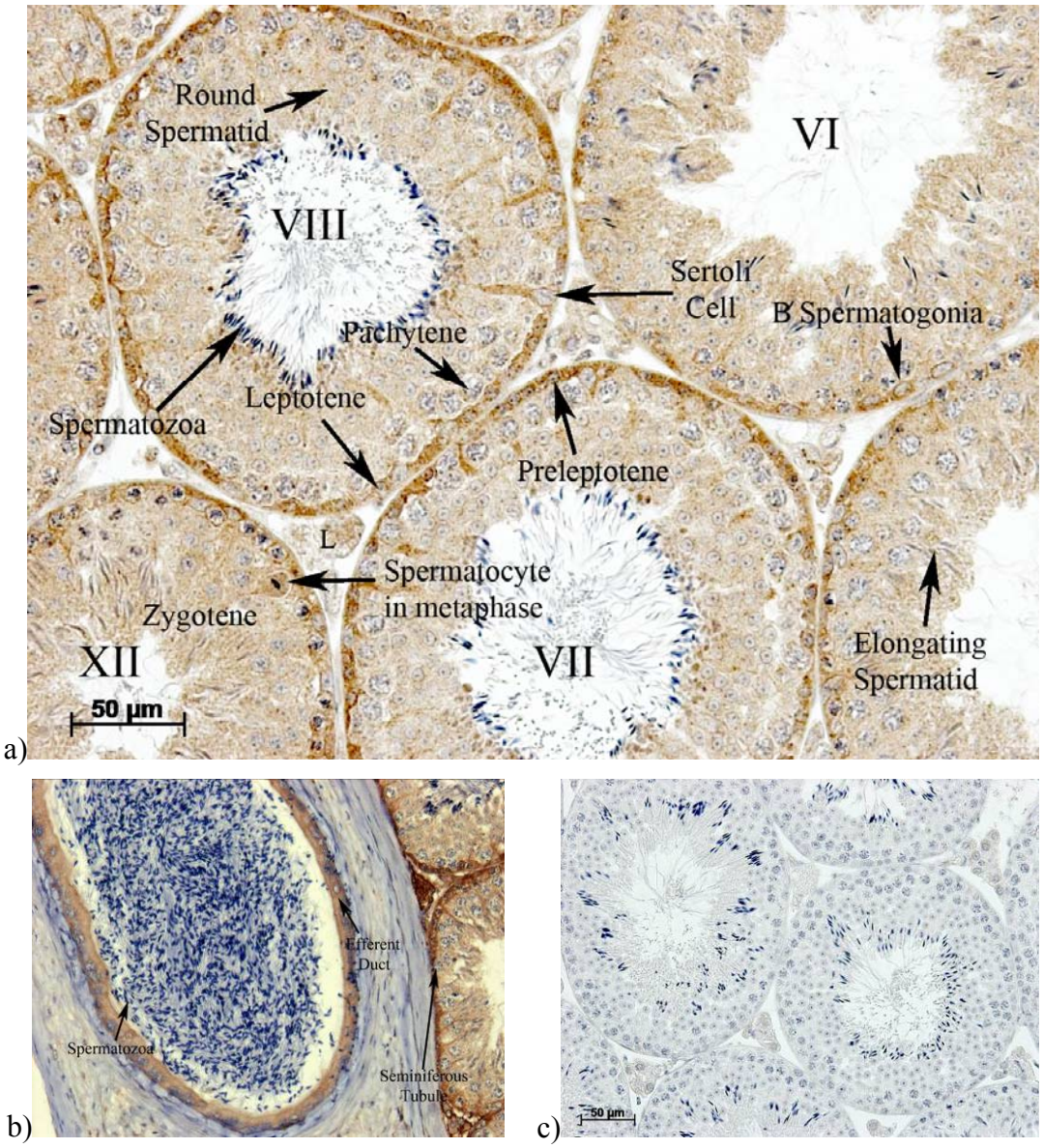


**Figure 4.7 - Pabp4 is expressed in germ and somatic cells in mouse adult gonads.** IHC analysis of mouse adult testes sections with an anti-PABP4 antibody (1/2000) in mouse adult testes. a – Pabp4 is robustly expressed in the cytoplasm of B-spermatogonia, preleptotene, leptotene, zygotene germ cells and Sertoli cells. The weak Pabp4 expression in the cytoplasm of pachytene spermatocytes, round spermatids, elongating spermatids and in Leydig cells (L) may represent background staining. b – no Pabp4 staining is observed in the spermatozoa within the efferent duct. c –no primary antibody control. X20 magnifications.

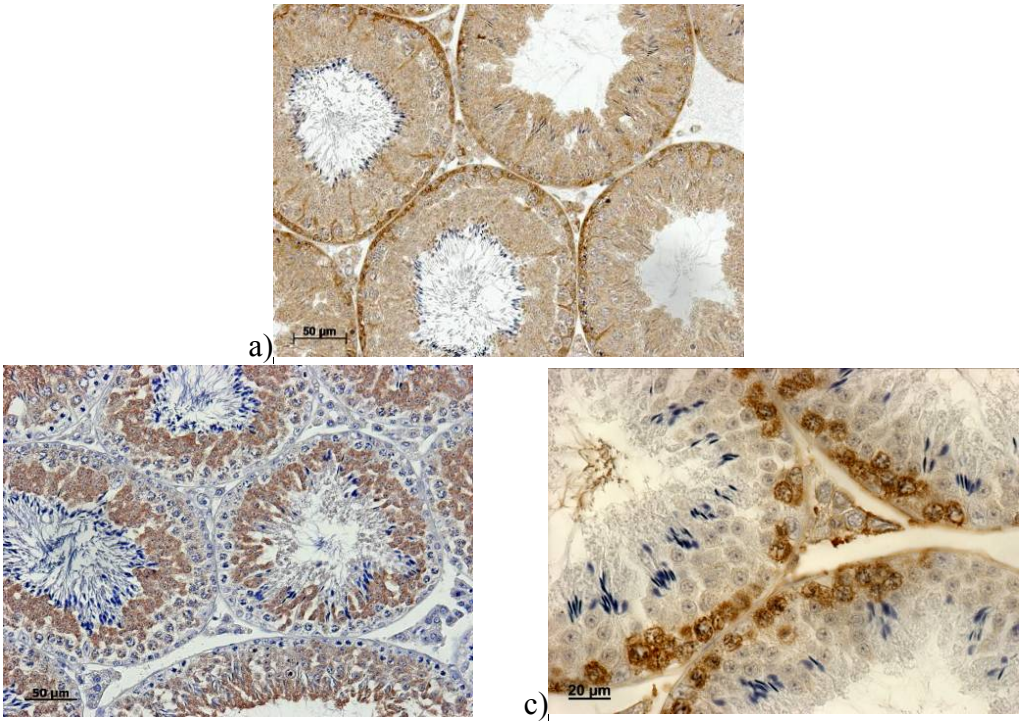


**Figure 4.8 - The expression pattern of Pabp4 in adult mouse testes is distinct from Pabp1, but significantly overlaps with that of Dazl.** IHC of adult mouse testes with DAB detection using: a – PABP4 (from Figure 4.7 - a); b – PABP1; c – Dazl antibodies. PABP4 and Dazl expression shows an intense peak in the cells close to the basement membrane (spermatogonia and early spermatocytes), whilst PABP1 expression is stronger in inner germ cells (round and elongating spermatids). a and and b - x20 magnification, c – x40 magnification.

#### 4.2.2.1 PABP4 expression pattern is conserved in mammalian testes

Since this data represents the first analysis of PABP4 expression and taking advantage of the conserved nature of peptide used to raise the antibody, PABP4 expression was also examined in other mammalian species to determine whether the observed pattern was recapitulated. Due to tissue availability, expression was analysed in adult rat and marmoset testes alongside mouse testes by two different detection systems: DAB and immunofluorescence (IF). In contrast to mouse, marmoset spermatogenesis progresses with a "helical" organisation within the seminiferous tubules, with different spermatogenic stages observed in the same tubule section (Millar *et al.*, 2000). In spite of this organisational difference, the pattern of Pabp4 expression in marmoset testes was broadly similar to that in mouse,

with stronger DAB staining in the early germ cells proximal to the basement membrane of the tubules and lighter staining in cells closer to the lumen (Figure 4.9). However, the cytoplasm of Sertoli cells was not clearly distinguishable, suggesting that Pabp4 may not be abundant in these cells in the marmoset.

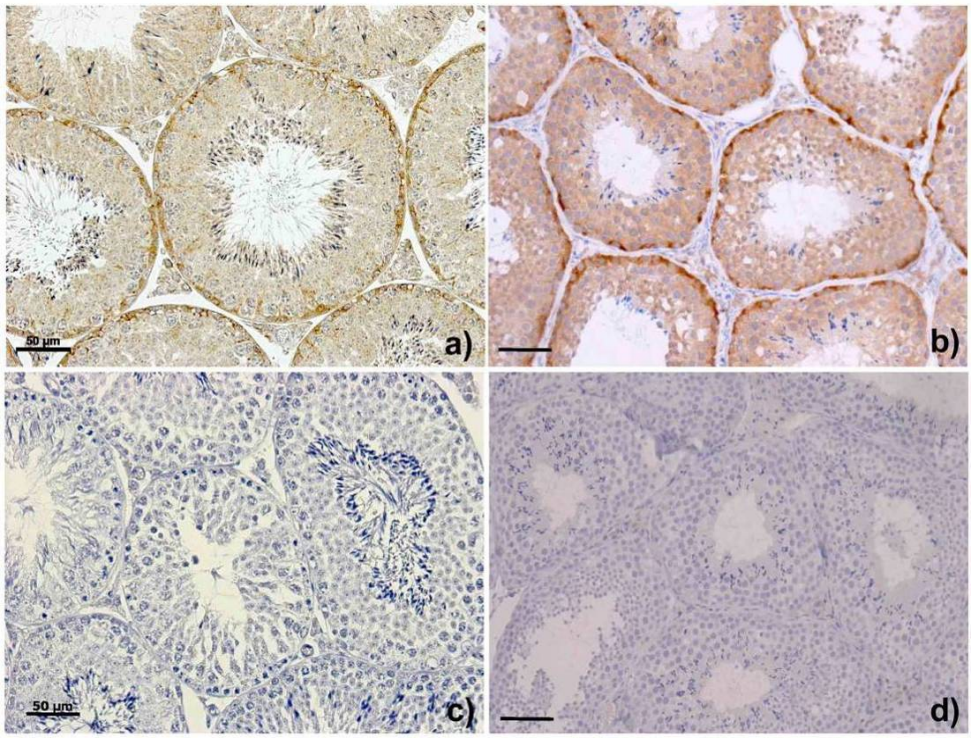


**Figure 4.9 - PABP4 expression is broadly similarly in mouse and marmoset testes.** a and b – IHC with anti-PABP4 antibody (1/2000); c and d – no primary antibody controls. a and c – mouse testes, b and d - marmoset testes. x20 magnification.

IF with tyramide detection in mouse and marmoset also gave results resembling those obtained with DAB detection, with the most intense signal being in the outermost germ cells and, in the case of mouse, also the Sertoli cells (Figure 4.10- a, b and c). The pattern observed in rat (Figure 4.10-b) most strongly resembled that obtained for mouse (see figure 4.7) with strong detection of PABP4 in early germ cells and in the extended cytoplasm of the Sertoli cells. Together these results suggest that PABP4 is predominantly expressed in the early germ cell stages of both rodent and primate species, with rodent species also showing significant staining within the Sertoli cells.

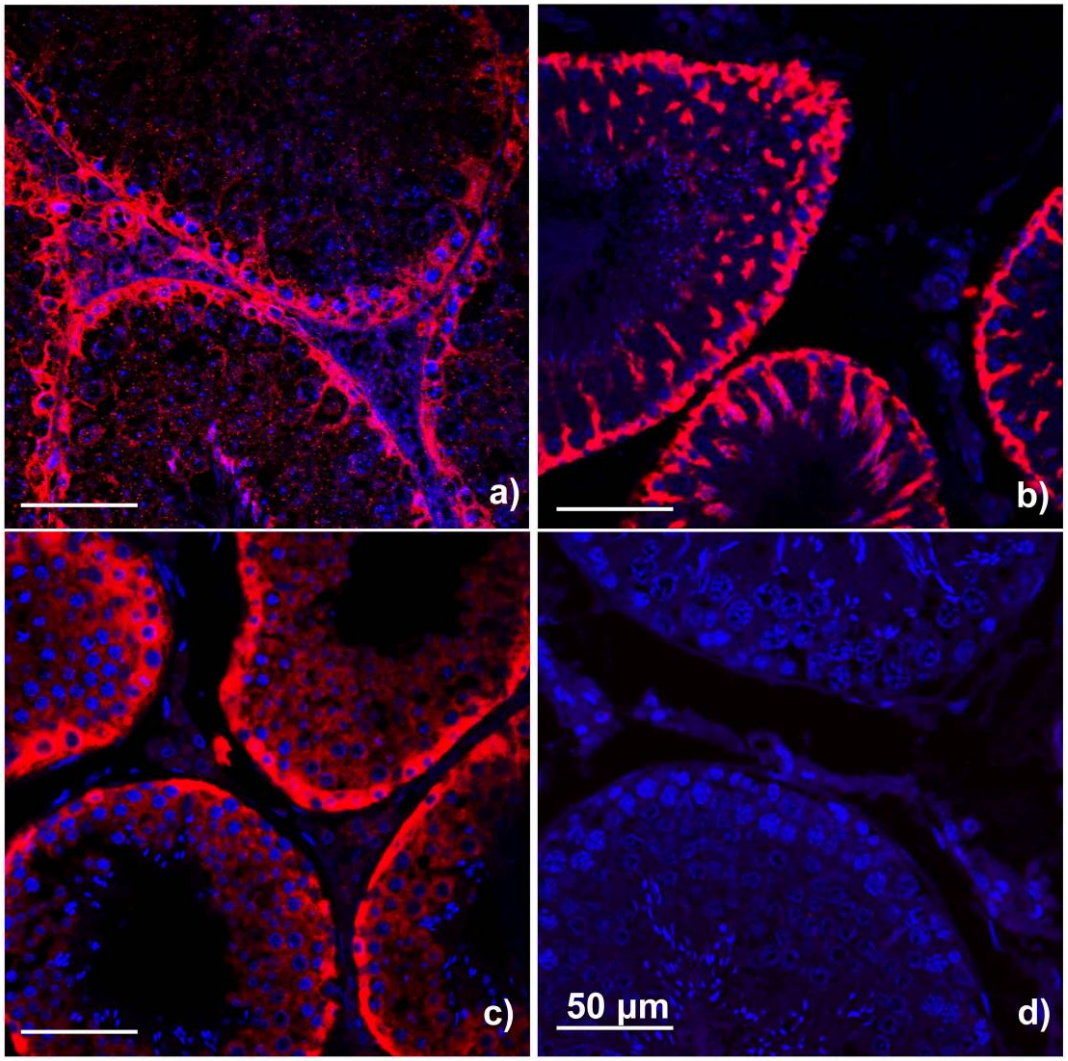


**Figure 4.10 - IF IHC analysis shows that PABP4 pattern of expression in mammalian testes is broadly similar.** Immunofluorescent (IF) detection of PABP4 (1/7500) in a – mouse; b – rat; and c - marmoset testes. d – rat testes negative control with no primary antibody. Red – PABP4, blue – DAPI nuclear counterstain. x40 magnifications.

#### 4.2.2.2 Dazl and Pabp4 are predominantly expressed in the same germ cell stages in adult mice testis.

Comparing the expression analysis of Pabp4 with that obtained for Dazl (see sections 3.2.1 and 4.2.2.1) supports the hypothesis that Pabp4, like Pabp1, may be utilised by Dazl to activate mRNA translation. Indeed the almost distinct patterns of Pabp1 and Pabp4 raise the possibility that Dazl may utilise Pabp4 in early germ cells and Pabp1 later in spermatogenesis to activate a cascade of mRNAs required for these different developmental stages. Thus to confirm that Dazl and Pabp4 co-reside

within the cytoplasm of the same germ cells, a dual-IF IHC assay with tyramide detection was utilised.

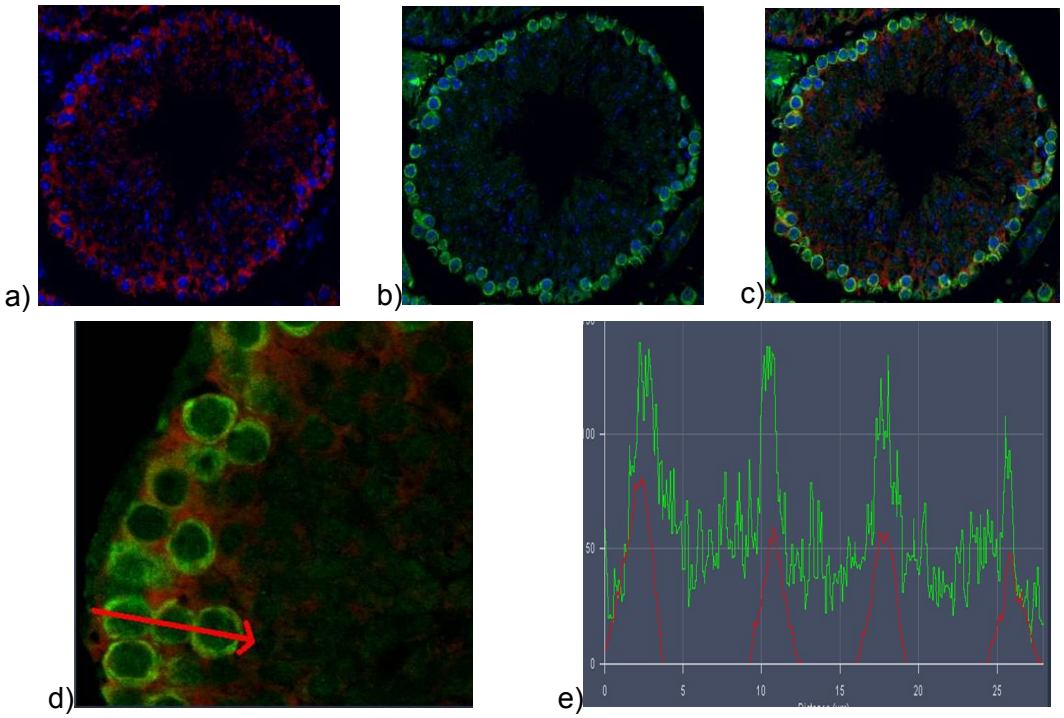


**Figure 4.11 - Pabp4 and Dazl colocalise within the cytoplasm of early germ cells in adult mouse testes.** Dual immunofluorescence with anti-Dazl and anti-PABP4 antibodies using tyramide detection a - anti-PABP4; b - anti-DAZL; c - merge of a and b; d and e. e - Colocalisation confirmed using intensity analysis software along the arrow shown in d (Zeiss Zen 2007). Red – Pabp4; Green – Dazl; Blue –DAPI nuclear counterstain. a, b and c – x40 magnification; d - x100 magnification.

In agreement with earlier data, both Pabp4 and Dazl expression was highest in the cytoplasm of the more peripheral germ cells (Figures 4.11- a and b) with their co-expression being confirmed in merged images (Figure 4.11- c). However, merging the images did not produce the expected distinctive yellow colour, due to the differing relative pixel intensities of the Dazl and Pabp4 signals. Therefore, to further confirm that both proteins co-reside within the cytoplasm of cells, a pixel intensity analysis was performed using the Zeiss Zen 2007 software focusing on the early germ cells where both proteins are highly expressed (Figures 4.11 - d and e). To this end, a cross-section of the picture was selected starting from the basement membrane towards the lumen and software used to read the pixel intensity for each

colour through the selected line (Figure 4.11- d). A graph depicting the pixel intensity throughout the marked line, with the X axis representing distance (basement membrane towards lumen), and Y axis representing pixel intensity is shown (Figure 4.11- e). This revealed that the expression of both proteins is very low at the basement membrane but dramatically increases within the cytoplasm of the first germ cell, decreases significantly in the nucleus and increases again in the cytoplasm. This nuclear/cytoplasmic variation continued through the analysed section with high pixel intensity for both proteins within the cytoplasm, and low intensity in the nucleus. These results establish that both proteins are found diffusely distributed within the same cellular compartment, the cytoplasm, during early stages of spermatogenesis, consistent with the hypothesis that they may interact to activate translation of a subset of mRNAs within germ cells.

#### 4.2.2.3 Pabp4 expression in mouse fetal gonads

The previous sections established that Dazl and Pabp4 are both present within the cytoplasm of spermatogonia and early spermatocytes, which represent germ cells undergoing mitotic or entering meiosis division, respectively. Thus in order to investigate the expression of Pabp4 during the equivalent stages in females, anti-PABP4 antibody was applied to the gonads of fetal female mice (Dazl - Figure 3.18; Pabp4 - Figure 4.12).

At 13.5 dpc Pabp4 was detected throughout the developing ovary Figure 4.12 - a. Despite this essentially ubiquitous pattern, Pabp4 could be identified within the cytoplasm of primordial germ cells (PGCs) within the germ cell cysts, which also express Dazl (Figure 3.18), and in the surrounding somatic cells. At day 15.5 dpc (Figure 4.12 - b) expression of Pabp4 was maintained throughout the ovary including the cytoplasm of oogonia, the site of Dazl expression.

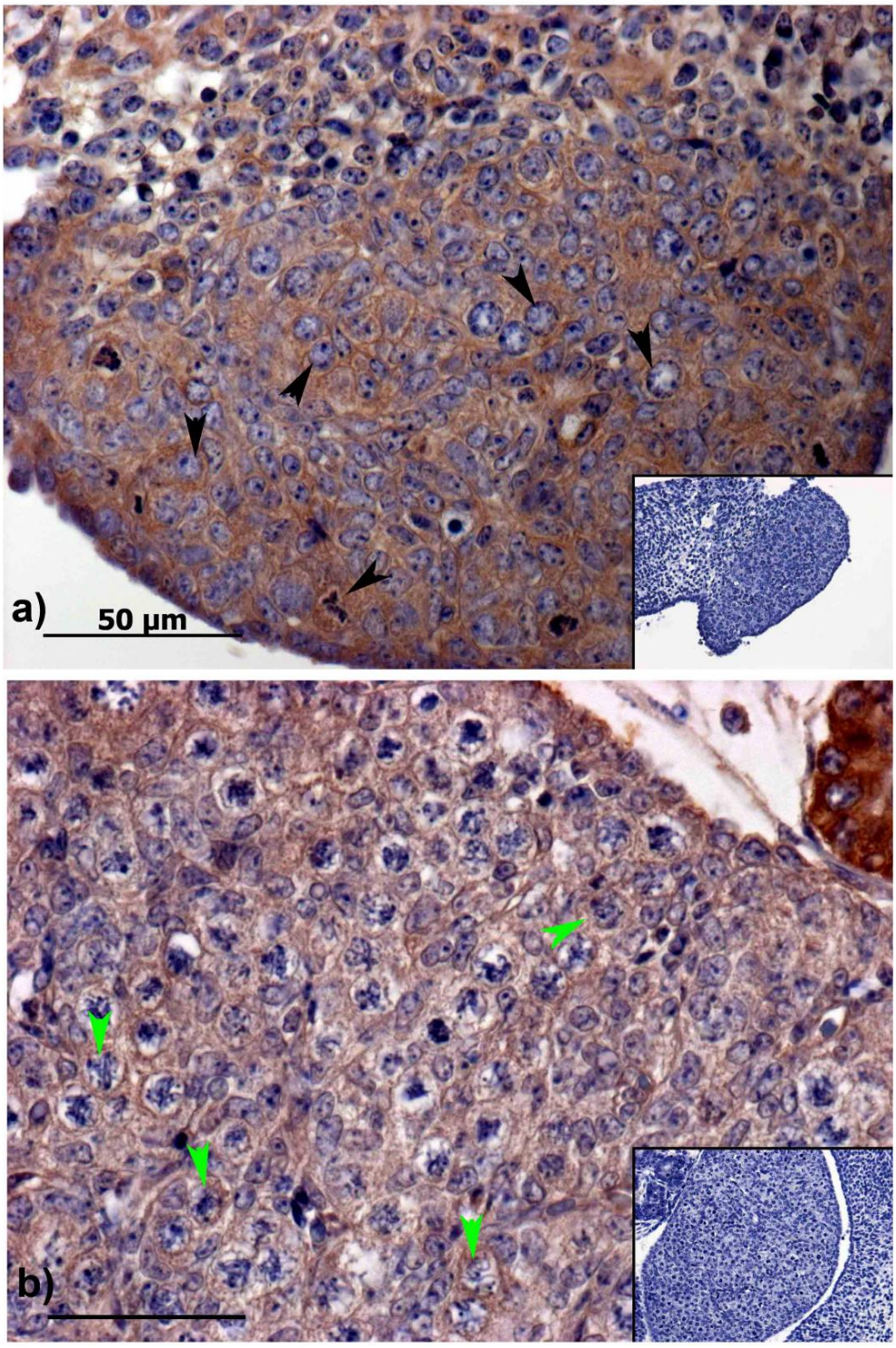


**Figure 4.12 - Pabp4 is widely expressed in female fetal gonads including the germ cells.** IHC with DAB detection was performed using the anti-DAZL antibody at different developmental stages: a – 13.5 dpc; b – 15.5 dpc. Arrowheads indicate germ cells: black – PGCss; green - oogonia. x40 magnifications; insets - no primary antibody controls.

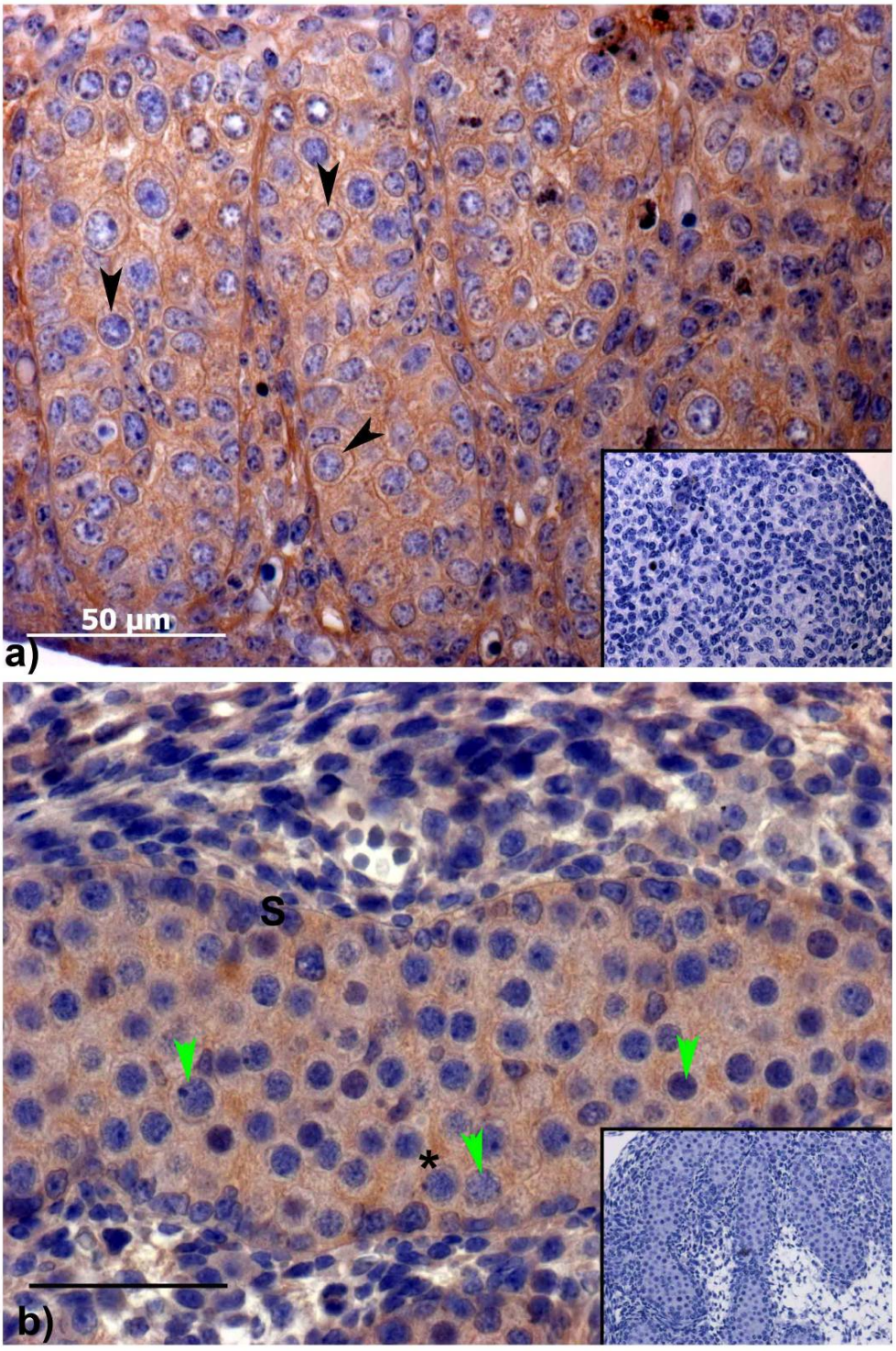


**Figure 4.13 - Pabp4 is widely expressed in male fetal gonads including the germ cells.** IHC with DAB detection was performed using the anti-DAZL antibody at different developmental stages: a – 13.5 dpc; b – 15.5 dpc. Arrowheads indicate germ cells: black – PGCs; green – prospermatogonia; * - inter germ cell space; S – Sertoli cells. x40 magnifications; insets - no primary antibody control.

As previously mentioned there is a marked sexual dimorphic status in germ cells at these stages of development, with only female gonocytes entering meiosis (13.5 dpc). Thus in order to determine whether Pabp4 is differentially expressed in males at these stages, 13.5 and 15.5 dpc fetal mouse testes were subject to IHC with the anti-PABP4 antibody. Similar to 13.5 dpc ovary, Pabp4 was widely expressed within the developing testes (Figure 4.13 - a), including the cytoplasm of PGCs within the developing seminiferous tubules, which express Dazl (Figure 3.20 -b) and the surrounding intra and intertubular somatic cells. At day 15.5 dpc (Figure 4.13 - b), Pabp4 was still expressed very widely, including in the prospermatogonia, but at low levels. The strongest expression appeared to be in the spaces between prospermatogonia cells (* in Figure 4.13 - b), which may represent early extensions of Sertoli cell cytoplasm starting to surround the germ cells (Mendis *et al.*, 2011). The absence of immunostaining in the absence of primary antibody (Figure 4.13 insets) suggests that this expression pattern although widespread was specific. Thus Pabp4 appears to be expressed alongside Dazl in the cytoplasm of fetal germ cells of both sexes (Figures 3.17 and 3.19), consistent with a potential role in mediating Dazl function at these stages.

#### 4.2.2.4 Pabp4 expression in female adult mouse gonads

Given the phenotypic consequences associated with loss of Dazl function in maturing oocytes (Chen *et al.*, 2011), the expression of Pabp4 was also compared to that of Dazl in adult ovaries. Pabp4 was strongly expressed in the oocytes of primordial, primary and secondary follicles, but became undetectable in oocytes in antral follicles. Interestingly, Pabp4 was also expressed in a subset of somatic cells including the granulosa and theca cells of the growing follicles (Figure 4.14). Granulosa cells are considered functionally equivalent to the Sertoli cells which also displayed robust Pabp4 expression (Figure 4.7), whilst theca cells functionally resemble Leydig cells. PABP4 was essentially absent from the stroma cells that sit between the follicles.

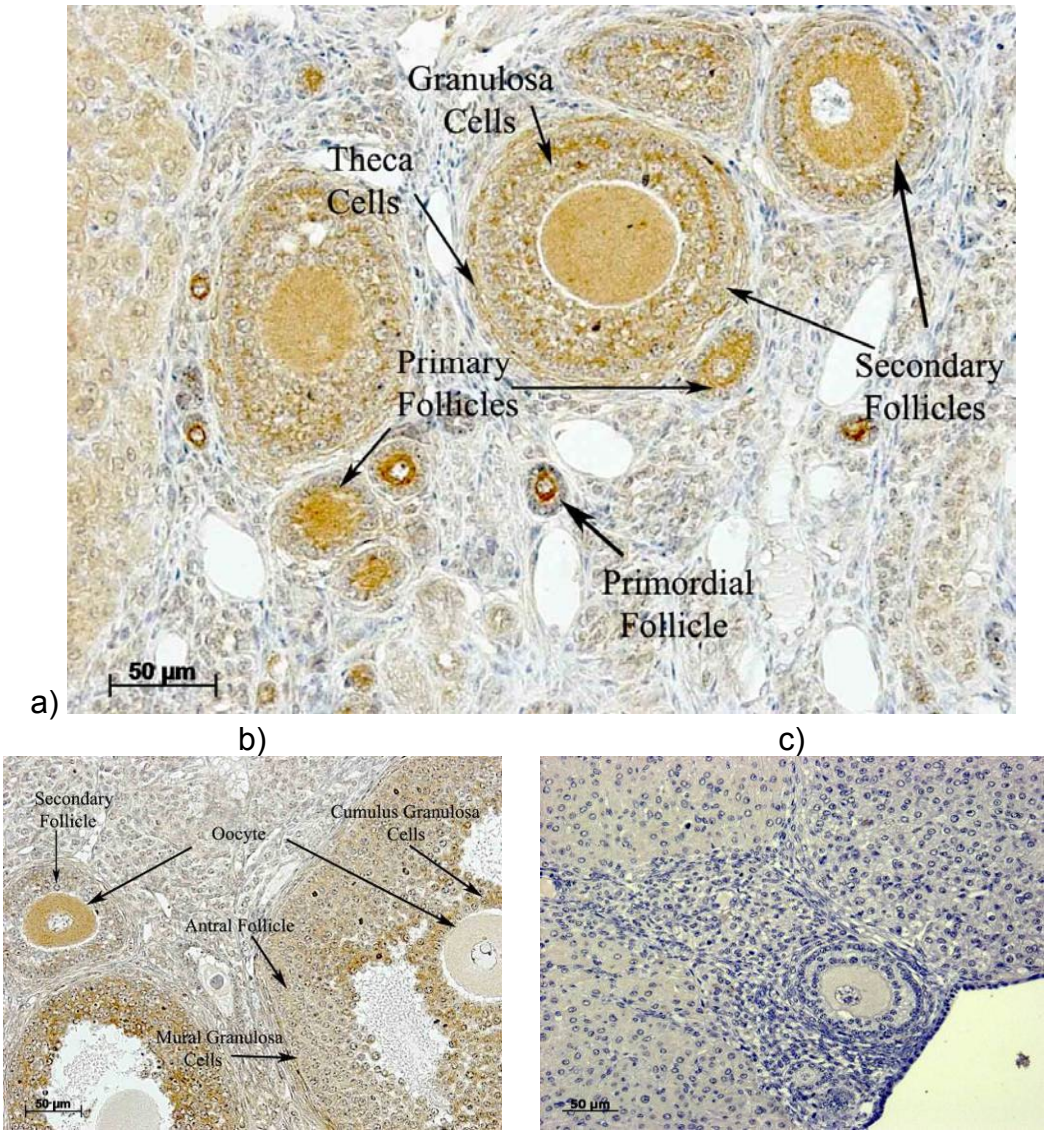


**Figure 4.14 - Pabp4 expression within adult mouse ovaries.** IHC analysis using the anti-PABP4 antibody (1/2000) in mouse adult ovaries using: a and b – IHC with anti-PABP4 antibody; c - negative control performed with no primary antibody. x40 magnifications. In mouse ovaries, Pabp4 is expressed in the cytoplasm of primordial, primary and secondary follicles. Pabp4 expression is also observed in granulosa and theca cells.

Importantly, the robust expression of Pabp4 within the oocytes of primordial, primary and secondary follicles resembles that of Dazl (Figure 3.22), indicating that both proteins are present within the cytoplasm of oocytes during early folliculogenesis. Interestingly, unlike the pattern observed in male germ cells, where Pabp4 and Pabp1 show almost reciprocal expression (Figure 4.8), the expression of these PABPs significantly overlapped in oocytes.

### 4.2.3 Mouse testes express four different splice-forms of Pabp4

To date no PABP-specific protein interactions have been described, and the finding that Pabp4 and Dazl show striking similarities in their expression during male and female germ cell development, provides the potential for these proteins to interact *in vivo*. Ensembl (Hubbard *et al.*, 2009) predicts four different potential splice-forms for mouse Pabp4 (mPabp4), created by inclusion and exclusion of 2 exons (Figure 4.15). Such alternative splicing would generate variation within the proline-rich linker that comprises part of the C-terminal region. This region of PABP1 is responsible for its interaction with DAZL (Collier *et al.*, 2005b). The predicted splice variants, named mPabp4-001, -002, -003 and -004 correspond to proteins of 660 amino acids (aa), 615 aa, 631 aa and 644 aa, respectively and appear conserved in humans (Hannah Burgess, personal communication), suggesting that they may be biological relevant. However, due to differences in nomenclature these putative isoforms are named differently: human PABP4-001 (hPABP4-001) corresponds to mPabp4.004, hPABP4-002 corresponds to mPabp4.001, hPABP4-003 corresponds to mPabp4.002 and hPABP4-004 corresponds to mPabp4.003.

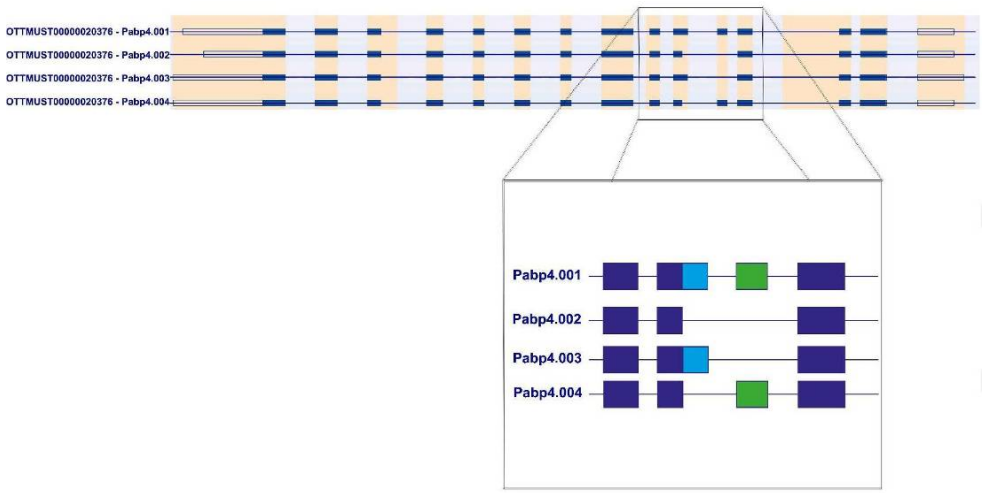


**Figure 4.15 - Schematic representation of the different mouse Pabp4 isoforms predicted by Ensembl.** Constitutive exons are represented in dark blue; alternative exons are represented in light blue and green. Unfilled regions represent UTRs.

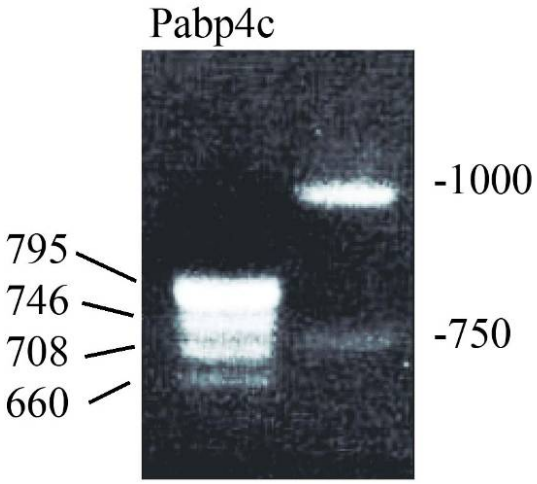


**Figure 4.16 - Mouse testes express 4 different splice forms of Pabp4.** RT-PCR performed in mouse testes RNA with oligonucleotides that flank the predicted variable region of mouse Pabp4.

To determine whether these predicted splice variants are actually expressed, RT-PCR was performed on mouse testes RNA (see 2.4.10 and 2.5.2) using oligonucleotides that flank the variable region. This produced four closely spaced bands (Figure 4.16) corresponding to the predicted sizes, with sequencing confirming their identity. Thus, at least at the RNA level, all four isoforms predicted by Ensembl are expressed in mouse testes.

## 4.2.4 DAZL and PABP4 interactions

### 4.2.4.1 Interspecies interaction between mammalian DAZL and *X. laevis* PABP4

It was shown previously that mDazl as well as *X. laevis* Dazl (xDazl) interacts with the C-terminus of *X. laevis* PABP1 (xPABP1) and ePABP (xePABP) (Collier *et al.*, 2005b). However, subsequently a homologue of PABP4 (xPABP4) was identified in *X. laevis* (Gorgoni *et al.*, 2011). Thus its ability to interact either with xDazl, or mDazl, was examined by yeast two-hybrid approach (Y2H) (Zhang *et al.*, 1999).

To this end, the C-terminal region of xPABP4 was cloned in frame with the lexA DNA-binding domain (see 2.16.2) and the respective DAZL proteins with the GAL4 activation domain. The characterised interaction between xPABP1 and xDazl

served as a positive control (Collier *et al.*, 2005b), whilst iron regulating protein (IRP) and MS2 as negative controls (Gray *et al.*, 2000).

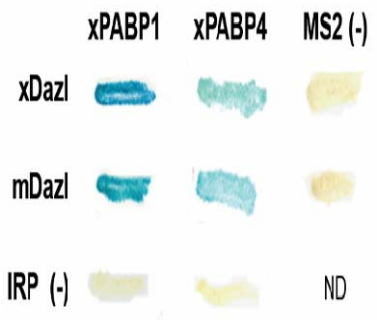


**Figure 4.17 - *X. laevis* and mouse Dazl interact with xPABP4.** Yeast two-hybrid assay between DAZL from different species and the C-terminus of *X. laevis* PABPs. Blue colour indicates a positive interaction. ND – not done.

Interestingly, this revealed that xPABP4 was able to interact with both xDazl and mDazl (Figure 4.17), despite the C-terminal regions of *X. laevis* PABP1 and PABP4 showing only 58% identity. The findings that interactions are conserved between different family members and between species (mDazl interacts with xPABP4) suggest that interaction between these families may be both important and complex.

#### 4.2.4.2 Mouse Dazl specifically interacts with different PABP family members

Dazl binding has been mapped to the C-terminal region of PABPs. This comprises a highly conserved PABC domain (e.g. almost 95% conserved between mPabp4 and xPABP4) and a much less conserved proline-rich linker region which is subject to alternative splicing in mouse (Figures 4.15 and 4.18).

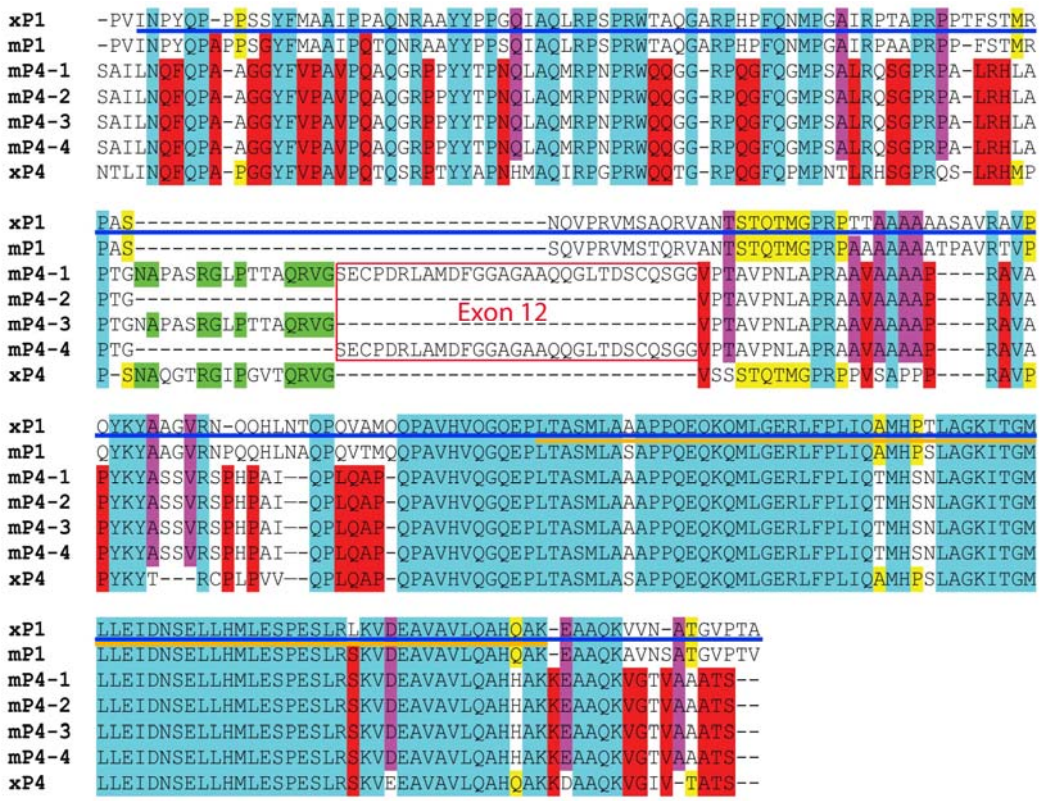


**Figure 4.18 - Comparison of the conservation within C-terminal regions of different PABPs.** There is a high degree of homology in the PABC domain (orange line) between PABP1 and PABP4 but the region containing the alternative exons in PABP4 is less conserved. Blue – conserved residues; Red – conserved residues between mouse and *X. laevis* PABP4; Yellow – conserved residues in mouse and *X. laevis* PABP1 and xPABP4 but not in mPabp4 isoforms; Purple – conserved residues between xP1, mP1 and mP4 isoforms. Blue line – region to which the Dazl interaction is mapped. mPabp – mouse Pabp; xPabp – *X. laevis* PABP.

The finding that xPABP4 interacts with both *X. laevis* and mouse Dazl suggests that mPabp4, or specific mPabp4 isoforms, are likely to interact with mDazl. To investigate this, Y2H assays were undertaken using the C-terminal regions of the mPabp4 isoforms as bait. Each of the mPabp4 isoforms interacted with the positive control protein PAIP-1 (blue colonies), but surprisingly, none interacted with mDazl (Figure 4.19). mDazl did show a positive interaction with mPabp1 indicating that it was expressed and capable of interaction. Thus despite the ability of xPABP4 and mDazl to interact, it appears none of the mPabp4 isoforms interact with mDazl.

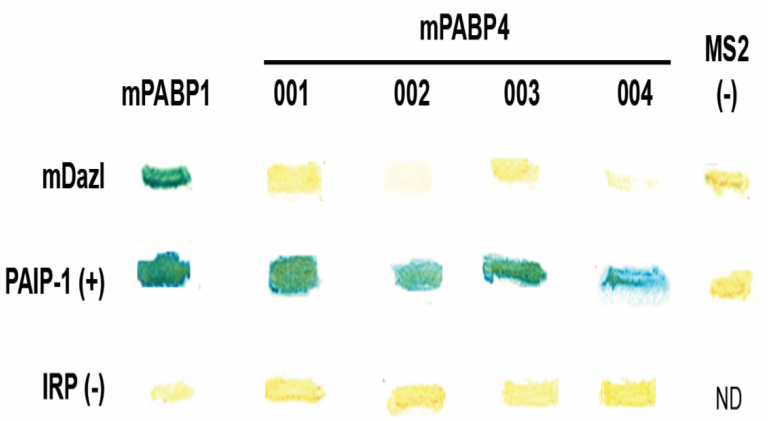


**Figure 4.19 - Mouse Dazl exhibits specificity in its interactions with different mammalian PABPs.** Y2H analysis using mDazl and the C-terminal regions of mPabp1 and mPabp4 isoforms. PABP-interacting protein 1 (PAIP-1) is used as a positive control. IRP and MS2 are used as negative controls. ND – not done.

### 4.2.4.3 Generation of recombinant mouse Pabp4 proteins

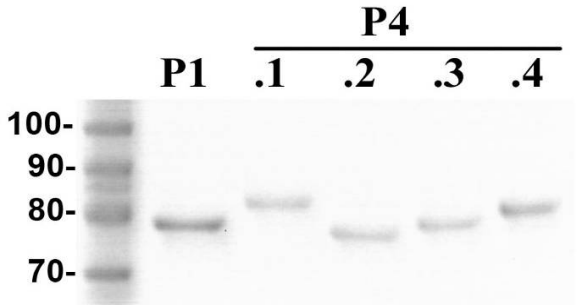


**Figure 4.20 - Recombinant mouse PABP proteins.** Lysates from *E. coli* expressing mouse His-Strep-tagged PABP proteins were purified by two step affinity chromatography. Eluted proteins were subjected to SDS-PAGE followed by staining with GelCode Blue. P1 – mouse Pabp1; P4 – mouse Pabp4; .1-.4 – mouse Pabp4 isoforms 1 to 4.

To confirm this surprising result, a GST-pull-down assay was performed. This required the generation of purified recombinant mPabp4 proteins. Thus, each of the four isoforms, together with mPabp1, were cloned into Isopropyl-β-D-thio-galactoside (IPTG) inducible expression vectors. Following induced expression, the recombinant proteins were purified from *E. coli* extracts by two-step affinity chromatography based on their N-terminal His tag and C-terminal Strep tag. This two-step approach produced highly pure full-length PABP proteins as determined by SDS-PAGE and GelCode blue staining (Figure 4.20).

#### 4.2.4.4 Mouse Pabp4 isoforms do not interact with DAZL in a pull-down assay

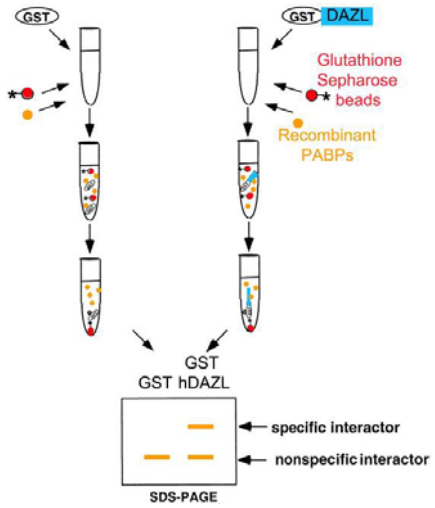


**Figure 4.21 - Schematic of GST-DAZL pull-down assay.** GST-DAZL was bound to Glutathione Sepharose 4B beads and incubated with recombinant purified PABP proteins. Following washes, bound proteins were eluted and analysed by Western blotting. Beads bound by GST alone control for non-specific interactions. GST – glutathione S-transferase and GST-DAZL – GST fused to human DAZL.

Equal amounts of the recombinant purified mPABP proteins were utilised in GST-pull-down assays with commercially available GST or GST-DAZL (Figure 4.21). Western blotting (anti-His) showed that each of the mPABP proteins was similarly retained by GST and GST-DAZL, suggesting non-specific binding of purified mPABP proteins to either GST and/or the beads (Figure 4.22).

Thus in order to reduce this non-specific background binding, more stringent washing conditions were utilised increasing the NaCl in the wash buffer to 300 mM (from 150 mM). Under these conditions (Figure 4.23) the signal with the anti-His antibody was significantly stronger in the GST-DAZL lane compared the control GST lane, suggesting a specific interaction between mPabp1 and DAZL. In contrast, Pabp4 isoforms that bound GST-DAZL (e.g. mPabp4.003) were also retained by GST alone, indicating that these represent non-specific interactions. Thus consistent with the Y2H results, the pull-down failed to detect specific interactions between DAZL and any of the mouse Pabp4 isoforms.

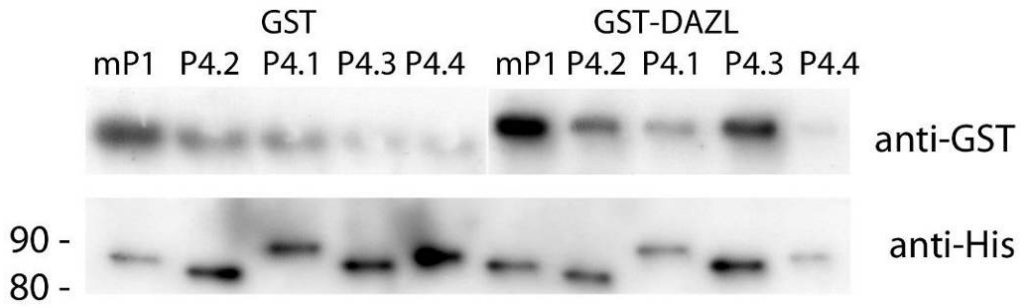


**Figure 4.22 - Recombinant PABP proteins bind non-specifically in low (150 mM NaCl) salt washes.** GST or GST-DAZL proteins (3 pmol) were bound to Glutathione sepharose 4B beads and incubated with purified recombinant mouse PABP proteins (30 pmol) for 1 hour. Beads were washed extensively and bound proteins eluted and subject to western blotting with anti-polyhistidine (anti-His) and anti-GST antibodies. mP1 – mouse Pabp1; P4.1-4 – mouse Pabp4.001 to 004; GST – glutathione S-transferase; GST-DAZL – GST bound to human DAZL.

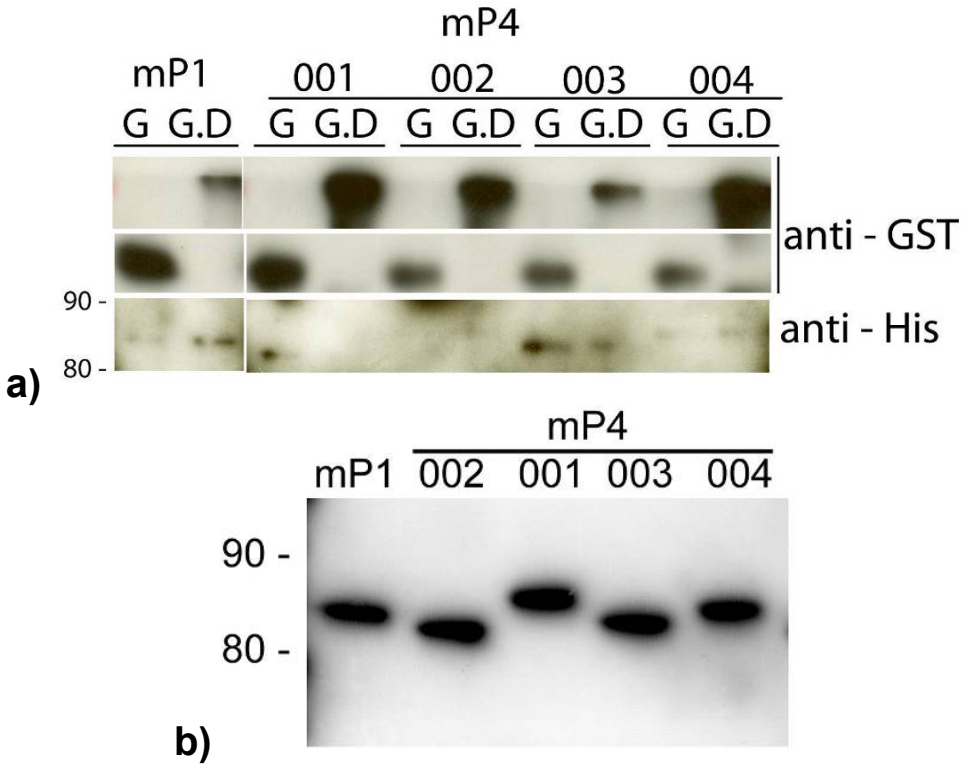


**Figure 4.23 - Recombinant mouse Pabp4 isoforms fail to interact with recombinant DAZL protein in pull-down assays.** a) GST or GST-DAZL proteins (3 pmol) were bound to Glutathione sepharose 4B beads and incubated with (30 pmol) purified recombinant mPABP proteins. Columns were washed with buffer containing 300 mM NaCl. Samples were eluted and western blotted with anti-polyhistidine (anti-His) and anti-GST antibodies. b) Input (3 pmol PABP proteins), Western blotted and exposed in parallel, represents 10% of the sample used for the pull-down. mP1 – mouse PABP1; P4.1-4 – mouse Pabp4.001 to 004. G - glutathione S-transferase; G.D – GST bound to human DAZL.

As it remained possible that mammalian or germ-cell specific post-translational modifications may be required for Dazl-Pabp4 interactions, the ability of the PABP4 antibody to co-isolate Dazl, and vice-versa, was tested by co-IP using mouse testes extracts. Mouse and rabbit IgGs were used as negative controls for the mouse anti-DAZL and the rabbit anti-PABP4 antibodies, respectively.

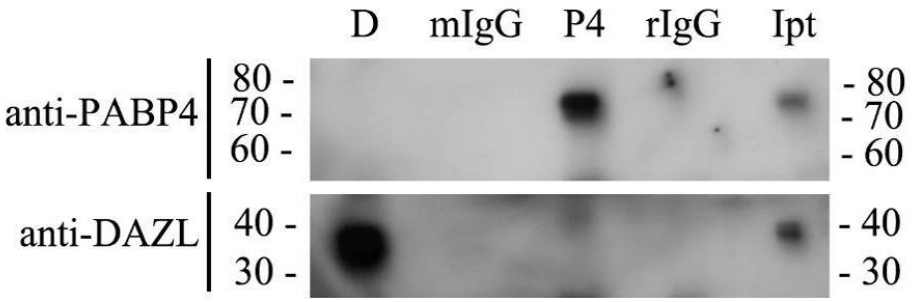


**Figure 4.24 - Endogenous mouse Pabp4 and Dazl fail to interact.** Immunoprecipitation (IP) with anti-DAZL (D), anti-mouse IgG (mIgG), anti-PABP4 (P4) and anti-rabbit IgG (rIgG) in adult mouse testes lysates. IPs were western blotted for PABP4 and DAZL. Input (Ipt) represents 1% of the material used for each IP. IPs were washed with co-IP buffer containing 200 mM NaCl.

Both the PABP4 and DAZL antibodies had efficacy for immunoprecipitation since they were able to IP themselves, as detected by western blotting (Figure 4.24). However, despite the co-IPs being performed under the same conditions as the Dazl-Pabp1 co-IP in Chapter 3 (Figure 3.34), the anti-Pabp4 antibody failed to co-IP mDazl and vice-versa.

Thus, three separate lines of evidence support the surprising finding that mouse Pabp4 and Dazl do not interact, identifying Dazl as the first PABP-specific protein partner.

### 4.2.5 Mouse Pabp4 isoforms interact with the DAZ family member Boule

As it was surprising that Pabp4 was unable to interact with DAZL, it was of interest to determine whether it could interact with Boule, the other DAZ family member expressed in mouse. Thus mouse Boule (mBoll) was retrieved by RT-PCR from mouse testes and cloned into an appropriate Y2H vector.

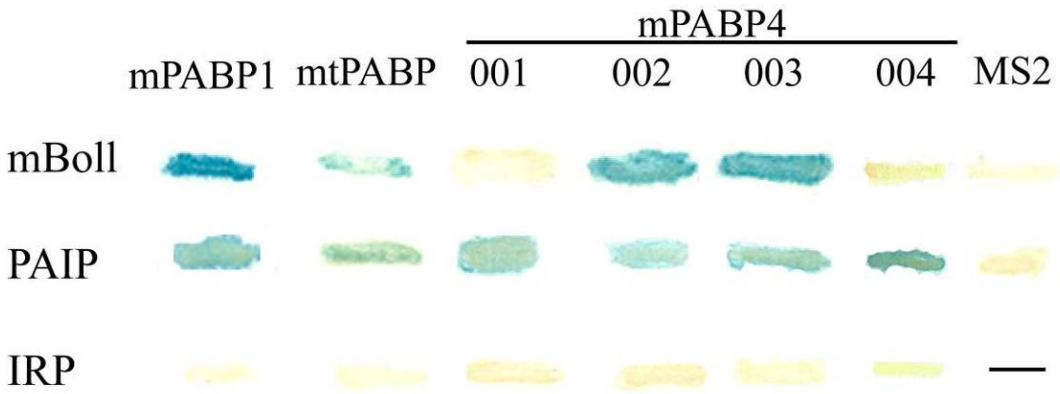


**Figure 4.25 - Mouse Pabp4 isoforms exhibit specificity in their interactions with Boule.** Yeast two-hybrid assay between mBoll (mouse Boule) and the C-terminus of mPabp1, mtPabp and mPabp4 isoforms. mBoll interacted with the C-terminal region of mPabp1, mtPabp, mPabp4.002 and mPabp4.003. PABP-interacting protein - 1 (PAIP) is used as a positive control. IRP and MS2 are used as negative controls. –: not done.

The Y2H assay with mBoll (Figure 4.25) showed that it can interact with two of the mPabp4 isoforms in addition to mPabp1 and mtPabp. Both Pabp4 isoforms that failed to interact with mBoll still interacted with the positive control PAIP-1. This not only suggests that there is divergence in the protein partners of Pabp1 and tPabp compared to Pabp4, but furthermore that the different Pabp4 isoforms also have partially distinct interactomes.

# 4.3 Discussion

Chapter 3 provided evidence that the DAZL-PABP1 interaction, first proposed in *X. laevis* (Collier *et al.*, 2005b), is conserved in mammals. In this chapter, the role of Pabp4 in promoting the ability of Dazl to stimulate translation in mammalian gametogenesis was studied by assessing the extent to which both proteins co-reside within the male and female germ cells of mouse gonads, together with a molecular analysis of their ability to interact. In doing so this provided the first insight into the expression of PABP4 protein and the first indication of both PABP and isoform specific protein partners.

## 4.3.1 Mammalian PABP4 expression

This work revealed that PABP4 is expressed in a wide variety of cell-types within the gonads including both germ and somatic cells. This finding is consistent with a northern blot of adult human tissues showing that human testis and ovaries contain substantial levels of PABP4 mRNA (Yang *et al.*, 1995). This work also provided insight into its expression during development where it was found to be significant in tissues including the developing liver, heart and pancreas which continue to express Pabp4 at high levels in the adult (Hannah Burgess personal communication) but also intriguingly in the kidney and lungs, where it is essentially undetectable in adults (Hannah Burgess personal communication). The presence of Pabp4 in many different cell types likely reflects available evidence suggesting that it shares global functions in regulating mRNAs with PABP1 (Gorgoni *et al.*, 2011).

Confidence in this pattern is provided by commercial antibodies raised against distinct epitopes which became available during this work (Table 2.10), one of which was found to specifically recognise Pabp4 and produced a pattern highly reminiscent of the results in this chapter (Appendix 4). In contrast to its pattern within adult gonads, Pabp4 was almost ubiquitously expressed within fetal gonads although its expression decreased somewhat between 13.5 and 15.5 dpc in both sexes. Comparison with the Pabp1 expression pattern shows that these widely expressed PABPs have distinct expression patterns. Some cell types (e.g. granulosa

cells) appear to express significant quantities of both Pabp1 and Pabp4. Multiple PABPs may be required in some cases due to a high protein synthetic load or in others because of functional differences between family members (Gorgoni *et al.*, 2011) which presumably allow for the complex regulation of subsets of mRNAs. However, their expression appears almost reciprocal during adult spermatogenesis. This is reminiscent of the reciprocal expression of ePABP and PABP1 during oogenesis and early embryonic development (Voeltz *et al.*, 2001, Seli *et al.*, 2005, Wilkie *et al.*, 2005), and is suggestive of a requirement for particular family members during the different stages of gametogenesis to achieve the necessary changes in protein synthesis.

Added complexity regarding the complement of PABPs within the different cell types comes from the observation that testis contains four alternatively spliced PABP4 transcripts. Although their presence does not establish that they are represented within the proteome, western blotting of a panel of mouse tissue lysates with PABP4 antibodies detected at least three distinct bands corresponding to their predicted sizes (mPabp4.001 – 72KDa; .002 – 68KDa; .003 – 69KDa; .004 – 71 KDa) in some but not all tissues (Hannah Burgess, personal communication). This observation also suggests that alternative splicing of Pabp4 may be tissue/cell type specific. However, as the PABP4 antibody recognises a shared peptide, it is not currently possible to distinguish whether these splice variants are differentially expressed between cell types from gonads.

### 4.3.2 DAZL and PABP4 regulation of mammalian gametogenesis

Surprisingly, despite the similarities between Dazl and Pabp4 expression within germ cells, these proteins failed to interact in Y2H or pull-down assays. These assays use recombinant proteins which may have failed to interact due to an absence of mammalian-specific post-translation modifications (PTMs), as human PABP1 contains PTMs which are predicted to alter its C-terminal protein-protein interactions (Brook *et al.*, 2012). However, endogenous proteins from mouse testes failed to co-IP, although this result cannot formal exclude the possibility that such modifications,

and therefore Dazl-Pabp4 interactions, only occur dynamically in a subset of germ cells.

Importantly, the inability of mPabp4 to interact with Dazl provides the first evidence that its functions in mRNA-specific regulation will not completely overlap with PABP1. Such functional differences may underlie the requirement for multiple PABPs in vertebrates (Gorgoni *et al.*, 2011). The finding also provides direct evidence for the hypothesis (Gorgoni *et al.*, 2011) that such functional differences between PABPs are, at least in part, due to differential protein-protein interactions mediated by the C-terminal region. Since the PABC domain is 95% identical between xPABP1, xPABP4, mPabp1, and the mPabp4 isoforms (Figures 4.18) it appears likely that the Dazl binding site lies, at least in part, in the highly variable proline rich region. A short amino acid stretch within this region is conserved in interacting but not in non-interacting PABPs (Figure 4.18), but its absence in Pabp4 isoforms that interact with Boule cast doubts on the role of this sequence or suggest that the binding sites for Dazl and Boule within PABPs are at least partially distinct.

### 4.3.3 PABP4 isoforms show specific interactions

Interestingly, while none of the mPabp4 isoforms interacted with mDazl two interacted with Boule, although further validation of this interaction is required. A role for these isoforms in Boule-mediated translation would show that they are functionally distinct.

Boule is conserved from worms to humans (Cheng *et al.*, 1998, Karashima *et al.*, 2000, Xu *et al.*, 2001, Tung *et al.*, 2006a), and is associated with the regulation of meiotic progression in female and male *C. elegans* (Eberhart *et al.*, 1996, Karashima *et al.*, 2000) and *Drosophila* (Xu *et al.*, 2001, Otori *et al.*, 2006), respectively. In mice, Boule is not required for meiotic progression (VanGompel and Xu, 2010) but knockout males fail to produce mature sperm due to a spermiogenesis defect, as germ cells do not progress past stage 6 round spermatids (VanGompel and Xu, 2010). Consistent with this phenotype, Boule is expressed in late spermatocytes and early round spermatids (VanGompel and Xu, 2010). However, preliminary results suggest that Boule and Pabp4 do not colocalise during mouse spermatogenesis.

Interestingly, the two Pabp4 isoforms that interact with Boule are those missing exon 12 (Figures 4.18 and 4.25). However, it is unlikely that amino acids spanning the splice site directly mediate Boule interaction, since they are different in the two interacting isoforms. This suggests that the amino acids encoded by this exon maybe incompatible with Boule interaction, perhaps by altering the conformation of Pabp4 to make the Boule binding site unavailable or by providing a binding site for a protein that interferes with Boule recruitment. Given that the isoforms show differential interactions in an Y2H assay, any such protein would need to be conserved in yeast.

# Chapter 5
# Functional studies of putative human DAZL mutations

# 5.1 Introduction

Infertility affects between 10-15% of couples worldwide (Matzuk and Lamb, 2002), with impaired gametogenesis being a major contributing factor (Matzuk and Lamb, 2008). Whilst many of the genetic causes of infertility remain to be determined, deletion of the Y-chromosome encoded DAZ gene is associated with azoospermia and oligozoospermia in man (Reijo *et al.*, 1995, Najmabadi *et al.*, 1996). The contribution of other family members to human fertility is less clear, but their roles in gametogenesis are supported by studies in multiple organisms. For instance Dazl-KO mice are infertile due to male azoospermia, and female loss of oocytes at birth (Ruggiu *et al.*, 1997, Saunders *et al.*, 2003), although heterozygous females have larger litter sizes due to increased ovulation rates (McNeilly *et al.*, 2011).

In 2006, Tung *et al*. sequenced the human DAZL (hDAZL) gene in small cohorts of patients with impaired fertility (Tung *et al.*, 2006b). This identified four putative missense mutations in a small number of individuals (Table 5.1) that were not present in controls (frequency of less than 1%).

| Amino acid change | Sex | Genotype | Phenotype |
|---|---|---|---|
| **P6H** | F | Het | Spontaneous early menopause at age 45<br>3 children previously |
| **N10C** | M | Hom | Azoospermia |
| | F | Het | Familial early menopause at age 44<br>4 children previously |
| **I37A** | F | Het | Spontaneous early menopause at age 43<br>1 child previously |
| **R115G** | F | Hom | Spontaneous premature ovarian failure at age 34<br>0 children previously |

**Table 5.1 - Putative hDAZL mutations.** hDAZL mutations identified in patients with impaired fertility. The position and identity of the amino acid substitutions are given. Adapted from Tung *et al.,* 2006.

Heterozygous mutations, P6H, N10C or I37A, were found in three female patients who underwent menopause in their mid-40s whilst a homozygous R115G mutation was identified in a patient with premature ovarian failure (POF) at age 34. POF is posited to be due to increased atresia of oocytes (e.g. during fetal

development) or increased recruitment of oocytes to undergo folliculogenesis prior to ovulation (reviewed in (Shelling, 2010)). A male patient homozygous for N10C suffered from azoospermia. However, as this study examined small non-familial cohorts and no functional studies have been carried out, it is unclear whether these putative mutations are causative. Two of the putative mutations I37A and R115G, are of particular interest as they are located in the RNA recognition motif (RRM) of DAZL, which is highly conserved between DAZ-family members (Yen, 2004) and mediates RNA and protein interactions necessary for DAZL function (Ruggiu and Cooke, 2000, Tsui *et al.*, 2000a, Tsui *et al.*, 2000b, Collier *et al.*, 2005b, Jenkins *et al.*, 2011).

Whilst several target mRNAs of mDazl have been validated in male and female mice (Reynolds *et al.*, 2005, Reynolds *et al.*, 2007, Chen *et al.*, 2011), to date potential translational targets of hDAZL have not been investigated experimentally, although a number of human mRNAs can be bound by hDAZL. These include SDAD1 (Fox *et al.*, 2005), the homolog of the yeast gene which regulates cell cycle (Zimmerman and Kellogg, 2001), and the family of testis-specific serine/threonine kinases (TSSK) (Zeng *et al.*, 2008). However, the ability of hDAZL to activate mRNA translation was established in stage VI *X. laevis* oocytes (Collier *et al.*, 2005b). *X. laevis* oocytes provide an excellent experimentally accessible germ cell model: single ovaries contain hundreds of stage VI oocytes which are large (approximately 1.3 mm), relatively easy to manipulate and micro-inject and provide enough material for biochemical analysis. These oocytes offer two additional advantages for the analysis of translation. Firstly, they are essentially transcriptional silent (Mendez and Richter, 2001), meaning that effects on translation can be studied in the absence of effects on transcription and splicing. This is important as many 3'UTR-binding proteins are multifunctional (reviewed in (Paronetto and Sette, 2009, Nguyen-Chi and Morello, 2011). Secondly, mRNAs can be injected directly into the cytoplasm and remain stable even if deadenylated (Colman and Drummond, 1986, Gillian-Daniel *et al.*, 1998), allowing effects on translation to be studied in isolation from changes in mRNA stability.

In this chapter, the functional consequences of the four putative mutations on the ability of hDAZL to stimulate translation were studied using reporter mRNAs

micro-injected into oocytes. One reporter mRNA contained the 3'UTR of a human mRNA which was found to be susceptible to regulation by hDAZL. A reporter containing tethering sites was also used to determine the effects of these mutations on the ability of hDAZL to mediate protein interactions independently of any effects on RNA binding.

## 5.2 Results

### 5.2.1 Growth differentiation factor 9 is a translational target for human DAZL

No human mRNAs have been shown to be susceptible to translational regulation by hDAZL. However, cross-species rescue experiments (Houston *et al.*, 1998, Slee *et al.*, 1999, Vogel *et al.*, 2002, Xu *et al.*, 2003) suggest that different family members share similar mRNA-binding specificity and a loose DAZL binding consensus "$U_{2\text{-}10}$[C/G]-$U_{2\text{-}10}$" has been identified from a combination of *in vitro* and *in vivo* studies (Venables *et al.*, 2001, Jiao *et al.*, 2002, Maegawa *et al.*, 2002, Reynolds *et al.*, 2005, Chen *et al.*, 2011). Intriguingly, as part of ongoing studies of oocyte expressed mRNAs in the laboratory, it was noted that the 3'UTR of human growth differentiation factor 9 (hGDF9) mRNA (Figure 5.1) contained at least one excellent putative consensus binding site (N. K. Gray, unpublished). This raised the possibility that hGDF9 may be utilised to study the functional consequences of the putative mutations on the ability of hDAZL to stimulate translation of oocyte-specific GDF9 (Richards, 1980, Elvin *et al.*, 1999, Moore *et al.*, 2004b). GDF9 is secreted from oocytes and is important for oocyte-granulosa communication at various stages of folliculogenesis (Knight and Glister, 2001). Communication between these cell types is thought to be crucial both for oocyte survival and the initiation of folliculogenesis and as a result mGdf9-KO female mice are infertile (Dong *et al.*, 1996) with folliculogenesis arresting at the primary follicle stage, slightly later than the described mDazl-KO phenotype (Ruggiu *et al.*, 1997, Saunders *et al.*, 2003). Moreover, homozygous Gdf9 mutations that result in female infertility, but increased offspring number in heterozygous animals due to increased ovulation

rates, have been reported in sheep (Nicol *et al.*, 2009), reminiscent of Dazl-KO mice (Ruggiu *et al.*, 1997, Saunders *et al.*, 2003, McNeilly *et al.*, 2011). In humans, missense mutations in *GDF9* have been associated with POF (Laissue *et al.*, 2006, Tung *et al.*, 2006b, Kovanci *et al.*, 2007) and heterozygous *GDF9* mutations with dizygotic human pregnancies (Palmer *et al.*, 2006).

CAAATGGTCCTCTTAAAACCTTGAGCCTATTTGGCAAAGTAACTACTGTGTGCCTATGTGTGC
CTTCAAGAGAAAGCTTCATATATTAAGTCTCTAAATGTAGCATATGTTATATAAAGAGGAGCC
TGTGTAGGTTAGTACCTTCTATGGCATCTATCAGGATAAAGGGATAACATCAATTGTTGCTAC
AGAGCCTTTTTTTATTTCCAAATTTAAATGAAATATAATTATTGTGGAGAACTTTACATTTTT
CCC
TTCCTTGAGTGATTTTTTTTCTTTTCATAGGAGTCTTATTCTTGATAGGGAAAAAACCTTAAT
TAGCATCAATCCTGGATGGACTTGCAGCTATAAATAGGCAATTCAGATTGCTGTAGTCTTAAT
AGAAGAATAAATTTCTGTCAATGGC

**Figure 5.1 - The 3'UTR sequence of hGDF9 has one very good putative hDAZL binding site.** The consensus "$U_{2\text{-}10}$[C/G]-$U_{2\text{-}10}$" DAZL binding site (Venables *et al.*, 2001, Reynolds *et al.*, 2005, Reynolds *et al.*, 2007, Chen *et al.*, 2011, Jenkins *et al.*, 2011) is highlighted in green, with the sequence to which it was mutated depicted in yellow. Alternative binding sites are presented in red (Venables *et al.*, 2001, Reynolds *et al.*, 2005, Reynolds *et al.*, 2007, Chen *et al.*, 2011) and blue (Venables *et al.*, 2001)).

Thus, to assess whether hGDF9 mRNA can be regulated by hDAZL, its 3'UTR was appended to a luciferase reporter mRNA (Figure 5.2). The luciferase-hGDF9-3'UTR reporter mRNA and a control β-gal mRNA, insensitive to Dazl, were co-injected into oocytes (Figure 5.2) expressing either hDAZL or U1A, and the levels of their translated products were subsequently assayed. U1A is an RRM-containing protein, which does not affect translation (Jovine *et al.*, 1996) and was utilised as a negative control, with stimulation or repression of translation by hDAZL being calculated relative to U1A. This revealed a modest but reproducible and highly statistically significant increase in hGDF9 translation in the presence of hDAZL (Figure 5.3). Thus, hGDF9 translation can be activated, albeit modestly, by hDAZL.

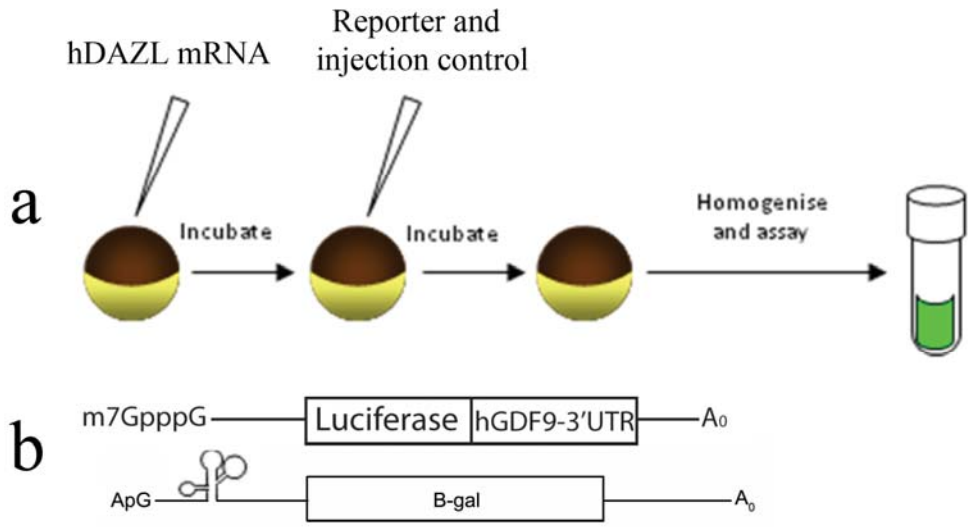


**Figure 5.2 - Luciferase reporter assay to test the ability of hDAZL to regulate the translation of reporter mRNAs.** a - *X. laevis* oocytes were injected with hDAZL or U1A mRNA. Following incubation to allow expression, they were co-injected with a luciferase reporter fused to the 3'UTR of hGDF9 and β-galactosidase (β-gal) control mRNA (mRNAs depicted in b). The oocytes were incubated overnight and the effect of hDAZL on translation was assessed by measuring luciferase production normalised against any minor differences in the β-gal activity. $m^7$GpppG cap and ApG caps are physiological or non-functional caps respectively, and the β-gal mRNA contains a internal ribosome entry site, denoted by a stem-loop structure. $A_0$ indicates that the mRNAs are unadenylated.

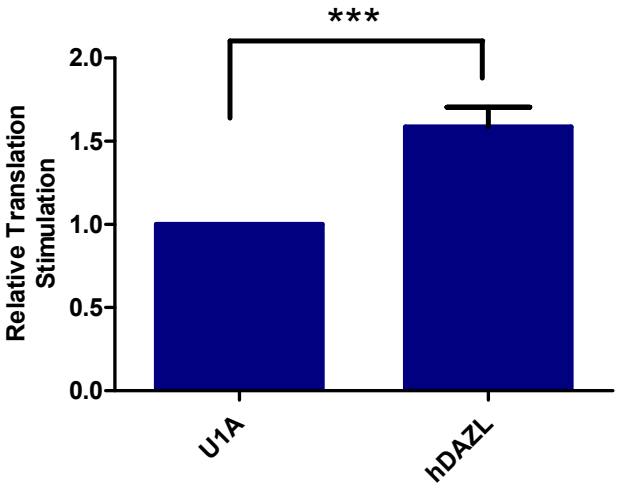


**Figure 5.3 - hDAZL stimulates translation of a mRNA containing the human growth differentiation factor-9 (hGDF9) 3'UTR.** *X. laevis* oocytes were injected with either hDAZL- or U1A-encoding mRNAs, and co-injected with a hGDF9 reporter mRNA and an β-gal control mRNA. The effect of hDAZL on translation of hGDF9 was normalised to the injection control β-gal. Stimulation was expressed relative to U1A which was set to 1. T-test, unpaired, 2 tails, p=0.0002, error bars indicate standard error of the mean. Statistical analyses were performed on transformed raw data values (Y=Ln(Y)) from 8 experiments.

#### 5.2.1.1 GDF9 appears to have more than one functional DAZL-binding site

Verified DAZL target mRNAs have multiple DAZL binding sites (Venables *et al.*, 2001, Jiao *et al.*, 2002, Fox *et al.*, 2005, Reynolds *et al.*, 2005, Reynolds *et al.*, 2007, Chen *et al.*, 2011) but hGDF9 only contains one significant match for the $U_{2\text{-}10}$[G/C]$U_{2\text{-}10}$ consensus ("UUUUUUUUCUUUU") (Venables *et al.*, 2001, Reynolds *et al.*, 2005, Reynolds *et al.*, 2007, Chen *et al.*, 2011), although it does contain other sequences that match the minimal or variant consensus sequences (Figure 5.1). Since the number of binding sites affects the level of translational stimulation (Collier *et al.*, 2005b), a single functional binding site in GDF9 may explain the relatively modest effect observed. Thus to determine whether the best match sequence is the only functional hDAZL binding site, this was mutated to "UUUUUCCCCUUUU" by site-directed mutagenesis (Figure 5.4).

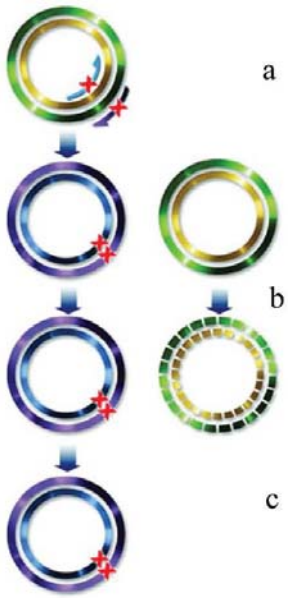


**Figure 5.4 - Site directed mutagenesis.** a and b - Oligonucleotide primers containing the desired mutations (represented by X) are used in a PCR reaction with *Pfu*Turbo DNA polymerase to replace the nucleotide(s) in the newly synthesised plasmid. c – The methylated parental vector (green/yellow) was digested with Dpn1, prior to transformation into *E. coli.* Adapted from https://www.genomics.agilent.com .

The ability of hDAZL to stimulate the translation of reporter mRNAs containing either the mutated or wild-type hGDF9-3'UTR was compared and no significant difference was observed (Figure 5.5), consistent with the presence of other binding sites. This result was unexpected as this sequence represented the best consensus site and only a small number of other matches to potential consensus sequences were present within the 3'UTR (Figure 5.1). This result highlights the need for a better definition of DAZL binding sites as many sequences are able to be bound by DAZL to some extent (Maines and Wasserman, 1999, Venables *et al.*, 2001, Jiao *et al.*, 2002, Maegawa *et al.*, 2002, Fox *et al.*, 2005, Reynolds *et al.*, 2005, Reynolds *et al.*, 2007, Chen *et al.*, 2011). This will be discussed further in section 5.3.1.

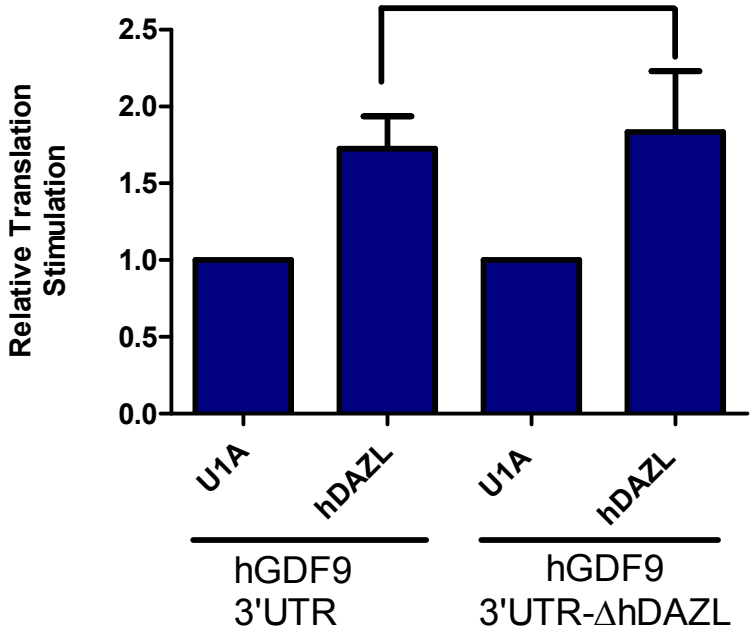


**Figure 5.5 - The hGDF9 mRNA 3'UTR may contain multiple functional DAZL binding sites.** *X. laevis* oocytes expressing hDAZL or U1A were co-injected with β-gal and the hGDF9 reporter mRNA containing the wild type hGDF9 3'UTR or the mutated version (ΔhDAZL). Luciferase values were normalised to the β-gal injection control. Translation stimulation was calculated relative to U1A, which was set to 1. T-test p = 0.8151, unpaired, 2 tails, error bars indicate standard error of the mean. Results represent the average of 6 experiments.

### 5.2.1.2 Endogenous *X. laevis* Dazl is not the cause of the modest extent of hGDF9 stimulation by hDAZL.

In tethering assays hDAZL stimulates translation by 4-fold (Collier *et al.*, 2005b) but the hGDF9 target reporter is only stimulated 1.5 fold (Figure 5.3), despite potentially containing multiple DAZL binding sites (Figure 5.1). However, the hGDF9 reporter mRNA, but not the tether reporter, contains natural binding sites that may bind the endogenous *X. laevis* DAZL (Xdazl). This may result in a degree of activation even in the absence of hDAZL, diminishing its effect. To address this, a competition strategy was devised in which an excess of an RNA fragment containing only the hGDF9-3'UTR was injected to sequester endogenous Xdazl and prevent it from binding the hGDF9 reporter mRNA. Thus, oocytes expressing U1A were injected with the hGDF9 reporter mRNA and control mRNAs in the presence or absence of a 100-fold excess of hGDF9 3'UTR.

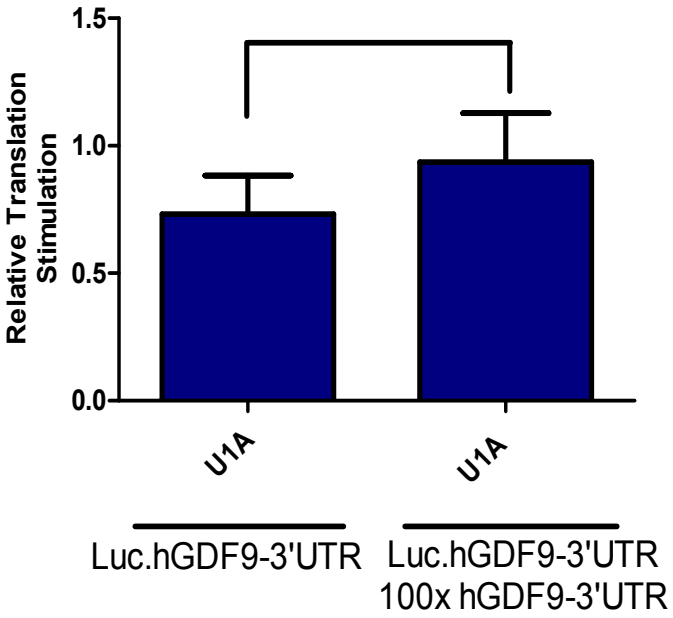


**Figure 5.5 - Xdazl is not the cause of the modest extent of hGDF9 stimulation by hDAZL**. *X. laevis* oocytes expressing U1A were injected with reporter and control mRNAs in the presence or absence of a 100x excess of hGDF9 3'UTR RNA. Luciferase activity was normalised to the injection control β-gal. T-test, unpaired, 2 tails p = 0.4299, error bars indicate standard error of the mean. Results represent the average of 6 experiments.

Despite a slight increase in translation of the hGDF9 reporter mRNA in the presence of excess hGDF9-3'UTR (Figure 5.6) there was no statistical significance between the two pools of oocytes indicating that activation by endogenous Xdazl did not underlie the modest extent of stimulation by hDAZL.

### 5.2.2 Putative hDAZL mutations have a compromised ability to stimulate translation of hGDF9

The previous section shows that the hGDF9 reporter mRNA can be used to assess the effect of the four putative mutations (Tung *et al.*, 2006b) on the ability of hDAZL to activate translation.

To this end, the putative mutations (Table 5.1) were introduced into hDAZL coding sequence by site directed mutagenesis (Figure 5.4), and mRNAs encoding these mutants or wild-type hDAZL were injected into *X. laevis* oocytes. These were then subsequently injected with the described hGDF9 reporter and β-gal control mRNAs (Figure 5.2).

Initially the ability of the P6H and N10C mutants to activate translation was tested. These putative mutations lie in the N-terminal portion of the RRM and showed no significant difference in activity compared to wild-type (Figure 5.7). This indicates that the observed phenotype in these patients (Table 5.1) does not appear to result from a compromised ability of DAZL, containing these amino acid substitutions, to stimulate translation.

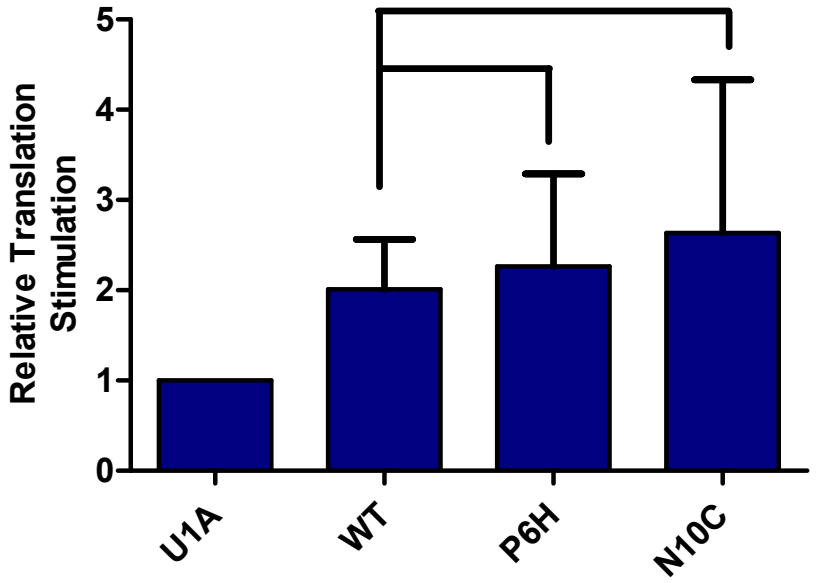


**Figure 5.6 - Putative mutations P6H and N10C do not disrupt the ability of hDAZL to stimulate translation in reporter assays.** *X. laevis* oocytes were injected with either hDAZL (WT, P6H, N10C) or U1A and subsequently with the hGDF9 luciferase reporter mRNA and the control β-gal mRNA. Luciferase levels were normalised for β-gal and translation stimulation compared to U1A (set to 1) and wild type hDAZL. T-test, paired, 2 tails; WT vs P6H p=0.6497; WT vs N10C p=0.6413; error bars indicate standard error of the mean. Results represent the average of 3 experiments.

The I37A and R115G substitutions lie within the functionally important RRM domain (amino acids 32-116) (Figure 5.8). The ability of the I37A mutant to stimulate translation of the hGDF9 reporter mRNA showed a modest but statistically significant decrease compared to wild type hDAZL (Figure 5.9). In contrast R115G mutation ablated the ability of hDAZL to stimulate translation, with luciferase levels being similar to those obtained in oocytes expressing the negative control U1A (Jovine *et al.*, 1996). Western blot analysis of hDAZL and mutants thereof showed that they were similarly expressed in oocytes indicating that the observed differences in activity are not a result of differential protein levels (Figure 5.10). Thus I37A and R115G appear to represent functionally relevant mutations in hDAZL.

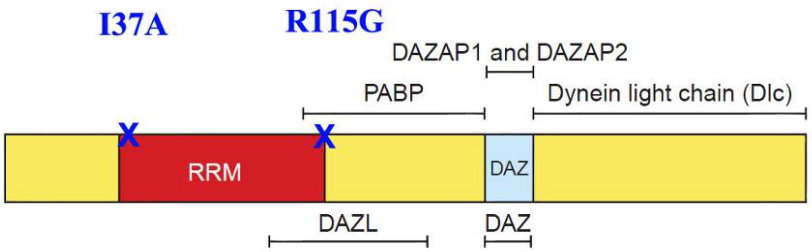


**Figure 5.7 - Mutations I37A and R115G are located in the RRM domain within hDAZL.** Diagram of the DAZL protein, depicting the location of the two putative hDAZL mutations (I37A and R115G), together with identified DAZL interacting proteins (adapted from (Brook *et al.*, 2009)). Pumilio-2 is also a protein partner of DAZL, with previously described roles in translation, but its binding site in DAZL has not been characterised although human pumilio-2 interacts with the region between the RRM and the DAZ motif in DAZ (Moore *et al.*, 2003). DZIP proteins which are also potential protein partner are not depicted.

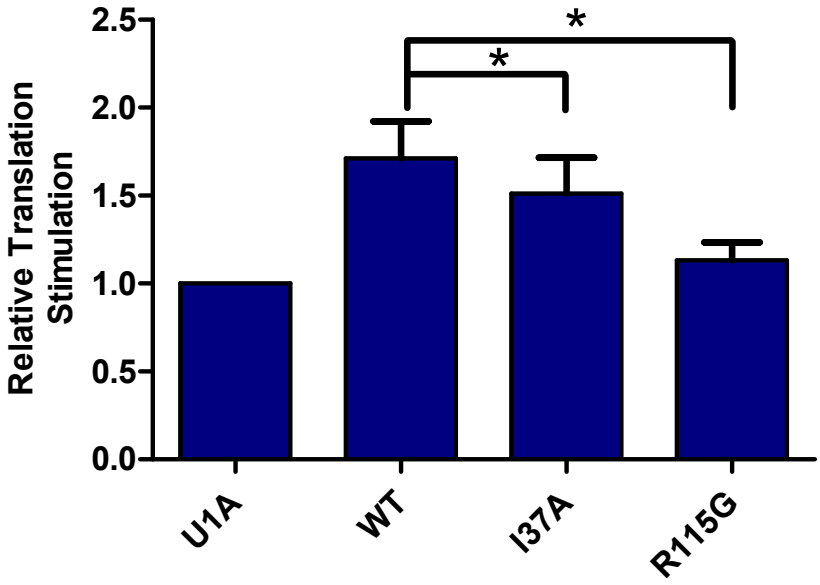


**Figure 5.8 - Putative mutations I37A and R115G disrupt the ability of hDAZL to stimulate translation in a luciferase reporter assay.** *X. laevis* oocytes were injected with either hDAZL (WT, I37A and R115G) or U1A and co-injected with the hGDF9 reporter mRNA and β-gal control mRNA. The effect of putative mutants on translation of hGDF9 was normalised to the injection control β-gal. U1A was set to 1 and the activity of the mutants compared to wild type hDAZL. T-test, paired, 2 tails; WT vs I37A p=0.0341; WT vs R115G p=0.0444 error bars indicate standard error of the mean. Results represent the average of 3 experiments.


**Figure 5.9 - Injected wild-type and mutant forms of hDAZL are expressed at similar levels in *X. laevis* oocytes.** Stage VI *X. laevis* oocytes were injected with hDAZL (wild type and mutants thereof) incubated for 6 hours and whole extracts were western blotted with an anti-DAZL antibody. WT- wild type hDAZL; 6 – P6H hDAZL; 10 – N10C hDAZL; 37 – I37A hDAZL; 115 – R115G hDAZL; n.inj – non-injected.

### 5.2.3 The ability of hDAZL to mediate protein-protein interactions required to stimulate translation appears compromised in I37A and R115G.

I37A and R115G mutants (Table 5.1) (Tung *et al.*, 2006b) both show a compromised ability to stimulate translation of the hGDF9 luciferase reporter compared to wild type hDAZL (Figure 5.3). These amino acids lie within the RRM (Tung *et al.*, 2006b) (Figure 5.8), which mediates RNA-binding (Tsui *et al.*, 2000b, Jenkins *et al.*, 2011), but outside of the core RNP motifs. However, RRM motifs including that of DAZL can also mediate protein-protein interactions (Ruggiu and Cooke, 2000, Tsui *et al.*, 2000a, Collier *et al.*, 2005b). Thus in order to understand whether the ability of hDAZL to mediate protein interactions required for its translation-stimulating ability are compromised by these mutations, a tethered function approach was used (Gray *et al.*, 2000, Collier *et al.*, 2005b).

In this assay, the function of the tethered protein is uncoupled from its ability to bind the mRNA target (Figure 5.11), as it is brought or "tethered" to the mRNA via the interaction between the RNA-binding protein MS2 and its binding sites within the 3'UTR of a luciferase mRNA (Gray *et al.*, 2000). Therefore this assay solely examines the ability of proteins (i.e. hDAZL and mutants thereof) to mediate

protein-protein interactions required to activate translation. Oocytes were injected with MS2-hDAZL and mutants thereof or MS2-U1A (Jovine *et al.*, 1996, Gray *et al.*, 2000) and subsequently with the MS2 reporter mRNA and a β-gal mRNA which lacks the MS2 binding sites as a co-injection control. Translational stimulation was normalised to MS2-U1A.

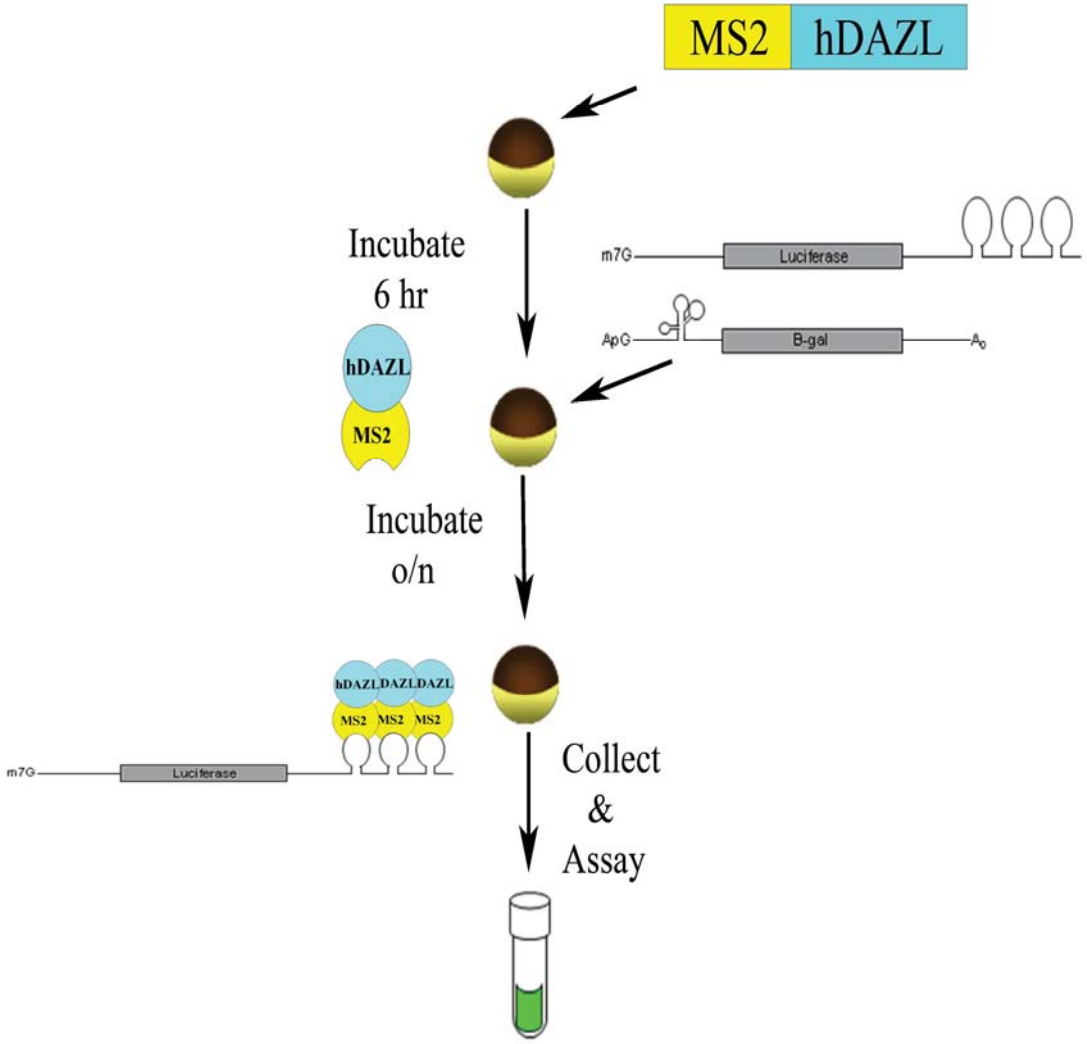


**Figure 5.10 - The tethered function assay.** *X. laevis* oocytes are injected with mRNAs encoding the bacteriophage MS2 coat protein fused to hDAZL (MS2-hDAZL) or U1A (MS2-U1A). Following incubation, oocytes are simultaneously injected with a luciferase reporter containing MS2-binding sites within its 3'-UTR, and a β-gal control mRNA. The MS2-hDAZL fusion protein binds the MS2-binding sites within the luciferase reporter mRNA 3'-UTR via MS2, independent of the ability of hDAZL to bind mRNA. The effect of hDAZL on translation of the reporter is assessed by measuring luciferase activity normalised against the injection control β-gal. Translation stimulation is normalised to MS2-U1A, set to 1 and compared to wild type MS2-hDAZL. Adapted from (Gray *et al.*, 2000).

Tethered hDAZL stimulated the translation of the MS2 reporter mRNA approximately 5-fold compared to U1A (Figure 5.12), consistent with published analyses (Collier *et al.*, 2005b). Critically, the ability of the I37A mutant to stimulate translation in this assay was compromised and that of the R115G mutant was almost completely abrogated. This pattern is highly reminiscent of that obtained with the hGDF9 reporter mRNA (Figure 5.9). Since both mutants were efficiently expressed (Figure 5.13), these results reveal that the compromised ability of these mutants to stimulate translation is, at least in part, due to impaired interactions with protein factors necessary for this function of hDAZL.

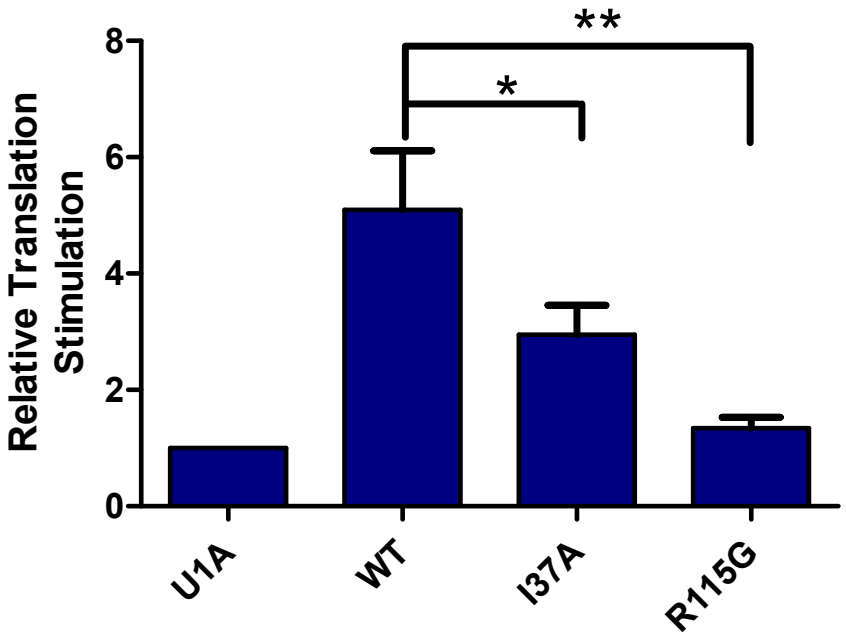


**Figure 5.11 - I37A and R115G mutations disrupt the ability of hDAZL to interact with proteins required for its function in stimulating translation.** *X. laevis* oocytes were injected with MS2 fusion proteins with either hDAZL (WT, I37A and R115G) or U1A and subsequently with luciferase reporter mRNA with three MS2 binding sites in its 3'UTR and a β-gal control mRNA. The effect of putative mutants on translation was normalised to the injection control β-gal. Translation stimulation was normalised to U1A =1 and compared to wild type MS2-hDAZL. T-test, paired, 2 tails; WT vs 37A p=0.0248; WT vs R115G p=0.0023. Error bars indicate standard error of the mean. Results represent the average of 10 experiments.

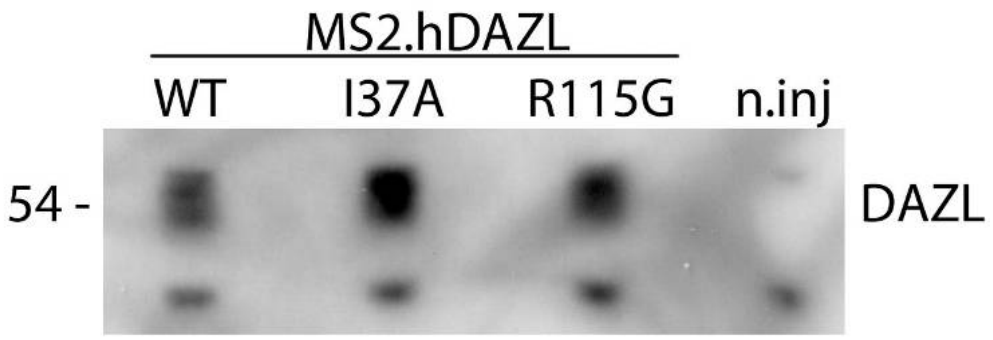


**Figure 5.12 - Expression of MS2-hDAZL wild-type and mutants in *X. laevis* oocytes.** Stage VI *X. laevis* oocytes were injected with MS2-hDAZL (wild type and mutant versions) and incubated for 6 hours. Subsequently, extracts were western blotted with an anti-DAZL antibody. WT - wild type hDAZL; 37 – I37A hDAZL; 115 – R115G hDAZL; n.inj – non-injected.

## 5.3 Discussion

In this chapter the association between the putative hDAZL mutations described in patients with impaired fertility (Table 5.1) (Tung *et al.*, 2006b) and the ability of hDAZL to stimulate translation (Collier *et al.*, 2005b) was examined. Importantly, two of the mutations were found to impair the function of hDAZL, suggesting that they may be causative. Further characterisation of these mutations indicated that loss of function is due, at least in part, to impaired protein-protein interactions.

### 5.3.1 hGDF9 is a translational target for hDAZL

In order to assess the role of the four putative mutations in the ability of hDAZL to stimulate translation, a mRNA (hGDF9) that could be regulated by hDAZL was identified. Since injected, as well as endogenous, mRNAs are highly stable in *X. laevis* oocytes (Ford *et al.*, 1977, Colman and Drummond, 1986), the observed effects likely reflect changes in translation rather than mRNA stability, consistent with the described functions of DAZL in this model system. However, a formal demonstration of reporter mRNA stability (e.g. Q-PCR or injection of radiolabelled mRNAs) is still desirable.

Translation of the hGDF9 reporter mRNA was only modestly enhanced by hDAZL. Nevertheless, this effect was statistically significant and some overlap exists

between the GDF9 and DAZL phenotypes, both show increased ovulation rates or infertility in heterozygous (Palmer *et al.*, 2006, Nicol *et al.*, 2009, McNeilly *et al.*, 2011) and homozygous animals respectively (Dong *et al.*, 1996, Ruggiu *et al.*, 1997, McNeilly *et al.*, 2000, Saunders *et al.*, 2003). Although this latter phenotype arises later in the Gdf9-KO animals, it is likely that DAZL activates cascades of mRNAs during oogenesis (see sections 3.2.5 and 3.2.7) suggesting that conditional knockout mice may display later phenotypes. Moreover, both proteins have been reported to be associated with POF in humans (Tung *et al.*, 2006b, Kovanci *et al.*, 2007).

Nonetheless, further work would be required before concluding whether GDF9 mRNA is a biologically significant target of DAZL in mammals. Such studies (e.g RNA-IPs from oocytes; IHC analysis of mGdf9 protein levels in wild type and mDazl-KO oocytes) would be facilitated by a conditional Dazl-KO mouse. However, recent technical progress in the in vitro development of human follicles (Telfer *et al.*, 2008, Telfer and McLaughlin, 2011, White *et al.*, 2012), opens the exciting possibility of addressing such questions in human oocytes in the future.

Although hDAZL stimulates translation to a lesser degree than mouse and *X. laevis* Dazl (4-fold compared to 10- and 8-fold) in tethering assays (Collier *et al.*, 2005b), stimulation of hGDF9 by hDAZL was significantly reduced (Figure 5.3) compared to tethered hDAZL (Figure 5.12) (Collier *et al.*, 2005b). Sequestration of endogenous Xdazl, using excess hGDF9 3'UTR excluded partial stimulation of this reporter by Xdazl as underlying the reduced stimulation. In contrast to the tether reporter mRNA that has three MS2 binding sites (Collier *et al.*, 2005b), the hGDF9 3'UTR only has one very good match to the consensus $U_{(2\text{-}10)}[G/C]U_{(2\text{-}10)}$. However mutation of this binding site did not significantly diminish stimulation, suggesting that either other functional binding sites are present or that these mutations did not significantly reduce hDAZL binding to this site.

This result draws attention to the debate regarding the nature of DAZL binding sites. In addition to the consensus $U_{2\text{-}10}[G/C]U_{2\text{-}10}$ present in validated mDazl targets in mouse (Reynolds *et al.*, 2005, Reynolds *et al.*, 2007, Chen *et al.*, 2011) other binding sites have been reported. DAZL has been reported to bind U-rich elements (Tsui *et al.*, 2000b, Fox *et al.*, 2005); $(GU_n)_n$ elements (Venables *et al.*, 2001), the sequence "GUUC" (Maegawa *et al.*, 2002); and most recently the crystal

structure of mDazl bound to Mvh and Sycp3 RNA showed high affinity for GUU[U\C] repeats (Jenkins *et al.*, 2011). Whilst these reports share common observations, they to do not allow for the accurate prediction of binding sites and may help to explain why mutation of the "best" site in the luciferase hGDF9'UTR reporter (Figure 5.1) did not reduce stimulation (Figure 5.5). Thus further RNA-binding studies (e.g. EMSAs and/or RNA-IP) to determine the efficacy of the mutations would be informative. Similarly, such studies may shed light on whether low affinity binding of hDAZL to this mRNA accounts for its limited translational stimulation.

### 5.3.2 I37A and R115G mutations reduce the ability of hDAZL to stimulate translation due to impaired protein-protein interactions

The hGDF9 reporter mRNA allowed for the functional characterisation of putative mutations. Two of these mutations, P6H and N10C, appeared not to impair the ability of hDAZL to stimulate translation, suggesting that these amino acids are not critical for this function. In keeping with this observation, proline 6 (P6) is maintained in human DAZ (Figure 5.14 - green) but not in DAZL proteins from other species indicating that it has a less important, or divergent, role. Asparagine at position 10 (N10) is maintained in DAZL proteins from different species and hDAZ but is absent in BOULE, despite its ability to stimulate translation (Figure 5.14 - red). Moreover, deletion of the amino acids 1-32 does not affect the ability of tethered mDazl to stimulate translation (Collier *et al.*, 2005b) suggesting that this region is not required for protein interactions that mediate this function. These results suggest that these putative mutations are either not causative of the observed phenotypes or that they affect another function of hDAZL.

In contrast R115G, and to a lesser extent I37A, mutation results in a compromised ability to stimulate translation, suggesting that they may play a causative role in the early menopause/POF that occurred in the patients in which they were identified. It is thought that increased oocyte atresia and/or activation of follicles both play an important role in diminishing the oocyte pool but the genetics

of POF are poorly understood. Moreover it was found that these mutations compromised the ability of hDAZL to mediate protein-protein interactions that are important for its ability to stimulate translation. Both these mutations occur in the RRM (Yen, 2004) and both are preserved in all DAZ family members in all studied species (Figure 5.14), indicating that they are important for DAZL function. Although these results implicate altered protein-protein interactions for the hDAZL mutants, they do not rule out additional effects on RNA-binding. Indeed recent structural studies of the isolated RRM bound to RNA shows a hydrogen bond between R115 and RNA, despite this residue being located outside the core RNP motifs. The R115G mutation decreased *in vitro* RNA-binding affinity 50-fold (Jenkins *et al.*, 2011), suggesting that this residue may be important for both RNA and protein binding. Structural studies have also indirectly implicate I37 in RNA-binding (Jenkins *et al.*, 2011) suggesting that the effects of I37A mutation could be due to altered protein-protein interactions and RNA binding. Whether this reflects an indirect role in maintaining hDAZL conformation in a manner favourable for partner interactions or whether it forms a protein-interaction site remain to be determined.

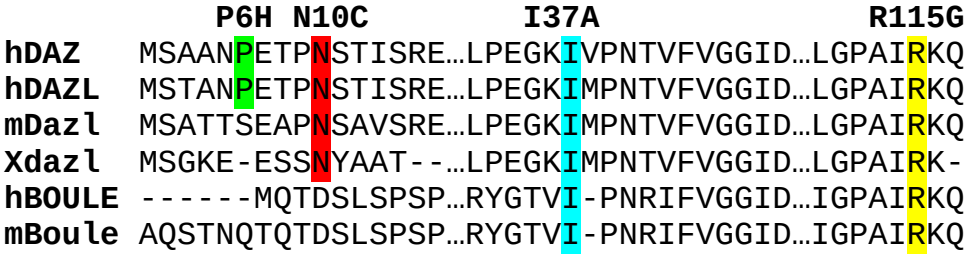


**Figure 5.13 - Conservation of putative hDAZL mutations amino acids in the DAZ family.** Amino acid 6 (proline) is only conserved in hDAZL and hDAZ whereas an asparagine at position 10 is present in both hDAZ and DAZL from different species. Both isoleucine at position 37 and arginine at position 115 are maintained in the three DAZ family members in all the species studied. h – human; m – mouse; x – *X. laevis.* Green – Pro 6; Red – Asn 10; Blue – Ile 37 Yellow – Arg 115.

# Chapter 6
# Final discussion

# 6.1 Introduction

This work examined the function of DAZL in mRNA-specific translational activation during mammalian gametogenesis. In particular it addressed whether this function in mammals may be mediated via recruitment of one or more members of the PABP family, and whether putative mutations identified in patients with reduced fertility alter its ability to stimulate translation. These results highlight the importance of translation regulation in gametogenesis and provide new lines of research for future work, into both the mechanisms of DAZL function and the potential clinical consequences of disrupting DAZL function.

## 6.1.1 PABP expression within mammalian gonads.

By providing the first detailed insight into the expression of PABP1 and PABP4 in mammals, this work has revealed that both proteins are widely but not ubiquitously expressed. Within the gonads they are both present in a subset of germ and somatic cells. This is in contrast to the other two family members that share the same domain organisation, tPABP and ePABP. In mice, tPabp is only expressed in round spermatids (Kimura *et al.*, 2009), and ePabp mRNA is mainly found in oocytes and pre-implantation embryos (Seli *et al.*, 2005). Taken together with this data, the work presented here provides a picture of the PABP complement within the germ cells of adult mice.

In primordial through pre-antral follicles, oocytes appear to simultaneous express three PABP-family members Pabp1, Pabp4 and ePabp. Although ePABP is the predominant PABP protein in *X. laevis* oocytes (Wilkie *et al.*, 2005), its relative abundance compared to Pabp1 and Pabp4 in mammalian oocytes remains to be determined as data is only available for ePabp mRNA (Seli *et al.*, 2005, Wilkie *et al.*, 2005). Nevertheless, a recent ePabp knock-out mouse has established the importance of this protein in regulating oocyte mRNAs (Guzeloglu-Kayisli *et al.*, 2012) that are required for oocyte maturation and cumulus expansion (Guzeloglu-Kayisli *et al.*, 2012). However, it is unclear whether phenotype onset corresponds to the time when ePabp mRNA is initially translated or whether ePabp is normally present prior to this

stage and has functions that can be compensated, to some degree, by the Pabp1 and Pabp4. A degree of functional redundancy would be consistent with analysis in *X. laevis* (Gorgoni *et al.*, 2011) and the ePabp phenotype arising at the point when Pabp1 and Pabp4 levels were found to diminish.

Although, Pabp1 and Pabp4 are co-expressed in oocytes, in male germ cells they show clear temporal differences in their expression pattern, being almost reciprocal. Both of their patterns of expression are distinct from that of tPabp, although tPabp and Pabp1 both appear relatively abundant in round spermatids (Kimura *et al.*, 2009), suggesting that higher overall levels of PABPs may be required at specific stages. Conversely, it also appears important to reduce PABP levels during spermiogenesis and spermiation, as Paip2-KO mice have aberrant expression of PABPs late in spermatogenesis and fail to activate the deadenylation-dependent translation of critical mRNAs, leading to morphological defects (Yanagiya *et al.*, 2010). The observed temporal regulation of individual PABPs may not only serve to modulate overall PABP levels but may also be a consequence of PABP-specific functions that are required within different germ cell stages. In support of such functional differences, the sub-cellular distribution of tPabp and Pabp1 within round spermatids is distinct: tPabp, but not Pabp1, is localised in chromatoid bodies and is not polysome associated, despite its ability to activate reporter mRNA translation and to interact with Pabp1 partners (Kimura *et al.*, 2009).

The expression pattern of Pabp1 and Pabp4 established here suggest that these PABPs likely play, at least partially, distinct physiological roles during gametogenesis, which are also likely to differ from that of tPabp and ePabp. Furthermore the protein interaction studies herein revealed functional differences that could also contribute to differences in their physiological roles: Pabp4 function, but not Pabp1 function, is entirely Dazl-independent. Given the multi-functional nature of Pabp1, many of its roles even within Dazl-expressing cells are also likely to be DAZL-independent. However, the generation of knock-out mice will be required to evaluate their individual physiological roles, with the limited expression analysis that was performed in mouse embryos suggesting that conditional approaches may be required. Breeding of compound knock-out mice would enable further assessment of the functional redundancy within this family.

### 6.1.2 Interplay between the DAZ-PABP families

Potential interactions between the mouse DAZ and PABP family members were examined. Pabp1 was found to be co-expressed with Dazl in multiple germ cells stages associated with Dazl-KO phenotypes and to maintain the interaction first described in *X. laevis*, consistent with the model in which PABPs are involved in DAZL-mediated translational activation of specific mRNAs in germ cells. Surprisingly, in males a role in Dazl-mediated translation activation appeared to be Pabp1-specific. tPabp expression does not overlap with Dazl and although Pabp4 expression is co-incident with Dazl in early male germ cells (spermatogonia and early spermatocytes), none of the mouse Pabp4 isoforms interacted with Dazl. Thus, Dazl represents the first PABP-specific protein partner, the potential existence of which was suggested by findings that the C-terminal regions of *X. laevis* PABPs are not functionally equivalent (Gorgoni *et al.*, 2011).

In females, Pabp1 and Dazl are co-expressed during fetal development in oogonia at 13.5 and 15.5 dpc and after birth in the oocytes of primordial through pre-antral follicles, suggesting that they may functionally interact within these cells. However, *in situ* hybridisation showed that ePabp transcripts are also present in oocytes from primary through pre-antral follicles (Seli *et al.*, 2005). Although the ePabp phenotype occurs much later than that of Dazl (Ruggiu *et al.*, 1997, Saunders *et al.*, 2003, Guzeloglu-Kayisli *et al.*, 2012), this does not preclude a functional interaction between these proteins, as Pabp1 may be able to compensate for loss of ePabp function in Dazl-mediated translation, as suggested by the expression analysis and protein-protein interaction data. However, the finding that DAZL and PABP4 can interact in *X. laevis* but not in mouse, caution any extrapolation from *X. laevis* that murine Dazl and ePabp interact. Indeed, the divergence between mouse and *X. laevis* ePABP is greater than that of PABP4, and the C-terminal region of mouse ePabp is subject to alternative splicing (Seli *et al.*, 2008) which may also influence any potential Dazl interaction.

Dazl has also recently been shown to function during mouse oocyte maturation and initial embryonic cleavages (Chen *et al.*, 2011). Meiosis II oocytes

and early embryos contain both Pabp1 and ePabp mRNA (Seli *et al.*, 2005), but their respective protein levels at these stages remain unknown.

Interactions with PABP family members may not be restricted to DAZL. In male mice, Pabp1 expression persists beyond the stages that express Dazl and overlaps with that of Boule which is present in late spermatocytes and peaks in round spermatids (VanGompel and Xu, 2010). Round spermatids also express tPabp (Kimura *et al.*, 2009). Since Pabp1 and tPabp interact with Boule, at least by Y2H, this suggests that Boule, unlike Dazl, may utilise multiple members of the PABP family to promote the translation of mRNAs during spermatogenesis. Boule is not expressed in female mice (Xu *et al.*, 2001). Moreover, the differential interaction of Pabp4 isoforms with Boule provides a potential explanation for Pabp4 alternative splicing within testes, suggesting that this modifies its protein interactome.

Whilst these results are consistent with a model in which PABPs are important for the function of DAZL and BOULE, establishing the physiological consequences of these interactions may ultimately require the generation of animal models. Identification of the minimal Pabp1 binding site within Dazl (or Boule) may allow for the identification of mutations that only disrupt PABP binding. Creating a mouse model where only the Dazl-Pabp1 interaction is disrupted would allow the physiological consequences of disrupting interaction to be assessed.

Such a model may also provide insight into the extent by which Dazl phenotypes are due to a loss of mRNA-specific translation. Whilst further work is required to delineate other functions of DAZL, suggested by multiple protein partners (Figure 5.8), evidence that it can localise mRNAs (Lee *et al.*, 2006) and is required for the formation of stress granules (Kim *et al.*, 2012) is available. Other functions are consistent with the expression of Dazl in male mice germ cell types that do not contain Pabp1, e.g. Dazl-dependent stress granules form in preleptotene and early pachytene spermatocytes (Kim *et al.*, 2012) which do not express Pabp1.

### 6.1.3 Translational targets of DAZL

Previous studies have identified but not experimentally investigated putative human targets for hDAZL. Here it was shown that a reporter mRNA with the 3’ UTR

of hGDF9 can be regulated by hDAZL although the level of stimulation was modest. Preliminary observations show that the putative binding site in hGDF9 mRNA is present in another mono-ovulatory species, sheep, but appears absent in mouse, arguing that it may not be physiologically important. However, mutation of this site in hGDF9 did not abrogate Dazl-mediated stimulation, suggesting other sequences, which may be present in mGdf9, are also important for its Dazl-mediated regulation. Thus, the extent to which GDF9 represents a physiologically important target mRNA remains unclear in the absence of further experimentation.

It also remains important to identify and validate the full spectrum of DAZL target mRNAs. For instance, Sycp3 has only been validated as a misregulated mRNA in the first wave of mouse spermatogenesis (Reynolds *et al.*, 2007). However, Sycp3 is also translationally activated with the onset of meiosis in females mice during fetal development, where Dazl and Pabp1 are both expressed, and prior to birth Dazl-deficient oocytes display defects in synapsis of homologous chromosomes, a function associated with synaptonemal complex formation of which Sycp3 is a component (Lammers *et al.*, 1994, Yuan *et al.*, 2000). Thus Dazl may also regulate Sycp3 translation in female mice.

Similarly, it would be valuable to identify target mRNAs whose misregulation may underlie other DAZL-associated phenotypes such as the failure to acquire sex specific imprinting (Haston *et al.*, 2009). In this regard it is interesting that Dnmt3L (DNA (cytosine-5)-methyltransferase 3-like) which regulates sex specific methylation during germ cell development ((Kato *et al.*, 2007) reviewed in (Smallwood and Kelsey, 2012)) was immunoprecipitated from mouse testes extract as a potential mDazl target mRNA (Zeng *et al.*, 2008), since both Dnmt3L$^{-/-}$ and Dazl-KO male mice show similar phenotypes (Ruggiu *et al.*, 1997, Saunders *et al.*, 2003, Webster *et al.*, 2005). Visual inspection of the 3'UTR of mouse Dnmt3L reveals the presence of putative DAZL binding sites, suggesting that further study of this putative target mRNA is warranted.

Boule-KO mice have post-meiotic defects in spermiogenesis and do not progress beyond stage VI spermatids (VanGompel and Xu, 2010). Intriguingly, levels of Crem protein, but not mRNA, a master transcription factor of spermiogenesis, are significantly reduced in these mice (VanGompel and Xu, 2010).

A similar reduction, but not complete loss of protein, was observed with Mvh and Sycp3 in Dazl-KO mice (Reynolds *et al.*, 2005, Reynolds *et al.*, 2007). Since Crem expression is required during the spermatid phase, when Boule is co-expressed with Pabp1 and tPabp (Kimura *et al.*, 2009), all of which can interact with Boule, this raises the possibility that Boule may be recruiting one, or more, of these PABPs to activate the translation of mRNAs, such as Crem. Such a role would be consistent with the ability of hBoule to stimulate translation in tethering assays (Collier *et al.*, 2005b) and Daz-1 to activate translation in *C. elegans* (Otori *et al.*, 2006).

### 6.1.4 Functional consequences of mutations in human DAZL

Two mutations, both within the RRM of hDAZL (Tung *et al.*, 2006b), were found to impair the ability of DAZL to stimulate translation. Whilst these may also affect RNA-binding (Jenkins *et al.*, 2011), their inability to activate translation in tethering assays directly implicates impaired protein interactions. More than ten proteins have been shown to interact with DAZ family members, although their binding sites within DAZL have only been partially characterised in six cases (Figure 5.8). Of these, the sites for PABP and DAZL itself overlap the RRM, including residue R115. Given the role of PABP in DAZL-mediated stimulation, disruption of this interaction would be an attractive hypothesis to explain the loss of function. However, the efficacy of translational stimulation is partly dependent on the number of DAZL molecules bound (Collier *et al.*, 2005b) and could be impacted by a reduction in the amount of DAZL loaded onto mRNAs due to a loss of DAZL-DAZL interactions.

Moreover it remains plausible that these mutations may disrupt protein binding at sites outside the RRM by altering the conformation of DAZL or by disrupting post-translational modifications (PTMs), such as arginine methylations, which can act as licensing events for PTMs at distant sites: structural information for full length DAZL is not available to rule out conformational effects and Xdazl is apparently subject to PTMs (Mita and Yamashita, 2000). Thus, effects of these

mutations on other known, or as yet to be identified, DAZL partners cannot be excluded with DAZAP-1 being of particular interest given its recently described role in translational activation (Smith *et al.*, 2011).

### 6.1.5 DAZ family mediated translational activation in human germ cells.

When germ cells colonize the gonodal ridges in developing mice they express Oct3/4, Dazl and Mvh (Fujiwara *et al.*, 1994, Pesce *et al.*, 1998, Seligman and Page, 1998, Toyooka *et al.*, 2000, Kehler *et al.*, 2004). At the equivalent developmental point, human germ cells contain OCT3/4 and nuclear DAZL, with VASA only becoming detectable in females once the oogonia stop expressing OCT3/4, enter meiosis, and DAZL translocates to the cytoplasm (Anderson *et al.*, 2007). However, VASA mRNA is detectable prior to the onset of meiosis (Anderson *et al.*, 2007) suggesting it may be subjected to translational control as observed in the first wave of spermatogenesis in mice (Reynolds *et al.*, 2005).

Such differences in the timing of markers (e.g. VASA) alludes to differences between the development of mouse and human germ cells that may affect our ability to extrapolate from genetic studies of DAZL and BOULE function in mice to human gametogenesis. Human males also encode an additional family member, DAZ. As a result, it would be desirable to examine the co-expression of DAZ- and PABP-family members in developing human and adult gonads, which could provide *in vivo* support for the observed interactions between human DAZL and PABP1 and tPABP. However such studies are severely restricted by the availability of tissue.

To date no direct evidence to support a role of DAZL or BOULE in human gametogenesis is available. However, the finding that mutations from patients with early menopause/POF, disrupt DAZL function is intriguing and opens the possibility that these mutations are causative. Given the advances in high-throughput sequencing, it would be of interest to investigate whether other patients with POF, or indeed those with other relevant defects in gametogenesis (e.g. azoospermia), also contain functional mutations in DAZL. In the case of POF, genome-wide association studies may also be informative.

Finally, the recent finding that mDazl is critical for oocyte maturation (Chen *et al.*, 2011), combined with advances in growing human follicles in culture which may increase the availability of GV oocytes for experimentation (Telfer *et al.*, 2008, White *et al.*, 2012), raises the possibility that morpholino knock-down of DAZL in human oocytes prior to *in vitro* maturation could confirm its importance, at least at this stage, in human germ cells.

# Chapter 7
# Appendices

# Appendix 1

# DAZL antibody validation

# A1.1 DAZL antibody Validation

## A1.1.1 Serotec Antibody

Published work, described in Chapter 1, examining the expression of DAZL utilised a discontinued mouse monoclonal antibody from Abcam. However, a mouse monoclonal antibody bearing the same clone number became available from Serotec (#MCA2336-3/11A). This antibody was raised against a C-terminal peptide within human DAZL (hDAZL), highly conserved in the mouse Dazl (mDazl) but not mouse Boule (mBoll) (Figure A1.1). The specificity of the new anti-DAZL antibody was assessed in mouse adult testes, using two different fixatives, Bouin's and 4% NBF. Bouin's better preserves tissue morphology within the testes, but previous analysis of Dazl expression pattern was performed on NBF fixed tissue (Niederberger *et al.*, 1997, Ruggiu *et al.*, 1997). Two dilutions were utilised and for comparison, the discontinued Abcam anti-DAZL antibody (gift from Alan McNeilly) was tested in parallel.

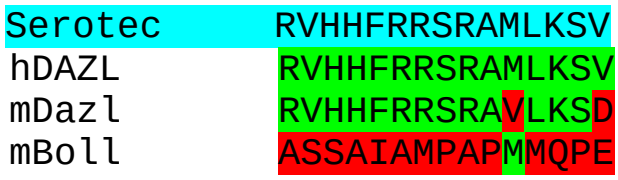


**Figure A1.1 - Serotec anti-DAZL antibody.** Sequence homology between the synthetic peptide corresponding to the sequence within the C terminal domain of human DAZL (hDAZL) used to raise the Serotec anti-DAZL antibody. mDazl – mouse Dazl and mBoll – mouse Boule. Blue - sequence used to raise antibody; Green - amino-acids matching the synthetic peptide; Red - amino-acid not matching the synthetic peptide.

In adult mouse testes, the new Serotec anti-DAZL antibody showed strongest Dazl expression in germ cells, with a peak of expression in early stages, namely spermatogonia and spermatocytes (Figure A1.2). However, at the lower dilution (1/100), it also detected Dazl in the round spermatids in both fixatives, inconsistent with the published literature. In contrast, the higher dilution (1/500) in NBF fixed tissue only showed Dazl expression in the spermatogonia and pachytene spermatocytes, as expected, whilst in Bouin's the spermatogonia and early

spermatocytes were not consistently immunostained. In the absence of primary antibody, the non-specific signal in Leydig cells, was also stronger in Bouin's compared to NBF fixed tissue.

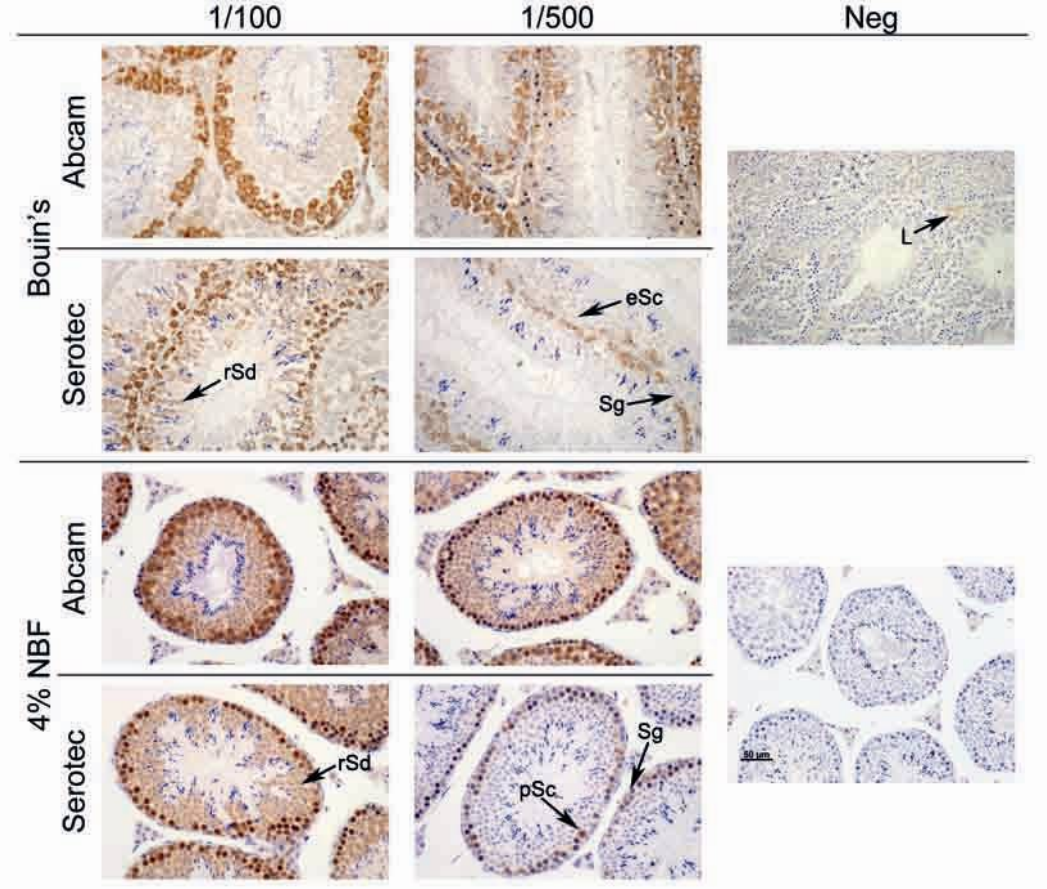


**Figure A1.2 - Serotec DAZL antibody validation in mouse adult testes.** A new Serotec anti-DAZL antibody was applied to adult mouse testes fixed in 4% NBF or Bouin's, at two different dilutions; 1/100 and 1/500. An Abcam antibody was used as a positive control. Neg; no primary antibody control. rSd – round spermatid; eSc – early spermatocytes; Sg – spermatogonium; L – Leydig cell; pSc – pachytene spermatocytes. x20 magnification.

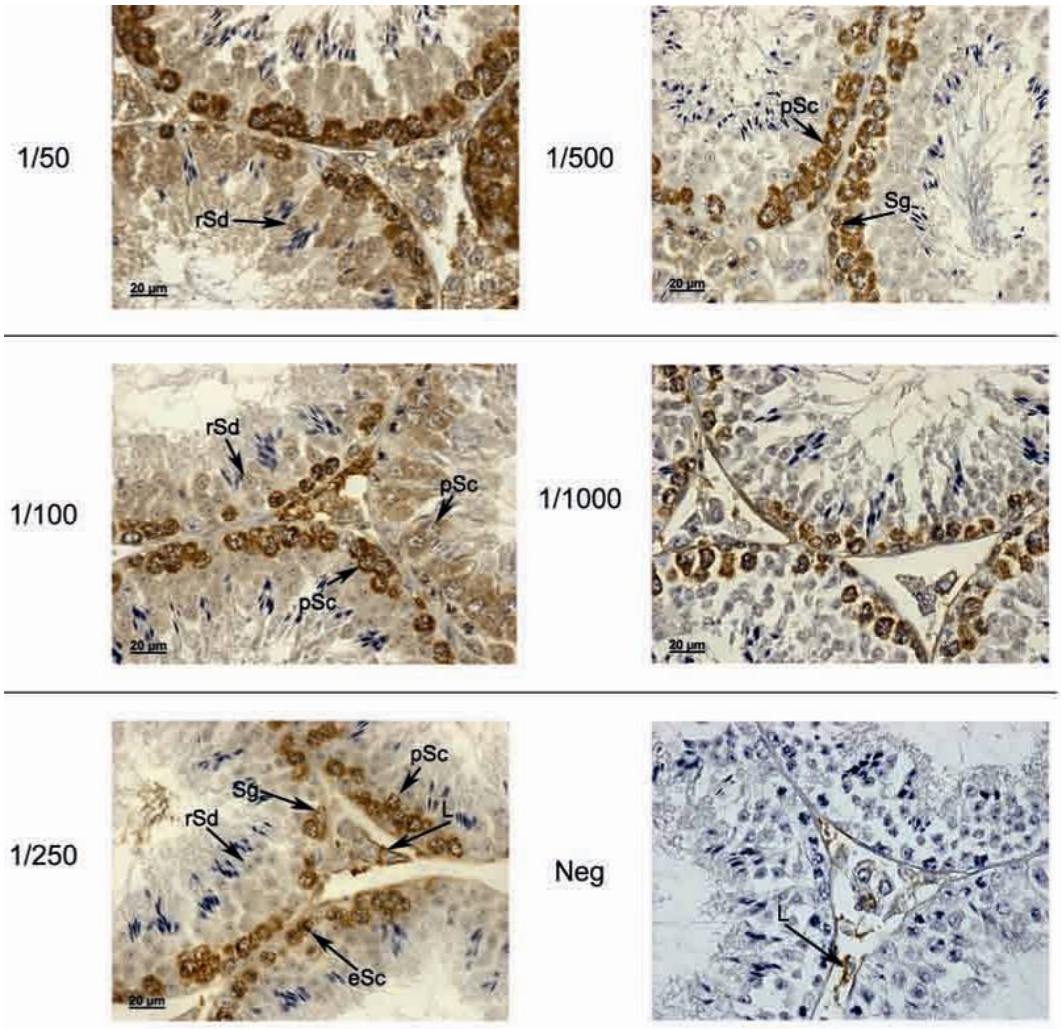


**Figure A1.3 - DAZL antibody titration in mouse testes.** Titration of the anti-DAZL Serotec antibody in mouse testes with five different dilutions in normal goat serum, ranging from 1/50 to 1/1000. Neg - negative control preformed with no primary antibody. rSd – round spermatid; eSc – early spermatocytes; Sg – spermatogonium; L – Leydig cell; pSc – pachytene spermatocytes. x40 magnification.

In summary, the new Serotec mouse monoclonal anti-DAZL gives a specific signal that agrees with published literature (Niederberger *et al.*, 1997, Ruggiu *et al.*, 1997), when used in NBF fixed tissue.

To further optimise this antibody, a titration was performed on mouse adult testes fixed in NBF. Figure A1.3 shows five different anti-DAZL antibody dilutions, ranging from 1/50 to 1/1000. Lower dilutions (1/50 and 1/100) detected Dazl in the cytoplasm of round spermatids, a pattern that does not agree with the published literature. Both the 1/250 and 1/500 anti-DAZL dilution gave the expected pattern of

Dazl expression (i.e. in the cytoplasm of spermatogonia, early and pachytene spermatocytes). The higher dilution of 1/1000 detected Dazl more weakly. Positive immunostainingwas observed in the Leydig cells even in the absence of primary antibody. Since, the Serotec anti-Dazl antibody is a mouse monoclonal some degree of non-specific immunostaining in mouse tissues was expected due to the presence of endogenous mouse immunoglobulins (IgG) that can be recognised by the secondary antibody. Therefore, a mouse on mouse block (Vector #BMK-2202) containing an affinity purified anti-mouse IgG was used to try to reduce the background signal by blocking endogenous IgG, but without success (data not shown). Fortunately, the Leydig cells lie outside the seminiferous tubules which contain the germ cells.

Throughout this project Dazl expression was assessed on NBF fixed tissue using the Serotec antibody at a 1/250 dilution.

## A1.1.2 Everest

A newly available anti-DAZL antibody (Everest #EB06857) raised in goat was tested for Dazl specificity in mouse testes to establish whether it could be used for PLA. This antibody was raised against a C-terminal peptide of hDAZL that is conserved in mouse Dazl (mDazl) but not Boule (mBoll) (Figure A1.4). Specificity was assessed over a range of concentrations indicated by the manufacturer (2-3 µg/ml).

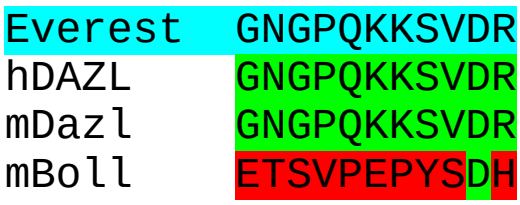


**Figure A1.4 - Everest anti-DAZL antibody.** Sequence homology between the human DAZL (hDAZL) peptide (shown in blue) used to raise the Everest anti-DAZL antibody and mouse Dazl (mDazl) and Boule (mBoll). Green - amino-acids matching the peptide; Red – mismatched amino-acids.

This antibody detected Dazl in spermatogonia and spermatocytes located in the more peripheral regions of the seminiferous tubules, as previously shown with the Serotec anti-DAZL antibody. However, it also cross-reacted with non-specific epitopes present in the cytoplasm of elongated spermatids (Figure A1.5): previously published RNA and protein expression data (Niederberger *et al.*, 1997, Ruggiu *et al.*, 1997), together with findings described earlier in this appendix , show that Dazl is not present in these cells. This pattern was not observed in the absence of primary antibody (Figure A1.5). These results indicate that the new anti-DAZL antibody from Everest is not specific for Dazl and is therefore unsuitable for use in the PLA.

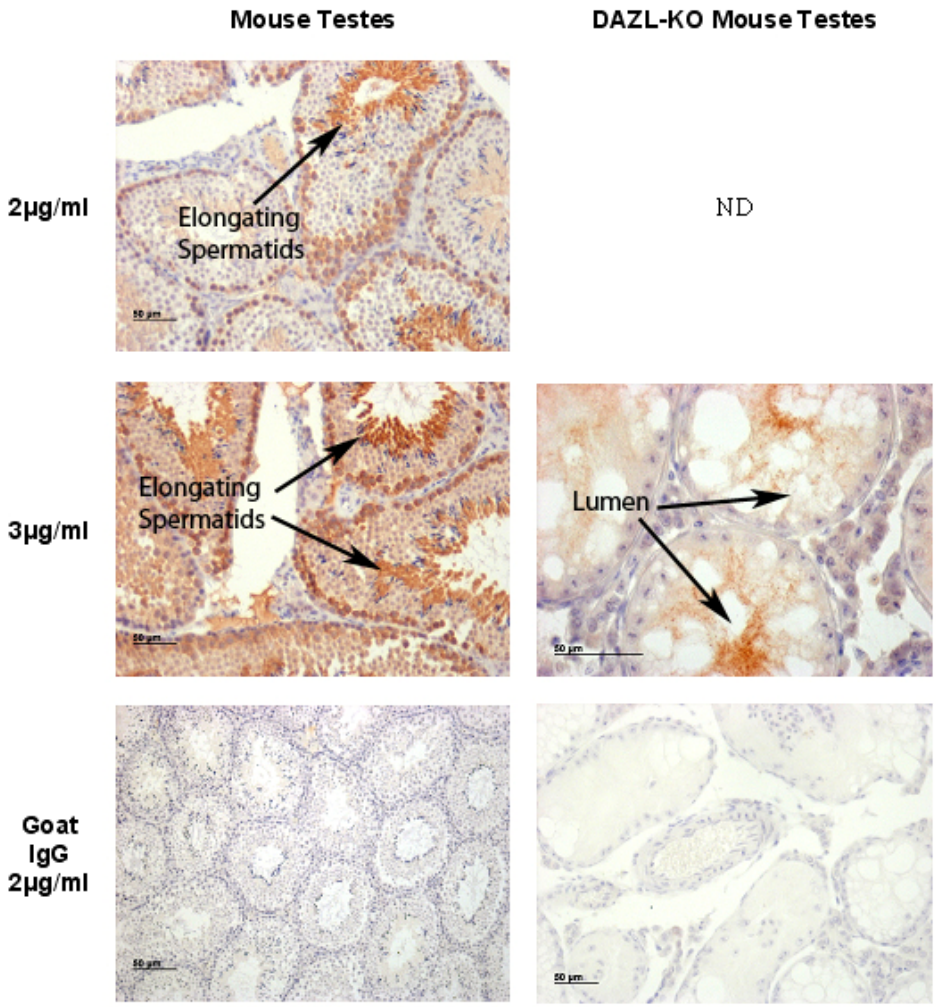


**Figure A1.5 - Testing a new Everest anti-DAZL antibody.** IHC using the anti-DAZL antibody from Everest Biotech #EB06857 in wild-type and DAZL-KO mouse testes at two different antibody concentrations with DAB detection. Anti-goat IgG was used as negative control. ND - not done.

# Appendix 2

# PABP1 antibody validation

# A2.1 PABP1 antibody validation for IHC

```
MARSHALL    AQKAVNSATGVPTV
mPabp1      AQKAVNSATGVPTV
mtPabp      AQKAVGSTSGVPTV
mPabp4-001  AQK-VG-TVAAATS
mPabp4-002  AQK-VG-TVAAATS
mPabp4-003  AQK-VG-TVAAATS
mPabp4-004  AQK-VG-TVAAATS
mePabp      DRN----------

VINPY       PVINPYQPAPPSGY
mPabp1      PVINPYQPAPPSGY
mtPabp      PV-NPYQPASSSYS
mPabp4-001  AILNQFQPAAG-GY
mPabp4-002  AILNQFQPAAG-GY
mPabp4-003  AILNQFQPAAG-GY
mPabp4-004  AILNQFQPAAG-GY
mePabp      PVLSSFQQPT-SYL
```

**Figure A2.1 - Peptide homology corresponding to sequence within the C terminal domain of mouse Pabp1 used to raise the Marshall and VINPY anti-PABP1 antibodies.** Blue - sequence used to raise the antibody; Green - amino-acids matching the peptide; Red - amino-acid not matching the peptide. mPabp1 – mouse Pabp1; mtPabp – mouse tPabp; mPabp4.001-004 – mouse Pabp4 isoforms 1 to 4; mePabp – mouse ePabp.

Previous literature describing the presence of PABPs in male germ cells did not discern between different PABP family members (Kleene *et al.*, 1994). Thus, in order to characterize Pabp1 expression two new antibodies were raised against C-terminal peptides: Marshall (AQKAVNSATGVPTV) and VINPY (PVINPYQPAPPSGY) in mouse Pabp1 that were not well conserved in different PABP family members (Figure A2.1). tPabp shares the highest degree of homology with these peptides due to its relatively high degree of conservation with Pabp1. Other potentially immunogenic peptides showing less conservation with tPabp were not identified during the original epitope selection.

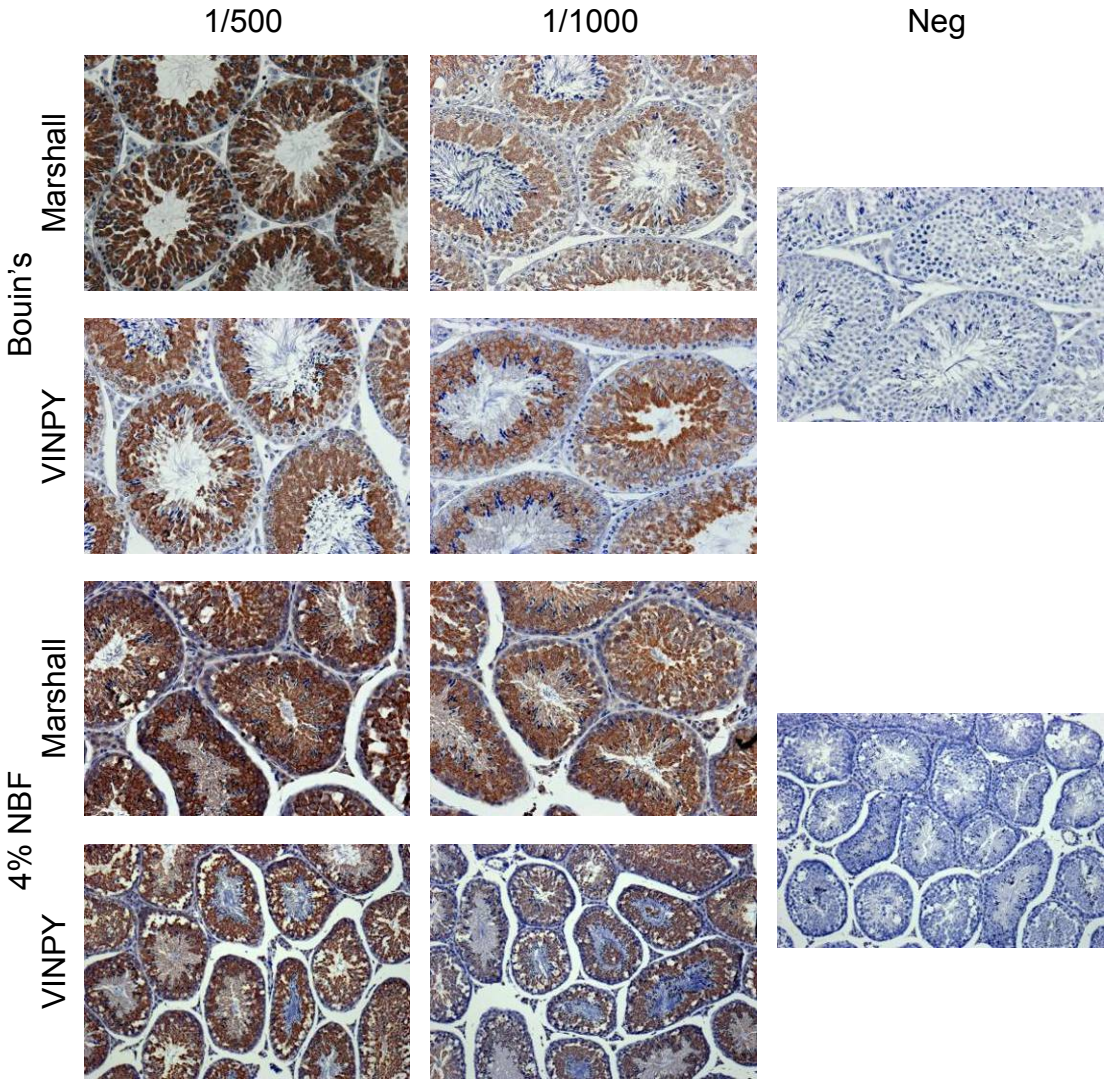


**Figure A2.2 - Anti-PABP1 antibodies validation in adult mouse testes.** Validation of anti-PABP1 antibodies in adult mouse testes fixed in 4%NBF or Bouin's, at two different dilutions; 1/500 and 1/1000. Negative control preformed with no primary antibody.

The efficacy and specificity of the antibodies was assessed using two dilutions in both Bouin's and 4% NBF-fixed adult mouse testes (Figure A2.2), for which Pabp1 mRNA expression data is available (Kleene *et al.*, 1994). Bouin's fixed tissue showed a peak of expression in round and elongating spermatids. The pattern obtained from testes fixed with NBF was more difficult to interpret, due to the poor morphology of the tissue. Further titration of these antibodies over a greater concentration range (1/500-1/5000) was therefore performed on Bouin's fixed tissue (Figure A2.3). This showed that the lowest dilution (1/500) appeared to produce some non-specific immunostaining since both antibodies detected proteins in early stage germ cells which do not contain PABP1 mRNA (Kleene *et al.*, 1994). This non-specific signal was also observed for Marshall using 1/1000 and 1/2500 dilutions but not 1/5000. At this dilution the Marshall anti-PABP1 antibody detects PABP1 in the pachytene spermatocytes through elongating spermatids signal, agreeing with the onset of PABP1 mRNA expression (Kleene *et al.*, 1994). This expression pattern was also observed at a 1/1000 dilution of the VINPY antibody, although further dilution of this antibody gave an increasing weak and diffuse signal. In the absence of primary antibody, or in the presence of rabbit IgG or normal rabbit serum (Ross Anderson; Figure A2.4), no signal was observed in any cells within or outside the seminiferous tubules. Since both antibodies (at different dilutions) give the same expression pattern, which is supported by the published RNA data (Kleene *et al.*, 1994, Kimura *et al.*, 2009), this suggests that both antibodies can be used for IHC (Marshall: 1/5000 dilution [0.025 ng/µl] and VINPY: 1/1000 dilution [0.06 ng/µl]). Since the specificity of the Marshall anti-PABP1 antibody was further supported by western blotting and immunofluroescence following PABP1 knockdown in cultured cells (Burgess *et al.*, 2011) this antibody was used for subsequent experiments.

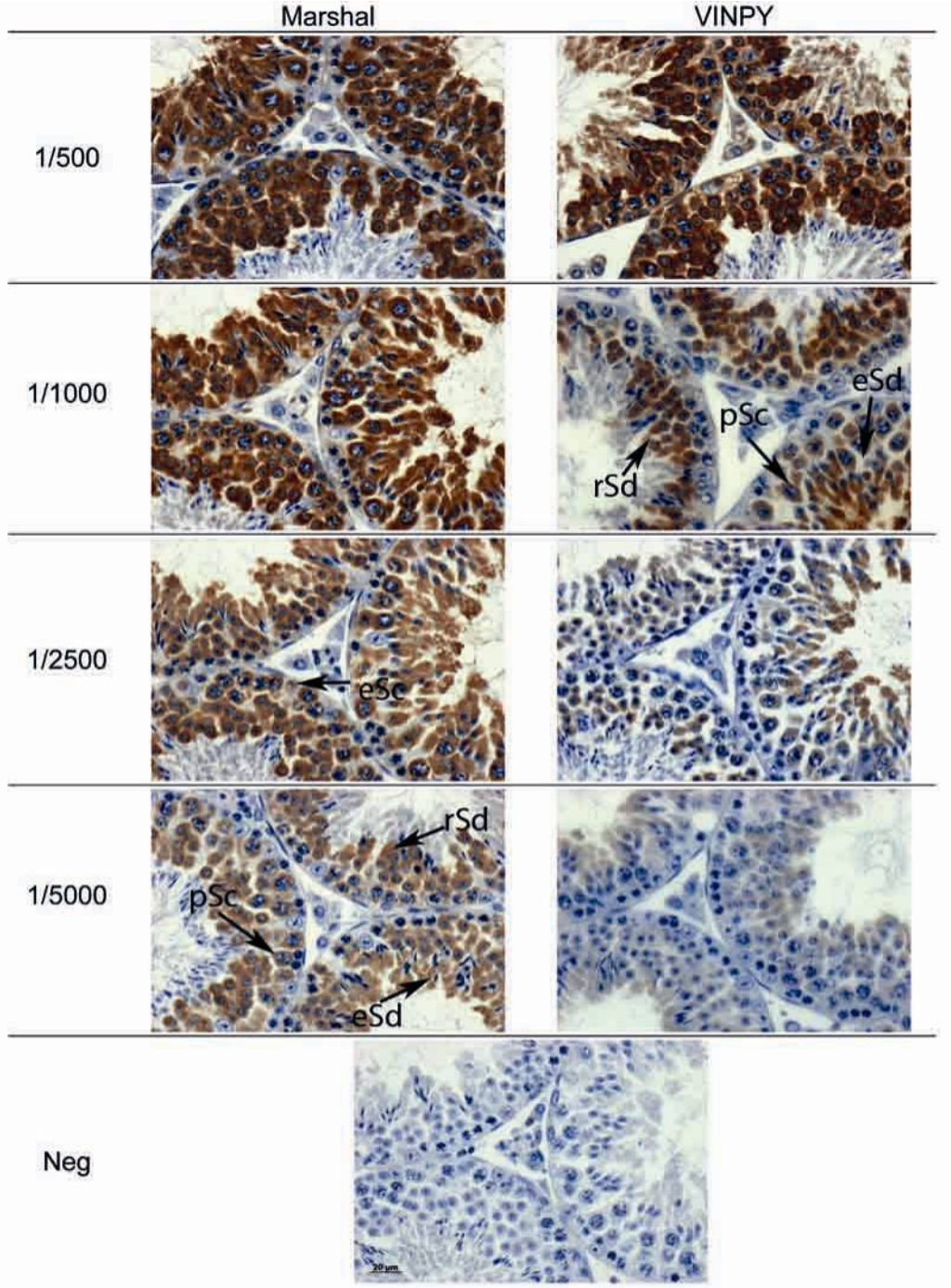


**Figure A2.3 - Titration of PABP1 antibodies in IHC using mouse testes.** Four dilutions (1/500 to 1/5000) of anti-PABP1 antibodies were applied to mouse testes in normal goat serum. Neg - no primary antibody. eSc – early spermatocytes; pSc – pachytene spermatocytes; rSd – round spermatid; eSd – elongating spermatids. x40 magnification.

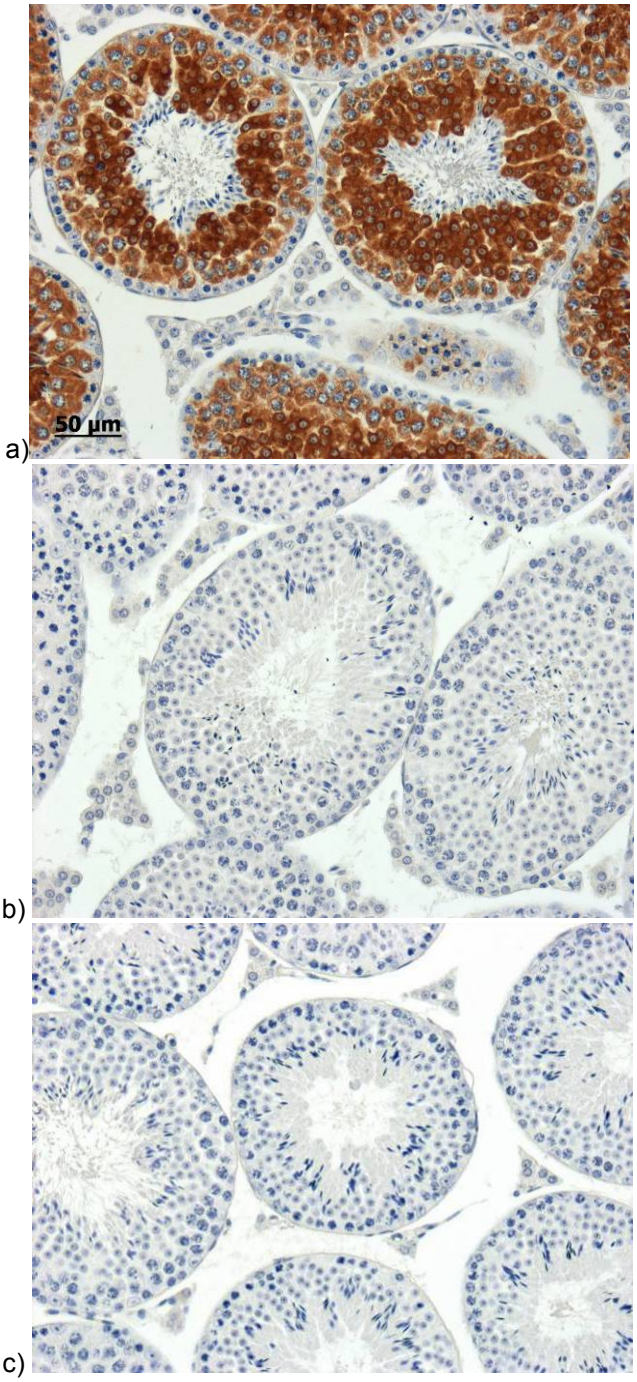


**Figure A2.4 - Additional controls further support the specificity of the Marshall anti-PABP1 antibody.** Sections of adult mouse testes were immunostained using a – Marshall anti-PABP1 antibody; b –rabbit IgG; c - normal rabbit serum. Performed by Ross Anderson.

# Appendix 3

# Optimising HeLa cell transfection

# A3.1 Optimising HeLa cell transfection

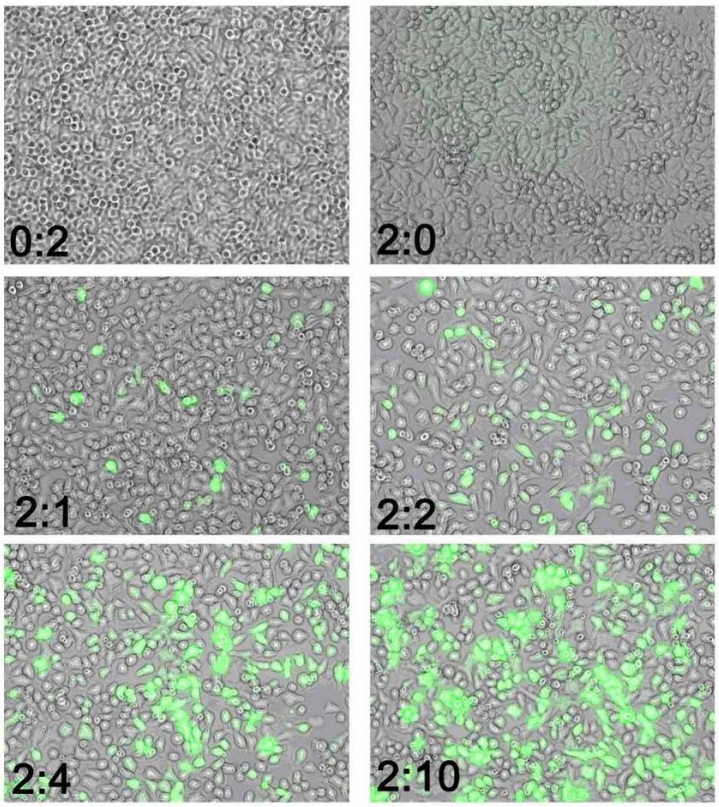


**Figure A3.1 - Optimisation of HeLa cell transfection with Lipofectamine 2000™.** 6 well plates were seeded with 1.8 x $10^4$/$cm^2$ of HeLa cells and incubated for 24 hours followed by transfection with different ratios between pEGFP-C1 plasmid DNA (2 µg): *Lipofectamine 2000*™(1-0 µl). No DNA (0:2) and no transfection reagent (2:0) controls are shown.

The transfection protocol was optimised using a plasmid expressing green fluorescent protein, pEGFP-C1, and different volumes of transfection reagent (Lipofectamine 2000™). Transfection efficiency was assessed 24 hours post–transfection using an axiovert 200 inverted microscope to identify GFP-expressing cells (Figure A3.1). For transfection of a sub-confluent 6-well plate well of HeLa cells with 2ug plasmid DNA, the best transfection efficiency was obtained using 10 µl Lipofectamine 2000™, with over 80% of the cells expressing GFP. No GFP expression was observed in the negative controls (no DNA or no transfection reagent) showing this was not due to autofluorescence. Higher cell density was observed in the absence of transfection reagent indicating a degree of toxicity associated with its use in HeLa cells.

# Appendix 4
# Validation of commercial PABP4 antibodies

# A4.1 Anti-PABP4 antibodies validation in HeLa cell extracts

The specificity of an Abnova anti-PABP4 antibody (# H000087610D1P) and a Bethyl labs antibody (#IHC-00561) was assessed by siRNAs in HeLa cells. The Abnova antibody detected a protein of around 90 kDa, larger than the predicted molecular weight (70 kDa), and the protein detected by the in house anti-PABP4 antibody (Figure A4.1). This larger protein was not diminished by PABP4 knockdown showing that this antibody is not specific for PABP4. Conversely, the Bethyl lab antibody recognised a protein of the expected size that was absent following PABP4 but not PABP1 knockdown providing evidence that it specifically recognised PABP4.

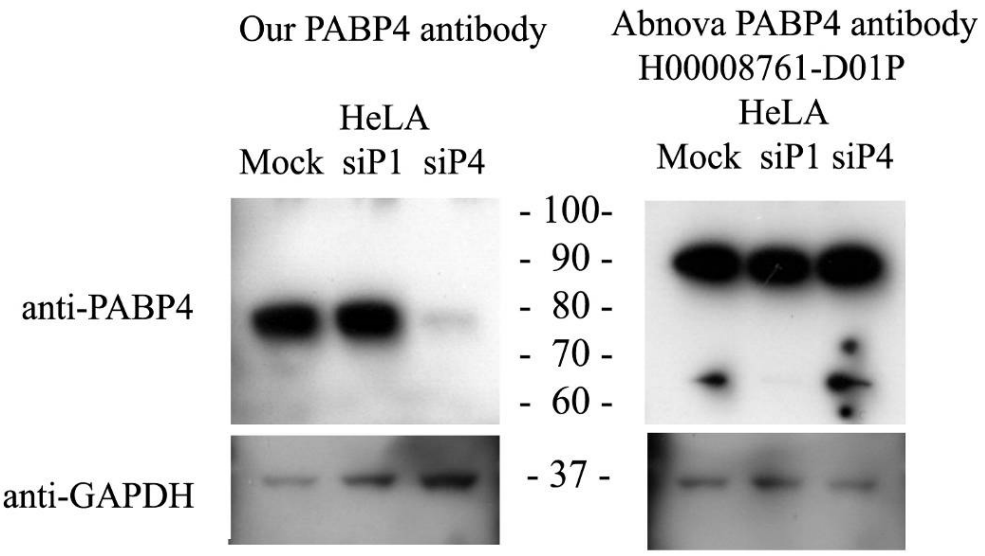


**Figure A4.1 - An anti-PABP4 antibody from Abnova is not specific for PABP4 in HeLa cells.** HeLa cells were transfected with 5 nM of siPABP1 (siP1), siPABP4 (siP4) or mock transfected and incubated for 48 hours prior to western blotting with the in house PABP4 antibody (left hand panel) or the Abnova antibody (right hand panel) and GAPDH which served as a loading control..

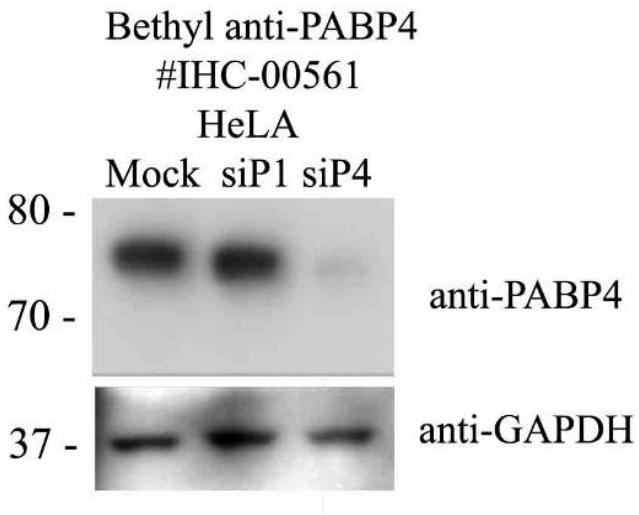


**Figure A4.2 - A Bethyl labs anti-PABP4 antibody specifically detects PABP4 in HeLa cells.** HeLa cells were transfected with 5 nM of siPABP1 (siP1), siPABP4 (siP4) or were mock transfected and incubated for 48 hours prior to Western blotting for PABP4. GAPDH served as a loading control.

## A4.2 Bethyl anti-PABP4 Anti-PABP4 #IHC-00561 antibody validation for IHC

To determine if this antibody would replicate the Pabp4 expression pattern observed with the in house antibody, IHC was performed using adult mouse testis (Figure A4.3). This showed robust expression of Pabp4 in the cytoplasm of spermatogonia (Sg), early spermatocytes (eSc), and Sertoli cells (S) and also within Leydig cells (L). The pattern obtained with this antibody is highly reminiscent of the results described with the in house anti-PABP4 antibody described in Chapter 4 (Figure 4.7).

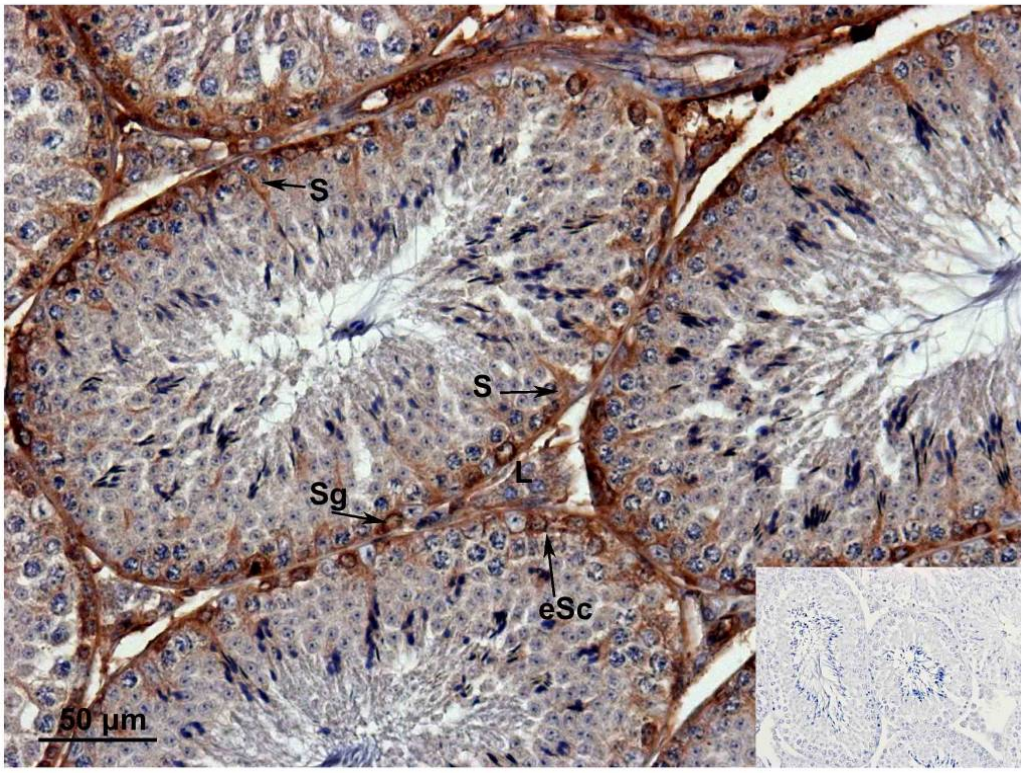


**Figure A4.3 - IHC using the Bethyl anti-PABP4 #IHC-00561 antibody in mouse adult testes.** IHC with DAB detection using the Bethyl anti-PABP4 antibody (1/150) in adult mouse testes. Inset shows a negative control performed with rabbit IgG. L – Leydig cell; S – Serolti cell; Sg – spermatogonia; eSc – early spermatocyte. X20 magnification**.**

# Chapter 8
# References

ABOU-HAILA, A. & TULSIANI, D. R. (2000) Mammalian sperm acrosome: formation, contents, and function. *Arch Biochem Biophys,* 379**,** 173-82.

ADASHI, E. Y. (1994) Endocrinology of the ovary. *Hum Reprod,* 9**,** 815-27.

AFONINA, E., STAUBER, R. & PAVLAKIS, G. N. (1998) The human poly(A)-binding protein 1 shuttles between the nucleus and the cytoplasm. *J Biol Chem,* 273**,** 13015-21.

ALBRECHT, M. & LENGAUER, T. (2004) Survey on the PABC recognition motif PAM2. *Biochem Biophys Res Commun,* 316**,** 129-38.

ALGIRE, M. A., MAAG, D. & LORSCH, J. R. (2005) Pi release from eIF2, not GTP hydrolysis, is the step controlled by start-site selection during eukaryotic translation initiation. *Mol Cell,* 20**,** 251-62.

AMRANI, N., GHOSH, S., MANGUS, D. A. & JACOBSON, A. (2008) Translation factors promote the formation of two states of the closed-loop mRNP. *Nature,* 453**,** 1276-80.

ANDERSON, E. L., BALTUS, A. E., ROEPERS-GAJADIEN, H. L., HASSOLD, T. J., DE ROOIJ, D. G., VAN PELT, A. M. & PAGE, D. C. (2008) Stra8 and its inducer, retinoic acid, regulate meiotic initiation in both spermatogenesis and oogenesis in mice. *Proc Natl Acad Sci U S A,* 105**,** 14976-80.

ANDERSON, P. & KEDERSHA, N. (2009) Stress granules. *Curr Biol,* 19**,** R397-8.

ANDERSON, R. A., FULTON, N., COWAN, G., COUTTS, S. & SAUNDERS, P. T. (2007) Conserved and divergent patterns of expression of DAZL, VASA and OCT4 in the germ cells of the human fetal ovary and testis. *BMC Dev Biol,* 7**,** 136.

ANDERSON, R. C. (2010) Expression and Characterisation of a Novel Poly(A)-Binding Protein, PABP5. Edinburgh Edinburgh University.

ATKINS, J. F., WEISS, R. B. & GESTELAND, R. F. (1990) Ribosome gymnastics - degree of difficulty 9.5, style 10.0. *Cell,* 62**,** 413-423.

BAER, B. W. & KORNBERG, R. D. (1983) The protein responsible for the repeating structure of cytoplasmic poly(A)-ribonucleoprotein. *J Cell Biol,* 96**,** 717-21.

BAILLET, A. & MANDON-PEPIN, B. (2011) Mammalian ovary differentiation - A focus on female meiosis. *Mol Cell Endocrinol,* 356**,** 13-23.

BAKER, S. J. & SPEARS, N. (1999) The role of intra-ovarian interactions in the regulation of follicle dominance. *Hum Reprod Update,* 5**,** 153-65.

BASHAW, G. J. & BAKER, B. S. (1997) The Regulation of the Drosophila *msl-2* Gene Reveals a Function for Sex-lethal in Translational Control. *Cell,* 89**,** 789-798.

BECKMANN, K., GRSKOVIC, M., GEBAUER, F. & HENTZE, M. W. (2005) A dual inhibitory mechanism restricts msl-2 mRNA translation for dosage compensation in Drosophila. *Cell,* 122**,** 529-40.

BELLVE, A. R., CAVICCHIA, J. C., MILLETTE, C. F., O'BRIEN, D. A., BHATNAGAR, Y. M. & DYM, M. (1977) Spermatogenic cells of the prepuberal mouse. Isolation and morphological characterization. *J Cell Biol,* 74**,** 68-85.

BENDEL-STENZEL, M., ANDERSON, R., HEASMAN, J. & WYLIE, C. (1998) The origin and migration of primordial germ cells in the mouse. *Semin Cell Dev Biol,* 9**,** 393-400.

BENOIT, B., MITOU, G., CHARTIER, A., TEMME, C., ZAESSINGER, S., WAHLE, E., BUSSEAU, I. & SIMONELIG, M. (2005) An essential cytoplasmic function for the nuclear poly(A) binding protein, PABP2, in poly(A) tail length control and early development in Drosophila. *Dev Cell,* 9**,** 511-22.

BERNSTEIN, P., PELTZ, S. W. & ROSS, J. (1989) The poly(A)-poly(A)-binding protein complex is a major determinant of mRNA stability in vitro. *Mol Cell Biol,* 9**,** 659-70.

BI, X. & GOSS, D. J. (2000) Wheat germ poly(A)-binding protein increases the ATPase and the RNA helicase activity of translation initiation factors eIF4A, eIF4B, and eIF-iso4F. *J Biol Chem,* 275**,** 17740-6.

BLANCO, P., SARGENT, C. A., BOUCHER, C. A., HOWELL, G., ROSS, M. & AFFARA, N. A. (2001) A novel poly(A)-binding protein gene (PABPC5) maps to an X-specific subinterval in the Xq21.3/Yp11.2 homology block of the human sex chromosomes. *Genomics,* 74**,** 1-11.

BLOBEL, G. (1973) A protein of molecular weight 78,000 bound to the polyadenylate region of eukaryotic messenger RNAs. *Proc Natl Acad Sci U S A,* 70**,** 924-8.

BONNAL, S., PILEUR, F., ORSINI, C., PARKER, F., PUJOL, F., PRATS, A. C. & VAGNER, S. (2005) Heterogeneous nuclear ribonucleoprotein A1 is a novel internal ribosome entry site trans-acting factor that modulates alternative initiation of translation of the fibroblast growth factor 2 mRNA. *J Biol Chem,* 280**,** 4144-53.

BORMAN, A. M., MICHEL, Y. M. & KEAN, K. M. (2000) Biochemical characterisation of cap-poly(A) synergy in rabbit reticulocyte lysates: the eIF4G-PABP interaction increases the functional affinity of eIF4E for the capped mRNA 5'-end. *Nucleic Acids Res,* 28**,** 4068-75.

BOWLES, J., KNIGHT, D., SMITH, C., WILHELM, D., RICHMAN, J., MAMIYA, S., YASHIRO, K., CHAWENGSAKSOPHAK, K., WILSON, M. J., ROSSANT, J., HAMADA, H. & KOOPMAN, P. (2006) Retinoid signaling determines germ cell fate in mice. *Science,* 312**,** 596-600.

BOWLES, J. & KOOPMAN, P. (2007) Retinoic acid, meiosis and germ cell fate in mammals. *Development,* 134**,** 3401-11.

BRAUN, R. E. (2001) Packaging paternal chromosomes with protamine. *Nat Genet,* 28**,** 10-2.

BREKHMAN, V., ITSKOVITZ-ELDOR, J., YODKO, E., DEUTSCH, M. & SELIGMAN, J. (2000) The DAZL1 gene is expressed in human male and female embryonic gonads before meiosis. *Mol Hum Reprod,* 6**,** 465-8.

BREWER, L. R., CORZETT, M. & BALHORN, R. (1999) Protamine-induced condensation and decondensation of the same DNA molecule. *Science,* 286**,** 120-3.

BROOK, M. & GRAY, N. K. (2012) The role of mammalian poly(A)-binding proteins in coordinating mRNA turnover. *Biochemical Society Transactions,* in press.

BROOK, M., MCCRACKEN, L., REDDINGTON, J. P., LU, Z. L., MORRICE, N. A. & GRAY, N. K. (2012) The multifunctional poly(A)-binding protein (PABP) 1 is subject to extensive dynamic post-translational modification,

which molecular modelling suggests plays an important role in co-ordinating its activities. *Biochem J,* 441**,** 803-12.

BROOK, M., SMITH, J. W. & GRAY, N. K. (2009) The DAZL and PABP families: RNA-binding proteins with interrelated roles in translational control in oocytes. *Reproduction,* 137**,** 595-617.

BRUNET, S., DUMONT, J., LEE, K. W., KINOSHITA, K., HIKAL, P., GRUSS, O. J., MARO, B. & VERLHAC, M. H. (2008) Meiotic regulation of TPX2 protein levels governs cell cycle progression in mouse oocytes. *PLoS One,* 3**,** e3338.

BUCHAN, J. R. & PARKER, R. (2009) Eukaryotic stress granules: the ins and outs of translation. *Mol Cell,* 36**,** 932-41.

BUONOMO, S. B., CLYNE, R. K., FUCHS, J., LOIDL, J., UHLMANN, F. & NASMYTH, K. (2000) Disjunction of homologous chromosomes in meiosis I depends on proteolytic cleavage of the meiotic cohesin Rec8 by separin. *Cell,* 103**,** 387-98.

BURD, C. G., MATUNIS, E. L. & DREYFUSS, G. (1991) The multiple RNA-binding domains of the mRNA poly(A)-binding protein have different RNA-binding activities. *Mol Cell Biol,* 11**,** 3419-24.

BURGESS, H. & GRAY , N. K. (2012) An integrated model for the nucleo-cytoplasmic transport of cytoplasmic poly(A)-binding proteins. *Communicative&Integrative Biology,* 5**,** in Press.

BURGESS, H. M. & GRAY, N. K. (2010) mRNA-specific regulation of translation by poly(A)-binding proteins. *Biochem Soc Trans,* 38**,** 1517-22.

BURGESS, H. M., RICHARDSON, W. A., ANDERSON, R. C., SALAUN, C., GRAHAM, S. V. & GRAY, N. K. (2011) Nuclear relocalisation of cytoplasmic poly(A)-binding proteins PABP1 and PABP4 in response to UV irradiation reveals mRNA-dependent export of metazoan PABPs. *J Cell Sci,* 124**,** 3344-3355.

BUSHELL, M., WOOD, W., CARPENTER, G., PAIN, V. M., MORLEY, S. J. & CLEMENS, M. J. (2001) Disruption of the interaction of mammalian protein synthesis eukaryotic initiation factor 4B with the poly(A)-binding protein by caspase- and viral protease-mediated cleavages. *J Biol Chem,* 276**,** 23922-8.

BYSKOV, A. G. (1975) The role of the rete ovarii in meiosis and follicle formation in the cat, mink and ferret. *J Reprod Fertil,* 45**,** 201-9.

CAKMAKCI, N. G., LERNER, R. S., WAGNER, E. J., ZHENG, L. & MARZLUFF, W. F. (2008) SLIP1, a factor required for activation of histone mRNA translation by the stem-loop binding protein. *Mol Cell Biol,* 28**,** 1182-94.

CALADO, A., KUTAY, U., KUHN, U., WAHLE, E. & CARMO-FONSECA, M. (2000) Deciphering the cellular pathway for transport of poly(A)-binding protein II. *RNA,* 6**,** 245-56.

CANIPARI, R. (2000) Oocyte--granulosa cell interactions. *Hum Reprod Update,* 6**,** 279-89.

CAO, Q., PADMANABHAN, K. & RICHTER, J. D. (2010) Pumilio 2 controls translation by competing with eIF4E for 7-methyl guanosine cap recognition. *RNA,* 16**,** 221-7.

CARMODY, S. R. & WENTE, S. R. (2009) mRNA nuclear export at a glance. *J Cell Sci,* 122**,** 1933-7.

CHANG, T. C., YAMASHITA, A., CHEN, C. Y., YAMASHITA, Y., ZHU, W., DURDAN, S., KAHVEJIAN, A., SONENBERG, N. & SHYU, A. B. (2004) UNR, a new partner of poly(A)-binding protein, plays a key role in translationally coupled mRNA turnover mediated by the c-fos major coding-region determinant. *Genes Dev,* 18**,** 2010-23.

CHEKULAEVA, M., HENTZE, M. W. & EPHRUSSI, A. (2006) Bruno acts as a dual repressor of oskar translation, promoting mRNA oligomerization and formation of silencing particles. *Cell,* 124**,** 521-33.

CHEN, J., MELTON, C., SUH, N., OH, J. S., HORNER, K., XIE, F., SETTE, C., BLELLOCH, R. & CONTI, M. (2011) Genome-wide analysis of translation reveals a critical role for deleted in azoospermia-like (Dazl) at the oocyte-to-zygote transition. *Genes Dev,* 25**,** 755-66.

CHEN, L., WERT, S. E., HENDRIX, E. M., RUSSELL, P. T., CANNON, M. & LARSEN, W. J. (1990) Hyaluronic acid synthesis and gap junction endocytosis are necessary for normal expansion of the cumulus mass. *Mol Reprod Dev,* 26**,** 236-47.

CHENG, M. H., MAINES, J. Z. & WASSERMAN, S. A. (1998) Biphasic subcellular localization of the DAZL-related protein boule in Drosophila spermatogenesis. *Dev Biol,* 204**,** 567-76.

CHEUNG, Y. N., MAAG, D., MITCHELL, S. F., FEKETE, C. A., ALGIRE, M. A., TAKACS, J. E., SHIROKIKH, N., PESTOVA, T., LORSCH, J. R. & HINNEBUSCH, A. G. (2007) Dissociation of eIF1 from the 40S ribosomal subunit is a key step in start codon selection in vivo. *Genes Dev,* 21**,** 1217-30.

CHUMA, S. & NAKATSUJI, N. (2001) Autonomous transition into meiosis of mouse fetal germ cells in vitro and its inhibition by gp130-mediated signaling. *Dev Biol,* 229**,** 468-79.

CIOSK, R., DEPALMA, M. & PRIESS, J. R. (2004) ATX-2, the C. elegans ortholog of ataxin 2, functions in translational regulation in the germline. *Development,* 131**,** 4831-41.

CLEMENS, M. J. (1996) Protein kinases that phosphorylate eIF-2 and eIF-2B, and their role in eukaryotic cell translational control. IN HERSHEY, J. W. B., MATHEWS, M. B. & SONENBERG, N. (Eds.) *Translational Control.* New York, Cold Spring Harbor Laboratory Press.

CLEMENS, M. J. (1997) PKR--a protein kinase regulated by double-stranded RNA. *Int J Biochem Cell Biol,* 29**,** 945-9.

CLEMENS, M. J. & ELIA, A. (1997) The Double-Stranded RNA-Dependent Protein Kinase PKR: Structureand Function. *Journal of Interferon and Cytokine Research,* 17**,** 503-524.

CLERMONT, Y. (1972) Kinetics of spermatogenesis in mammals: seminiferous epithelium cycle and spermatogonial renewal. *Physiol Rev,* 52**,** 198-236.

COLLIER, B., GORGONI, B., LOVERIDGE, C., COOKE, H. & GRAY, N. K. (2005a) The DAZL family of proteins are PABP binding proteins that regulate translation in germ cells. *EMBO J,* 24**,** 2656-2666.

COLLIER, B., GORGONI, B., LOVERIDGE, C., COOKE, H. J. & GRAY, N. K. (2005b) The DAZL family proteins are PABP-binding proteins that regulate translation in germ cells. *EMBO J,* 24**,** 2656-66.

COLMAN, A. & DRUMMOND, D. (1986) The stability and movement of mRNA in Xenopus oocytes and embryos. *J Embryol Exp Morphol,* 97 Suppl**,** 197-209.

COLVIN, J. S., GREEN, R. P., SCHMAHL, J., CAPEL, B. & ORNITZ, D. M. (2001) Male-to-female sex reversal in mice lacking fibroblast growth factor 9. *Cell,* 104**,** 875-89.

CONTI, M., HSIEH, M., ZAMAH, A. M. & OH, J. S. (2011) Novel signaling mechanisms in the ovary during oocyte maturation and ovulation. *Mol Cell Endocrinol,* 356**,** 65-73.

COOKE, H. J., LEE, M., KERR, S. & RUGGIU, M. (1996) A murine homologue of the human DAZ gene is autosomal and expressed only in male and female gonads. *Hum Mol Genet,* 5**,** 513-6.

CORMACK, B. P., VALDIVIA, R. H. & FALKOW, S. (1996) FACS-optimized mutants of the green fluorescent protein (GFP). *Gene,* 173**,** 33-8.

COSSON, B., BERKOVA, N., COUTURIER, A., CHABELSKAYA, S., PHILIPPE, M. & ZHOURAVLEVA, G. (2002a) Poly(A)-binding protein and eRF3 are associated in vivo in human and Xenopus cells. *Biol Cell,* 94**,** 205-16.

COSSON, B., BRAUN, F., PAILLARD, L., BLACKSHEAR, P. & BEVERLEY OSBORNE, H. (2004) Identification of a novel Xenopus laevis poly (A) binding protein. *Biol Cell,* 96**,** 519-27.

COSSON, B., COUTURIER, A., CHABELSKAYA, S., KIKTEV, D., INGE-VECHTOMOV, S., PHILIPPE, M. & ZHOURAVLEVA, G. (2002b) Poly(A)-binding protein acts in translation termination via eukaryotic release factor 3 interaction and does not influence [PSI(+)] propagation. *Mol Cell Biol,* 22**,** 3301-15.

COSSON, B., COUTURIER, A., LE GUELLEC, R., MOREAU, J., CHABELSKAYA, S., ZHOURAVLEVA, G. & PHILIPPE, M. (2002c) Characterization of the poly(A) binding proteins expressed during oogenesis and early development of Xenopus laevis. *Biol Cell,* 94**,** 217-31.

CRAIG, A. W., HAGHIGHAT, A., YU, A. T. & SONENBERG, N. (1998) Interaction of polyadenylate-binding protein with the eIF4G homologue PAIP enhances translation. *Nature,* 392**,** 520-3.

DAI, T., VERA, Y., SALIDO, E. C. & YEN, P. H. (2001) Characterization of the mouse Dazap1 gene encoding an RNA-binding protein that interacts with infertility factors DAZ and DAZL. *BMC Genomics,* 2**,** 6.

DASGUPTA, T. & LADD, A. N. (2012) The importance of CELF control: molecular and biological roles of the CUG-BP, Elav-like family of RNA-binding proteins. *Wiley Interdiscip Rev RNA,* 3**,** 104-21.

DAY, D. A. & TUITE, M. F. (1998) Post-transcriptional gene regulatory mechanisms in eukaryotes: an overview. *J Endocrinol,* 157**,** 361-71.

DE GREGORIO, E., PREISS, T. & HENTZE, M. W. (1999) Translation driven by an eIF4G core domain in vivo. *EMBO J,* 18**,** 4865-74.

DE MELO NETO, O. P., STANDART, N. & MARTINS DE SA, C. (1995) Autoregulation of poly(A)-binding protein synthesis in vitro. *Nucleic Acids Res,* 23**,** 2198-205.

DE MOOR, C. H. & RICHTER, J. D. (1999) Cytoplasmic polyadenylation elements mediate masking and unmasking of cyclin B1 mRNA. *EMBO J,* 18**,** 2294-303.

DEARDORFF, J. A. & SACHS, A. B. (1997) Differential effects of aromatic and charged residue substitutions in the RNA binding domains of the yeast poly(A)-binding protein. *J Mol Biol,* 269**,** 67-81.

DEO, R. C., BONANNO, J. B., SONENBERG, N. & BURLEY, S. K. (1999) Recognition of polyadenylate RNA by the poly(A)-binding protein. *Cell,* 98**,** 835-45.

DEVER, T. E., DAR, A. C. & SICHERI, F. (2007) The eIF2α kinases. IN MATTHEWS, M. B., SONENBERG, N. & HERSHEY, J. W. B. (Eds.) *Translational Control in Biology and Medicine.* New York, Cold Spring Harbor Laboratory Press.

DI CARLO, A. D., TRAVIA, G. & DE FELICI, M. (2000) The meiotic specific synaptonemal complex protein SCP3 is expressed by female and male primordial germ cells of the mouse embryo. *Int J Dev Biol,* 44**,** 241-4.

DOBSON, M. J., PEARLMAN, R. E., KARAISKAKIS, A., SPYROPOULOS, B. & MOENS, P. B. (1994) Synaptonemal complex proteins: occurrence, epitope mapping and chromosome disjunction. *J Cell Sci,* 107 ( Pt 10)**,** 2749-60.

DONG, J., ALBERTINI, D. F., NISHIMORI, K., KUMAR, T. R., LU, N. & MATZUK, M. M. (1996) Growth differentiation factor-9 is required during early ovarian folliculogenesis. *Nature,* 383**,** 531-5.

DORFMAN, D. M., GENEST, D. R. & REIJO PERA, R. A. (1999) Human DAZL1 encodes a candidate fertility factor in women that localizes to the prenatal and postnatal germ cells. *Hum Reprod,* 14**,** 2531-6.

DUNCAN, K., GRSKOVIC, M., STREIN, C., BECKMANN, K., NIGGEWEG, R., ABAZA, I., GEBAUER, F., WILM, M. & HENTZE, M. W. (2006) Sex-lethal imparts a sex-specific function to UNR by recruiting it to the msl-2 mRNA 3' UTR: translational repression for dosage compensation. *Genes Dev,* 20**,** 368-79.

DUNCAN, K. E., STREIN, C. & HENTZE, M. W. (2009) The SXL-UNR corepressor complex uses a PABP-mediated mechanism to inhibit ribosome recruitment to msl-2 mRNA. *Mol Cell,* 36**,** 571-82.

DURLINGER, A. L., VISSER, J. A. & THEMMEN, A. P. (2002) Regulation of ovarian function: the role of anti-Mullerian hormone. *Reproduction,* 124**,** 601-9.

EBERHART, C. G., MAINES, J. Z. & WASSERMAN, S. A. (1996) Meiotic cell cycle requirement for a fly homologue of human Deleted in Azoospermia. *Nature,* 381**,** 783-5.

ELVIN, J. A., YAN, C., WANG, P., NISHIMORI, K. & MATZUK, M. M. (1999) Molecular characterization of the follicle defects in the growth differentiation factor 9-deficient ovary. *Mol Endocrinol,* 13**,** 1018-34.

EPPIG, J. J. (2001) Oocyte control of ovarian follicular development and function in mammals. *Reproduction,* 122**,** 829-38.

EYERS, P. A. & MALLER, J. L. (2004) Regulation of Xenopus Aurora A activation by TPX2. *J Biol Chem,* 279**,** 9008-15.

EZZEDDINE, N., CHANG, T. C., ZHU, W., YAMASHITA, A., CHEN, C. Y., ZHONG, Z., YAMASHITA, Y., ZHENG, D. & SHYU, A. B. (2007) Human TOB, an antiproliferative transcription factor, is a poly(A)-binding protein-

dependent positive regulator of cytoplasmic mRNA deadenylation. *Mol Cell Biol,* 27**,** 7791-801.

FARINI, D., SCALDAFERRI, M. L., IONA, S., LA SALA, G. & DE FELICI, M. (2005) Growth factors sustain primordial germ cell survival, proliferation and entering into meiosis in the absence of somatic cells. *Dev Biol,* 285**,** 49-56.

FEKETE, C. A., MITCHELL, S. F., CHERKASOVA, V. A., APPLEFIELD, D., ALGIRE, M. A., MAAG, D., SAINI, A. K., LORSCH, J. R. & HINNEBUSCH, A. G. (2007) N- and C-terminal residues of eIF1A have opposing effects on the fidelity of start codon selection. *EMBO J,* 26**,** 1602-14.

FERAL, C., GUELLAEN, G. & PAWLAK, A. (2001) Human testis expresses a specific poly(A)-binding protein. *Nucleic Acids Res,* 29**,** 1872-83.

FIELDS, S. & SONG, O. (1989) A novel genetic system to detect protein-protein interactions. *Nature,* 340**,** 245-6.

FORD, P. J., MATHIESON, T. & ROSBASH, M. (1977) Very long-lived messenger RNA in ovaries of Xenopus laevis. *Dev Biol,* 57**,** 417-26.

FOX, C. A., SHEETS, M. D., WAHLE, E. & WICKENS, M. (1992) Polyadenylation of maternal mRNA during oocyte maturation: poly(A) addition in vitro requires a regulated RNA binding activity and a poly(A) polymerase. *EMBO J,* 11**,** 5021-32.

FOX, M., URANO, J. & REIJO PERA, R. A. (2005) Identification and characterization of RNA sequences to which human PUMILIO-2 (PUM2) and deleted in Azoospermia-like (DAZL) bind. *Genomics,* 85**,** 92-105.

FRIEDMAN, R. C., FARH, K. K., BURGE, C. B. & BARTEL, D. P. (2009) Most mammalian mRNAs are conserved targets of microRNAs. *Genome Res,* 19**,** 92-105.

FRIEND, K., BROOK, M., BEZIRCI, F. B., SHEETS, M. D., GRAY, N. K. & SELI, E. (2012) Embryonic poly(A)-binding protein (ePAB) phosphorylation is required for Xenopus oocyte maturation. *Biochem J*.

FUJIWARA, Y., KOMIYA, T., KAWABATA, H., SATO, M., FUJIMOTO, H., FURUSAWA, M. & NOCE, T. (1994) Isolation of a DEAD-family protein gene that encodes a murine homolog of Drosophila vasa and its specific expression in germ cell lineage. *Proc Natl Acad Sci U S A,* 91**,** 12258-62.

FUNAKOSHI, Y., DOI, Y., HOSODA, N., UCHIDA, N., OSAWA, M., SHIMADA, I., TSUJIMOTO, M., SUZUKI, T., KATADA, T. & HOSHINO, S. (2007) Mechanism of mRNA deadenylation: evidence for a molecular interplay between translation termination factor eRF3 and mRNA deadenylases. *Genes Dev,* 21**,** 3135-48.

GALLIE, D. R. (1991) The cap and the poly (A) tail function synergistically to regulate mRNA translational efficiency. *Genes & Dev.,* 5**,** 2108-2116.

GARCIA-BONILLA, L., CID, C., ALCAZAR, A., BURDA, J., AYUSO, I. & SALINAS, M. (2007) Regulatory proteins of eukaryotic initiation factor 2-alpha subunit (eIF2 alpha) phosphatase, under ischemic reperfusion and tolerance. *J Neurochem,* 103**,** 1368-80.

GARNEAU, N. L., WILUSZ, J. & WILUSZ, C. J. (2007) The highways and byways of mRNA decay. *Nat Rev Mol Cell Biol,* 8**,** 113-26.

GAVIS, E. R., SINGER, R. H. & HUETTELMAIER, S. (2007) Localized translation through mRNA localization. IN MATTHEWS, M. B., SONENBERG, N. & HERSHEY, J. W. B. (Eds.) *Translational control in biology and medicine.* New York, CSHL Press.

GEBAUER, F. & HENTZE, M. W. (2001) Fertility facts: male and female germ cell development requires translational control by CPEB. *Mol Cell,* 8**,** 247-9.

GEBAUER, F. & HENTZE, M. W. (2004) Molecular mechanisms of translational control. *Nat Rev Mol Cell Biol,* 5**,** 827-35.

GEBAUER, F. & RICHTER, J. D. (1997) Synthesis and function of Mos: the control switch of vertebrate oocyte meiosis. *Bioessays,* 19**,** 23-8.

GEBAUER, F., XU, W., COOPER, G. M. & RICHTER, J. D. (1994) Translational control by cytoplasmic polyadenylation of c-mos mRNA is necessary for oocyte maturation in the mouse. *EMBO J,* 13**,** 5712-20.

GILL, M. E., HU, Y. C., LIN, Y. & PAGE, D. C. (2011) Licensing of gametogenesis, dependent on RNA binding protein DAZL, as a gateway to sexual differentiation of fetal germ cells. *Proc Natl Acad Sci U S A,* 108**,** 7443-8.

GILLIAN-DANIEL, D. L., GRAY, N. K., ASTROM, J., BARKOFF, A. & WICKENS, M. (1998) Modifications of the 5' cap of mRNAs during Xenopus oocyte maturation: independence from changes in poly(A) length and impact on translation. *Mol Cell Biol,* 18**,** 6152-63.

GOOD, P. J., ABLER, L., HERRING, D. & SHEETS, M. D. (2004) Xenopus embryonic poly(A) binding protein 2 (ePABP2) defines a new family of cytoplasmic poly(A) binding proteins expressed during the early stages of vertebrate development. *Genesis,* 38**,** 166-75.

GORGONI, B., ANDREWS, S., SCHALLER, A., SCHUMPERLI, D., GRAY, N. K. & MULLER, B. (2005) The stem-loop binding protein stimulates histone translation at an early step in the initiation pathway. *RNA,* 11**,** 1030-42.

GORGONI, B. & GRAY, N. K. (2004) The roles of cytoplasmic poly(A)-binding proteins in regulating gene expression: a developmental perspective. *Brief Funct Genomic Proteomic,* 3**,** 125-41.

GORGONI, B., RICHARDSON, W. A., BURGESS, H. M., ANDERSON, R. C., WILKIE, G. S., GAUTIER, P., MARTINS, J. P., BROOK, M., SHEETS, M. D. & GRAY, N. K. (2011) Poly(A)-binding proteins are functionally distinct and have essential roles during vertebrate development. *Proc Natl Acad Sci USA,* 108**,** 7844-9.

GORLACH, M., BURD, C. G. & DREYFUSS, G. (1994) The mRNA poly(A)-binding protein: localization, abundance, and RNA-binding specificity. *Exp Cell Res,* 211**,** 400-7.

GRAY, N. K. (1998) Translational control by repressor proteins binding to the 5UTR of mRNAs. *Meth. Mol. Biol.,* **77,** 379-397.

GRAY, N. K., COLLER, J. M., DICKSON, K. S. & WICKENS, M. (2000) Multiple portions of poly(A)-binding protein stimulate translation in vivo. *EMBO J,* 19**,** 4723-33.

GRAY, N. K. & HENTZE, M. W. (1994) Iron regulatory protein prevents binding of the 43S translation pre-initiation complex to ferritin and eALAS mRNAs. *EMBO J,* 13**,** 3882-91.

GRAY, N. K. & WICKENS, M. (1998) Control of translation initiation in animals. *Annu Rev Cell Dev Biol,* 14**,** 399-458.

GROSSET, C., CHEN, C. Y., XU, N., SONENBERG, N., JACQUEMIN-SABLON, H. & SHYU, A. B. (2000) A mechanism for translationally coupled mRNA turnover: interaction between the poly(A) tail and a c-fos RNA coding determinant via a protein complex. *Cell,* 103**,** 29-40.

GRUNERT, S. & JACKSON, R. J. (1994) The immediate downstream codon strongly influences the efficiency of utilization of eukaryotic translation initiation codons. *EMBO J,* 13**,** 3618-30.

GU, W., KWON, Y., OKO, R., HERMO, L. & HECHT, N. B. (1995) Poly (A) binding protein is bound to both stored and polysomal mRNAs in the mammalian testis. *Mol Reprod Dev,* 40**,** 273-85.

GUZELOGLU-KAYISLI, O., LALIOTI, M. D., AYDINER, F., SASSON, I., ILBAY, O., SAKKAS, D., LOWTHER, K. M., MEHLMANN, L. M. & SELI, E. (2012) Embryonic poly(A) binding protein (EPAB) is required for oocyte maturation and female fertility in mice. *Biochem J,* In Press.

GUZELOGLU-KAYISLI, O., PAULI, S., DEMIR, H., LALIOTI, M. D., SAKKAS, D. & SELI, E. (2008) Identification and characterization of human embryonic poly(A) binding protein (EPAB). *Mol Hum Reprod,* 14**,** 581-588.

HANDEL, M. A. & EPPIG, J. J. (1998) Sexual dimorphism in the regulation of mammalian meiosis. *Curr Top Dev Biol,* 37**,** 333-58.

HASEGAWA, E., KARASHIMA, T., SUMIYOSHI, E. & YAMAMOTO, M. (2006) C. elegans CPB-3 interacts with DAZ-1 and functions in multiple steps of germline development. *Dev Biol,* 295**,** 689-99.

HASHIMOTO, Y., MAEGAWA, S., NAGAI, T., YAMAHA, E., SUZUKI, H., YASUDA, K. & INOUE, K. (2004) Localized maternal factors are required for zebrafish germ cell formation. *Dev Biol,* 268**,** 152-61.

HASTON, K. M., TUNG, J. Y. & REIJO PERA, R. A. (2009) Dazl functions in maintenance of pluripotency and genetic and epigenetic programs of differentiation in mouse primordial germ cells in vivo and in vitro. *PLoS One,* 4**,** e5654.

HERMO, L., PELLETIER, R. M., CYR, D. G. & SMITH, C. E. (2009) Surfing the wave, cycle, life history, and genes/proteins expressed by testicular germ cells. Part 1: background to spermatogenesis, spermatogonia, and spermatocytes. *Microsc Res Tech,* 73**,** 241-78.

HERMO, L. & SMITH, C. E. (2011) Thirsty business: cell, region, and membrane specificity of aquaporins in the testis, efferent ducts, and epididymis and factors regulating their expression. *J Androl,* 32**,** 565-75.

HINNEBUSCH, A. G., DEVER, T. E. & ASANO, K. (2007) Mechanism of Translation Initiation in the Yeast Saccharomyces cerevisiae. IN MATHEWS, M. B., SONENBERG, N. & HERSHEY, J. W. B. (Eds.) *Translational Control in Biology and Medicine.* New York, Cold Spring Harbor Laboratory Press.

HIRSHFIELD, A. N. & DESANTI, A. M. (1995) Patterns of ovarian cell proliferation in rats during the embryonic period and the first three weeks postpartum. *Biol Reprod,* 53**,** 1208-21.

HODGMAN, R., TAY, J., MENDEZ, R. & RICHTER, J. D. (2001) CPEB phosphorylation and cytoplasmic polyadenylation are catalyzed by the kinase IAK1/Eg2 in maturing mouse oocytes. *Development,* 128**,** 2815-22.

HOLCIK, M. & SONENBERG, N. (2005) Translational control in stress and apoptosis. *Nat Rev Mol Cell Biol,* 6**,** 318-27.

HOOPFER, E. D., PENTON, A., WATTS, R. J. & LUO, L. (2008) Genomic analysis of Drosophila neuronal remodeling: a role for the RNA-binding protein Boule as a negative regulator of axon pruning. *J Neurosci,* 28**,** 6092-103.

HORNSTEIN, E., GIT, A., BRAUNSTEIN, I., AVNI, D. & MEYUHAS, O. (1999) The expression of poly(A)-binding protein gene is translationally regulated in a growth-dependent fashion through a 5'-terminal oligopyrimidine tract motif. *J Biol Chem,* 274**,** 1708-14.

HOSHINO, S., IMAI, M., KOBAYASHI, T., UCHIDA, N. & KATADA, T. (1999) The eukaryotic polypeptide chain releasing factor (eRF3/GSPT) carrying the translation termination signal to the 3'-Poly(A) tail of mRNA. Direct association of erf3/GSPT with polyadenylate-binding protein. *J Biol Chem,* 274**,** 16677-80.

HOSODA, N., KOBAYASHI, T., UCHIDA, N., FUNAKOSHI, Y., KIKUCHI, Y., HOSHINO, S. & KATADA, T. (2003) Translation termination factor eRF3 mediates mRNA decay through the regulation of deadenylation. *J Biol Chem,* 278**,** 38287-91.

HOUNG, A. K., MAGGINI, L., CLEMENT, C. Y. & REED, G. L. (1997) Identification and structure of activated-platelet protein-1, a protein with RNA-binding domain motifs that is expressed by activated platelets. *Eur J Biochem,* 243**,** 209-18.

HOUSTON, D. W. & KING, M. L. (2000) A critical role for Xdazl, a germ plasm-localized RNA, in the differentiation of primordial germ cells in Xenopus. *Development,* 127**,** 447-56.

HOUSTON, D. W., ZHANG, J., MAINES, J. Z., WASSERMAN, S. A. & KING, M. L. (1998) A Xenopus DAZ-like gene encodes an RNA component of germ plasm and is a functional homologue of Drosophila boule. *Development,* 125**,** 171-80.

HSIEH, M., ZAMAH, A. M. & CONTI, M. (2009) Epidermal growth factor-like growth factors in the follicular fluid: role in oocyte development and maturation. *Semin Reprod Med,* 27**,** 52-61.

HUANG, W. J., LIN, Y. W., HSIAO, K. N., EILBER, K. S., SALIDO, E. C. & YEN, P. H. (2008) Restricted expression of the human DAZ protein in premeiotic germ cells. *Hum Reprod,* 23**,** 1280-9.

HUBBARD, T. J., AKEN, B. L., AYLING, S., BALLESTER, B., BEAL, K., BRAGIN, E., BRENT, S., CHEN, Y., CLAPHAM, P., CLARKE, L., COATES, G., FAIRLEY, S., FITZGERALD, S., FERNANDEZ-BANET, J., GORDON, L., GRAF, S., HAIDER, S., HAMMOND, M., HOLLAND, R., HOWE, K., JENKINSON, A., JOHNSON, N., KAHARI, A., KEEFE, D., KEENAN, S., KINSELLA, R., KOKOCINSKI, F., KULESHA, E., LAWSON, D., LONGDEN, I., MEGY, K., MEIDL, P., OVERDUIN, B., PARKER, A., PRITCHARD, B., RIOS, D., SCHUSTER, M., SLATER, G.,

SMEDLEY, D., SPOONER, W., SPUDICH, G., TREVANION, S., VILELLA, A., VOGEL, J., WHITE, S., WILDER, S., ZADISSA, A., BIRNEY, E., CUNNINGHAM, F., CURWEN, V., DURBIN, R., FERNANDEZ-SUAREZ, X. M., HERRERO, J., KASPRZYK, A., PROCTOR, G., SMITH, J., SEARLE, S. & FLICEK, P. (2009) Ensembl 2009. *Nucleic Acids Res,* 37**,** D690-7.

HUMPHREYS, D. T., WESTMAN, B. J., MARTIN, D. I. & PREISS, T. (2005) MicroRNAs control translation initiation by inhibiting eukaryotic initiation factor 4E/cap and poly(A) tail function. *Proc Natl Acad Sci U S A,* 102**,** 16961-6.

IDLER, R. K. & YAN, W. (2012) Control of Messenger RNA Fate by RNA-Binding Proteins: An Emphasis on Mammalian Spermatogenesis. *J Androl,* 33**,** 309-37.

IMATAKA, H., GRADI, A. & SONENBERG, N. (1998) A newly identified N-terminal amino acid sequence of human eIF4G binds poly(A)-binding protein and functions in poly(A)-dependent translation. *EMBO J,* 17**,** 7480-9.

IMATAKA, H. & SONENBERG, N. (1997) Human eukaryotic translation initiation factor 4G (eIF4G) possesses two separate and independent binding sites for eIF4A. *Mol Cell Biol,* 17**,** 6940-7.

IVANOV, P. V., GEHRING, N. H., KUNZ, J. B., HENTZE, M. W. & KULOZIK, A. E. (2008) Interactions between UPF1, eRFs, PABP and the exon junction complex suggest an integrated model for mammalian NMD pathways. *EMBO J,* 27**,** 736-47.

JACKSON, R. J., HELLEN, C. U. & PESTOVA, T. V. (2010) The mechanism of eukaryotic translation initiation and principles of its regulation. *Nat Rev Mol Cell Biol,* 11**,** 113-27.

JENKINS, H. T., MALKOVA, B. & EDWARDS, T. A. (2011) Kinked beta-strands mediate high-affinity recognition of mRNA targets by the germ-cell regulator DAZL. *Proc Natl Acad Sci U S A,* 108**,** 18266-71.

JIAO, X., TRIFILLIS, P. & KILEDJIAN, M. (2002) Identification of target messenger RNA substrates for the murine deleted in azoospermia-like RNA-binding protein. *Biol Reprod,* 66**,** 475-85.

JINEK, M., FABIAN, M. R., COYLE, S. M., SONENBERG, N. & DOUDNA, J. A. (2010) Structural insights into the human GW182-PABC interaction in microRNA-mediated deadenylation. *Nat Struct Mol Biol,* 17**,** 238-40.

JOHNSON, J., BAGLEY, J., SKAZNIK-WIKIEL, M., LEE, H. J., ADAMS, G. B., NIIKURA, Y., TSCHUDY, K. S., TILLY, J. C., CORTES, M. L., FORKERT, R., SPITZER, T., IACOMINI, J., SCADDEN, D. T. & TILLY, J. L. (2005) Oocyte generation in adult mammalian ovaries by putative germ cells in bone marrow and peripheral blood. *Cell,* 122**,** 303-15.

JOHNSON, J., CANNING, J., KANEKO, T., PRU, J. K. & TILLY, J. L. (2004) Germline stem cells and follicular renewal in the postnatal mammalian ovary. *Nature,* 428**,** 145-50.

JOHNSON, M. H. (2007) *Essential Reproduction*, Blackwell Publishing.

JOINER, M. L. & WU, C. F. (2004) Nervous system function for the testis RNA-binding protein boule in Drosophila. *J Neurogenet,* 18**,** 341-63.

JOVINE, L., OUBRIDGE, C., AVIS, J. M. & NAGAI, K. (1996) Two structurally different RNA molecules are bound by the spliceosomal protein U1A using the same recognition strategy. *Structure,* 4**,** 621-31.

KAHVEJIAN, A., ROY, G. & SONENBERG, N. (2001) The mRNA closed-loop model: the function of PABP and PABP-interacting proteins in mRNA translation. *Cold Spring Harb Symp Quant Biol,* 66**,** 293-300.

KAHVEJIAN, A., SVITKIN, Y. V., SUKARIEH, R., M'BOUTCHOU, M. N. & SONENBERG, N. (2005) Mammalian poly(A)-binding protein is a eukaryotic translation initiation factor, which acts via multiple mechanisms. *Genes Dev,* 19**,** 104-13.

KAMISCHKE, A., GROMOLL, J., SIMONI, M., BEHRE, H. M. & NIESCHLAG, E. (1999) Transmission of a Y chromosomal deletion involving the deleted in azoospermia (DAZ) and chromodomain (CDY1) genes from father to son through intracytoplasmic sperm injection: case report. *Hum Reprod,* 14**,** 2320-2.

KARASHIMA, T., SUGIMOTO, A. & YAMAMOTO, M. (2000) Caenorhabditis elegans homologue of the human azoospermia factor DAZ is required for oogenesis but not for spermatogenesis. *Development,* 127**,** 1069-79.

KATO, Y., KANEDA, M., HATA, K., KUMAKI, K., HISANO, M., KOHARA, Y., OKANO, M., LI, E., NOZAKI, M. & SASAKI, H. (2007) Role of the Dnmt3 family in de novo methylation of imprinted and repetitive sequences during male germ cell development in the mouse. *Hum Mol Genet,* 16**,** 2272-80.

KEE, K., ANGELES, V. T., FLORES, M., NGUYEN, H. N. & REIJO PERA, R. A. (2009) Human DAZL, DAZ and BOULE genes modulate primordial germ-cell and haploid gamete formation. *Nature,* 462**,** 222-5.

KEENEY, S., GIROUX, C. N. & KLECKNER, N. (1997) Meiosis-specific DNA double-strand breaks are catalyzed by Spo11, a member of a widely conserved protein family. *Cell,* 88**,** 375-84.

KEHLER, J., TOLKUNOVA, E., KOSCHORZ, B., PESCE, M., GENTILE, L., BOIANI, M., LOMELI, H., NAGY, A., MCLAUGHLIN, K. J., SCHOLER, H. R. & TOMILIN, A. (2004) Oct4 is required for primordial germ cell survival. *EMBO Rep,* 5**,** 1078-83.

KELLEY, R. L., WANG, J., BELL, L. & KURODA, M. I. (1997) *Sex lethal* contols dosage compensation in *Drosophila* by a non-splicing mechanism. *Nature,* 387**,** 195-199.

KERR, C. L. & CHENG, L. (2009) The dazzle in germ cell differentiation. *J Mol Cell Biol,* 2**,** 26-9.

KERR, J. B., DUCKETT, R., MYERS, M., BRITT, K. L., MLADENOVSKA, T. & FINDLAY, J. K. (2006) Quantification of healthy follicles in the neonatal and adult mouse ovary: evidence for maintenance of primordial follicle supply. *Reproduction,* 132**,** 95-109.

KHALEGHPOUR, K., KAHVEJIAN, A., DE CRESCENZO, G., ROY, G., SVITKIN, Y. V., IMATAKA, H., O'CONNOR-MCCOURT, M. & SONENBERG, N. (2001) Dual interactions of the translational repressor Paip2 with poly(A) binding protein. *Mol Cell Biol,* 21**,** 5200-13.

KIM, B., COOKE, H. J. & RHEE, K. (2012) DAZL is essential for stress granule formation implicated in germ cell survival upon heat stress. *Development,* 139**,** 568-78.

KIM, J. H. & RICHTER, J. D. (2006) Opposing polymerase-deadenylase activities regulate cytoplasmic polyadenylation. *Mol Cell,* 24**,** 173-83.

KIM, J. H. & RICHTER, J. D. (2007) RINGO/cdk1 and CPEB mediate poly(A) tail stabilization and translational regulation by ePAB. *Genes Dev,* 21**,** 2571-9.

KIMBLE, J. & CRITTENDEN, S. L. (2007) Controls of germline stem cells, entry into meiosis, and the sperm/oocyte decision in Caenorhabditis elegans. *Annu Rev Cell Dev Biol,* 23**,** 405-33.

KIMURA, M., ISHIDA, K., KASHIWABARA, S. & BABA, T. (2009) Characterization of two cytoplasmic poly(A)-binding proteins, PABPC1 and PABPC2, in mouse spermatogenic cells. *Biol Reprod,* 80**,** 545-54.

KITAJIMA, T. S., SAKUNO, T., ISHIGURO, K., IEMURA, S., NATSUME, T., KAWASHIMA, S. A. & WATANABE, Y. (2006) Shugoshin collaborates with protein phosphatase 2A to protect cohesin. *Nature,* 441**,** 46-52.

KLEENE, K. C., MULLIGAN, E., STEIGER, D., DONOHUE, K. & MASTRANGELO, M. A. (1998) The mouse gene encoding the testis-specific isoform of Poly(A) binding protein (Pabp2) is an expressed retroposon: intimations that gene expression in spermatogenic cells facilitates the creation of new genes. *J Mol Evol,* 47**,** 275-81.

KLEENE, K. C., WANG, M. Y., CUTLER, M., HALL, C. & SHIH, D. (1994) Developmental expression of poly(A) binding protein mRNAs during spermatogenesis in the mouse. *Mol Reprod Dev,* 39**,** 355-64.

KNIGHT, P. G. & GLISTER, C. (2001) Potential local regulatory functions of inhibins, activins and follistatin in the ovary. *Reproduction,* 121**,** 503-12.

KOCER, A., REICHMANN, J., BEST, D. & ADAMS, I. R. (2009) Germ cell sex determination in mammals. *Mol Hum Reprod,* 15**,** 205-13.

KOUBOVA, J., MENKE, D. B., ZHOU, Q., CAPEL, B., GRISWOLD, M. D. & PAGE, D. C. (2006) Retinoic acid regulates sex-specific timing of meiotic initiation in mice. *Proc Natl Acad Sci U S A,* 103**,** 2474-9.

KOVANCI, E., ROHOZINSKI, J., SIMPSON, J. L., HEARD, M. J., BISHOP, C. E. & CARSON, S. A. (2007) Growth differentiating factor-9 mutations may be associated with premature ovarian failure. *Fertil Steril,* 87**,** 143-6.

KOZAK, M. (1989) Circumstances and mechanisms of inhibition of translation by secondary structure in eucaryotic mRNAs. *Mol. Cell. Biol.,* 9**,** 5134-5142.

KOZAK, M. (1990) Downstream secondary structure facilitates recognition of initiator codons by eukaryotic ribosomes. *Proc. Natl. Acad. Sci. USA,* 87**,** 8301-8305.

KOZAK, M. (1991a) Effects of long 5' leader sequences on initiation by eukaryotic ribosomes in vitro. *Gene Expression,* 1**,** 117-125.

KOZAK, M. (1991b) A short leader sequence impairs the fidelity of initiation by eukaryotic ribosomes. *Gene Expression,* 1**,** 111-115.

KOZAK, M. (1991c) Structural features in eukaryotic mRNAs that modulate the initiation of translation. *J. Biol. Chem.,* 266**,** 19867-19870.

KOZLOV, G., TREMPE, J. F., KHALEGHPOUR, K., KAHVEJIAN, A., EKIEL, I. & GEHRING, K. (2001) Structure and function of the C-terminal PABC

domain of human poly(A)-binding protein. *Proc Natl Acad Sci U S A,* 98**,** 4409-13.

KRISHNAMOORTHY, T., PAVITT, G. D., ZHANG, F., DEVER, T. E. & HINNEBUSCH, A. G. (2001) Tight binding of the phosphorylated alpha subunit of initiation factor 2 (eIF2alpha) to the regulatory subunits of guanine nucleotide exchange factor eIF2B is required for inhibition of translation initiation. *Mol Cell Biol,* 21**,** 5018-30.

KUALES, G., DE MULDER, K., GLASHAUSER, J., SALVENMOSER, W., TAKASHIMA, S., HARTENSTEIN, V., BEREZIKOV, E., SALZBURGER, W. & LADURNER, P. (2011) Boule-like genes regulate male and female gametogenesis in the flatworm Macrostomum lignano. *Dev Biol,* 357**,** 117-32.

KUDO, N. R., WASSMANN, K., ANGER, M., SCHUH, M., WIRTH, K. G., XU, H., HELMHART, W., KUDO, H., MCKAY, M., MARO, B., ELLENBERG, J., DE BOER, P. & NASMYTH, K. (2006) Resolution of chiasmata in oocytes requires separase-mediated proteolysis. *Cell,* 126**,** 135-46.

KUENG, P., NIKOLOVA, Z., DJONOV, V., HEMPHILL, A., ROHRBACH, V., BOEHLEN, D., ZUERCHER, G., ANDRES, A. C. & ZIEMIECKI, A. (1997) A novel family of serine/threonine kinases participating in spermiogenesis. *J Cell Biol,* 139**,** 1851-9.

KUERSTEN, S. & GOODWIN, E. B. (2003) The power of the 3' UTR: translational control and development. *Nat Rev Genet,* 4**,** 626-37.

KUHN, U. & PIELER, T. (1996) Xenopus poly(A) binding protein: functional domains in RNA binding and protein-protein interaction. *J Mol Biol,* 256**,** 20-30.

KUHN, U. & WAHLE, E. (2004) Structure and function of poly(A) binding proteins. *Biochim Biophys Acta,* 1678**,** 67-84.

LACKNER, D. H. & BAHLER, J. (2008) Translational control of gene expression from transcripts to transcriptomes. *Int Rev Cell Mol Biol,* 271**,** 199-251.

LAHN, B. T., TANG, Z. L., ZHOU, J., BARNDT, R. J., PARVINEN, M., ALLIS, C. D. & PAGE, D. C. (2002) Previously uncharacterized histone acetyltransferases implicated in mammalian spermatogenesis. *Proc Natl Acad Sci U S A,* 99**,** 8707-12.

LAISSUE, P., CHRISTIN-MAITRE, S., TOURAINE, P., KUTTENN, F., RITVOS, O., AITTOMAKI, K., BOURCIGAUX, N., JACQUESSON, L., BOUCHARD, P., FRYDMAN, R., DEWAILLY, D., REYSS, A. C., JEFFERY, L., BACHELOT, A., MASSIN, N., FELLOUS, M. & VEITIA, R. A. (2006) Mutations and sequence variants in GDF9 and BMP15 in patients with premature ovarian failure. *Eur J Endocrinol,* 154**,** 739-44.

LAMMERS, J. H., OFFENBERG, H. H., VAN AALDEREN, M., VINK, A. C., DIETRICH, A. J. & HEYTING, C. (1994) The gene encoding a major component of the lateral elements of synaptonemal complexes of the rat is related to X-linked lymphocyte-regulated genes. *Mol Cell Biol,* 14**,** 1137-46.

LAWSON, K. A. & HAGE, W. J. (1994) Clonal analysis of the origin of primordial germ cells in the mouse. *Ciba Found Symp,* 182**,** 68-84; discussion 84-91.

LE, H., TANGUAY, R. L., BALASTA, M. L., WEI, C. C., BROWNING, K. S., METZ, A. M., GOSS, D. J. & GALLIE, D. R. (1997) Translation initiation

factors eIF-iso4G and eIF-4B interact with the poly(A)-binding protein and increase its RNA binding activity. *J Biol Chem,* 272**,** 16247-55.

LE HIR, H., GATFIELD, D., IZAURRALDE, E. & MOORE, M. J. (2001) The exon-exon junction complex provides a binding platform for factors involved in mRNA export and nonsense-mediated mRNA decay. *EMBO J,* 20**,** 4987-97.

LE HIR, H., IZAURRALDE, E., MAQUAT, L. E. & MOORE, M. J. (2000a) The spliceosome deposits multiple proteins 20-24 nucleotides upstream of mRNA exon-exon junctions. *EMBO J,* 19**,** 6860-9.

LE HIR, H., MOORE, M. J. & MAQUAT, L. E. (2000b) Pre-mRNA splicing alters mRNP composition: evidence for stable association of proteins at exon-exon junctions. *Genes Dev,* 14**,** 1098-108.

LEE, K. H., LEE, S., KIM, B., CHANG, S., KIM, S. W., PAICK, J. S. & RHEE, K. (2006) Dazl can bind to dynein motor complex and may play a role in transport of specific mRNAs. *EMBO J,* 25**,** 4263-70.

LEE, S. L., SADOVSKY, Y., SWIRNOFF, A. H., POLISH, J. A., GODA, P., GAVRILINA, G. & MILBRANDT, J. (1996) Luteinizing hormone deficiency and female infertility in mice lacking the transcription factor NGFI-A (Egr-1). *Science,* 273**,** 1219-21.

LEE, Y. Y., CEVALLOS, R. C. & JAN, E. (2009) An upstream open reading frame regulates translation of GADD34 during cellular stresses that induce eIF2alpha phosphorylation. *J Biol Chem,* 284**,** 6661-73.

LIN, Y., GILL, M. E., KOUBOVA, J. & PAGE, D. C. (2008) Germ cell-intrinsic and -extrinsic factors govern meiotic initiation in mouse embryos. *Science,* 322**,** 1685-7.

LIN, Y. & PAGE, D. C. (2005) Dazl deficiency leads to embryonic arrest of germ cell development in XY C57BL/6 mice. *Dev Biol,* 288**,** 309-16.

LING, J., MORLEY, S. J., PAIN, V. M., MARZLUFF, W. F. & GALLIE, D. R. (2002) The histone 3'-terminal stem-loop-binding protein enhances translation through a functional and physical interaction with eukaryotic initiation factor 4G (eIF4G) and eIF3. *Mol Cell Biol,* 22**,** 7853-67.

LUETJENS, C. M., XU, E. Y., REJO PERA, R. A., KAMISCHKE, A., NIESCHLAG, E. & GROMOLL, J. (2004) Association of meiotic arrest with lack of BOULE protein expression in infertile men. *J Clin Endocrinol Metab,* 89**,** 1926-33.

LYABIN, D. N., ELISEEVA, I. A., SKABKINA, O. V. & OVCHINNIKOV, L. P. (2011) Interplay between Y-box-binding protein 1 (YB-1) and poly(A) binding protein (PABP) in specific regulation of YB-1 mRNA translation. *RNA Biol,* 8.

MAAG, D., ALGIRE, M. A. & LORSCH, J. R. (2006) Communication between eukaryotic translation initiation factors 5 and 1A within the ribosomal pre-initiation complex plays a role in start site selection. *J Mol Biol,* 356**,** 724-37.

MAAG, D., FEKETE, C. A., GRYCZYNSKI, Z. & LORSCH, J. R. (2005) A conformational change in the eukaryotic translation preinitiation complex and release of eIF1 signal recognition of the start codon. *Mol Cell,* 17**,** 265-75.

MACIEJOWSKI, J., AHN, J. H., CIPRIANI, P. G., KILLIAN, D. J., CHAUDHARY, A. L., LEE, J. I., VOUTEV, R., JOHNSEN, R. C.,

BAILLIE, D. L., GUNSALUS, K. C., FITCH, D. H. & HUBBARD, E. J. (2005) Autosomal genes of autosomal/X-linked duplicated gene pairs and germ-line proliferation in Caenorhabditis elegans. *Genetics,* 169**,** 1997-2011.

MAEGAWA, S., YAMASHITA, M., YASUDA, K. & INOUE, K. (2002) Zebrafish DAZ-like protein controls translation via the sequence 'GUUC'. *Genes Cells,* 7**,** 971-84.

MAEGAWA, S., YASUDA, K. & INOUE, K. (1999) Maternal mRNA localization of zebrafish DAZ-like gene. *Mech Dev,* 81**,** 223-6.

MAHADEVAIAH, S. K., TURNER, J. M., BAUDAT, F., ROGAKOU, E. P., DE BOER, P., BLANCO-RODRIGUEZ, J., JASIN, M., KEENEY, S., BONNER, W. M. & BURGOYNE, P. S. (2001) Recombinational DNA double-strand breaks in mice precede synapsis. *Nat Genet,* 27**,** 271-6.

MAINES, J. Z. & WASSERMAN, S. A. (1999) Post-transcriptional regulation of the meiotic Cdc25 protein Twine by the Dazl orthologue Boule. *Nat Cell Biol,* 1**,** 171-4.

MAJUMDAR, R., BANDYOPADHYAY, A. & MAITRA, U. (2003) Mammalian translation initiation factor eIF1 functions with eIF1A and eIF3 in the formation of a stable 40 S preinitiation complex. *J Biol Chem,* 278**,** 6580-7.

MANGUS, D. A., EVANS, M. C. & JACOBSON, A. (2003) Poly(A)-binding proteins: multifunctional scaffolds for the post-transcriptional control of gene expression. *Genome Biol,* 4**,** 223.

MARATOU, K., FORSTER, T., COSTA, Y., TAGGART, M., SPEED, R. M., IRELAND, J., TEAGUE, P., ROY, D. & COOKE, H. J. (2004) Expression profiling of the developing testis in wild-type and Dazl knockout mice. *Mol Reprod Dev,* 67**,** 26-54.

MARSTON, A. L. & AMON, A. (2004) Meiosis: cell-cycle controls shuffle and deal. *Nat Rev Mol Cell Biol,* 5**,** 983-97.

MARTIN, F., SCHALLER, A., EGLITE, S., SCHUMPERLI, D. & MULLER, B. (1997) The gene for histone RNA hairpin binding protein is located on human chromosome 4 and encodes a novel type of RNA binding protein. *Embo J,* 16**,** 769-78.

MARTINEAU, Y., DERRY, M. C., WANG, X., YANAGIYA, A., BERLANGA, J. J., SHYU, A. B., IMATAKA, H., GEHRING, K. & SONENBERG, N. (2008) The poly(A)-binding protein-interacting protein 1 binds to eIF3 to stimulate translation. *Mol Cell Biol*.

MARUYAMA, R., ENDO, S., SUGIMOTO, A. & YAMAMOTO, M. (2005) Caenorhabditis elegans DAZ-1 is expressed in proliferating germ cells and directs proper nuclear organization and cytoplasmic core formation during oogenesis. *Dev Biol,* 277**,** 142-54.

MARZLUFF, W. F., WAGNER, E. J. & DURONIO, R. J. (2008) Metabolism and regulation of canonical histone mRNAs: life without a poly(A) tail. *Nat Rev Genet,* 9**,** 843-54.

MATZUK, M. M., BURNS, K. H., VIVEIROS, M. M. & EPPIG, J. J. (2002) Intercellular communication in the mammalian ovary: oocytes carry the conversation. *Science,* 296**,** 2178-80.

MATZUK, M. M. & LAMB, D. J. (2002) Genetic dissection of mammalian fertility pathways. *Nat Cell Biol,* 4 Suppl**,** s41-9.

MATZUK, M. M. & LAMB, D. J. (2008) The biology of infertility: research advances and clinical challenges. *Nat Med,* 14**,** 1197-213.

MAU KAI, C., JUUL, A., MCELREAVEY, K., OTTESEN, A. M., GARN, I. D., MAIN, K. M., LOFT, A., JORGENSEN, N., SKAKKEBAEK, N. E., ANDERSEN, A. N. & RAJPERT-DE MEYTS, E. (2008) Sons conceived by assisted reproduction techniques inherit deletions in the azoospermia factor (AZF) region of the Y chromosome and the DAZ gene copy number. *Hum Reprod,* 23**,** 1669-78.

MAZUMDER, B., SESHADRI, V. & FOX, P. L. (2003) Translational control by the 3'-UTR: the ends specify the means. *Trends Biochem Sci,* 28**,** 91-8.

MCLAREN, A. (2003) Primordial germ cells in the mouse. *Dev Biol,* 262**,** 1-15.

MCLAREN, A. & LAWSON, K. A. (2005) How is the mouse germ-cell lineage established? *Differentiation,* 73**,** 435-7.

MCNEILLY, J. R., SAUNDERS, P. T., TAGGART, M., CRANFIELD, M., COOKE, H. J. & MCNEILLY, A. S. (2000) Loss of oocytes in Dazl knockout mice results in maintained ovarian steroidogenic function but altered gonadotropin secretion in adult animals. *Endocrinology,* 141**,** 4284-94.

MCNEILLY, J. R., WATSON, E. A., WHITE, Y. A., MURRAY, A. A., SPEARS, N. & MCNEILLY, A. S. (2011) Decreased oocyte DAZL expression in mice results in increased litter size by modulating follicle-stimulating hormone-induced follicular growth. *Biol Reprod,* 85**,** 584-93.

MEIKAR, O., DA ROS, M., KORHONEN, H. & KOTAJA, N. (2011) Chromatoid body and small RNAs in male germ cells. *Reproduction,* 142**,** 195-209.

MELO, E. O., DHALIA, R., MARTINS DE SA, C., STANDART, N. & DE MELO NETO, O. P. (2003) Identification of a C-terminal poly(A)-binding protein (PABP)-PABP interaction domain: role in cooperative binding to poly (A) and efficient cap distal translational repression. *J Biol Chem,* 278**,** 46357-68.

MENDEZ, R. & RICHTER, J. D. (2001) Translational control by CPEB: a means to the end. *Nat Rev Mol Cell Biol,* 2**,** 521-9.

MENDIS, S. H., MEACHEM, S. J., SARRAJ, M. A. & LOVELAND, K. L. (2011) Activin A balances Sertoli and germ cell proliferation in the fetal mouse testis. *Biol Reprod,* 84**,** 379-91.

MEUWISSEN, R. L., OFFENBERG, H. H., DIETRICH, A. J., RIESEWIJK, A., VAN IERSEL, M. & HEYTING, C. (1992) A coiled-coil related protein specific for synapsed regions of meiotic prophase chromosomes. *Embo J,* 11**,** 5091-100.

MICHEL, Y. M., PONCET, D., PIRON, M., KEAN, K. M. & BORMAN, A. M. (2000) Cap-Poly(A) synergy in mammalian cell-free extracts. Investigation of the requirements for poly(A)-mediated stimulation of translation initiation. *J Biol Chem,* 275**,** 32268-76.

MIGNONE, F., CARMELA, G., LIUNI, S. & PESOLE, G. (2002) Untranslated regions of mRNAs. *Genome Biology,* 3**,** 4.1-4.10.

MILLAR, M. R., SHARPE, R. M., WEINBAUER, G. F., FRASER, H. M. & SAUNDERS, P. T. (2000) Marmoset spermatogenesis: organizational similarities to the human. *Int J Androl,* 23**,** 266-77.

MITA, K. & YAMASHITA, M. (2000) Expression of Xenopus Daz-like protein during gametogenesis and embryogenesis. *Mech Dev,* 94**,** 251-5.

MONK, M. & MCLAREN, A. (1981) X-chromosome activity in foetal germ cells of the mouse. *J Embryol Exp Morphol,* 63**,** 75-84.

MONTERO, H., ARIAS, C. F. & LOPEZ, S. (2006) Rotavirus Nonstructural Protein NSP3 is not required for viral protein synthesis. *J Virol,* 80**,** 9031-8.

MOORE, F. L., JARUZELSKA, J., DORFMAN, D. M. & REIJO-PERA, R. A. (2004a) Identification of a novel gene, DZIP (DAZ-interacting protein), that encodes a protein that interacts with DAZ (deleted in azoospermia) and is expressed in embryonic stem cells and germ cells. *Genomics,* 83**,** 834-43.

MOORE, F. L., JARUZELSKA, J., FOX, M. S., URANO, J., FIRPO, M. T., TUREK, P. J., DORFMAN, D. M. & PERA, R. A. (2003) Human Pumilio-2 is expressed in embryonic stem cells and germ cells and interacts with DAZ (Deleted in AZoospermia) and DAZ-like proteins. *Proc Natl Acad Sci U S A,* 100**,** 538-43.

MOORE, R. K., ERICKSON, G. F. & SHIMASAKI, S. (2004b) Are BMP-15 and GDF-9 primary determinants of ovulation quota in mammals? *Trends Endocrinol Metab,* 15**,** 356-61.

MORELLI, M. A. & COHEN, P. E. (2005) Not all germ cells are created equal: aspects of sexual dimorphism in mammalian meiosis. *Reproduction,* 130**,** 761-81.

MORRIS, D. R. & GEBALLE, A. P. (2000) Upstream open reading frames as regulators of mRNA translation. *Mol Cell Biol,* 20**,** 8635-42.

MUCKENTHALER, M., GRAY, N. K. & HENTZE, M. W. (1998) IRP-1 binding to ferritin mRNA prevents the recruitment of the small ribosomal subunit by the cap-binding complex eIF4F. *Mol Cell,* 2**,** 383-8.

MUNROE, D. & JACOBSON, A. (1990) mRNA poly(A) tail, a 3' enhancer of translational initiation. *Mol Cell Biol,* 10**,** 3441-55.

MURRAY, S. M., YANG, S. Y. & VAN DOREN, M. (2010) Germ cell sex determination: a collaboration between soma and germline. *Curr Opin Cell Biol,* 22**,** 722-9.

NAJMABADI, H., HUANG, V., YEN, P., SUBBARAO, M. N., BHASIN, D., BANAAG, L., NASEERUDDIN, S., DE KRETSER, D. M., BAKER, H. W., MCLACHLAN, R. I. & ET AL. (1996) Substantial prevalence of microdeletions of the Y-chromosome in infertile men with idiopathic azoospermia and oligozoospermia detected using a sequence-tagged site-based mapping strategy. *J Clin Endocrinol Metab,* 81**,** 1347-52.

NAKAMURA, A., SATO, K. & HANYU-NAKAMURA, K. (2004) Drosophila cup is an eIF4E binding protein that associates with Bruno and regulates oskar mRNA translation in oogenesis. *Dev Cell,* 6**,** 69-78.

NAKAMURA, T., ARAI, Y., UMEHARA, H., MASUHARA, M., KIMURA, T., TANIGUCHI, H., SEKIMOTO, T., IKAWA, M., YONEDA, Y., OKABE, M., TANAKA, S., SHIOTA, K. & NAKANO, T. (2007) PGC7/Stella protects against DNA demethylation in early embryogenesis. *Nat Cell Biol,* 9**,** 64-71.

NANDA, J. S., CHEUNG, Y. N., TAKACS, J. E., MARTIN-MARCOS, P., SAINI, A. K., HINNEBUSCH, A. G. & LORSCH, J. R. (2009) eIF1 controls

multiple steps in start codon recognition during eukaryotic translation initiation. *J Mol Biol,* 394**,** 268-85.

NAPOLI, I., MERCALDO, V., BOYL, P. P., ELEUTERI, B., ZALFA, F., DE RUBEIS, S., DI MARINO, D., MOHR, E., MASSIMI, M., FALCONI, M., WITKE, W., COSTA-MATTIOLI, M., SONENBERG, N., ACHSEL, T. & BAGNI, C. (2008) The fragile X syndrome protein represses activity-dependent translation through CYFIP1, a new 4E-BP. *Cell,* 134**,** 1042-54.

NAVARRO-COSTA, P., NOGUEIRA, P., CARVALHO, M., LEAL, F., CORDEIRO, I., CALHAZ-JORGE, C., GONCALVES, J. & PLANCHA, C. E. (2010) Incorrect DNA methylation of the DAZL promoter CpG island associates with defective human sperm. *Hum Reprod,* 25**,** 2647-54.

NEWBURY, S. F. (2006) Control of mRNA stability in eukaryotes. *Biochem Soc Trans,* 34**,** 30-4.

NGUYEN-CHI, M. & MORELLO, D. (2011) RNA-binding proteins, RNA granules, and gametes: is unity strength? *Reproduction,* 142**,** 803-17.

NICOL, L., BISHOP, S. C., PONG-WONG, R., BENDIXEN, C., HOLM, L. E., RHIND, S. M. & MCNEILLY, A. S. (2009) Homozygosity for a single base-pair mutation in the oocyte-specific GDF9 gene results in sterility in Thoka sheep. *Reproduction,* 138**,** 921-33.

NIEDERBERGER, C., AGULNIK, A. I., CHO, Y., LAMB, D. & BISHOP, C. E. (1997) In situ hybridization shows that Dazla expression in mouse testis is restricted to premeiotic stages IV-VI of spermatogenesis. *Mamm Genome,* 8**,** 277-8.

NIETFELD, W., MENTZEL, H. & PIELER, T. (1990) The Xenopus laevis poly(A) binding protein is composed of multiple functionally independent RNA binding domains. *Embo J,* 9**,** 3699-705.

NISHI, S., HOSHI, N., KASAHARA, M., ISHIBASHI, T. & FUJIMOTO, S. (1999) Existence of human DAZLA protein in the cytoplasm of human oocytes. *Mol Hum Reprod,* 5**,** 495-7.

OATLEY, J. M. & BRINSTER, R. L. (2008) Regulation of spermatogonial stem cell self-renewal in mammals. *Annu Rev Cell Dev Biol,* 24**,** 263-86.

OHH, M., YAUCH, R. L., LONERGAN, K. M., WHALEY, J. M., STEMMER-RACHAMIMOV, A. O., LOUIS, D. N., GAVIN, B. J., KLEY, N., KAELIN, W. G., JR. & ILIOPOULOS, O. (1998) The von Hippel-Lindau tumor suppressor protein is required for proper assembly of an extracellular fibronectin matrix. *Mol Cell,* 1**,** 959-68.

OHINATA, Y., PAYER, B., O'CARROLL, D., ANCELIN, K., ONO, Y., SANO, M., BARTON, S. C., OBUKHANYCH, T., NUSSENZWEIG, M., TARAKHOVSKY, A., SAITOU, M. & SURANI, M. A. (2005) Blimp1 is a critical determinant of the germ cell lineage in mice. *Nature,* 436**,** 207-13.

OKOCHI, K., SUZUKI, T., INOUE, J., MATSUDA, S. & YAMAMOTO, T. (2005) Interaction of anti-proliferative protein Tob with poly(A)-binding protein and inducible poly(A)-binding protein: implication of Tob in translational control. *Genes Cells,* 10**,** 151-63.

OLDFIELD, S., JONES, B. L., TANTON, D. & PROUD, C. G. (1994) Use of monoclonal antibodies to study the structure and function of eukaryotic protein synthesis initiation factor eIF-2B. *Eur J Biochem,* 221**,** 399-410.

ORPHANIDES, G. & REINBERG, D. (2002) A unified theory of gene expression. *Cell,* 108**,** 439-51.

OTORI, M., KARASHIMA, T. & YAMAMOTO, M. (2006) The Caenorhabditis elegans homologue of deleted in azoospermia is involved in the sperm/oocyte switch. *Mol Biol Cell,* 17**,** 3147-55.

PADMANABHAN, K. & RICHTER, J. D. (2006) Regulated Pumilio-2 binding controls RINGO/Spy mRNA translation and CPEB activation. *Genes Dev,* 20**,** 199-209.

PALMER, J. S., ZHAO, Z. Z., HOEKSTRA, C., HAYWARD, N. K., WEBB, P. M., WHITEMAN, D. C., MARTIN, N. G., BOOMSMA, D. I., DUFFY, D. L. & MONTGOMERY, G. W. (2006) Novel variants in growth differentiation factor 9 in mothers of dizygotic twins. *J Clin Endocrinol Metab,* 91**,** 4713-6.

PAN, H. A., LEE, Y. C., TENG, Y. N., TSAI, S. J., LIN, Y. M. & KUO, P. L. (2008) CDC25 protein expression and interaction with DAZL in human corpus luteum. *Fertil Steril*.

PAN, H. A., LEE, Y. C., TENG, Y. N., TSAI, S. J., LIN, Y. M. & KUO, P. L. (2009) CDC25 protein expression and interaction with DAZL in human corpus luteum. *Fertil Steril,* 92**,** 1997-2003.

PAN, H. A., TSAI, S. J., CHEN, C. W., LEE, Y. C., LIN, Y. M. & KUO, P. L. (2002) Expression of DAZL protein in the human corpus luteum. *Mol Hum Reprod,* 8**,** 540-5.

PARASKEVA, E., GRAY, N. K., SCHLAGER, B., WEHR, K. & HENTZE, M. W. (1999) Ribosomal pausing and scanning arrest as mechanisms of translational regulation from cap-distal iron-responsive elements. *Mol Cell Biol,* 19**,** 807-16.

PARONETTO, M. P. & SETTE, C. (2009) Role of RNA-binding proteins in mammalian spermatogenesis. *Int J Androl,* 33**,** 2-12.

PASSMORE, L. A., SCHMEING, T. M., MAAG, D., APPLEFIELD, D. J., ACKER, M. G., ALGIRE, M. A., LORSCH, J. R. & RAMAKRISHNAN, V. (2007) The eukaryotic translation initiation factors eIF1 and eIF1A induce an open conformation of the 40S ribosome. *Mol Cell,* 26**,** 41-50.

PATEL, G. P. & BAG, J. (2006) IMP1 interacts with poly(A)-binding protein (PABP) and the autoregulatory translational control element of PABP-mRNA through the KH III-IV domain. *FEBS J,* 273**,** 5678-90.

PELTTARI, J., HOJA, M. R., YUAN, L., LIU, J. G., BRUNDELL, E., MOENS, P., SANTUCCI-DARMANIN, S., JESSBERGER, R., BARBERO, J. L., HEYTING, C. & HOOG, C. (2001) A meiotic chromosomal core consisting of cohesin complex proteins recruits DNA recombination proteins and promotes synapsis in the absence of an axial element in mammalian meiotic cells. *Mol Cell Biol,* 21**,** 5667-77.

PEPLING, M. E. (2006) From primordial germ cell to primordial follicle: mammalian female germ cell development. *Genesis,* 44**,** 622-32.

PEPLING, M. E. & SPRADLING, A. C. (1998) Female mouse germ cells form synchronously dividing cysts. *Development,* 125**,** 3323-8.

PESCE, M., WANG, X., WOLGEMUTH, D. J. & SCHOLER, H. (1998) Differential expression of the Oct-4 transcription factor during mouse germ cell differentiation. *Mech Dev,* 71**,** 89-98.

PESTOVA, T. V., BORUKHOV, S. I. & HELLEN, C. U. (1998) Eukaryotic ribosomes require initiation factors 1 and 1A to locate initiation codons. *Nature,* 394**,** 854-9.

PESTOVA, T. V. & KOLUPAEVA, V. G. (2002) The roles of individual eukaryotic translation initiation factors in ribosomal scanning and initiation codon selection. *Genes Dev,* 16**,** 2906-22.

PESTOVA, T. V., LORSCH, J. R. & HELLEN, C. U. (2007a) The mechanism of translation initiation in eukaryotes. IN MATHEWS, M. B., SONENBERG, N. & HERSHEY, J. W. B. (Eds.) *Translational control in biology and medicine.* New York, Cold Spring Harbor Laboratory Press.

PESTOVA, T. V., LORSCH, J. R. & HELLEN, C. U. T. (2007b) Mechanism of Trnaslation Initiation in Eukaryotes. IN MB, M., N, S. & JWB, H. (Eds.) *Translational Control in Biology and Medicine.* New York, Cold Spring Harbor Press.

PETERSEN, C. P., BORDELEAU, M. E., PELLETIER, J. & SHARP, P. A. (2006) Short RNAs repress translation after initiation in mammalian cells. *Mol Cell,* 21**,** 533-42.

PETRONCZKI, M., SIOMOS, M. F. & NASMYTH, K. (2003) Un menage a quatre: the molecular biology of chromosome segregation in meiosis. *Cell,* 112**,** 423-40.

PILLAI, R. S., BHATTACHARYYA, S. N., ARTUS, C. G., ZOLLER, T., COUGOT, N., BASYUK, E., BERTRAND, E. & FILIPOWICZ, W. (2005) Inhibition of translational initiation by Let-7 MicroRNA in human cells. *Science,* 309**,** 1573-6.

PIQUE, M., LOPEZ, J. M., FOISSAC, S., GUIGO, R. & MENDEZ, R. (2008) A combinatorial code for CPE-mediated translational control. *Cell,* 132**,** 434-48.

POLACEK, C., FOLEY, J. E. & HARRIS, E. (2009a) Conformational changes in the solution structure of the dengue virus 5' end in the presence and absence of the 3' untranslated region. *J Virol,* 83**,** 1161-6.

POLACEK, C., FRIEBE, P. & HARRIS, E. (2009b) Poly(A)-binding protein binds to the non-polyadenylated 3' untranslated region of dengue virus and modulates translation efficiency. *J Gen Virol,* 90**,** 687-92.

POPE, C., MCNEILLY, J. R., COUTTS, S., MILLAR, M., ANDERSON, R. A. & MCNEILLY, A. S. (2006) Gonadotrope and thyrotrope development in the human and mouse anterior pituitary gland. *Dev Biol,* 297**,** 172-81.

PRASAD, C. K., MAHADEVAN, M., MACNICOL, M. C. & MACNICOL, A. M. (2008) Mos 3' UTR regulatory differences underlie species-specific temporal patterns of Mos mRNA cytoplasmic polyadenylation and translational recruitment during oocyte maturation. *Mol Reprod Dev,* 75**,** 1258-68.

PRIETO, I., SUJA, J. A., PEZZI, N., KREMER, L., MARTINEZ, A. C., RUFAS, J. S. & BARBERO, J. L. (2001) Mammalian STAG3 is a cohesin specific to sister chromatid arms in meiosis I. *Nat Cell Biol,* 3**,** 761-6.

QUENAULT, T., LITHGOW, T. & TRAVEN, A. (2011) PUF proteins: repression, activation and mRNA localization. *Trends Cell Biol,* 21**,** 104-12.

RACKI, W. J. & RICHTER, J. D. (2006) CPEB controls oocyte growth and follicle development in the mouse. *Development,* 133**,** 4527-37.

REIJO, R., ALAGAPPAN, R. K., PATRIZIO, P. & PAGE, D. C. (1996a) Severe oligozoospermia resulting from deletions of azoospermia factor gene on Y chromosome. *Lancet,* 347**,** 1290-3.

REIJO, R., LEE, T. Y., SALO, P., ALAGAPPAN, R., BROWN, L. G., ROSENBERG, M., ROZEN, S., JAFFE, T., STRAUS, D., HOVATTA, O. & ET AL. (1995) Diverse spermatogenic defects in humans caused by Y chromosome deletions encompassing a novel RNA-binding protein gene. *Nat Genet,* 10**,** 383-93.

REIJO, R., SELIGMAN, J., DINULOS, M. B., JAFFE, T., BROWN, L. G., DISTECHE, C. M. & PAGE, D. C. (1996b) Mouse autosomal homolog of DAZ, a candidate male sterility gene in humans, is expressed in male germ cells before and after puberty. *Genomics,* 35**,** 346-52.

REIJO, R. A., DORFMAN, D. M., SLEE, R., RENSHAW, A. A., LOUGHLIN, K. R., COOKE, H. & PAGE, D. C. (2000) DAZ family proteins exist throughout male germ cell development and transit from nucleus to cytoplasm at meiosis in humans and mice. *Biol Reprod,* 63**,** 1490-6.

REPPING, S., DE VRIES, J. W., VAN DAALEN, S. K., KORVER, C. M., LESCHOT, N. J. & VAN DER VEEN, F. (2003) The use of spermHALO-FISH to determine DAZ gene copy number. *Mol Hum Reprod,* 9**,** 183-8.

REYNOLDS, N., COLLIER, B., BINGHAM, V., GRAY, N. K. & COOKE, H. J. (2007) Translation of the synaptonemal complex component Sycp3 is enhanced in vivo by the germ cell specific regulator Dazl. *RNA,* 13**,** 974-81.

REYNOLDS, N., COLLIER, B., MARATOU, K., BINGHAM, V., SPEED, R. M., TAGGART, M., SEMPLE, C. A., GRAY, N. K. & COOKE, H. J. (2005) Dazl binds in vivo to specific transcripts and can regulate the pre-meiotic translation of Mvh in germ cells. *Hum Mol Genet,* 14**,** 3899-909.

RICHARDS, J. S. (1980) Maturation of ovarian follicles: actions and interactions of pituitary and ovarian hormones on follicular cell differentiation. *Physiol Rev,* 60**,** 51-89.

RICHARDS, J. S. (2005) Ovulation: new factors that prepare the oocyte for fertilization. *Mol Cell Endocrinol,* 234**,** 75-9.

RICHARDS, J. S., RUSSELL, D. L., OCHSNER, S. & ESPEY, L. L. (2002) Ovulation: new dimensions and new regulators of the inflammatory-like response. *Annu Rev Physiol,* 64**,** 69-92.

RICHTER, J. D. (2007) CPEB: a life in translation. *Trends Biochem Sci,* 32**,** 279-85.

RICHTER, J. D. & SONENBERG, N. (2005) Regulation of cap-dependent translation by eIF4E inhibitory proteins. *Nature,* 433**,** 477-80.

ROUAULT, T. A. (2006) The role of iron regulatory proteins in mammalian iron homeostasis and disease. *Nat Chem Biol,* 2**,** 406-14.

ROY, G., DE CRESCENZO, G., KHALEGHPOUR, K., KAHVEJIAN, A., O'CONNOR-MCCOURT, M. & SONENBERG, N. (2002) Paip1 interacts with poly(A) binding protein through two independent binding motifs. *Mol Cell Biol,* 22**,** 3769-82.

RUGGIU, M. & COOKE, H. J. (2000) In vivo and in vitro analysis of homodimerisation activity of the mouse Dazl1 protein. *Gene,* 252**,** 119-26.

RUGGIU, M., SAUNDERS, P. T. & COOKE, H. J. (2000) Dynamic subcellular distribution of the DAZL protein is confined to primate male germ cells. *J Androl,* 21**,** 470-7.

RUGGIU, M., SPEED, R., TAGGART, M., MCKAY, S. J., KILANOWSKI, F., SAUNDERS, P., DORIN, J. & COOKE, H. J. (1997) The mouse Dazla gene encodes a cytoplasmic protein essential for gametogenesis. *Nature,* 389**,** 73-7.

RUSSEL, L. D. (1993) *Role of Sertoli cells in spermiation.*, Cache River Press.

RUSSELL, L., ETTLIN, R., HIKIM, A. & CLEGG, E. (1990) *Histological and Histopathological Evaluation of the Testis,* Clearwater, Cache River Press.

SACHS, A. B., BOND, M. W. & KORNBERG, R. D. (1986) A single gene from yeast for both nuclear and cytoplasmic polyadenylate-binding proteins: domain structure and expression. *Cell,* 45**,** 827-35.

SACHS, A. B., DAVIS, R. W. & KORNBERG, R. D. (1987) A single domain of yeast poly(A)-binding protein is necessary and sufficient for RNA binding and cell viability. *Mol Cell Biol,* 7**,** 3268-76.

SAITOU, M., BARTON, S. C. & SURANI, M. A. (2002) A molecular programme for the specification of germ cell fate in mice. *Nature,* 418**,** 293-300.

SAITOU, M., PAYER, B., O'CARROLL, D., OHINATA, Y. & SURANI, M. A. (2005) Blimp1 and the emergence of the germ line during development in the mouse. *Cell Cycle,* 4**,** 1736-40.

SARKISSIAN, M., MENDEZ, R. & RICHTER, J. D. (2004) Progesterone and insulin stimulation of CPEB-dependent polyadenylation is regulated by Aurora A and glycogen synthase kinase-3. *Genes Dev,* 18**,** 48-61.

SAUNDERS, P. T., TURNER, J. M., RUGGIU, M., TAGGART, M., BURGOYNE, P. S., ELLIOTT, D. & COOKE, H. J. (2003) Absence of mDazl produces a final block on germ cell development at meiosis. *Reproduction,* 126**,** 589-97.

SAXENA, R., BROWN, L. G., HAWKINS, T., ALAGAPPAN, R. K., SKALETSKY, H., REEVE, M. P., REIJO, R., ROZEN, S., DINULOS, M. B., DISTECHE, C. M. & PAGE, D. C. (1996) The DAZ gene cluster on the human Y chromosome arose from an autosomal gene that was transposed, repeatedly amplified and pruned. *Nat Genet,* 14**,** 292-9.

SAXENA, R., DE VRIES, J. W., REPPING, S., ALAGAPPAN, R. K., SKALETSKY, H., BROWN, L. G., MA, P., CHEN, E., HOOVERS, J. M. & PAGE, D. C. (2000) Four DAZ genes in two clusters found in the AZFc region of the human Y chromosome. *Genomics,* 67**,** 256-67.

SCHALK, J. A., DIETRICH, A. J., VINK, A. C., OFFENBERG, H. H., VAN AALDEREN, M. & HEYTING, C. (1998) Localization of SCP2 and SCP3 protein molecules within synaptonemal complexes of the rat. *Chromosoma,* 107**,** 540-8.

SCHOENBERG, D. R. & MAQUAT, L. E. (2012) Regulation of cytoplasmic mRNA decay. *Nat Rev Genet,* 13**,** 246-59.

SCHRANS-STASSEN, B. H., SAUNDERS, P. T., COOKE, H. J. & DE ROOIJ, D. G. (2001) Nature of the spermatogenic arrest in Dazl -/- mice. *Biol Reprod,* 65**,** 771-6.

SCHWANHAUSSER, B., BUSSE, D., LI, N., DITTMAR, G., SCHUCHHARDT, J., WOLF, J., CHEN, W. & SELBACH, M. (2011) Global quantification of mammalian gene expression control. *Nature,* 473**,** 337-42.

SCHWARTZ, D. C. & PARKER, R. (2000) mRNA decapping in yeast requires dissociation of the cap binding protein, eukaryotic translation initiation factor 4E. *Mol Cell Biol,* 20**,** 7933-42.

SEKIDO, R., BAR, I., NARVAEZ, V., PENNY, G. & LOVELL-BADGE, R. (2004) SOX9 is up-regulated by the transient expression of SRY specifically in Sertoli cell precursors. *Dev Biol,* 274**,** 271-9.

SEKIDO, R. & LOVELL-BADGE, R. (2008) Sex determination involves synergistic action of SRY and SF1 on a specific Sox9 enhancer. *Nature,* 453**,** 930-4.

SELI, E., LALIOTI, M. D., FLAHERTY, S. M., SAKKAS, D., TERZI, N. & STEITZ, J. A. (2005) An embryonic poly(A)-binding protein (ePAB) is expressed in mouse oocytes and early preimplantation embryos. *Proc Natl Acad Sci U S A,* 102**,** 367-72.

SELI, E., YABA, A., GUZELOGLU-KAYISLI, O. & LALIOTI, M. D. (2008) Alternative splicing of the mouse embryonic poly(A) binding protein (Epab) mRNA is regulated by an exonic splicing enhancer: a model for post-transcriptional control of gene expression in the oocyte. *Mol Hum Reprod,* 14**,** 393-8.

SELIGMAN, J. & PAGE, D. C. (1998) The Dazh gene is expressed in male and female embryonic gonads before germ cell sex differentiation. *Biochem Biophys Res Commun,* 245**,** 878-82.

SENGUPTA, D. J., ZHANG, B., KRAEMER, B., POCHART, P., FIELDS, S. & WICKENS, M. (1996) A three-hybrid system to detect RNA-protein interactions in vivo. *Proc Natl Acad Sci U S A,* 93**,** 8496-501.

SEYDOUX, G. & BRAUN, R. E. (2006) Pathway to totipotency: lessons from germ cells. *Cell,* 127**,** 891-904.

SHAH, C., VANGOMPEL, M. J., NAEEM, V., CHEN, Y., LEE, T., ANGELONI, N., WANG, Y. & XU, E. Y. (2010) Widespread presence of human BOULE homologs among animals and conservation of their ancient reproductive function. *PLoS Genet,* 6**,** e1001022.

SHARPE, R. M. (1994) Regulation of Spermatogenesis. IN KNOBIL, E. & NEIL, J. D. (Eds.) *The Physiology of Reproduction.* New York, Raven Press.

SHEETS, M. D., FOX, C. A., HUNT, T., VANDE WOUDE, G. & WICKENS, M. (1994) The 3'-untranslated regions of c-mos and cyclin mRNAs stimulate translation by regulating cytoplasmic polyadenylation. *Genes Dev,* 8**,** 926-38.

SHEETS, M. D., WU, M. & WICKENS, M. (1995) Polyadenylation of c-mos mRNA as a control point in Xenopus meiotic maturation. *Nature,* 374**,** 511-6.

SHELLING, A. N. (2010) Premature ovarian failure. *Reproduction,* 140**,** 633-41.

SIDDIQUI, N., MANGUS, D. A., CHANG, T. C., PALERMINO, J. M., SHYU, A. B. & GEHRING, K. (2007) Poly(A) nuclease interacts with the C-terminal domain of polyadenylate-binding protein domain from poly(A)-binding protein. *J Biol Chem,* 282**,** 25067-75.

SIGRIST, S. J., THIEL, P. R., REIFF, D. F., LACHANCE, P. E., LASKO, P. & SCHUSTER, C. M. (2000) Postsynaptic translation affects the efficacy and morphology of neuromuscular junctions. *Nature,* 405**,** 1062-5.

SINGH, G., REBBAPRAGADA, I. & LYKKE-ANDERSEN, J. (2008) A competition between stimulators and antagonists of Upf complex recruitment governs human nonsense-mediated mRNA decay. *PLoS Biol,* 6**,** e111.

SKABKINA, O. V., LYABIN, D. N., SKABKIN, M. A. & OVCHINNIKOV, L. P. (2005) YB-1 autoregulates translation of its own mRNA at or prior to the step of 40S ribosomal subunit joining. *Mol Cell Biol,* 25**,** 3317-23.

SKABKINA, O. V., SKABKIN, M. A., POPOVA, N. V., LYABIN, D. N., PENALVA, L. O. & OVCHINNIKOV, L. P. (2003) Poly(A)-binding protein positively affects YB-1 mRNA translation through specific interaction with YB-1 mRNA. *J Biol Chem,* 278**,** 18191-8.

SLADIC, R. T., LAGNADO, C. A., BAGLEY, C. J. & GOODALL, G. J. (2004) Human PABP binds AU-rich RNA via RNA-binding domains 3 and 4. *Eur J Biochem,* 271**,** 450-7.

SLEE, R., GRIMES, B., SPEED, R. M., TAGGART, M., MAGUIRE, S. M., ROSS, A., MCGILL, N. I., SAUNDERS, P. T. & COOKE, H. J. (1999) A human DAZ transgene confers partial rescue of the mouse Dazl null phenotype. *Proc Natl Acad Sci U S A,* 96**,** 8040-5.

SMALLWOOD, S. A. & KELSEY, G. (2012) De novo DNA methylation: a germ cell perspective. *Trends Genet,* 28**,** 33-42.

SMITH, J. W. S. (2007) Investigating the mechanism of translational stimulation by Deleted in Azoospermia-like. Edinburgh Edinburgh University.

SMITH, R. W., ANDERSON, R. C., SMITH, J. W., BROOK, M., RICHARDSON, W. A. & GRAY, N. K. (2011) DAZAP1, an RNA-binding protein required for development and spermatogenesis, can regulate mRNA translation. *RNA,* 17**,** 1282-95.

SMITH, R. W. & GRAY, N. K. (2010) Poly(A)-binding protein (PABP): a common viral target. *Biochem J,* 426**,** 1-12.

SODERBERG, O., GULLBERG, M., JARVIUS, M., RIDDERSTRALE, K., LEUCHOWIUS, K. J., JARVIUS, J., WESTER, K., HYDBRING, P., BAHRAM, F., LARSSON, L. G. & LANDEGREN, U. (2006) Direct observation of individual endogenous protein complexes in situ by proximity ligation. *Nat Methods,* 3**,** 995-1000.

SOLOVYEVA, E. V., HAYASHI, M., MARGI, K., BARKATS, C., KLEIN, C., AMSTERDAM, A., HSUEH, A. J. & TSAFRIRI, A. (2000) Growth differentiation factor-9 stimulates rat theca-interstitial cell androgen biosynthesis. *Biol Reprod,* 63**,** 1214-8.

SONENBERG, N. & HINNEBUSCH, A. G. (2009a) Regulation of translation initiation in eukaryotes: mechanisms and biological targets. *Cell,* 136**,** 731-45.

SONENBERG, N. & HINNEBUSCH, A. G. (2009b) Regulation of Translation Initiation in Eukaryotes: Mechanisms and Biological Targets. *Cell,* 136**,** 731-745.

SPRIGGS, K. A., BUSHELL, M. & WILLIS, A. E. (2010) Translational regulation of gene expression during conditions of cell stress. *Mol Cell,* 40**,** 228-37.

SPRIGGS, K. A., STONELEY, M., BUSHELL, M. & WILLIS, A. E. (2008) Re-programming of translation following cell stress allows IRES-mediated translation to predominate. *Biol Cell,* 100**,** 27-38.

STANDART, N. & MINSHALL, N. (2008) Translational control in early development: CPEB, P-bodies and germinal granules. *Biochem Soc Trans,* 36**,** 671-6.

STEBBINS-BOAZ, B., CAO, Q., DE MOOR, C. H., MENDEZ, R. & RICHTER, J. D. (1999) Maskin is a CPEB-associated factor that transiently interacts with elF-4E. *Mol Cell,* 4**,** 1017-27.

STEWART, M. (2007) Ratcheting mRNA out of the nucleus. *Mol Cell,* 25**,** 327-30.

STRIPECKE, R. & HENTZE, M. W. (1992) Bacteriophage and spliceosomal proteins function as position-dependent cis/trans repressors of mRNA translation in vitro. *Nucleic Acids Res,* 20**,** 5555-64.

SUGIURA, K., PENDOLA, F. L. & EPPIG, J. J. (2005) Oocyte control of metabolic cooperativity between oocytes and companion granulosa cells: energy metabolism. *Dev Biol,* 279**,** 20-30.

SUZUKI, A. & SAGA, Y. (2008) Nanos2 suppresses meiosis and promotes male germ cell differentiation. *Genes Dev,* 22**,** 430-5.

TAKEDA, Y., MISHIMA, Y., FUJIWARA, T., SAKAMOTO, H. & INOUE, K. (2009) DAZL relieves miRNA-mediated repression of germline mRNAs by controlling poly(A) tail length in zebrafish. *PLoS One,* 4**,** e7513.

TAM, P. P. & SNOW, M. H. (1981) Proliferation and migration of primordial germ cells during compensatory growth in mouse embryos. *J Embryol Exp Morphol,* 64**,** 133-47.

TANAKA, M. & HERR, W. (1990) Differential transcriptional activation by Oct-1 and Oct-2: interdependent activation domains induce Oct-2 phosphorylation. *Cell,* 60**,** 375-86.

TANAKA, S. S., TOYOOKA, Y., AKASU, R., KATOH-FUKUI, Y., NAKAHARA, Y., SUZUKI, R., YOKOYAMA, M. & NOCE, T. (2000) The mouse homolog of Drosophila Vasa is required for the development of male germ cells. *Genes Dev,* 14**,** 841-53.

TARUN, S. Z., JR. & SACHS, A. B. (1995) A common function for mRNA 5' and 3' ends in translation initiation in yeast. *Genes Dev,* 9**,** 2997-3007.

TARUN, S. Z., JR. & SACHS, A. B. (1996) Association of the yeast poly(A) tail binding protein with translation initiation factor eIF-4G. *EMBO J,* 15**,** 7168-77.

TAY, J., HODGMAN, R. & RICHTER, J. D. (2000) The control of cyclin B1 mRNA translation during mouse oocyte maturation. *Dev Biol,* 221**,** 1-9.

TAY, J., HODGMAN, R., SARKISSIAN, M. & RICHTER, J. D. (2003) Regulated CPEB phosphorylation during meiotic progression suggests a mechanism for temporal control of maternal mRNA translation. *Genes Dev,* 17**,** 1457-62.

TAY, J. & RICHTER, J. D. (2001) Germ cell differentiation and synaptonemal complex formation are disrupted in CPEB knockout mice. *Dev Cell,* 1**,** 201-13.

TELFER, E. E. & MCLAUGHLIN, M. (2011) In vitro development of ovarian follicles. *Semin Reprod Med,* 29**,** 15-23.

TELFER, E. E., MCLAUGHLIN, M., DING, C. & THONG, K. J. (2008) A two-step serum-free culture system supports development of human oocytes from primordial follicles in the presence of activin. *Hum Reprod,* 23**,** 1151-8.

TIRONE, E., D'ALESSANDRIS, C., HASCALL, V. C., SIRACUSA, G. & SALUSTRI, A. (1997) Hyaluronan synthesis by mouse cumulus cells is regulated by interactions between follicle-stimulating hormone (or epidermal

growth factor) and a soluble oocyte factor (or transforming growth factor beta1). *J Biol Chem,* 272**,** 4787-94.

TOTH, A., RABITSCH, K. P., GALOVA, M., SCHLEIFFER, A., BUONOMO, S. B. & NASMYTH, K. (2000) Functional genomics identifies monopolin: a kinetochore protein required for segregation of homologs during meiosis i. *Cell,* 103**,** 1155-68.

TOYOOKA, Y., TSUNEKAWA, N., TAKAHASHI, Y., MATSUI, Y., SATOH, M. & NOCE, T. (2000) Expression and intracellular localization of mouse Vasa-homologue protein during germ cell development. *Mech Dev,* 93**,** 139-49.

TSUDA, M., SASAOKA, Y., KISO, M., ABE, K., HARAGUCHI, S., KOBAYASHI, S. & SAGA, Y. (2003) Conserved role of nanos proteins in germ cell development. *Science,* 301**,** 1239-41.

TSUI, S., DAI, T., ROETTGER, S., SCHEMPP, W., SALIDO, E. C. & YEN, P. H. (2000a) Identification of two novel proteins that interact with germ-cell-specific RNA-binding proteins DAZ and DAZL1. *Genomics,* 65**,** 266-73.

TSUI, S., DAI, T., WARREN, S. T., SALIDO, E. C. & YEN, P. H. (2000b) Association of the mouse infertility factor DAZL1 with actively translating polyribosomes. *Biol Reprod,* 62**,** 1655-60.

TUNG, J. Y., LUETJENS, C. M., WISTUBA, J., XU, E. Y., REIJO PERA, R. A. & GROMOLL, J. (2006a) Evolutionary comparison of the reproductive genes, DAZL and BOULE, in primates with and without DAZ. *Dev Genes Evol,* 216**,** 158-68.

TUNG, J. Y., ROSEN, M. P., NELSON, L. M., TUREK, P. J., WITTE, J. S., CRAMER, D. W., CEDARS, M. I. & REIJO-PERA, R. A. (2006b) Novel missense mutations of the Deleted-in-AZoospermia-Like (DAZL) gene in infertile women and men. *Reprod Biol Endocrinol,* 4**,** 40.

UCHIDA, N., HOSHINO, S., IMATAKA, H., SONENBERG, N. & KATADA, T. (2002) A novel role of the mammalian GSPT/eRF3 associating with poly(A)-binding protein in Cap/Poly(A)-dependent translation. *J Biol Chem,* 277**,** 50286-92.

UCHIDA, N., HOSHINO, S. & KATADA, T. (2004) Identification of a human cytoplasmic poly(A) nuclease complex stimulated by poly(A)-binding protein. *J Biol Chem,* 279**,** 1383-91.

URANO, J., FOX, M. S. & REIJO PERA, R. A. (2005) Interaction of the conserved meiotic regulators, BOULE (BOL) and PUMILIO-2 (PUM2). *Mol Reprod Dev,* 71**,** 290-8.

VANGOMPEL, M. J. & XU, E. Y. (2010) A novel requirement in mammalian spermatid differentiation for the DAZ-family protein Boule. *Hum Mol Genet,* 19**,** 2360-9.

VANGOMPEL, M. J. W. & XU, E. Y. (2011) The roles of the DAZ family in spermatogenesis: More than just translation? *Spermatogenesis,* 1**,** 36-46.

VENABLES, J. P., RUGGIU, M. & COOKE, H. J. (2001) The RNA-binding specificity of the mouse Dazl protein. *Nucleic Acids Res,* 29**,** 2479-83.

VENDE, P., PIRON, M., CASTAGNE, N. & PONCET, D. (2000) Efficient translation of rotavirus mRNA requires simultaneous interaction of NSP3 with the eukaryotic translation initiation factor eIF4G and the mRNA 3' end. *J Virol,* 74**,** 7064-71.

VILLARD, J. (2004) Transcription regulation and human diseases. *Swiss Med Wkly,* 134**,** 571-9.

VINCENT, S. D., DUNN, N. R., SCIAMMAS, R., SHAPIRO-SHALEF, M., DAVIS, M. M., CALAME, K., BIKOFF, E. K. & ROBERTSON, E. J. (2005) The zinc finger transcriptional repressor Blimp1/Prdm1 is dispensable for early axis formation but is required for specification of primordial germ cells in the mouse. *Development,* 132**,** 1315-25.

VOELTZ, G. K., ONGKASUWAN, J., STANDART, N. & STEITZ, J. A. (2001) A novel embryonic poly(A) binding protein, ePAB, regulates mRNA deadenylation in Xenopus egg extracts. *Genes Dev,* 15**,** 774-88.

VOGEL, T., SPEED, R. M., ROSS, A. & COOKE, H. J. (2002) Partial rescue of the Dazl knockout mouse by the human DAZL gene. *Mol Hum Reprod,* 8**,** 797-804.

VOGT, P. H., EDELMANN, A., HIRSCHMANN, P. & KOHLER, M. R. (1995) The azoospermia factor (AZF) of the human Y chromosome in Yq11: function and analysis in spermatogenesis. *Reprod Fertil Dev,* 7**,** 685-93.

WALTERS, R. W., BRADRICK, S. S. & GROMEIER, M. (2010) Poly(A)-binding protein modulates mRNA susceptibility to cap-dependent miRNA-mediated repression. *RNA,* 16**,** 239-50.

WANG, J. & PANTOPOULOS, K. (2011) Regulation of cellular iron metabolism. *Biochem J,* 434**,** 365-81.

WANG, Z. & KILEDJIAN, M. (2000) The poly(A)-binding protein and an mRNA stability protein jointly regulate an endoribonuclease activity. *Mol Cell Biol,* 20**,** 6334-41.

WEBSTER, K. E., O'BRYAN, M. K., FLETCHER, S., CREWTHER, P. E., AAPOLA, U., CRAIG, J., HARRISON, D. K., AUNG, H., PHUTIKANIT, N., LYLE, R., MEACHEM, S. J., ANTONARAKIS, S. E., DE KRETSER, D. M., HEDGER, M. P., PETERSON, P., CARROLL, B. J. & SCOTT, H. S. (2005) Meiotic and epigenetic defects in Dnmt3L-knockout mouse spermatogenesis. *Proc Natl Acad Sci U S A,* 102**,** 4068-73.

WEI, C. C., BALASTA, M. L., REN, J. & GOSS, D. J. (1998) Wheat germ poly(A) binding protein enhances the binding affinity of eukaryotic initiation factor 4F and (iso)4F for cap analogues. *Biochemistry,* 37**,** 1910-6.

WEIBRECHT, I., LEUCHOWIUS, K. J., CLAUSSON, C. M., CONZE, T., JARVIUS, M., HOWELL, W. M., KAMALI-MOGHADDAM, M. & SODERBERG, O. (2010) Proximity ligation assays: a recent addition to the proteomics toolbox. *Expert Rev Proteomics,* 7**,** 401-9.

WEINBAEUR, G. F. & NIECHLAG, E. (1993) Hormonal Control of Spermatogenesis. IN DE KRETSER, D. M. (Ed.) *Molecular Physiology of the Male Reproductive System.* San Diego, Academic Press.

WEK, R. C., JIANG, H. Y. & ANTHONY, T. G. (2006) Coping with stress: eIF2 kinases and translational control. *Biochem Soc Trans,* 34**,** 7-11.

WELLS, S. E., HILLNER, P. E., VALE, R. D. & SACHS, A. B. (1998) Circularization of mRNA by eukaryotic translation initiation factors. *Mol Cell,* 2**,** 135-40.

WERT, S. E. & LARSEN, W. J. (1990) Preendocytotic alterations in cumulus cell gap junctions precede meiotic resumption in the rat cumulus-oocyte complex. *Tissue Cell,* 22**,** 827-51.

WHITE, Y. A., WOODS, D. C., TAKAI, Y., ISHIHARA, O., SEKI, H. & TILLY, J. L. (2012) Oocyte formation by mitotically active germ cells purified from ovaries of reproductive-age women. *Nat Med,* 18**,** 413-21.

WICKENS, M., BERNSTEIN, D. S., KIMBLE, J. & PARKER, R. (2002) A PUF family portrait: 3'UTR regulation as a way of life. *Trends Genet,* 18**,** 150-7.

WILKIE, G. S., GAUTIER, P., LAWSON, D. & GRAY, N. K. (2005) Embryonic poly(A)-binding protein stimulates translation in germ cells. *Mol Cell Biol,* 25**,** 2060-71.

WOODS, A. J., KANTIDAKIS, T., SABE, H., CRITCHLEY, D. R. & NORMAN, J. C. (2005) Interaction of paxillin with poly(A)-binding protein 1 and its role in focal adhesion turnover and cell migration. *Mol Cell Biol,* 25**,** 3763-73.

XU, E. Y., LEE, D. F., KLEBES, A., TUREK, P. J., KORNBERG, T. B. & REIJO PERA, R. A. (2003) Human BOULE gene rescues meiotic defects in infertile flies. *Hum Mol Genet,* 12**,** 169-75.

XU, E. Y., MOORE, F. L. & PERA, R. A. (2001) A gene family required for human germ cell development evolved from an ancient meiotic gene conserved in metazoans. *Proc Natl Acad Sci U S A,* 98**,** 7414-9.

YANAGIYA, A., DELBES, G., SVITKIN, Y. V., ROBAIRE, B. & SONENBERG, N. (2010) The poly(A)-binding protein partner Paip2a controls translation during late spermiogenesis in mice. *J Clin Invest,* 120**,** 3389-400.

YANAGIYA, A., SUYAMA, E., ADACHI, H., SVITKIN, Y. V., AZA-BLANC, P., IMATAKA, H., MIKAMI, S., MARTINEAU, Y., RONAI, Z. A. & SONENBERG, N. (2012) Translational Homeostasis via the mRNA Cap-Binding Protein, eIF4E. *Mol Cell*.

YANAGIYA, A., SVITKIN, Y. V., SHIBATA, S., MIKAMI, S., IMATAKA, H. & SONENBERG, N. (2009) Requirement of RNA binding of mammalian eukaryotic translation initiation factor 4GI (eIF4GI) for efficient interaction of eIF4E with the mRNA cap. *Mol Cell Biol.,* 29**,** 1661-1669.

YANG, F., ECKARDT, S., LEU, N. A., MCLAUGHLIN, K. J. & WANG, P. J. (2008a) Mouse TEX15 is essential for DNA double-strand break repair and chromosomal synapsis during male meiosis. *J Cell Biol,* 180**,** 673-9.

YANG, F., GELL, K., VAN DER HEIJDEN, G. W., ECKARDT, S., LEU, N. A., PAGE, D. C., BENAVENTE, R., HER, C., HOOG, C., MCLAUGHLIN, K. J. & WANG, P. J. (2008b) Meiotic failure in male mice lacking an X-linked factor. *Genes Dev,* 22**,** 682-91.

YANG, H., DUCKETT, C. S. & LINDSTEN, T. (1995) iPABP, an inducible poly(A)-binding protein detected in activated human T cells. *Mol Cell Biol,* 15**,** 6770-6.

YEN, P. H. (2004) Putative biological functions of the DAZ family. *Int J Androl,* 27**,** 125-9.

YEN, P. H., CHAI, N. N. & SALIDO, E. C. (1996) The human autosomal gene DAZLA: testis specificity and a candidate for male infertility. *Hum Mol Genet,* 5**,** 2013-7.

YEN, P. H., CHAI, N. N. & SALIDO, E. C. (1997) The human DAZ genes, a putative male infertility factor on the Y chromosome, are highly polymorphic in the DAZ repeat regions. *Mamm Genome,* 8**,** 756-9.

YOSHIDA, S., SUKENO, M., NAKAGAWA, T., OHBO, K., NAGAMATSU, G., SUDA, T. & NABESHIMA, Y. (2006) The first round of mouse spermatogenesis is a distinctive program that lacks the self-renewing spermatogonia stage. *Development,* 133**,** 1495-505.

YUAN, L., LIU, J. G., ZHAO, J., BRUNDELL, E., DANEHOLT, B. & HOOG, C. (2000) The murine SCP3 gene is required for synaptonemal complex assembly, chromosome synapsis, and male fertility. *Mol Cell,* 5**,** 73-83.

ZEKRI, L., HUNTZINGER, E., HEIMSTADT, S. & IZAURRALDE, E. (2009) The silencing domain of GW182 interacts with PABPC1 to promote translational repression and degradation of microRNA targets and is required for target release. *Mol Cell Biol,* 29**,** 6220-31.

ZENG, M., DENG, W., WANG, X., QIU, W., LIU, Y., SUN, H., TAO, D., ZHANG, S. & MA, Y. (2008) DAZL binds to the transcripts of several Tssk genes in germ cells. *BMB Rep,* 41**,** 300-4.

ZENG, M., LU, Y., LIAO, X., LI, D., SUN, H., LIANG, S., ZHANG, S., MA, Y. & YANG, Z. (2009) DAZL binds to 3'UTR of Tex19.1 mRNAs and regulates Tex19.1 expression. *Mol Biol Rep,* 36**,** 2399-403.

ZHANG, B., KRAEMER, B., SENGUPTA, D., FIELDS, S. & WICKENS, M. (1999) Yeast three-hybrid system to detect and analyze interactions between RNA and protein. *Methods Enzymol,* 306**,** 93-113.

ZHAO, W. M., JIANG, C., KROLL, T. T. & HUBER, P. W. (2001) A proline-rich protein binds to the localization element of Xenopus Vg1 mRNA and to ligands involved in actin polymerization. *EMBO J,* 20**,** 2315-25.

ZICKLER, D. & KLECKNER, N. (1999) Meiotic chromosomes: integrating structure and function. *Annu Rev Genet,* 33**,** 603-754.

ZIMMERMAN, Z. A. & KELLOGG, D. R. (2001) The Sda1 protein is required for passage through start. *Mol Biol Cell,* 12**,** 201-19.